Department of Electrical & Electronics Engineering

Course File

EHVAC Transmission

(Professional Elective-VI)

(Course Code: EE861PE**)**

IV B.Tech II Semester

2023-24

BOILLA SRINU

Assistant Professor

Anurag ENGINEERING COLLEGE

Ananthagiri, Kodad, Telangana 508 206, India.

Department of Electrical & Electronics Engineering

EHVAC Transmission

Check List

S.No	Name of the Format	Page No.
1	Syllabus	1
2	Timetable	2
3	Program Educational Objectives	4
4	Program Objectives	4
5	Course Objectives	5
6	Course Outcomes	5
7	Guidelines to study the course	6
8	Course Schedule	7
9	Course Plan	8
10	Unit Plan	8
11	Lesson Plan	14
12	Assignment Sheets	17
13	Tutorial Sheets	19
14	Evaluation Strategy	20
15	Assessment in relation to COb's and CO's	22
16	Mappings of CO's and PO's	22
17	Rubric for course	23
18	Mid-I and Mid-II question papers	24
19	Mid-I mark	30
20	Mid-II mark	34
21	Sample answer scripts and Assignments	38
22	Course materials like Notes, PPT's, etc.	50

Department of Electrical & Electronics Engineering

Int. Marks:25 Ext. Marks:75 Total Marks:100

(EE861PE) EHVAC Transmission

(Professional Elective-VI)

IV Year B.Tech. EEE - II Sem **L T/P/D C**
3 -/-/- 3

UNIT – I
Preliminaries Necessity of EHV AC transmission – advantages and problems–power handling capacity and line losses- mechanical considerations — bundle conductor systems. Line inductance and capacitances – sequence inductances and capacitances – modes of propagation.
UNIT – II
Voltage gradients of conductors Electrostatics – field of sphere gap – field of line changes and properties – charge – potential relations for multi-conductors – surface voltage gradient on conductors – distribution of voltage gradient on sub-conductors of bundle – Examples.
UNIT – III
Corona Effects Corona in E.H.V. lines – Corona loss formulae- attention of traveling waves due to Corona – Audio noise due to Corona, its generation, characteristic and limits. Measurements of audio noise radio interference due to Corona - properties of radio noise – frequency spectrum of RI fields – Measurements of RI and RIV.
UNIT – IV
Electro Static Field Electrostatic field: calculation of electrostatic field of EHV/AC lines – effect on humans, animals and plants – electrostatic induction in unenergised circuit of double-circuit line – electromagnetic interference-Examples. Traveling wave expression and solution- source of excitation- terminal conditions-open circuited and short-circuited end- reflection and refraction coefficients-Lumped parameters of distributed lines-generalized constants-No load voltage conditions and charging current.
UNIT –V
Voltage control Power circle diagram and its use – voltage control using synchronous condensers – cascade connection of shunt and series compensation – sub synchronous resonance in series capacitor – compensated lines – static VAR compensating system.

Text Books:

1. R. D. Begamudre, “EHVAC Transmission Engineering”, New Age International (p) Ltd, 3rd Edition, 2006.
2. 2. S.Rao, “EHVAC and HVDC Transmission Engineering and Practice”, Khanna Publishers, 2015(Reprint). Reference

Books:

1. E Rakesh Das Begamudre, “Extra High Voltage AC Transmission Engineering”, Wiley Eastern LTD., New Delhi, 1987.
2. Edison,”EHV Transmission line”, Electric Institution - (GEC 1968).

Department of Electrical & Electronics Engineering

Timetable

IV B.Tech. II Semester – EHVAC Transmissiom

Day/Hour	9.30-10.20	10.20-11.10	11.20-12.10	12.10-0100	01.40-02.25	2.25-3.10	3.15-4.0
Monday	EHVACT						
Tuesday							
Wednesday	EHVACT						
Thursday	EHVACT						
Friday			EHVACT				
Saturday			EHVACT				

Department of Electrical & Electronics Engineering

Vision of the Institute

To be a premier Institute in the country and region for the study of Engineering, Technology and Management by maintaining high academic standards which promotes the analytical thinking and independent judgment among the prime stakeholders, enabling them to function responsibly in the globalized society.

Mission of the Institute

To be a world-class Institute, achieving excellence in teaching, research and consultancy in cutting-edge Technologies and be in the service of society in promoting continued education in Engineering, Technology and Management.

Quality Policy

To ensure high standards in imparting professional education by providing world-class infrastructure, top-quality-faculty and decent work culture to sculpt the students into Socially Responsible Professionals through creative team-work, innovation and research

Vision of the Department

To impart technical knowledge and skills required to succeed in life, career and help society to achieve self sufficiency.

Mission of the Department

- To become an internationally leading department for higher learning.
- To build upon the culture and values of universal science and contemporary education.
- To be a center of research and education generating knowledge and technologies which lay groundwork in shaping the future in the fields of electrical and electronics engineering.
- To develop partnership with industrial, R&D and government agencies and actively participate in conferences, technical and community activities.

Department of Electrical & Electronics Engineering

Program Educational Objectives (B.Tech. – EEE)

Graduates will be able to

PEO 1: To prepare students to excel in technical profession/industry and/or higher education by acquiring knowledge in mathematics, science and engineering principles.

PEO 2: Able to formulate, analyze, design and create novel products and solutions to electrical and electronics engineering problems those are economically feasible and socially acceptable.

PEO 3: Able to adopt multi-disciplinary environments, leadership qualities, effective communication, professional ethics and lifelong learning process.

Program Outcomes (B.Tech. – EEE)

At the end of the Program, a graduate will have the ability to

PO 1: An ability to apply the knowledge of mathematics, science and engineering fundamentals.

PO 2: An ability to conduct Investigations using design of experiments, analysis and interpretation of data to arrive at valid conclusions.

PO 3: An ability to design Electrical and Electronics Engineering components and processes within economic, environmental, ethical and manufacturability constraints.

PO 4: An ability to function effectively in multidisciplinary teams.

PO 5: An ability to identify, formulate, analyze and solve Electrical and Electronics Engineering problems.

PO 6: An ability to understand professional, ethical and social responsibility.

PO 7: An ability to communicate effectively through written reports or oral presentations.

PO 8: The broad education necessary to understand the impact of engineering solutions in a global, economic, environmental, and societal context.

PO 9: An ability to recognize the need and to engage in independent and life-long learning.

PO 10: Knowledge on contemporary issues.

PO 11: An ability to use the appropriate techniques and modern engineering tools necessary for engineering practice.

PO 12: Demonstrate an ability to design electrical and electronic circuits, power electronics, power systems; electrical machines analyze and interpret data and also an ability to design digital and analog systems and programming them.

Department of Electrical & Electronics Engineering

COURSE OBJECTIVES

On completion of this Subject/Course the student shall be able to:

S.No	Objectives
1	This course introduces the necessity of EHVAC transmission line.
2	It introduces calculation of voltage gradient of conductors corona effects in EHV line.
3	Deals with the corona effects.
4	Calculation of electro static field of EHVAC lines and studying voltage control along with power circle diagram and analyze the test performed large transmission lines over bulk power lines.
5	• Deals with the voltage control aspects

COURSE OUTCOMES

The expected outcomes of the Course/Subject are:

S.No	Outcomes
1.	Evaluating the loss coefficients, capacitances and inductances.
2.	Voltage gradient relations for various conductors.
3.	Corona formulations and its remedies.
4.	Electrostatic field computations.
5.	Compensating methods, power circle diagram approach.

Signature of faculty

Note: Please refer to Bloom's Taxonomy, to know the illustrative verbs that can be used to state the outcomes.

Department of Electrical & Electronics Engineering

GUIDELINES TO STUDY THE COURSE / SUBJECT

Course Design and Delivery System (CDD):

- The Course syllabus is written into number of learning objectives and outcomes.
- Every student will be given an assessment plan, criteria for assessment, scheme of evaluation and grading method.
- The Learning Process will be carried out through assessments of Knowledge, Skills and Attitude by various methods and the students will be given guidance to refer to the text books, reference books, journals, etc.

The faculty be able to –

- Understand the principles of Learning
- Understand the psychology of students
- Develop instructional objectives for a given topic
- Prepare course, unit and lesson plans
- Understand different methods of teaching and learning
- Use appropriate teaching and learning aids
- Plan and deliver lectures effectively
- Provide feedback to students using various methods of Assessments and tools of Evaluation
- Act as a guide, advisor, counselor, facilitator, motivator and not just as a teacher alone

Signature of HOD　　　　　　　　　　Signature of faculty

Date:　　　　　　　　　　Date:

Department of Electrical & Electronics Engineering
COURSE SCHEDULE

The Schedule for the whole Course / Subject is:

S. No.	Description	Duration (Date)		Total No. of Periods
		From	To	
1.	**UNIT – I** Preliminaries Necessity of EHV AC transmission – advantages and problems–power handling capacity and line losses-mechanical considerations — bundle conductor systems. Line inductance and capacitances – sequence inductances and capacitances – modes of propagation.	15-11-2023	16-12-2023	13
2.	**UNIT – II** Voltage gradients of conductors Electrostatics – field of sphere gap – field of line changes and properties – charge – potential relations for multi-conductors – surface voltage gradient on conductors – distribution of voltage gradient on sub-conductors of bundle – Examples.	17-12-2023	11-01-2024	14
3.	**UNIT – III** Corona Effects Corona in E.H.V. lines – Corona loss formulae- attention of traveling waves due to Corona – Audio noise due to Corona, its generation, characteristic and limits. Measurements of audio noise radio interference due to Corona - properties of radio noise – frequency spectrum of RI fields – Measurements of RI and RIV.	12-01-2024	12-02-2024	15
4.	**UNIT – IV** Electro Static Field Electrostatic field: calculation of electrostatic field of EHV/AC lines – effect on humans, animals and plants – electrostatic induction in unenergised circuit of double-circuit line – electromagnetic interference-Examples. Traveling wave expression and solution- source of excitation- terminal conditions- open circuited and short-circuited end- reflection and refraction coefficients-Lumped parameters of distributed lines-generalized constants-No load voltage conditions and charging current.	13-02-2024	08-03-2024	15
5.	**UNIT –V** Voltage control Power circle diagram and its use – voltage control using synchronous condensers – cascade connection of shunt and series compensation – sub synchronous resonance in series capacitor – compensated lines – static VAR compensating system.	09-03-2024	04-04-2024	13

Total No. of Instructional periods available for the course: 73 Hours

Department of Electrical & Electronics Engineering

SCHEDULE OF INSTRUCTIONS - COURSE PLAN

Unit No.	Lesson No.	Date	No. of Periods	Topics / Sub-Topics	Objectives & Outcomes Nos.	References (Textbook, Journal)
1.	1	15-11-2023	1	Introduction of Preliminaries	1 1	“EHVAC Transmission Engineering”, R.D.Begamudre
	2	16-11-2023	1	Necessity of EHV AC transmission	1 1	“EHVAC Transmission Engineering”, R.D.Begamudre
	3	17-11-2023	1	Advantages	1 1	“EHVAC Transmission Engineering”, R.D.Begamudre
	4	18-11-2023	1	Problems	1 1	“EHVAC Transmission Engineering”, R.D.Begamudre
	5	20-11-2023	1	Power Handling Capacity	1 1	“EHVAC Transmission Engineering”, R.D.Begamudre
	6	22-11-2023	1	Line Losses	1 1	“EHVAC Transmission Engineering”, R.D.Begamudre
	7	23-11-2023	1	Problems	1 1	“EHVAC Transmission Engineering”, R.D.Begamudre
	8	24-11-2023	1	Mechanical Considerations	1 1	“EHVAC Transmission Engineering”, R.D.Begamudre
	9	25-11-2023	1	Bundle Conductor Systems	1 1	“EHVAC Transmission Engineering”, R.D.Begamudre
	10	27-11-2023	1	Line Inductance	1 1	“EHVAC Transmission Engineering”, R.D.Begamudre
	11	30-11-2023	1	Line Capacitances	1 1	“EHVAC Transmission Engineering”, R.D.Begamudre
	12	04-12-2023	1	Sequence Inductances And Capacitances	1 1	“EHVAC Transmission

						Engineering", R.D.Begamudre
	13	06-12-2023	1	Modes Of Propagation	1 1	"EHVAC Transmission Engineering", R.D.Begamudre
2.	1	07-12-2023	1	Voltage Gradients Of Conductors Electrostatics	2 2	"EHVAC Transmission Engineering", R.D.Begamudre
	2	08-12-2023	1	Field Of Sphere Gap	2 2	"EHVAC Transmission Engineering", R.D.Begamudre
	3	11-12-2023	1	Field Of Sphere Gap	2 2	"EHVAC Transmission Engineering", R.D.Begamudre
	4	13-12-2023	1	Field Of Line Changes And Properties	2 2	"EHVAC Transmission Engineering", R.D.Begamudre
	5	14-12-2023	1	Field Of Line Changes And Properties	2 2	"EHVAC Transmission Engineering", R.D.Begamudre
	6	16-12-2023	1	Charge	2 2	"EHVAC Transmission Engineering", R.D.Begamudre
	7	18-12-2023	1	Potential Relations For Multi-Conductors	2 2	"EHVAC Transmission Engineering", R.D.Begamudre
	8	20-12-2023	1	Potential Relations For Multi-Conductors	2 2	"EHVAC Transmission Engineering", R.D.Begamudre
	9	21-12-2024	1	Surface Voltage Gradient On Conductors	2 2	"EHVAC Transmission Engineering", R.D.Begamudre
	10	22-12-2024	1	Surface Voltage Gradient On Conductors	2 2	"EHVAC Transmission Engineering", R.D.Begamudre
	11	23-12-2024	1	Distribution Of Voltage Gradient On Sub-Conductors Of Bundle	2 2	"EHVAC Transmission Engineering", R.D.Begamudre

	12	27-12-2024	1	Distribution Of Voltage Gradient On Sub-Conductors Of Bundle	2 2	"EHVAC Transmission Engineering", R.D.Begamudre
	13	28-12-2024	1	Examples	2 2	"EHVAC Transmission Engineering", R.D.Begamudre
	14	03-01-2024	1	Examples	2 2	"EHVAC Transmission Engineering", R.D.Begamudre
3.	1	04-01-2024	1	Corona Effects Corona In E.H.V	3 3	"EHVAC Transmission Engineering", R.D.Begamudre
	2	05-01-2024	1	Corona Loss Formulae	3 3	"EHVAC Transmission Engineering", R.D.Begamudre
	3	06-01-2024	1	Attention Of Traveling Waves Due To Corona	3 3	"EHVAC Transmission Engineering", R.D.Begamudre
	4	08-01-2024	1	Audio Noise Due To Corona	3 3	"EHVAC Transmission Engineering", R.D.Begamudre
	5	22-01-2024	1	Lines, Its Generation,	3 3	"EHVAC Transmission Engineering", R.D.Begamudre
	6	24-01-2024	1	Characteristic And Limits	3 3	"EHVAC Transmission Engineering", R.D.Begamudre
	7	25-01-2024	1	Measurements Of Audio Noise Radio Interference Due To Corona	3 3	"EHVAC Transmission Engineering", R.D.Begamudre
	8	25-01-2024	1	Measurements Of Audio Noise Radio Interference Due To Corona	3 3	"EHVAC Transmission Engineering", R.D.Begamudre
	9	27-01-2024	1	Properties Of Radio Noise	3 3	"EHVAC Transmission Engineering", R.D.Begamudre
	10	01-02-2024	1	Frequency Spectrum Of RI Fields	3 3	"EHVAC Transmission Engineering", R.D.Begamudre

Department of Electrical & Electronics Engineering

	11	03-02-2024	1	Frequency Spectrum Of RI Fields	3 3	“EHVAC Transmission Engineering”, R.D.Begamudre
	12	08-02-2024	1	Measurements Of RI	3 3	“EHVAC Transmission Engineering”, R.D.Begamudre
	13	12-02-2024	1	Measurements Of RIV.	3 3	“EHVAC Transmission Engineering”, R.D.Begamudre
4	1	16-02-2024	1	Electro Static Field Electrostatic Field	4 4	“EHVAC Transmission Engineering”, R.D.Begamudre
	2	17-02-2024	1	Calculation Of Electrostatic Field Of EHV/AC Lines	4 4	“EHVAC Transmission Engineering”, R.D.Begamudre
	3	17-02-2024	1	Effect On Humans, Animals And Plants	4 4	“EHVAC Transmission Engineering”, R.D.Begamudre
	4	21-02-2024	1	Electrostatic Induction In Unenergised Circuit Of Double Circuit Line	4 4	“EHVAC Transmission Engineering”, R.D.Begamudre
	5	22-02-2024	1	Electromagnetic Interference	4 4	“EHVAC Transmission Engineering”, R.D.Begamudre
	6	23-02-2024	1	Electromagnetic Interference-Examples	4 4	“EHVAC Transmission Engineering”, R.D.Begamudre
	7	24-02-2024	1	Traveling Wave Expression	4 4	“EHVAC Transmission Engineering”, R.D.Begamudre
	8	26-02-2024	1	Traveling Wave Expression And Solution	4 4	“EHVAC Transmission Engineering”, R.D.Begamudre
	9	28-02-2024	1	Source Of Excitation	4 4	“EHVAC Transmission Engineering”, R.D.Begamudre
	10	29-02-2024	1	Terminal Conditions	4 4	“EHVAC Transmission Engineering”, R.D.Begamudre

	11	01-03-2024	1	Open Circuited And Short-Circuited End	4 4	"EHVAC Transmission Engineering", R.D.Begamudre
	12	02-03-2024	1	Reflection And Refraction Coefficients	4 4	"EHVAC Transmission Engineering", R.D.Begamudre
	13	04-03-2024	1	Lumped Parameters Of Distributed Lines	4 4	"EHVAC Transmission Engineering", R.D.Begamudre
	14	06-03-2024	1	Generalized Constants-No Load Voltage Conditions	4 4	"EHVAC Transmission Engineering", R.D.Begamudre
	15	08-03-2024	1	Generalized Constants	4 4	"EHVAC Transmission Engineering", R.D.Begamudre
	16	08-03-2024	1	No Load Voltage Conditions And Charging Current.	4 4	"EHVAC Transmission Engineering", R.D.Begamudre
5	1	11-03-2024	1	Voltage Control Power Circle Diagram And Its Use	5 5	"EHVAC Transmission Engineering", R.D.Begamudre
	2	13-03-2024	1	Voltage Control Using Synchronous Condensers	5 5	"EHVAC Transmission Engineering", R.D.Begamudre
	3	14-03-2024	1	Voltage Control Using Synchronous Condensers	5 5	"EHVAC Transmission Engineering", R.D.Begamudre
	4	15-03-2024	1	Cascade Connection Of Shunt And Series Compensation	5 5	"EHVAC Transmission Engineering", R.D.Begamudre
	5	16-03-2024	1	Cascade Connection Of Shunt And Series Compensation	5 5	"EHVAC Transmission Engineering", R.D.Begamudre
	6	18-03-2024	1	Sub Synchronous Resonance In Series Capacitor	5 5	"EHVAC Transmission Engineering", R.D.Begamudre
	7	20-03-2024	1	Compensated Lines	5 5	"EHVAC Transmission Engineering", R.D.Begamudre

Department of Electrical & Electronics Engineering

	8	25-03-2024	1	Static VAR Compensating System	5 5	“EHVAC Transmission Engineering”, R.D.Begamudre
	9	28-03-2024	1	Static VAR Compensating System	5 5	“EHVAC Transmission Engineering”, R.D.Begamudre
	10	30-03-2024	1	Static VAR Compensating System	5 5	“EHVAC Transmission Engineering”, R.D.Begamudre
	11	01-04-2024	1	Revision	1, 2, 3, 4, 5 1, 2, 3, 4, 5	“EHVAC Transmission Engineering”, R.D.Begamudre
	12	03-04-2024	1	Revision	1, 2 1, 2	“EHVAC Transmission Engineering”, R.D.Begamudre
	13	04-04-2024	1	Revision	3, 4 3, 4	“EHVAC Transmission Engineering”, R.D.Begamudre

Signature of HOD Signature of faculty

Date: Date:

Note:

1. Ensure that all topics specified in the course are mentioned.
2. Additional topics covered, if any, may also be specified in bold.
3. Mention the corresponding course objective and outcome numbers against each topic.

Department of Electrical & Electronics Engineering
LESSON PLAN (U-I)

Lesson No: 01 Duration of Lesson: 50 min

Lesson Title: Introduction to EHVAC Transmission

<u>Instructional / Lesson Objectives:</u>

- To make students understand Preliminaries Necessity of EHV AC transmission
- To familiarize students on Voltage gradients of conductors Electrostatics
- To understand students the concept of Corona Effects Corona in E.H.V. lines.
- To provide information on Electro Static Field Electrostatic field.
- To understand students the concept of Voltage control Power circle diagram and its use.

Teaching AIDS : PPTs, Digital Board
Time Management of Class :

5 mins for taking attendance
35 min for the lecture delivery
10 min for doubts session

Signature of faculty

Department of Electrical & Electronics Engineering

Unit No.	Lesson No.	Date	Day Of The Week	Topics / Sub-Topics
1.	1	15-11-2023	Wed	Introduction of Preliminaries
	2	16-11-2023	Thu	Necessity of EHV AC transmission
	3	17-11-2023	Mon	Advantages
	4	18-11-2023	Thu	Problems
	5	20-11-2023	Fri	Power Handling Capacity
	6	22-11-2023	Mon	Line Losses
	7	23-11-2023	Wed	Problems
	8	24-11-2023	Thu	Mechanical Considerations
	9	25-11-2023	Mon	Bundle Conductor Systems
	10	27-11-2023	Thu	Line Inductance
	11	30-11-2023	Mon	Line Capacitances
	12	04-12-2023	Thu	Sequence Inductances And Capacitances
	13	06-12-2023	Sat	Modes Of Propagation
2.	14	07-12-2023	Mon	Voltage Gradients Of Conductors Electrostatics
	15	08-12-2023	Wed	Field Of Sphere Gap
	16	11-12-2023	Fri	Field Of Sphere Gap
	17	13-12-2023	Sat	Field Of Line Changes And Properties
	18	14-12-2023	Wed	Field Of Line Changes And Properties
	19	16-12-2023	Thu	Charge
	20	18-12-2023	Fri	Potential Relations For Multi-Conductors
	21	20-12-2023	Sat	Potential Relations For Multi-Conductors
	22	21-12-2024	Wed	Surface Voltage Gradient On Conductors
	23	22-12-2024	Thu	Surface Voltage Gradient On Conductors
	24	23-12-2024	Fri	Distribution Of Voltage Gradient On Sub-Conductors Of Bundle
	25	27-12-2024	Sat	Distribution Of Voltage Gradient On Sub-Conductors Of Bundle
	26	28-12-2024	Mon	Examples
	27	03-01-2024	Thu	Examples
3.	28	04-01-2024	Wed	Corona Effects Corona In E.H.V
	29	05-01-2024	Thu	Corona Loss Formulae
	30	06-01-2024	Fri	Attention Of Traveling Waves Due To Corona
	31	08-01-2024	Sat	Audio Noise Due To Corona
	32	22-01-2024	Mon	Lines, Its Generation,
	33	24-01-2024	Wed	Characteristic And Limits
	34	25-01-2024	Thu	Measurements Of Audio Noise Radio Interference Due To Corona
	35	25-01-2024	Sat	Measurements Of Audio Noise Radio Interference Due To Corona
	36	27-01-2024	Mon	Properties Of Radio Noise
	37	01-02-2024	Thu	Frequency Spectrum Of RI Fields
	38	03-02-2024	Sat	Frequency Spectrum Of RI Fields
	39	08-02-2024	Fri	Measurements Of RI

	40	12-02-2024	Mon	Measurements Of RIV.
4	41	16-02-2024	Wed	Electro Static Field Electrostatic Field
	42	17-02-2024	Fri	Calculation Of Electrostatic Field Of EHV/AC Lines
	43	17-02-2024	Sat	Effect On Humans, Animals And Plants
	44	21-02-2024	Wed	Electrostatic Induction In Unenergised Circuit Of Double Circuit Line
	45	22-02-2024	Thu	Electromagnetic Interference
	46	23-02-2024	Fri	Electromagnetic Interference-Examples
	47	24-02-2024	Sat	Traveling Wave Expression
	48	26-02-2024	Mon	Traveling Wave Expression And Solution
	49	28-02-2024	Wed	Source Of Excitation
	50	29-02-2024	Thu	Terminal Conditions
	51	01-03-2024	Fri	Open Circuited And Short-Circuited End
	52	02-03-2024	Sat	Reflection And Refraction Coefficients
	53	04-03-2024	Mon	Lumped Parameters Of Distributed Lines
	54	06-03-2024	Wed	Generalized Constants-No Load Voltage Conditions
	55	08-03-2024	Thu	Generalized Constants
	56	08-03-2024	Fri	No Load Voltage Conditions And Charging Current.
5	57	11-03-2024	Mon	Voltage Control Power Circle Diagram And Its Use
	58	13-03-2024	Wed	Voltage Control Using Synchronous Condensers
	59	14-03-2024	Thu	Voltage Control Using Synchronous Condensers
	60	15-03-2024	Fri	Cascade Connection Of Shunt Compensation
	61	16-03-2024	Sat	Cascade Connection Of Series Compensation
	62	18-03-2024	Mon	Sub Synchronous Resonance In Series Capacitor
	63	20-03-2024	Wed	Compensated Lines
	64	25-03-2024	Mon	Static VAR Compensating System
	65	28-03-2024	Thu	Static VAR Compensating System
	66	30-03-2024	Sat	Static VAR Compensating System
	67	01-04-2024	Mon	Revision
	68	03-04-2024	Wed	Revision
	69	04-04-2024	Thu	Revision

Signature of faculty

Department of Electrical & Electronics Engineering

ASSIGNMENT – I

Answer all the questions. Each question carry equal marks **Total Marks=5**

Q.NO	Question	Course Outcome	Bloom's Level
UNIT- I			
1.	Explain power handling capacity and line losses of EHVAC Transmission?	CO 1	L3
2.	What are the mechanical consideration of EHVAC transmission system	CO 1	L3
UNIT- II			
3.	Explain field of sphere gap and What are the properties of field of line charges	CO 2	L3
4.	Describe in detail the potential relation for multi conductor.	CO 2	L4
UNIT- III			
5.	Write short notes on microphones and octave band audible noise measurement devices.	CO 3	L3

Signature of HOD

Date:

Signature of faculty

Date:

Department of Electrical & Electronics Engineering

ASSIGNMENT – II

Answer all the questions. Each question carry equal marks **Total Marks=5**

Q.NO	Question	Course Outcome	Bloom's Level
	UNIT- III		
1.	Discuss the lines for radio interference fields in EHV AC transmission line?	CO 3	L3
	UNIT- IV		
2.	Derive the expression for charging current and MVAR rating of EHV line?	CO 4	L4
3.	Explain the effect of electrostatic fields of EHV AC line on human, plants and animals	CO 4	L3
	UNIT- V		
4.	Write short notes on electrostatic induction on unenerged circuit on a double circuit line?	CO 5	L3
5.	Write a short notes on cascade connection of shunt and series compensation?	CO 5	L3

Signature of HOD

Date:

Signature of faculty

Date:

Department of Electrical & Electronics Engineering
TUTORIAL – 1

Q1. By increasing the transmission voltage double of its original value, the same power can be dispatched keeping the line loss,
a) Equal to its original value b) Half of original value
c) Double the original value d) One-forth of original value

Q2. Which of the following distribution systems is preferred for good efficiency and high economy
a) Single-phase, 2-wire system b) 2-ph, 3-wire system
c) 3-ph, 3-wire system d) 3-ph, 4-wire system

Q3. The highest transmission voltage used in India is
a) 400 kv b) 220 kv c) 132 kv d) 765 kv

Q4. With bundled conductors
a) The corona inception voltage increases
b) The corona inception voltage decreases
c) The corona inception voltage remain unaffected

Q5. HVDC Transmission Needs
a) Pulse converters b) Dc generators
c) Ac filters d) Dc filters

Q6. For power factor improvement static capacitors have the drawback of
a) Short-service life
b) Getting damaged by high voltage
c) Not repairable
d) All of the above

Q7. Static capacitors are rated in terms of
a) kVAR b) Kw c) kVA d) kWh

Q8. For a consumer the most economical power factor is usually
a) 0.25-0.5 lagging b) 0.25-0.5 leading c) 0.85-0.95 lagging d) 0.85-0.95 leading

Q9. Corona loss in a transmission line is dependent on
a) Diameter of a conductor
b) Material of the conductor
c) Height of the conductor

Q10. Extra high voltage transmission means
a) Voltage less than 400kv
b) Voltage in the range of 400-750kv
c) Voltage grater than 750

Q11. Corona is
a) Partial breakdown of air
b) Complete breakdown of air
c) Sparking between lines

Q12. The main reason for using high voltage for long distance power transmission is
a) Reduction in transmission losses b) Reduction in time of transmission
c) Increase in system reliability d) None of the above

Department of Electrical & Electronics Engineering

EVALUATION STRATEGY

Target (s)

a. Percentage of Pass : 95%

Assessment Method (s) (Maximum Marks for evaluation are defined in the Academic Regulations)

a. Daily Attendance
b. Assignments
c. Online Quiz (or) Seminars
d. Continuous Internal Assessment
e. Semester / End Examination

List out any new topic(s) or any innovation you would like to introduce in teaching the subjects in this semester

Case Study of any one existing application

Signature of HOD | Signature of faculty

Date: | Date:

Department of Electrical & Electronics Engineering

COURSE COMPLETION STATUS

Actual Date of Completion & Remarks if any

Units	Remarks	Objective No. Achieved	Outcome No. Achieved
Unit 1	completed on 16.12.2023	1	1
Unit 2	completed on 1.01.2024	2	2
Unit 3	completed on 12.02.2024	3	3
Unit 4	completed on 08.03.2024	4	4
Unit 5	completed on 04.04.2024	5	5

Signature of HOD

Date:

Signature of faculty

Date:

Department of Electrical & Electronics Engineering
Mappings

1. Course Objectives-Course Outcomes Relationship Matrix

(Indicate the relationships by mark "X")

Course-Outcomes / Course-Objectives	1	2	3	4	5
1	H		M		
2		H			M
3			H		
4		M		H	
5					H

2. Course Outcomes-Program Outcomes (POs) & PSOs Relationship Matrix

(Indicate the relationships by mark "X")

P-Outcomes / C-Outcomes	a	b	c	d	e	f	g	h	i	j	k	l	PSO 1	PSO 2
1		M			M		M				H	M	H	
2	M	H						M		H			H	H
3	H				H	M			H			M		M
4	M		M		M			H				H	M	
5		M	M					H				H		

Department of Electrical & Electronics Engineering
Rubric for Evaluation

Performance Criteria	Unsatisfactory	Developing	Satisfactory	Exemplary
	1	2	3	4
Research & Gather Information	Does not collect any information that relates to the topic	Collects very little information some relates to the topic	Collects some basic Information most relates to the topic	Collects a great deal of Information all relates to the topic
Fulfill team role's duty	Does not perform any duties of assigned team role.	Performs very little duties.	Performs nearly all duties.	Performs all duties of assigned team role.
Share Equally	Always relies on others to do the work.	Rarely does the assigned work - often needs reminding.	Usually does the assigned work - rarely needs reminding.	Always does the assigned work without having to be reminded
Listen to other team mates	Is always talking—never allows anyone else to speak.	Usually doing most of the talking-- rarely allows others to speak	Listens, but sometimes talks too much.	Listens and speaks a fair amount.

Department of Electrical & Electronics Engineering

ANURAG Engineering College

(An Autonomous Institution)

Ananthagiri (V&M), Suryapet (Dt), Telangana – 508206.

IV B.Tech II Semester I MID Examinations, Jan 2024

Branch: EEE		**Max. Marks: 20**
Date: 11-01-2024 AN	**Subject : EHVAC TRANSMISSION**	**Time: 90 Min.**

Instructions for preparing Question Paper:
1. **For Each Subject you have to prepare 3 SET'S of Question paper**
2. Text Font Style : Times New Roman
3. Text Font Size : 12
4. Questions Should Not be Repeated in any 3 Sets
5. Question Paper Saving File Name format : **Example** (IV-II-I-MID-Branch Name-Subject Name-SET-A)
6. If any Additional Property Like Graphs/Sign Table/Log Tables etc. The Faculty should inform Clearly in Question paper itself

PART-A

Answer all the questions **5 X 1M=5 Marks**

Q.NO	Question	Course Outcome	Bloom's Level
1.	What is necessity of EHVAC transmission?	CO1	L1
2.	What are the advantages of EHVAC transmission?	CO1	L1
3.	Write short notes on the field of line charges?	CO2	L1
4.	What are the properties of field of line charges?	CO2	L1
5.	What do you understand by audible noise on over head transmission lines?	CO3	L1

PART-B

Answer the following **3 X 5M=15 Marks**

Q.NO	Question	Course Outcome	Bloom's Level
6.	Explain power handling capacity and line losses of EHVAC Transmission?	CO1	L3
	OR		
7.	Discuss the convenience offered by using modes of propagation?	CO1	L3
8.	Obtain the maximum charge conditions on 3-phase EHV line?	CO2	L4
	OR		
9.	A point charge Q = 10–6 coulomb (1mC) is kept on the surface of a conducting sphere of radius r = 1 cm, which can be considered as a point charge located at the centre of the sphere. Calculate the field strength and potential at a distance of 0.5 cm from the surface of the sphere. Also find the capacitance of the sphere, e r . = 1	CO2	L3
10.	Write short notes on various formulae of corona power loss.	CO3	L3
	OR		
11.	Write short notes on microphones and octave band audible noise measurement devices.	CO3	L3

Department of Electrical & Electronics Engineering

ANURAG Engineering College

(An Autonomous Institution)

Ananthagiri (V&M), Suryapet (Dt), Telangana – 508206.

IV B.Tech II Semester I MID Examinations, Jan 2024

Branch: EEE		**Max. Marks: 20**
Date: 11-01-2024 AN	**Subject : EHVAC TRANSMISSION**	**Time: 90 Min.**

Instructions for preparing Question Paper:
1. **For Each Subject you have to prepare 3 SET'S of Question paper**
2.Text Font Style : Times New Roman
3. Text Font Size : 12
4. Questions Should Not be Repeated in any 3 Sets
5. Question Paper Saving File Name format : **Example** (IV-II-I-MID-Branch Name-Subject Name-SET-A)
6.If any Additional Property Like Graphs/Sign Table/Log Tables etc. The Faculty should inform Clearly in Question paper itself

PART-A

Answer all the questions **5 X 1M=5 Marks**

Q.NO	Question	Course Outcome	Bloom's Level
1.	What are disadvantages of EHVAC transmission line?	CO1	L1
2.	Write properties of bundle conductor?	CO1	L1
3.	What is surface voltage gradient?	CO2	L1
4.	Write short nots on field of line charges?	CO2	L1
5.	What are the factors effecting the corona loss?	CO3	L1

PART-B

Answer the following **3 X 5M=15 Marks**

Q.NO	Question	Course Outcome	Bloom's Level
6.	Discuss the convenience offered by using modes of propagation?	CO1	L3
	OR		
7.	What are the mechanical consideration of EHVAC transmission system	CO1	L3
8.	Explain the field of line charges and their properties?	CO2	L3
	OR		
9.	Explain in detail the potential relation for multi conductor.	CO2	L3
10.	Explain the generation and characteristics of audio noise due to corona in EHV lines?	CO3	L3
	OR		
11.	Describe the charge voltage diagram and corona loss?	CO3	L4

Department of Electrical & Electronics Engineering

ANURAG Engineering College

(An Autonomous Institution)

Ananthagiri (V&M), Suryapet (Dt), Telangana – 508206.

IV B.Tech II Semester I MID Examinations, Jan 2024

Branch: EEE		Max. Marks: 20
Date: 11-01-2024 AN	Subject : EHVAC TRANSMISSION	Time: 90 Min.

Instructions for preparing Question Paper:
1. **For Each Subject you have to prepare 3 SET'S of Question paper**
2. Text Font Style : Times New Roman
3. Text Font Size : 12
4. Questions Should Not be Repeated in any 3 Sets
5. Question Paper Saving File Name format : **Example** (IV-II-I-MID-Branch Name-Subject Name-SET-A)
6. If any Additional Property Like Graphs/Sign Table/Log Tables etc. The Faculty should inform Clearly in Question paper itself

PART-A

Answer all the questions **5 X 1M=5 Marks**

Q.NO	Question	Course Outcome	Bloom's Level
1.	What are the properties of bundle conductor?	CO1	L1
2.	Write expression for power handling capacity and line losses for EHV AC transmission line	CO1	L1
3.	Write short notes on electric potential?	CO2	L1
4.	What is the need of bundle conductor in EHV transmission line?	CO2	L1
5.	How can measure the audible noise(AN) in EHVAC transmission line	CO3	L1

PART-B

Answer the following **3 X 5M=15 Marks**

Q.NO	Question	Course Outcome	Bloom's Level
6.	The configurations of some e.h.v. lines for 400 kV to 1200 kV are given. Calculate r_{eq} for each. (a) 400 kV : N = 2, d = 2r = 3.18 cm, B = 45 cm (b) 750 kV : N = 4, d = 3.46 cm, B = 45 cm (c) 1000 kV : N = 6, d = 4.6 cm, B = 12 d (d) 1200 kV : N = 8, d = 4.6 cm, R = 0.6 m	CO1	L4
	OR		
7.	Explain power handling capacity and line losses of EHVAC Transmission?	CO1	L3
8.	Explain in detail the potential relation for multi conductor. Drive the necessary equations?	CO2	L3
	OR		
9.	Explain field of sphere gap and What are the properties of field of line charges	CO2	L3
10.	Explain attenuation of travelling waves due to corona.	CO3	L3
	OR		
11.	What is corona ? Discuss the factors effecting corona loss	CO3	L3

Department of Electrical & Electronics Engineering

ANURAG Engineering College

(An Autonomous Institution)

Ananthagiri (V&M), Suryapet (Dt), Telangana – 508206.

IV B.Tech II Semester II MID Examinations, April 2024

Branch: EEE		**Max. Marks: 20**
Date: 08-04-2024 AN	**Subject : EHVAC TRANSMISSION**	**Time: 90 Min.**

Instructions for preparing Question Paper:
1. **For Each Subject you have to prepare 3 SET'S of Question paper**
2.Text Font Style : Times New Roman
3. Text Font Size : 12
4. Questions Should Not be Repeated in any 3 Sets
5. Question Paper Saving File Name format : **Example** (IV-II-I-MID-Branch Name-Subject Name-SET-A)
6.If any Additional Property Like Graphs/Sign Table/Log Tables etc. The Faculty should inform Clearly in Question paper itself

PART-A

Answer all the questions **5 X 1M=5 Marks**

Q.NO	Question	Course Outcome	Bloom's Level
1.	What are the factors to be considered to minimize the corona in transmission line?	CO3	L1
2.	What is reflection and refraction of travelling waves?	CO4	L1
3.	What you mean by travelling waves?	CO4	L1
4.	Define term compensation?	CO5	L1
5.	What is sub synchronous resonance in series capacitor in EHV line?	CO5	L1

PART-B

Answer the following **3 X 5M=15 Marks**

Q.NO	Question	Course Outcome	Bloom's Level
6.	Describe the charge voltage diagram and corona loss?	CO3	L3
	OR		
7.	Explain the procedure of measuring radio interference voltage (RIV) with the help of a Radio noise meter?	CO3	L3
8.	Derive the expression for charging current and MVAR rating of EHVAC lines?	CO4	L4
	OR		
9.	Explain the effects of electrostatic fields of EHVAC line on human, plants and animals?	CO4	L3
10.	Explain static VAR compensators for reactive power control in EHVAC systems?	CO5	L4
	OR		
11.	Explain the shunt series compensation techniques used for voltage control ?	CO5	L3

Department of Electrical & Electronics Engineering

ANURAG Engineering College

(An Autonomous Institution)

Ananthagiri (V&M), Suryapet (Dt), Telangana – 508206.

IV B.Tech II Semester II MID Examinations, April 2024

Branch: EEE		**Max. Marks: 20**
Date: 08-04-2024 AN	**Subject : EHVAC TRANSMISSION**	**Time: 90 Min.**

Instructions for preparing Question Paper:
1. **For Each Subject you have to prepare 3 SET'S of Question paper**
2.Text Font Style : Times New Roman
3. Text Font Size : 12
4. Questions Should Not be Repeated in any 3 Sets
5. Question Paper Saving File Name format : **Example** (IV-II-I-MID-Branch Name-Subject Name-SET-A)
6.If any Additional Property Like Graphs/Sign Table/Log Tables etc. The Faculty should inform Clearly in Question paper itself

PART-A

Answer all the questions **5 X 1M=5 Marks**

Q.NO	Question	Course Outcome	Bloom's Level
1.	What is the purpose of Radio noise meter	CO3	L1
2.	What is the effects of light load conditions?	CO4	L1
3.	What are the effects of high electrostatic fields on biological organism and human beings?	CO4	L1
4.	What is the use of power circle diagram?	CO5	L1
5.	How can we achieve voltage control by using by using static VAR compensation?	CO5	L1

PART-B

Answer the following **3 X 5M=15 Marks**

Q.NO	Question	Course Outcome	Bloom's Level
6.	Describe the mechanism of formation of pulse train from positive polarity conductor?	CO3	L3
	OR		
7.	Explain the procedure of measuring radio interference voltage (RIV) with the help of a Radio noise meter	CO3	L4
8.	Explain the procedure to calculate the electrostatic field of a single circuit 3- phase AC line is computed?	CO4	L4
	OR		
9.	Explain electrostatic induction on energized circuit of a double circuit line?	CO4	L3
10.	What is sub synchronous resonance in the steady state and transient conditions in series – capacitor compensated lines?	CO5	L4
	OR		
11.	Explain various static VAR compensators for reactive power control in EHVAC systems?	CO5	L4

Department of Electrical & Electronics Engineering

ANURAG Engineering College

(An Autonomous Institution)

Ananthagiri (V&M), Suryapet (Dt), Telangana – 508206.

IV B.Tech II Semester II MID Examinations, April 2024

Branch: EEE		**Max. Marks: 20**
Date: 08-04-2024 AN	**Subject : EHVAC TRANSMISSION**	**Time: 90 Min.**

Instructions for preparing Question Paper:

1. **For Each Subject you have to prepare 3 SET'S of Question paper**
2. Text Font Style : Times New Roman
3. Text Font Size : 12
4. Questions Should Not be Repeated in any 3 Sets
5. Question Paper Saving File Name format : **Example** (IV-II-I-MID-Branch Name-Subject Name-SET-A)
6. If any Additional Property Like Graphs/Sign Table/Log Tables etc. The Faculty should inform Clearly in Question paper itself

PART-A

Answer all the questions **5 X 1M=5 Marks**

Q.NO	Question	Course Outcome	Bloom's Level
1.	How can measure the audible noise(AN) in EHVAC transmission line?	CO3	L1
2.	State the lumped parameter?	CO4	L1
3.	What is the necessity of double conductor?	CO4	L1
4.	Write advantages of static VAR compensator?	CO5	L1
5.	Differentiate between shunt and series compensation?	CO5	L1

PART-B

Answer the following **3 X 5M=15 Marks**

Q.NO	Question	Course Outcome	Bloom's Level
6.	Describe the mechanism of formation of pulse train from positive polarity conductor?	CO3	L3
	OR		
7.	Illustrate the frequency spectrum of RI fields and explain the measurements of RI and RIV?	CO3	L3
8.	Explain electrostatic induction on energized circuit of a double circuit line?	CO4	L4
	OR		
9.	Explain the effects of electrostatic fields of EHVAC line on human, plants and animals ?	CO4	L3
10.	Write a short notes on cascade connection of shunt and series compensation?	CO5	L3
	OR		
11.	What is the reasons for the existence of sub synchronous resonance in the steady state and transient conditions in series – capacitor compensated lines?	CO5	L4

Department of Electrical & Electronics Engineering

First Internal Examination Marks

Programme **: B Tech** Year: **IV** Course: **Theory** **A.Y: 2023-24**

Course: EHVACT Section: A Faculty Name: BOILLA SRINU

S. No	Roll No	Assignment/Objective Marks (5)	Subjective Marks (20)	Total Marks (25)
1	19C11A0201	5	13	18
2	20C11A0201	5	19	24
3	20C11A0202	5	18	23
4	20C11A0203	5	18	23
5	20C11A0204	5	11	16
6	20C11A0205	5	14	19
7	20C11A0206	5	AB	0
8	20C11A0207	5	12	17
9	20C11A0208	5	11	16
10	20C11A0209	5	10	15
11	20C11A0210	5	19	24
12	20C11A0211	5	18	23
13	20C11A0212	5	20	25

14	20C11A0214	5	AB	0
15	20C11A0215	5	18	23
16	20C11A0216	5	AB	0
17	20C11A0217	5	18	23
18	20C11A0218	5	19	24
19	20C11A0219	5	13	18
20	20C11A0220	5	19	24
21	20C11A0221	5	8	13
22	21C15A0201	5	19	24
23	21C15A0202	5	18	23
24	21C15A0203	5	9	14
25	21C15A0204	5	14	19
26	21C15A0205	5	20	25
27	21C15A0206	5	9	14
28	21C15A0207	5	20	25
29	21C15A0208	5	17	22
30	21C15A0209	5	15	20

31	21C15A0210	5	16	21
32	21C15A0211	5	14	19
33	21C15A0212	5	17	22
34	21C15A0213	5	18	23
35	21C15A0214	5	20	25
36	21C15A0215	5	18	23
37	21C15A0216	5	13	18
38	21C15A0217	5	12	17
39	21C15A0218	5	12	17
40	21C15A0219	5	20	25
41	21C15A0220	5	17	22
42	21C15A0221	5	14	19
43	21C15A0222	5	19	24
44	21C15A0223	5	20	25
45	21C15A0224	5	12	17
46	21C15A0225	5	12	17
47	21C15A0226	5	16	21

48	21C15A0227	5	19	24
49	21C15A0228	5	20	25
50	21C15A0229	5	12	17
51	21C15A0230	5	18	23
52	21C15A0231	5	20	25
53	21C15A0232	5	14	19
54	21C15A0233	5	18	23
55	21C15A0234	5	17	22
56	21C15A0235	5	16	21
57	21C15A0236	5	10	15
58	21C15A0237	5	15	20
59	21C15A0238	5	12	17

No. of Absentees: **03**

Total Strength: **56**

Signature of Faculty

: **Signature of HoD**

Department of Electrical & Electronics Engineering
Second Internal Examination Marks

Programme **: B Tech** Year: **IV** Course: **Theory** **A.Y: 2023-24**

Course: EHVACT Section: A Faculty Name: BOILLA SRINU

S. No	Roll No	Assignment/Objective Marks (5)	Subjective Marks (20)	Total Marks (25)
1	19C11A0201	5	17	22
2	20C11A0201	5	13	18
3	20C11A0202	5	17	22
4	20C11A0203	5	19	24
5	20C11A0204	5	9	14
6	20C11A0205	5	10	15
7	20C11A0206	AB	AB	0
8	20C11A0207	5	11	16
9	20C11A0208	5	10	15
10	20C11A0209	5	8	13
11	20C11A0210	5	14	19
12	20C11A0211	5	12	17
13	20C11A0212	5	19	24
14	20C11A0214	AB	AB	0

15	20C11A0215	5	14	19
16	20C11A0216	AB	AB	0
17	20C11A0217	5	12	17
18	20C11A0218	5	17	22
19	20C11A0219	5	19	24
20	20C11A0220	5	11	16
21	20C11A0221	5	10	15
22	21C15A0201	5	20	25
23	21C15A0202	5	20	25
24	21C15A0203	5	14	19
25	21C15A0204	5	11	16
26	21C15A0205	5	17	22
27	21C15A0206	5	11	16
28	21C15A0207	5	20	25
29	21C15A0208	5	16	21
30	21C15A0209	5	11	16
31	21C15A0210	5	12	17
32	21C15A0211	5	10	15

33	21C15A0212	5	13	18
34	21C15A0213	5	12	17
35	21C15A0214	5	13	18
36	21C15A0215	5	11	16
37	21C15A0216	5	13	18
38	21C15A0217	5	11	16
39	21C15A0218	5	13	18
40	21C15A0219	5	20	25
41	21C15A0220	5	16	21
42	21C15A0221	5	7	12
43	21C15A0222	5	20	25
44	21C15A0223	5	11	16
45	21C15A0224	5	9	14
46	21C15A0225	5	8	13
47	21C15A0226	5	4	9
48	21C15A0227	5	20	25
49	21C15A0228	5	16	21
50	21C15A0229	5	13	18

51	21C15A0230	5	12	17
52	21C15A0231	5	17	22
53	21C15A0232	5	10	15
54	21C15A0233	5	11	16
55	21C15A0234	5	12	17
56	21C15A0235	5	18	23
57	21C15A0236	5	11	16
58	21C15A0237	5	9	14
59	21C15A0238	5	10	15

No. of Absentees: **03**

Total Strength: **59**

Signature of Faculty

Signature of HoD

EXTRA HIGH VOLTAGE AC TRANSMISSION

Y. Bhavana
21C15D0201

ASSIGNMENT - II

25/25
5

BSN

1 Discuss the limits for radio interference fields in EHVAC transmission lines and also give short notes on measurement of RI and RIV

LIMITS FOR RADIO INTERFERENCE FIELDS:

Radio Interference (RI) resulting from a transmission line is a man-made phenomenon.

Interference to communication systems is described through signal-to-Noise Ratio designated as S/N Ratio, with both quantities, measured on the same weighting circuit of a suitable standard meter.

However, it has been the practice to designate the signal from a broadcast station in terms of the average signal strength called the Field Intensity (FI) setting of the field-strength metre, while the interface signal to a radio receiver due to line noise is measured on the Quasi-Peak (QP) detector circuit. The difference in weighting circuits will be will be known. There are proposals to change this custom and have both signal and noise measured on the same weighting circuit.

It is the duty or responsibility of a designer to keep noise level from a line below a limiting value at the edge of the right-of-way (ROW) of the line corridor. The value to be used for this RI limit is causing considerable discussion and we shall describe two points of view currently used in the world. Some countries, particularly in Europe, have set definite limits for the RI field from power lines, while in North America only the minimum acceptable S/N ratio at the receiver location has been recommended.

In North America the following practise is adopted in the U.S.A and Canada.

U.S.A recommended practice is to guarantee a minimum S/N ratio of 24dB at the receiver for broadcast signals having a minimum strength of 54dB at the receiver.

Canada for satisfactory reception, a S/N ratio of 22dB or better must be provided in fair weather in suburban regions for stations with a mean signal strength of 54dB (500 μV/m). In urban regions, this limit to can be increased by 10dB, and in rural areas lowered by 3dB.

Based on these two points of view, namely.

1. setting a definite RI limit. and
2. providing a minimum S/N ratio at the receiver, the procedures required line design will be different.

RI Limits in Various countries of the World (Loop Antenna):

Country	Distance from Line	RI Limit	Frequency	Remarks
1 Switzerland	20m from outermost phase	800 μV/m (46dB above 1μV/m)	500 kHz	Dry weather 10°c
2. Poland	20m from outerphase	750 μV/m (57.5dB)	500kHz ±10kHz	Air humidity< 80%. Temp. 5°c
3. Czechoslovakia	voltage kV / Distance from line centre: 220 – 50m; 400 – 55m; 750 – 70m	40dB	500kHz	Air humidity=90% Dry weather.
4. CIS	100m from outerphase	40dB	500 kHz	For 80% of the year limit should not be exceeded.

Station strengths and allowable noise at the station frequencies:

Frequency of station	0.5	0.8	1	1.1	1.3	1.52	mHz
Received signal strength	55	60	50	75	57	52	dB
Allowable Noise Level (signal strength -24dB)	31	36	26	51	33	28	dB

For the station broadcasting at 0.5mHz, the recommended minimum S/N ratio of 24dB cannot be guaranteed. The situation is represented pictorially in figure.

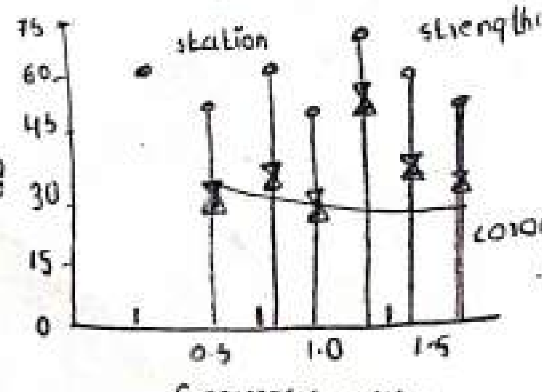

Fig. station signal strength(.), -24dB (x), & corona noise (-). Illustrating basis for design based upon minimum S/N ratio of 24 dB

(x(station strength -24dB))

Measurement of RI & RIV:

The interface of AM broadcast in the frequency range 0.5 MHz to 1.6 MHz is measured in terms of 3 quantities: Radio Interference Field Intensity (RIFI or RI), the Radio Influence Voltage (RIV), and more recently through the Excitation function. The units are μV/m, μV, and μA/√m or the decibel values above their reference values of 1 unit (μV/m, μV, μA/√m). A block diagram of radio noise meter is shown.

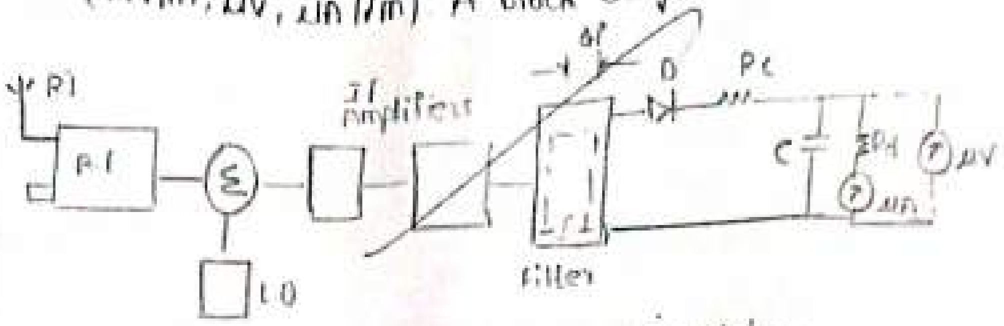

Fig: Block diagram of Radio Noise Meter.

For radiated interference measurement RI, the front end of the meter is fitted with either a rod antenna of 0.5 to 2 m in length or a loop antenna of this size of side. For conducted measurement, the interfering voltage RIV is fed through a jack. The input impedance of the meter is 50 ohms.

The following formulas due to Nigol apply to the various settings of the noise meter for repetitive pulses:

Peak value: $V_p = \sqrt{2} \cdot A \cdot \tau \, \Delta f$

Quasi Peak: $V_{qp} = k V_p$

Average: $V_{av} = \sqrt{2} \cdot A \cdot \tau \cdot f_0$

R.m.s value: $V_{rms} = \sqrt{2} \cdot A \cdot \tau \cdot \sqrt{f_0 \cdot \Delta f}$

Where, A - amplitude of repetitive pulses,

τ = pulse duration,

Δf = bandwidth of meter,

f_0 = repetition frequency of pulses, $< \Delta f$,

k = a constant = 0.9 - 0.95.

Relations can be found among these four quantities if necessary.

Conducted RIV is measured by a circuit shown.

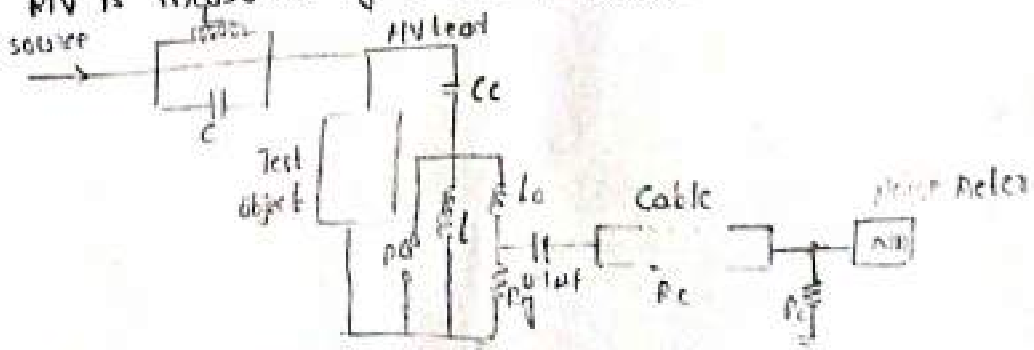

Fig: Circuit for measuring radio influence voltage (RIV)

The object under test, which could be an insulator string with guard is energized by a high voltage source at power frequency or impulse. A fi interposed such that any r-f energy produced by partial discharge in the te object is prevented from flowing into the source & all r-f energy goes to the measuring circuit. The value of L is chosen such that the voltage drop is not more than 5 volts so that the measuring equipment does not experience a high power-frequency voltage.

Let v - applied power frequency voltage from line to ground,

V_L - voltage across L,

X_C - reactance of coupling capacitor.

$X_L = 2\pi f L$ = reactance of inductor.

Then, $V_L = V \cdot X_L / (X_C - X_L) \approx V X_L / X_C = 4\pi^2 f^2 L C_c \cdot V$.

2. Derive the expression for charging current and MVAR rating of EHV line.

No-Load Voltage conditions & Charging current,

When there is no-load at the receiving end, $I_r = 0$, the control of voltage at line ends poses certain problems due to overvoltage conditions. Unlike dc lines, ac lines have the shunt charging current flowing through the series inductance of line causing a rise in the output voltage at the receiving end. This is the well-known Ferranti Effect".

By proper voltage division, the source voltage will be

$E_s = (1/j\omega c + j\omega L) E_r / (1/j\omega c) = (1 - \omega^2 L C) E_r$.

E_s is less than E_r and in phase with it.

In a distributed-parameter line, neglecting series resistance for understanding the phenomenon, at no load

$$E_s = (\cosh j\omega L / v_0) E_r = E_r \cdot \cos(\omega L / v_0) = E_r \cdot \cos(2\pi L / \lambda)$$

Charging current and MVAR:

The current supplied by the source into the line at no load ($I_r = 0$) is, from

$E_s = A E_r + B I_r$ & $I_s = C E_r + D I_r$

$I_s = C E_r = \frac{1}{Z_0} \sinh pL \cdot E_r$.

When resistance is neglected,

$Z_{00} = \sqrt{l/c}$ and $p = j\omega / v_0 = j2\pi / \lambda$

$\therefore I_s = j \sqrt{\frac{c}{l}} \sin(\omega L / v_0) \cdot E_r = j E_r \cdot \sqrt{\frac{c}{l}} \sin(2\pi L / \lambda)$.

It leads the receiving end voltage by 90°. An effective capacitance for the distributed lines connected across the receiving end voltage E_r, and drawing the same current has the value

$$C_0 = \frac{1}{\omega Z_0} \sin(2\pi L/\lambda), \text{ farad.}$$

The corresponding charging reactive power supplied by the source per phase will be

$$Q_0 = E_s \cdot I_0 = E_s \cdot E_r \sqrt{\frac{c}{l}} \cdot \sin(2\pi L/\lambda).$$

If E_r & E_s are line-to line voltages in kV, rms then Q_0 will be the 3-phase charging MVAR. Also,

$$Q_0 = E_s^2 \cdot \sqrt{\frac{c}{l}} \tan(2\pi L/\lambda), \text{ since } E_r = E_s / \cos(2\pi L/\lambda).$$

Note that for a resistanceless line, when $L = \lambda/2$, there is no charging current, and furthermore, $E_r = -E_s$.

3. Explain the effect of electrostatic fields of EHVAC line on human, plants and animals.

Effect of High Electrostatic Field on Human, Animals and Plants:

The use of ehv lines is increasing danger of the high e.s field to (a) human beings, (b) animals, (c) plant life, (d) vehicles, (e) fences, and (f) buried pipe lines under and near these lines. A case-by-case study must be made if great accuracy is needed to observe the effect of the distortion field.

a. Human Beings:

The effect of high e.s field on human beings has been studied to a much greater extent than on any other animals or objects because of its grave and shocking effects which has resulted in loss of life. It has been ascertained experimentally that the limit for the undistributed field is 15 kV/m, rms. for human beings to experience possible shock. An e.h.v or u.h.v. line must be designed such that this limit is not exceeded.

b. Animals:

Experiments carried out in cages under ehv lines have shown that pigeons & hens are affected by e.s field at about 30 kV/m. They are unable to pick up grain because of the chattering of their beaks which will affect their growth. Other animals get a charge on their bodies and when they proceed to a water trough to drink water, a spark usually jump from their nose to grounded pipe or trough.

c. Plant Life:

Plants such as wheat, rice, sugarcane, etc., suffer the following types of damage. At a field strength of 20 kV/m (rms), the sharp edges of the stalk give corona discharges so that damage occurs to the upper portion of the grain-bearing pools.

d. Vehicles:

vehicles parked under a line or driving through acquire electrostatic charge, their tyres are made of insulating material. If parking lots are located under a line the minimum recommended safe clearance is 17m for 345kV and 20m for 400kV lines. Trucks and lorries will require an extra 3m clearance. The danger lies in a human being attempting to open the door and getting a shock thereby.

e. Others

fences, buried cables, and pipe lines are important pieces of equipment to require careful layout. Metallic fences parallel to a line must be grounded preferably every 75m. Pipelines longer than 2km and larger than 15cm in diameter are recommended to be buried at least 30m laterally from the line centre to avoid dangerous eddy currents that could cause corrosion.

4. Write short note on electrostatic induction on unenergized circuit of D/C Line.

Electrostatic Induction on Unenergized circuit of D/c Line:

This is a very specialized topic useful for line crew, telephone line interference etc, and control the EHV lines must be provided with wide range enough right-of-way so that other low-voltage lines are located far enough as when they cross, the crossing must be at right angles.

Consider fig. in which a double-circuit line configuration is shown with 3 conductors energized by a 3-phase system of voltages $V_1 = V_m \sin\omega t$, $V_2 = V_m\sin(\omega t - 120^\circ)$, $V_3 = V_m \sin(\omega t + 120^\circ)$. The other circuit consisting of conductors 4, 5 & 6 is not energized.

We will calculate the voltage on these conductors due to electrostatic induction which a line-man may experience.

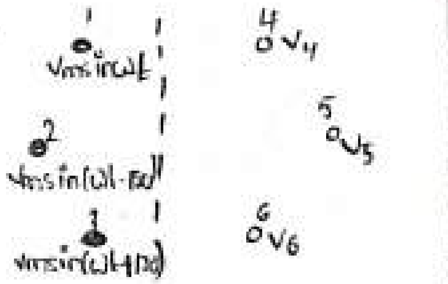

fig: D/c line: one line energized & the other unenergized to illustrate induction

Now,
$$V_4 = \frac{q_1}{2\pi\epsilon_0}\ln(I_{14}/A_{14}) + \frac{q_2}{2\pi\epsilon_0}\ln(I_{24}/A_{24}) + \frac{q_3}{2\pi\epsilon_0}\ln(I_{34}/A_{34})$$
$$V_4 = \frac{q_1}{2\pi\epsilon_0}P_{14} + \frac{q_2}{2\pi\epsilon_0}P_{24} + \frac{q_3}{2\pi\epsilon_0}P_{34}$$

The charge coefficients q_1, q_2, q_3 are obtained from the applied voltages.
$$\begin{bmatrix} V_1 \\ V_2 \\ V_3 \end{bmatrix} = \begin{bmatrix} P_{11} & P_{12} & P_{13} \\ P_{21} & P_{22} & P_{23} \\ P_{31} & P_{32} & P_{33} \end{bmatrix} \begin{bmatrix} q_1 \\ q_2 \\ q_3 \end{bmatrix} (1/2\pi\epsilon_0) = [P][q](1/2\pi\epsilon_0)$$

so that $(q/2\pi\epsilon_0) = [m][V]$

$$V_4 = V_m P_{14}[m_{11}\sin\omega t + m_{12}\sin(\omega t-120) + m_{13}\sin(\omega t+120)] + V_m P_{24}[m_{21}\sin\omega t + m_{22}\sin(\omega t-120) + m_{23}\sin(\omega t+120)] + P_{34}[m_{31}\sin\omega t + m_{32}\sin(\omega t-120) + m_{33}\sin(\omega t+120)]$$

$$V_4 = V_m[(P_{14}m_{11} + P_{24}m_{21} + P_{34}m_{31})\sin\omega t + (P_{14}m_{12} + P_{24}m_{22} + P_{34}m_{32})\sin(\omega t-120) + (P_{14}m_{13} + P_{24}m_{23} + P_{34}m_{33})\sin(\omega t+120)]$$

$$V_4 = V_m\left[\lambda_1 \sin\omega t + \lambda_2 \sin(\omega t - 120^\circ) + \lambda_3 \sin(\omega t + 120^\circ)\right]$$

In phasor form, $V_4 = V[\lambda_1 \angle 0^\circ + \lambda_2 \angle -120^\circ + \lambda_3 \angle +120^\circ]$, r.m.s.

$$V_4 = V(\lambda_1^2 + \lambda_2^2 + \lambda_3^2 - \lambda_1\lambda_2 - \lambda_2\lambda_3 - \lambda_3\lambda_1)^{1/2}$$

similarly, $V_5 = V[\lambda_4^2 + \lambda_5^2 + \lambda_6^2 - \lambda_4\lambda_5 - \lambda_5\lambda_6 - \lambda_6\lambda_4]^{1/2}$ &

$$V_6 = V[\lambda_7^2 + \lambda_8^2 + \lambda_9^2 - \lambda_7\lambda_8 - \lambda_8\lambda_9 - \lambda_9\lambda_7]^{1/2}$$

where $\lambda_1 = P_{14}m_{11} + P_{24}m_{21} + P_{34}m_{31}$; $\lambda_2 = P_{14}m_{12} + P_{24}m_{22} + P_{34}m_{32}$; $\lambda_3 = P_{14}m_{13} + P_{24}m_{23} + P_{34}m_{33}$

$\lambda_4 = P_{15}m_{11} + P_{25}m_{21} + P_{35}m_{31}$; $\lambda_5 = P_{15}m_{12} + P_{25}m_{22} + P_{35}m_{32}$; $\lambda_6 = P_{15}m_{13} + P_{25}m_{23} + P_{35}m_{33}$;

$\lambda_7 = P_{16}m_{11} + P_{26}m_{21} + P_{36}m_{31}$; $\lambda_8 = P_{16}m_{12} + P_{26}m_{22} + P_{36}m_{32}$; $\lambda_9 = P_{16}m_{13} + P_{26}m_{23} + P_{36}m_{33}$

6. Write short note on cascade connection of shunt & series compensation.

Cascade connection of components - shunt and series compensation:

In practice, shunt compensation reactors are provided for no-load conditions which are controlled by the line-charging current entirely, and by switched capacitors for full load conditions when the load has a lagging power factor.

Generalized Equations:

For no-load conditions, $Z_L = \infty$, and the equations for sending end & receiving end voltages are

$$E_r = E_s / [\cosh pL + (Z_0/Z_{sh})\sinh pL]$$

For simplicity, let $r = 0$. Then,

$$p = j\omega / v_0 = j\omega/\lambda,\ Z_0 = Z_{00} = \sqrt{L/C},\ Z_{sh} = jX_{sh},$$

so that $E_s/E_r = \cos 2\pi L/\lambda + (Z_{00}/X_{sh})\sin 2\pi L/\lambda$.

When the ratio E_s/E_r is given for a system, the value of X_{sh} is easily determined.

In particular, when $E_s = E_r$,

$$Z_{sh} = Z_{00}/(\operatorname{cosec} 2\pi L/\lambda - \cot 2\pi L/\lambda).$$

Chain Rule:

For the reactor only, the generalized constants are given by,

$$\begin{bmatrix} E_s \\ I_s \end{bmatrix} = \begin{bmatrix} 1 & 0 \\ -jB_{sh} & 1 \end{bmatrix}\begin{bmatrix} E_s' \\ I_s' \end{bmatrix}$$

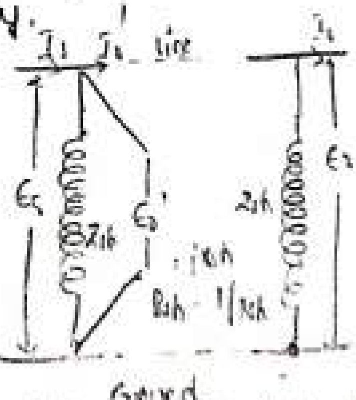

Fig: Transmission line with shunt reactor compensation for voltage control at no-load

Where $B_{sh} = 1/X_{sh}$ = admittance of each reactor per phase. If (E_s, I_s) refer to the input voltage and current from the source and (E_r, I_r) the output quantities at the load end, then the generalized constants (A_T, B_T, C_T, D_T) for the entire system is obtained by chain multiplication of three matrices for the cascade-connected components.

This is
$$\begin{bmatrix} A_T & B_T \\ C_T & D_T \end{bmatrix} = \begin{bmatrix} 1 & 0 \\ -jB_{sh} & 1 \end{bmatrix}\begin{bmatrix} A & B \\ C & D \end{bmatrix}_{Line}\begin{bmatrix} 1 & 0 \\ -jB_{sh} & 1 \end{bmatrix} = \begin{bmatrix} A & B \\ C & D \end{bmatrix}_{Line} - jB_{sh}\begin{bmatrix} B & 0 \\ 2A - jB_{sh}B & B \end{bmatrix}$$

The main requirement for the shunt reactors is control of voltage at no-load. For this case,

$$E_s = A_T E_r = (A - jB_{sh}B)E_r$$

$$B_{sh} = (A - E_s/E_r)/jB = j(E_s/E_r - A)/B$$

Shunt reactor compensation of very long line with intermediate switching station:

For very long lines, longer than 400km at 400kV, or at higher voltages, an intermediate station is sometimes preferable in lieu of series-capacitor compensation. Fig shows the arrangement where the line section has the generalized constants (A, B, C, D)

$$\begin{pmatrix} A_T & B_T \\ C_T & D_T \end{pmatrix} = \begin{bmatrix} A - jB_{in}B & B \\ C - j2B_{in}A - B_{in}^2B & D - jB_{in}B \end{bmatrix}^2$$

$$= \begin{bmatrix} A^2+BC & 2AB \\ 2AC & A^2+BC \end{bmatrix} - B_{in}^2 B \begin{bmatrix} 2B & 0 \\ 6A & 2B \end{bmatrix}$$

$$- jB_{in} \begin{bmatrix} 4AB & B^2 \\ 2(2A^2+2B_{in}^2B) & 4AB \end{bmatrix}$$

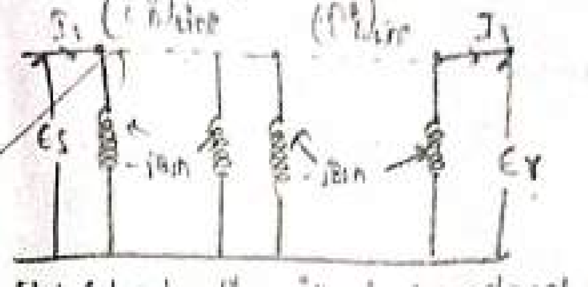

Fig: Extra-long line with shunt reactors at ends & at an intermediate station.

For $B_{in}=0$, this reduces to

$$\begin{pmatrix} A_T & B_T \\ C_T & D_T \end{pmatrix}_{B_{in}=0} = \begin{bmatrix} A^2+BC & 2AB \\ 2AC & A^2+BC \end{bmatrix} = \begin{pmatrix} A & B \\ C & D \end{pmatrix}^2$$

The voltage & current at the intermediate station are

$$\begin{bmatrix} E_i' \\ I_i' \end{bmatrix} = \begin{bmatrix} A - jB_{in}B & B \\ C - j2AB_{in} - B_{in}^2B & D - jB_{in}B \end{bmatrix} \begin{bmatrix} E_r \\ I_r \end{bmatrix}$$

Series-capacitor compensation at line center:

For each half of the line section of length $L/2$,

$$A' = D' = \cosh\sqrt{ZY}/4, \quad B' = Z_0 \sinh\sqrt{ZY}/4,$$

$$C' = \frac{1}{Z_0}\sinh\sqrt{ZY}/4$$

Where Z & Y refer to total line of length L.

For the series capacitor, voltages & currents

$$\begin{bmatrix} E_c' \\ I_c' \end{bmatrix} = \begin{bmatrix} 1 & -jX_c \\ 0 & 1 \end{bmatrix} \begin{bmatrix} E_r' \\ I_r' \end{bmatrix}$$

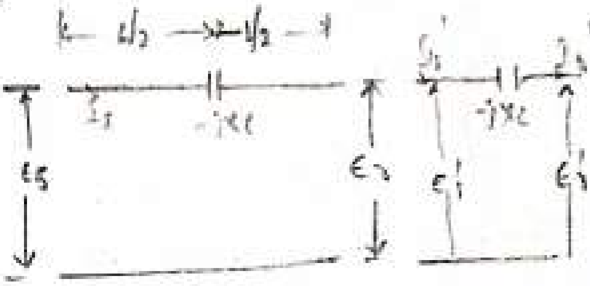

Fig: Transmission line with series-capacitor compensation in middle of line.

By the chain rule of multiplication:

$$\begin{pmatrix} A_T, & B_T \\ C_T, & D_T \end{pmatrix} = \begin{bmatrix} \cosh\sqrt{ZY}/4, & Z_0\sinh\sqrt{ZY}/4 \\ \frac{1}{Z_0}\sinh\sqrt{ZY}/4, & \cosh\sqrt{ZY}/4 \end{bmatrix} \begin{bmatrix} 1 & -jX_c \\ 0 & 1 \end{bmatrix} \times \begin{bmatrix} \cosh\sqrt{ZY}/4, & Z_0\sinh\sqrt{ZY}/4 \\ \frac{1}{Z_0}\sinh\sqrt{ZY}/4, & \cosh\sqrt{ZY}/4 \end{bmatrix}.$$

$$\begin{pmatrix} A_T, & B_T \\ C_T, & D_T \end{pmatrix} = \begin{bmatrix} \cosh\sqrt{ZY}, & Z_0\sinh\sqrt{ZY} \\ \frac{1}{Z_0}\sinh\sqrt{ZY}, & \cosh\sqrt{ZY} \end{bmatrix} - j\frac{X_c}{2Z_0} \begin{bmatrix} \sinh\sqrt{ZY}, & Z_0(\cosh\sqrt{ZY}+1) \\ \frac{1}{Z_0}(\cosh\sqrt{ZY}-1), & \sinh\sqrt{ZY} \end{bmatrix}$$

$$\begin{pmatrix} A_T, & B_T \\ C_T, & D_T \end{pmatrix} = \begin{bmatrix} A & B \\ C & D \end{bmatrix}_{Line} - j\frac{X_C}{2Z_0} \begin{bmatrix} \sinh pL, & Z_0(\cosh pL+1) \\ \frac{1}{Z_0}(\cosh pL-1), & \sinh pL \end{bmatrix}$$

Shunt reactor at both ends & series capacitor in middle of line:

$$\begin{pmatrix} A_T & B_T \\ C_T, & D_T \end{pmatrix} = \begin{pmatrix} A & B \\ C & D \end{pmatrix}_{line} - jB_{in} \begin{bmatrix} B & 0 \\ 2A - jB_{in} & BB \end{bmatrix}$$

$$- j\frac{X_c}{Z_0} \begin{bmatrix} \sinh pL & Z_0(\cosh pL+1) \\ \frac{1}{Z_0}(\cosh pL-1) & \sinh pL \end{bmatrix}$$

$$- \frac{X_c B_{in}}{2} \begin{bmatrix} \cosh pL+1 & 0 \\ \frac{2}{Z_0}\sinh pL - jB_{in}(\cosh pL+1) & \cosh pL+1 \end{bmatrix}$$

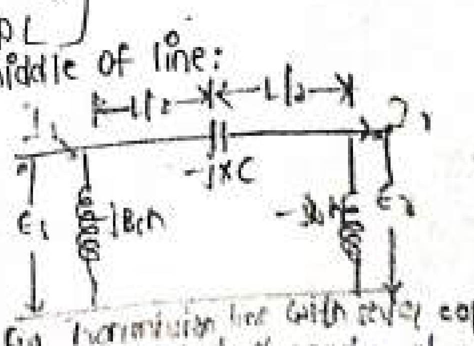

Fig: Transmission line with series capacitor in middle & shunt reactor at ends.

ANURAG ENGINEERING COLLEGE

(An Autonomous Institution)
(Approved by AICTE, New Delhi, Affiliated to JNTUH, Hyderabad, Accredited by NAAC with A+ Grade)
Ananthagiri (V & M), Kodad, Suryapet (Dist), Telangana.

Program			YEAR	SEMESTER	MID EXAMINATION
B.Tech. ✓	M.Tech.	M.B.A.	IV	II	II

HALL TICKET NO.: 2 1 C 1 5 A 0 2 0 7

Regulation : R18

Branch or Specialization: EEE

Course: EHVAC Transmission.

Signature of Student: Skoteshwar.

Signature of invigilator with date: [signature] 18/4/24

Signature of the Evaluator: BSA

Q.No. and Marks Awarded

1	2	3	4	5	6	7	8	9	10	11
1	1	1	1	1	5	-	5	-	5	-

Maximum Marks: 20 | Marks Obtained: 20

(Start Writing From Here)

PART-B $3\times5=15M$

6A:- Charge Voltage Diagram and Corona loss

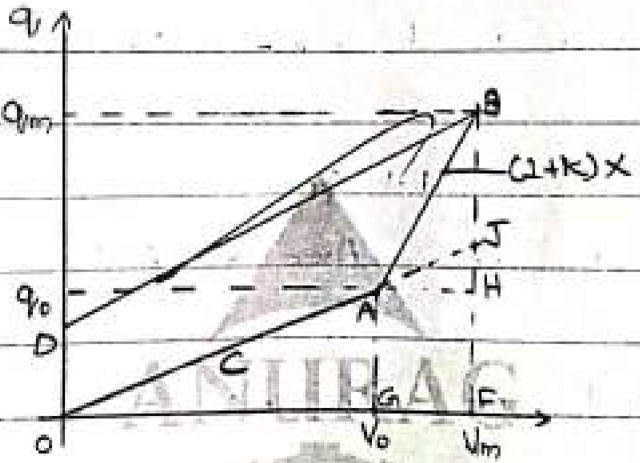

Fig: Charge Voltage (q-v) diagram with Corona loss

The diagram shows the charge voltage (q-v) with corona loss. When the corona is absent the area is calculated by considering the radius of the conductor only. The corona forms a extra layer in the vincity / surround of the conductor. This cause the increase of radius of the conductor. The charge-voltage is drawn, the V_0 is the

For very long lines, which ... ... , an

motion.

[AIB(I.D)

The energy loss is given by $\frac{1}{2}KC(V_m^2 - V_0^2)$

It is found by finding the area of DOAB.

Area DOAB = Area DOFB - Area (AOG) - Area (AHFG) - Area (AHB).

$$= \text{Area DOFB} - \frac{1}{2}q_0V_0 - q_0(V_m - V_0) - \frac{1}{2}(V_m - V_0)(q_m - q_0)$$

$$= \text{Area DOFB} - \frac{1}{2}q_0V_0 - q_0V_m + q_0V_0 - \frac{1}{2}(V_mq_m - V_mq_0 - V_0q_m + V_0 ...$$

$$= \text{Area DOFB} - \frac{1}{2}q_0V_0 - q_0V_m + q_0V_0 - \frac{1}{2}V_mq_m + \frac{1}{2}V_mq_0 + \frac{1}{2}V_0q_m ...$$

$$-\frac{1}{2}V_0q_0.$$

$$= \text{Area DOFB} + \frac{1}{2}q_0V_m - \frac{1}{2}V_mq_m + \frac{1}{2}V_0q_m.$$

$$\text{Area DOAB} = \text{Area DOFB} + \frac{1}{2}[q_0V_m + q_m(V_m - V_0)]$$

Therefore $BH = q_m$, $FH = q_0$,

Area of AOG $= \frac{1}{2}q_0V_0$, Area of (AHFG) $= q_0(V_m - V_0)$

Area of (AHB) $= \frac{1}{2}(V_m - V_0)(q_m - q_0)$.

$\therefore$ Area DOAB $= \frac{1}{2}Kq_0(V_m^2 - V_0^2)/V_0$.

The energy loss in the system $= \frac{1}{2}KC(V_m^2 - V_0^2)$

The power loss in the system $P_0 = f\frac{1}{2}KC(V_m^2 - V_0^2)$

Finally the area DOAB = energy lost

$$= \frac{1}{2}KC(V_m^2 - V_0^2).$$

Charging Current and MVAR rating of EHVAC line:

The supply current when the receiving end has no-load ($I_r=0$) the equation is: $I_s = C E_r$.

$$I_s = \frac{1}{Z_0} \sinh p.L E_r$$

when the resistance is less

$$Z_{00} = \sqrt{L/C} \quad , p = j\omega/x = j2\pi/\lambda$$

sub in I_s.

$$I_s = \sqrt{\frac{C}{L}} \sin(j\omega L/x) E_r$$

$$I_s = \sqrt{\frac{C}{L}} \sin(j2\pi L/\lambda) E_r$$

The current leads the voltage by 90°. The capacitance of the circuit when E_r is supplied is.

$$C_0 = \frac{1}{Z_{00}} E_r . \sin(2\pi L/\lambda)$$

The reactive power Q_c in the system is given by.

$$Q_c = E_s . E_r$$

$$Q_c = E_s^2 (2\pi L/\lambda) \qquad E_r = E_s / \cos(2\pi L/\lambda)$$

$$Q_c = E_s^2 \tan(2\pi L/\lambda)$$

when the resistance is less $L = 1/\lambda$ then the reactive power is zero.

The reactive power Q_c acts as MVAR rating.

For very long lines, ...

10)h) Static VAR Compensators

There are different schemes for reactive power in EHVAC systems. In static VAR compensators there are five schemes to control the reactive power in EHVAC systems. They are:

1) TCR-FC scheme
2) TCT scheme
3) TSC-TCR
4) MSC-TCR
5) SR scheme.

1) TCR-FC Scheme:-

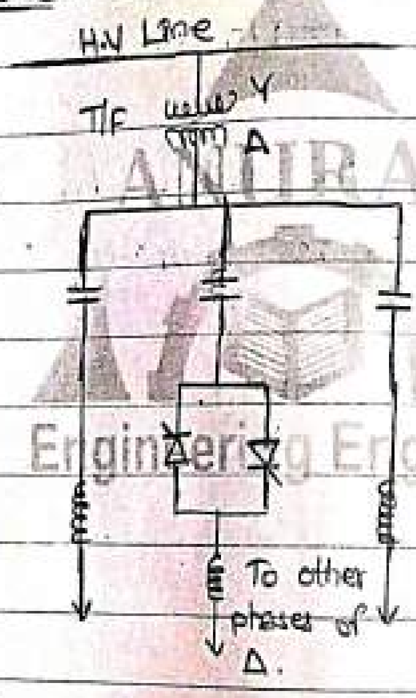

Diagram shows the Thyristor controlled reactor - Fixed capacitor. When the reactive power is more the thyristor controlled reactor (TCR) comes into conduction and when the reactive power is less (or) required to the system the fixed capacitors comes into conduction. By using the switching the harmonics are increased. The 12 switches produce 13th harmonic components, these can be limit before the damage occurs.

The reactors with small size are being placed to ...

shunt reac...

For many factors are required these cause bulk ...

inform...

2) TCT Scheme:

Thyristor Controlled Transformer. A transformer with zero leakage reactance on secondary has been taken and the switches are being connected. It operates more effectively than TCR but cost is more.

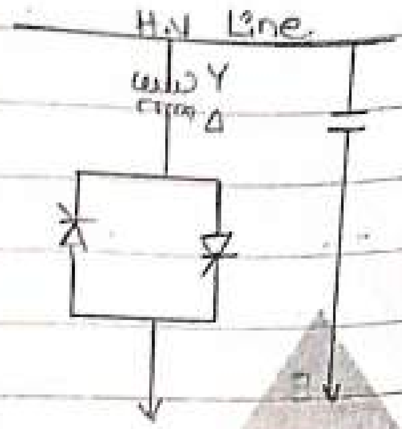

Diagram shows Thyristor Controlled transformer scheme.

3) TSC-TCR Scheme:

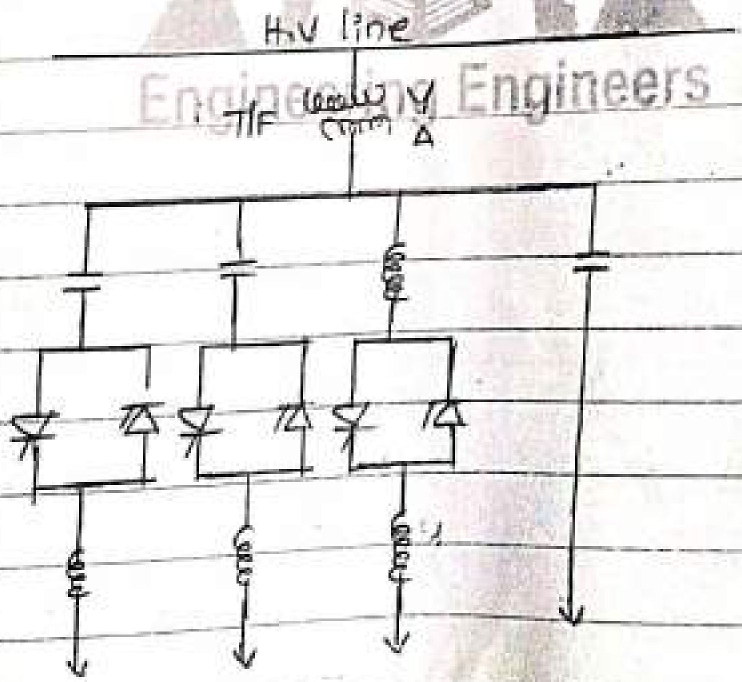

The diagram shows the ~~Thyristor controlled reactor~~ Thyristor switched capacitor - Thyristor controlled reactor scheme. The capacitors are switched according to the requirement of system. More number of switches

10

EHVAC lines has been done.

4) MSC-TCR Scheme:

Mechanically switched capacitor - Thyristor control reactor scheme is similar to TSC-TCR scheme. the thyristor / SCR switches are being replaced by the mechanical / SF6 switches. The harmonics are limited. The switching time is long but operation is similar.

5) SR Scheme:

SR scheme the reactors and fixed capacitors are used. One the dependance of requirement the step capacitor are used the B-H characteristics are changed.

5

ANURAG Engineering Engineers

PART-A 5X1=5M

1)A:- The factors to be considered to minimize the corona in transmission line are:

→ distance between the conductors i.e spacing

→ dielectric strength

c

2)A:- Reflection of travelling waves is, the travelling waves are obstructed by a object and turns back to other direction is known as Reflection.

Refraction of travelling waves is, the travelling waves are passed through the object and continue to travel in same direction with some reduced speed is known as Refraction.

c

Ans: **Travelling waves:** The waves which goes (or) travel to one place from other place are known as travelling waves.

Ans: **Compensation:** Compensation is the addition / reduction of inductive reactors (or) capacitors into the line for the operation / control of reactive power is known as compensation.

Ans: **Sub synchronous resonance:**

Sub synchronous resonance is the low reactive power present in the line with the compensation.

1

Introduction to EHV AC Transmission

1.1 ROLE OF EHV AC TRANSMISSION

Industrial-minded countries of the world require a vast amount of energy of which electrical energy forms a major fraction. There are other types of energy such as oil for transportation and industry, natural gas for domestic and industrial consumption, which form a considerable proportion of the total energy consumption. Thus, electrical energy does not represent the only form in which energy is consumed but an important part nevertheless. It is only 150 years since the invention of the dynamo by Faraday and 120 years since the installation of the first central station by Edison using dc. But the world has already consumed major portion of its natural resources in this short period and is looking for sources of energy other than hydro and thermal to cater for the rapid rate of consumption which is outpacing the discovery of new resources. This will not slow down with time and therefore there exists a need to reduce the rate of annual increase in energy consumption by any intelligent society if resources have to be preserved for posterity. After the end of the Second World War, countries all over the world have become independent and are showing a tremendous rate of industrial development, mostly on the lines of North-American and European countries, the U.S.S.R. and Japan. Therefore, the need for energy is very urgent in these developing countries, and national policies and their relation to other countries are sometimes based on energy requirements, chiefly nuclear. Hydro-electric and coal or oil-fired stations are located very far from load centres for various reasons which requires the transmission of the generated electric power over very long distances. This requires very high voltages for transmission. The very rapid strides taken by development of dc transmission since 1950 is playing a major role in extra-long-distance transmission, complementing or supplementing e.h.v. ac transmission. They have their roles to play and a country must make intelligent assessment of both in order to decide which is best suited for the country's economy. This book concerns itself with problems of e.h.v. ac transmission only.

1.2 BRIEF DESCRIPTION OF ENERGY SOURCES AND THEIR DEVELOPMENT

Any engineer interested in electrical power transmission must concern himself or herself with energy problems. Electrical energy sources for industrial and domestic use can be divided into two broad categories: (1) Transportable; and (2) Locally Usable.

Transportable type is obviously hydro-electric and conventional thermal power. But locally generated and usable power is by far more numerous and exotic. Several countries, including India, have adopted national policies to investigate and develop them, earmarking vast sums of money in their multi-year plans to accelerate the rate of development. These are also called 'Alternative Sources of Power'. Twelve such sources of electric power are listed here, but there are others also which the reader will do well to research.

Locally Usable Power

(1) Conventional thermal power in urban load centres;

(2) Micro-hydel power stations;

(3) Nuclear Thermal: Fission and Fusion;

(4) Wind Energy;

(5) Ocean Energy: (*a*) Tidal Power, (*b*) Wave Power, and (*c*) Ocean thermal gradient power;

(6) Solar thermal;

(7) Solar cells, or photo-voltaic power;

(8) Geo-thermal;

(9) Magneto hydro-dynamic or fluid dynamic;

(10) Coal gasification and liquefaction;

(11) Hydrogen power; and last but not least,

(12) Biomass Energy: (*a*) Forests; (*b*) Vegetation; and (*c*) Animal refuse.

To these can also be added bacterial energy sources where bacteria are cultured to decompose forests and vegetation to evolve methane gas. The water hyacinth is a very rich source of this gas and grows wildly in waterlogged ponds and lakes in India. A brief description of these energy sources and their limitation as far as India is concerned is given below, with some geographical points.

1. *Hydro-Electric Power:* The known potential in India is 50,000 MW (50 GW) with 10 GW in Nepal and Bhutan and the rest within the borders of India. Of this potential, almost 30% or 12 GW lies in the north-eastern part in the Brahmaputra Valley which has not been tapped. When this power is developed it will necessitate transmission lines of 1000 to 1500 kilometres in length so that the obvious choice is extra high voltage, ac or dc. The hydel power in India can be categorized as (*a*) high-head (26% of total potential), (*b*) medium-head (47%), (*c*) low-head (7%, less then 30 metres head), and (*d*) run-of-the-river (20%). Thus, micro-hydel plants and run-of-the-river plants (using may be bulb turbines) have a great future for remote loads in hilly tracts.

2. *Coal:* The five broad categories of coal available in India are Peat (4500 *BTU*/*LB**), Lignite (6500), Sub-Bituminous (7000-12000), Bituminous (14,000), and Anthracite (15,500 *BTU*/*LB*). Only non-coking coal of the sub-bituminous type is available for electric power production whose deposit is estimated at 50 giga tonnes in the Central Indian coal fields, With 50% of this allocated for thermal stations, it is estimated that the life of coal deposits will be 140 years if

---

*1000 *BTU/LB*–555.5 k-cal/kg.

the rate of annual increase in installed capacity is 5%. Thus, the country cannot rely on this source of power to be perennial. Nuclear thermal power must be developed rapidly to replace conventional thermal power.

3. *Oil and Natural Gas:* At present, all oil is used for transportation and none is available for electric power generation. Natural gas deposits are very meager at the oil fields in the North-Eastern region and only a few gas-turbine stations are installed to provide the electric power for the oil operations.

4. *Coal Liquefaction and Gasification:* Indian coal contains 45% ash and the efficiency of a conventional thermal station rarely exceeds 25% to 30%. Also transportation of coal from mines to urban load centres is impossible because of the 45% ash, pilferage of coal at stations where coal-hauling trains stop, and more importantly the lack of availability of railway wagons for coal transportation. These are needed for food transportation only. Therefore, the national policy is to generate electric power in super thermal stations of 2100 MW capacity located at the mine mouths and transmit the power by e.h.v. transmission lines. If coal is liquified and pumped to load centres, power up to 7 times its weight in coal can be generated in high efficiency internal cumbustion engines.

5. *Nuclear Energy:* The recent advances made in Liquid Metal Fast Breeder Reactors (*LMFBR)* are helping many developing countries, including India, to install large nuclear thermal plants. Although India has very limited Uranium deposits, it does possess nearly 50% of the world's Thorium deposits. The use of this material for *LMFBR* is still in infant stages and is being developed rapidly.

6. *Wind Energy:* It is estimated that 20% of India's power requirement can be met with development of wind energy. There are areas in the Deccan Plateau in South-Central India where winds of 30 km/hour blow nearly constantly. Wind power is intermittent and storage facilities are required which can take the form of storage batteries or compressed air. For an electrical engineer, the challenge lies in devising control circuitry to generate a constant magnitude constant-frequency voltage from the variable-speed generator and to make the generator operate in synchronism with an existing grid system.

7. *Solar-Cell Energy:* Photo-voltaic power is very expensive, being nearly the same as nuclear power costing U.S.$ 1000/kW of peak power. (At the time of writing, 1 U.S$ = Rs. 35). Solar cells are being manufactured to some extent in India, but the U.S.A. is the largest supplier still. Indian insolation level is 600 calories/ sq. cm/day on the average which will generate 1.5 kW, and solar energy is renewable as compared to some other sources of energy.

8. *Magneto Hydro-Dynamic:* The largest MHD generator successfully completed in the world is a 500 kW unit of AVCO in the U.S.A. Thus, this type of generation of electric energy has very local applications.

9. *Fuel-Cell Energy:* The fuel-cell uses H-O interaction through a Phosphoric Acid catalyzer to yield a flow of electrons in a load connected externally. The most recent installation is by the Consolidated Edison Co. of New York which uses a module operating at 190°C. Each cell develops 0.7 V and there are sufficient modules in series to yield an output voltage of 13.8 kV, the same as a conventional central-station generator. The power output is expected to reach 1 MW.

10. *Ocean Energy:* Energy from the vast oceans of the earth can be developed in 3 different ways: (*i*) Tidal; (*ii*) Wave; and (*iii*) Thermal Gradient.

(*i*) Tidal Power: The highest tides in the world occur at 40 to 50° latitudes with tides up to 12 m existing twice daily. Therefore, Indian tides are low being about 3.5 m in the Western Coast and Eastern rivers in estuaries. France has successfully operated a 240 MW station at the Rance-River estuary using bulb turbines. Several installations in the world have followed suit. The development of Indian tidal power at the Gujarat Coast in the West is very ambitious and is taking shape very well. Like wind power, tidal power is intermittent in nature.

The seawater during high tides is allowed to run in the same or different passage through the turbine-generators to fill a reservoir whose retaining walls may be up to 30 km long. At low-tide periods, the stored water flows back to the sea through the turbines and power is generated.

(*ii*) Wave Energy: An average power of 25 to 75 kW can be developed per metre of wave length depending on the wave height. The scheme uses air turbines coupled to generators located in chambers open to the sea at the bottom and closed at the top. There may be as many as 200-300 such chambers connected together at the top through pipes. A wave crest underneath some chambers will compress the air which will flow into other chambers underneath which the wave-trough is passing resulting in lower pressure. This runs the air turbines and generates power. Others are Salter's Ducks and Cockerrel's 3-part ship.

(*iii*) Ocean Thermal Power: This scheme utilizes the natural temperature difference between the warm surface water (20°-25°C) and the cooler oceanbed water at 5°C. The turbine uses NH_3 as the working fluid in one type of installation which is vaporized in a heat-exchanger by the warm water. The condenser uses the cooler ocean-bed water and the cycle is complete as in a conventional power station. The cost of such an installation is nearly the same as a nuclear power station.

This brief description of 'alternative' sources of electric power should provide the reader with an interest to delve deeper into modern energy sources and their development.

1.3 DESCRIPTION OF SUBJECT MATTER OF THIS BOOK

Extra High Voltage (EHV) ac transmission can be assumed to have seen its development since the end of the Second World War, with the installation of 345 kV in North America and 400 kV in Europe. The distance between generating stations and load centres as well as the amount of power to be handled increased to such an extent that 220 kV was inadequate to handle the problem. In these nearly 50 years, the highest commercial voltage has increased to 1150 kV (1200 kV maximum) and research is under way at 1500 kV by the AEP-ASEA group. In India, the highest voltage used is 400 kV ac, but will be increased after 1990 to higher levels. The problems posed in using such high voltages are different from those encountered at lower voltages. These are:

(*a*) Increased Current Density because of increase in line loading by using series capacitors.

(*b*) Use of bundled conductors.

(*c*) High surface voltage gradient on conductors.

(*d*) Corona problems: Audible Noise, Radio Interference, Corona Energy Loss, Carrier Interference, and TV Interference.

(*e*) High electrostatic field under the line.

(*f*) Switching Surge Overvoltages which cause more havoc to air-gap insulation than lightning or power frequency voltages.

(*g*) Increased Short-Circuit currents and possibility of ferro resonance conditions.

(*h*) Use of gapless metal-oxide arresters replacing the conventional gap-type Silicon Carbide arresters, for both lightning and switching-surge duty.

(*i*) Shunt reactor compensation and use of series capcitors, resulting in possible sub-synchronous resonance conditions and high shortcircuit currents.

(*j*) Insulation coordination based upon switching impulse levels.

(*k*) Single-pole reclosing to improve stability, but causing problems with arcing.

The subject is so vast that no one single book can hope to handle with a description, analysis, and discussion of all topics. The book has been limited to the transmission line only and has not dealt with transient and dynamic stability, load flow, and circuit breaking. Overvoltages and characteristics of long airgaps to withstand them have been discussed at length which can be classified as transient problems. Items (*a*) to (*e*) are steady-state problems and a line must be designed to stay within specified limits for interference problems, corona loss, electrostatic field, and voltages at the sending end and receiving end buses through proper reactive-power compensation.

Chapter 2 is devoted to an introduction to the e.h.v. problem, such as choice of voltage for transmission, line losses and power-handling capacity for a given line length between source and load and bulk power required to be transmitted. The problem of vibration of bundled conductors is touched upon since this is the main mechanical problem in e.h.v lines. Chapters 3 and 4 are basic to the remaining parts of the book and deal with calculation of line resistance, inductance, capacitance, and ground-return parameters, modes of propagation, electrostatics to understand charge distribution and the resulting surface voltage gradients. All these are directed towards an *N*-conductor bundle. Corona loss and Audible Noise from e.h.v. lines are consequences of high surface voltage gradient on conductors. This is dealt fully in Chapter 5. In several cases of line design, the audible noise has become a controlling factor with its attendant pollution of the environment of the line causing psycho-acoustics problems. The material on interference is continued in Chapter 6 where Radio Interference is discussed. Since this problem has occupied researchers for longer than AN, the available literature on RI investigation is more detailed than AN and a separate chapter is devoted to it. Commencing with corona pulses, their frequency spectrum, and the lateral profile of RI from lines, the reader is led into the modern concept of 'Excitation Function' and its utility in pre-determining the RI level of a line yet to be designed. For lines up to 750 kV, the C.I.G.R.E. formula applies. Its use in design is also discussed, and a relation between the excitation function and RI level calculated by the C.I.G.R.E. formula is given.

Chapter 7 relates to power frequency electrostatic field near an e.h.v. line which causes harmful effects to human beings, animals, vehicles, plant life, etc. The limits which a designer has to bear in mind in evolving a line design are discussed. Also a new addition has been made in this chapter under the title Magnetic Field Effects of E.H.V. Lines. Chapters 8-11 are devoted

2

Transmission Line Trends and Preliminaries

2.1 STANDARD TRANSMISSION VOLTAGES

Voltages adopted for transmission of bulk power have to conform to standard specifications formulated in all countries and internationally. They are necessary in view of import, export, and domestic manufacture and use. The following voltage levels are recognized in India as per IS-2026 for line-to-line voltages of 132 kV and higher.

Nominal System Voltage kV	132	220	275	345	400	500	750
Maximum Operating Voltage, kV	145	245	300	362	420	525	765

There exist two further voltage classes which have found use in the world but have not been accepted as standard. They are: 1000 kV (1050 kV maximum) and 1150 kV (1200 kV maximum). The maximum operating voltages specified above should in no case be exceeded in any part of the system, since insulation levels of all equipment are based upon them. It is therefore the primary responsibility of a design engineer to provide sufficient and proper type of reactive power at suitable places in the system. For voltage rises, inductive compensation and for voltage drops, capacitive compensation must usually be provided. As example, consider the following cases.

Example 2.1. A single-circuit 3-phase 50 Hz 400 kV line has a series reactance per phase of 0.327 ohm/km. Neglect line resistance. The line is 400 km long and the receiving-end load is 600 MW at 0.9 p.f. lag. The positive-sequence line capacitance is 7.27 nF/km. In the absence of any compensating equipment connected to ends of line, calculate the sending-end voltage. Work with and without considering line capacitance. The base quantities for calculation are 400 kV, 1000 MVA.

Solution. Load voltage $V = 1.0$ per unit. Load current $I = 0.6\ (1 - j0.483) = 0.6 - j0.29$ p.u. Base impedance $Z_b = 400^2/1000 = 160$ ohms. Base admittance $Y_b = 1/160$ mho.

Total series reactance of line

$$X = j0.327 \times 400 = j130.8 \text{ ohms} = j\ 0.8175 \text{ p.u.}$$

Total shunt admittance of line

$$\text{Y} = j\ 314 \times 7.27 \times 10^{-9} \times 400$$
$$= j\ 0.9136 \times 10^{-3} \text{ mho} = j\ 0.146 \text{ p.u.}$$

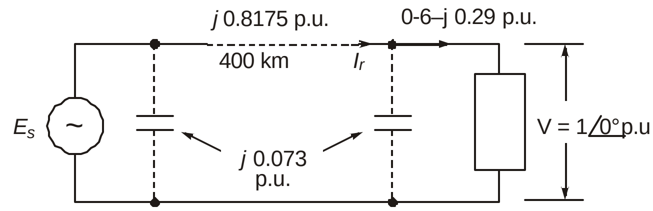

Fig. 2.1 (*a*)

When considering the line capacitance, one half will be concentrated at load end across the load and the other half at the entrance to the line at the sending end, as shown in Figure 2.1. Then, the receiving-end current is

$$I_r = 0.6 - j0.29 + j0.073 = 0.6 - j0.217 \text{ p.u.}$$

∴ The sending-end voltage will be

$$E_s = 1 + j\,(0.6 - j0.217)\ 0.8175 = 1.1774 + j0.49$$
$$= 1.2753\ \angle 22.6° = 510\ \angle 22.6°, \text{kV}.$$

When line capacitance is omitted, the sending-end voltage is

$$E_s = 1 + j\,(0.6 - j0.29)\ 0.8175 = 1.33\ \angle 21.6° = 532\ \angle 21.6°, \text{kV}.$$

Note that in both cases, the sending-end voltage, that is, the generating station h.v. bus voltage exceeds the IS limit of 420 kV.

Example 2.2. In the previous example, suggest suitable reactive compensation equipment to be provided at the load end to maintain 400 kV (1 p.u. voltage) at both ends of line.

Solution. Since the load is drawing lagging (inductive) current, obviously we have to provide capacitive compensating equipment across the load in order to reduce the line current. Figure 2.1 (*b*) shows the overall arrangement. If I_c is the current drawn by this compensating equipment, considering line capacitance, the total receiving-end line current will be $I_r = 0.6 - j0.217 + j\,I_c$, p.u., and the resulting sending-end voltage will be

$$E_s = 1 + j\,(0.6 - j0.217 + j\,I_c)\ 0.8175 = (1.1774 - 0.8175\ I_c) + j0.49.$$

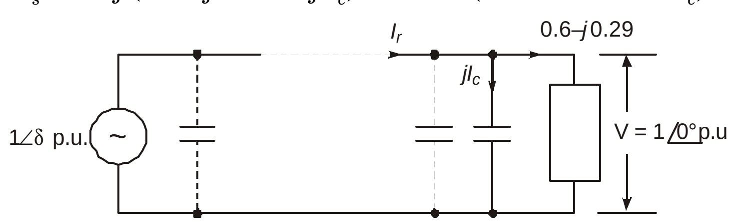

Fig. 2.1 (***b***)

Now, since $|E_s| = 1$ p.u. also, there results $I_c = 0.374$ p.u. The resulting rating of the compensating capacitor is 374 MVAR.

When the presence of line capacitance is neglected, $I_c = 0.447$ p.u. and the required compensation is 447 MVAR, which is of course higher than 374 MVAR by 73 MVAR.

Detailed discussion of line compensation for voltage control at the sending- and receiving-end busses will be considered in Chapter 12. We note in passing that voltage control in e.h.v. systems is a very expensive proposition. In addition to switched capacitors which provide variable capacitive reactive power to suit variation of load from no load to full load, variable inductive compensation will be required which takes the form of thyristor-controlled reactors (TCR) which are also known as Static VAR Systems. Unfortunately, these give rise to undesirable harmonics which are injected into the line and may cause maloperation of signalling and some communication equipment. These problems and use of proper filters to limit the harmonic injection will also be discussed in Chapter 12.

2.2 AVERAGE VALUES OF LINE PARAMETERS

Detailed calculation of line parameters will be described in Chapter 3. In order to be able to estimate how much power a single-circuit at a given voltage can handle, we need to know the value of positive-sequence line inductance and its reactance at power frequency. Furthermore, in modern practice, line losses caused by I^2R heating of the conductors is gaining in importance because of the need to conserve energy. Therefore, the use of higher voltages than may be dictated by purely economic consideration might be found in order not only to lower the current I to be transmitted but also the conductor resistance R by using bundled conductors comprising of several sub-conductors in parallel. We will utilize average values of parameters for lines with horizontal configuration as shown in Table 2.1 for preliminary estimates.

When line resistance is neglected, the power that can be transmitted depends upon (*a*) the magnitudes of voltages at the ends (E_s, E_r), (*b*) their phase difference δ, and (*c*) the total positive-sequence reactance X per phase, when the shunt caspacitive admittance is neglected.

Thus, $$P = E_s\, E_r \sin \delta / (L.x) \qquad ...(2.1)$$

where P = power in MW, 3-phase, E_s, E_r = voltages at the sending-end and receiving end, respectively, in kV line-line, δ = phase difference between E_s and E_r, x = positive-sequence reactance per phase, ohm/km, and L = line length, km.

Table 2.1. Average Values of Line Parameters

System kV	400	750	1000	1200
Average Height, m	15	18	21	21
Phase Spacing, m	12	15	18	21
Conductor	2 × 32 mm	4 × 30 mm	6 × 46 mm	8 × 46 mm
Bundle Spacing, m	0.4572	0.4572	–	–
Bundle Dia., m	–	–	1.2	1.2
*r, ohm/km**	0.031	0.0136	0.0036	0.0027
x, ohm/km (50 Hz)	0.327	0.272	0.231	0.231
x/r	10.55	20	64.2	85.6

*At 20°C. Increase by 12.5% for 50°C.

From consideration of stability, δ is limited to about 30°, and for a preliminary estimate of P, we will take $E_s = E_r = E$.

2.3 POWER-HANDLING CAPACITY AND LINE LOSS

According to the above criteria, the power-handling capacity of a single circuit is $P = E^2 \sin\delta / Lx$. At unity power factor, at the load P, the current flowing is

$$I = E \sin \delta / \sqrt{3}\, Lx \qquad ...(2.2)$$

and the total power loss in the 3-phases will amount to

$$p = 3I^2rL = E^2.\ \sin^2\ \delta\ .r/Lx^2 \qquad ...(2.3)$$

Therefore, the percentage power loss is

$$\%p = 100\ p/P = 100.\ \sin\delta\ .(r/x) \qquad ...(2.4)$$

Table 2.2. shows the percentage power loss and power-handling capacity of lines at various voltage levels shown in Table 2.1, for δ = 30° and without series-capacitor compensation.

Table 2.2. Percent Power Loss and Power-Handling Capacity

System kV	400	750	1000	1200
Percentage, Power Loss	$\frac{50}{10.55} = 4.76$	$\frac{50}{20} = 2.5$	$\frac{50}{64.2} = 0.78$	$\frac{50}{85.6} = 0.584$
Line Length, km	$P = 0.5E^2/Lx, MW$			
400	670	2860	6000	8625
600	450	1900	4000	5750
800	335	1430	3000	4310
1000	270	1140	2400	3450
1200	225	950	2000	2875

The following important and useful conclusions can be drawn for preliminary understanding of trends relating to power-handling capacity of a.c. transmission lines and line losses.

(1) One 750-kV line can normally carry as much power as four 400-kV circuits for equal distance of transmission.

(2) One 1200-kV circuit can carry the power of three 750-kV circuits and twelve 400-kV circuits for the same transmission distance.

(3) Similar such relations can be found from the table.

(4) The power-handling capacity of line at a given voltage level decreases with line length, being inversely proportional to line length *L*.

From equation (2.2) the same holds for current to be carried.

(5) From the above property, we observe that if the conductor size is based on current rating, as line length increases, smaller sizes of conductor will be necessary. This will increase the danger of high voltage effects caused by smaller diameter of conductor giving rise to corona on the conductors and intensifying radio interference levels and audible noise as well as corona loss.

(6) However, the *percentage* power loss in transmission remains independent of line length since it depends on the *ratio* of conductor resistance to the positive-sequence reactance per unit length, and the phase difference δ between E_s and E_r.

(7) From the values of $\%p$ given in Table 2.2, it is evident that it decreases as the system voltage is increased. This is very strongly in favour of using higher voltages if energy is to be conserved. With the enormous increase in world oil prices and the need for

conserving natural resources, this could sometimes become the governing criterion for selection of voltage for transmission. The Bonneville Power Administration (B.P.A.) in the U.S.A. has based the choice of 1150 kV for transmission over only 280 km length of line since the power is enormous (10,000 MW over one circuit).

(8) In comparison to the % power loss at 400 kV, we observe that if the same power is transmitted at 750 kV, the line loss is reduced to (2.5/4.76) = 0.525, at 1000 kV it is 0.78/4.76 = 0.165, and at 1200 kV it is reduced further to 0.124.

Some examples will serve to illustrate the benefits accrued by using very high transmission voltages.

Example 2.3. A power of 12,000 MW is required to be transmitted over a distance of 1000 km. At voltage levels of 400 kV, 750 kV, 1000 kV, and 1200 kV, determine:

(1) Possible number of circuits required with equal magnitudes for sending and receiving-end voltages with 30° phase difference;

(2) The currents transmitted; and

(3) The total line losses.

Assume the values of x given in Table 2.1. Omit series-capacitor compensation.

Solution. This is carried out in tabular form.

	System, kv	400	750	1000	1200
	x, ohm/km	0.327	0.272	0.231	0.231
	$P = 0.5\,E^2/Lx$, *MW*	268	1150	2400	3450
(*a*)	No. of circuits				
	(=12000/P)	45	10–11	5	3–4
(*b*)	Current, kA	17.31	9.232	6.924	5.77
(*c*)	% power loss, p	4.76	2.5	0.78	0.584
	Total power loss, MW	571	300	93.6	70

The above situation might occur when the power potential of the Brahmaputra River in North-East India will be harnessed and the power transmitted to West Bengal and Bihar. Note that the total power loss incurred by using 1200 kV ac transmission is almost one-eighth that for 400 kV. The width of land required is far less while using higher voltages, as will be detailed later on.

Example 2.4. A power of 2000 MW is to be transmitted from a super thermal power station in Central India over 800 km to Delhi. Use 400 kV and 750 kV alternatives. Suggest the number of circuits required with 50% series capacitor compensation, and calculate the total power loss and loss per km.

Solution. With 50% of line reactance compensated, the total reactance will be half of the positive-sequence reactance of the 800-km line.

Therefore $P = 0.5 \times 400^2/400 \times 0.327 = 670$ MW/Circuit at 400 kV

and $P = 0.5 \times 750^2/400 \times 0.272 = 2860$ MW/Circuit at 750 kV

	400 *kV*	750 *kV*
No. of circuits required	3	1
Current per circuit, kA	$667/\sqrt{3} \times 400 = 0.963$	1.54
Resistance for 800 km, ohms	$0.031 \times 800 = 24.8$	$0.0136 \times 800 = 10.88$
Loss per circuit, MW	$3 \times 24.8 \times 0.963^2 = 69$ MW	$3 \times 10.88 \times 1.54^2$
		= 77.4 MW
Total power loss, MW	$3 \times 69 = 207$	77.4
Loss/km, kW	86.25 kW/km	97 kW/km

2.4 EXAMPLES OF GIANT POWER POOLS AND NUMBER OF LINES

From the discussion of the previous section it becomes apparent that the choice of transmission voltage depends upon (*a*) the total power transmitted, (*b*) the distance of transmission, (*c*) the % power loss allowed, and (*d*) the number of circuits permissible from the point of view of land acquisition for the line corridor. For example, a single circuit 1200 kV line requires a width of 56 m, 3 – 765 kV require 300 m, while 6 single-circuit 500 kV lines for transmitting the same power require 220 m-of-right-of-way (R-O-W). An additional factor is the technological know-how in the country. Two examples of similar situations with regard to available hydro-electric power will be described in order to draw a parallel for deciding upon the transmission voltage selection. The first is from Canada and the second from India. These ideas will then be extended to thermal generation stations situated at mine mouths requiring long transmission lines for evacuating the bulk power to load centres.

2.4.1 Canadian Experience

The power situation in the province of Quebec comes closest to the power situation in India, in that nearly equal amounts of power will be developed eventually and transmitted over nearly the same distances. Hence the Canadian experience might prove of some use in making decisions in India also. The power to be developed from the La Grande River located in the James Bay area of Northern Quebec is as follows : Total 11,340 MW split into 4 stations [LG–1: 1140, LG–2 : 5300, LG–3 : 2300, and LG–4: 2600 MW]. The distance to load centres at Montreal and Quebec cities is 1100 km. The Hydro-Quebec company has vast ecperience with their existing 735 kV system from the earlier hydroelectric development at Manicouagan-Outardes Rivers so that the choice of transmission voltage fell between the existing 735 kV or a future 1200 kV. However, on account of the vast experience accumulated at the 735 kV level, this voltage was finally chosen. The number of circuits required from Table 2.2 can be seen to be 10–11 for 735 kV and 3–4 for 1200 kV. The lines run practically in wilderness and land acquisition is not as difficult a problem as in more thickly populated areas. Plans might however change as the development proceeds. The 1200 kV level is new to the industry and equipment manufacture is in the infant stages for this level. As an alternative, the company could have investigated the possibility of using e.h.v. dc transmission. But the final decision was to use 735 kV, ac. In 1987, a $\pm$ 450 kV h.v. d.c. link has been decided for James Bay-New England Hydro line (U.S.A.) for a power of 6000 MW.

2.4.2 Indian Requirement

The giant hydro-electric power pools are located in the northern border of the country on the Himalayan Mountain valleys. These are in Kashmir, Upper Ganga on the Alakhananda and Bhagirathi Rivers, Nepal, Bhutan, and the Brahmaputra River. Power surveys indicate the following power generation and distances of transmission:

(1) 2500 MW, 250 km, (2) 3000 MW, 300 km, (3) 4000 MW, 400 km, (4) 5000 MW, 300 km, (5) 12000 MW over distances of (*a*) 250 km, (*b*) 450 km, and (*c*) 1000-1200 km.

Using the power-handling capacities given in Table 2.2 we can construct a table showing the possible number of circuits required at differenct voltage levels (Table 2.3).

Table 2.3: Voltage Levels and Number of Circuits for Evacuating from Hydro-Electric Power Pools in India

Power, MW	2500	3000	4000	5000		12000	
Distance, km	250	300	400	300	250	450	1000
No. of Circuits /	3/400	4/400	6/400	6/400	12/400	20/400	48/400
Voltage Level		1/750	2/750	2/750	3/750	6/750	12/750
Voltage Level			(70%	(75%)	1/1200	2/1200	6/1000
(*Ac only*)			loaded)				4/1200

One can draw certain conclusions from the above table. For example, for powers up to 5000 MW, 400 kV transmission might be adequate. For 12000 MW, we observe that 750 kV level for distances up to 450 km and 1200 kV for 1000 km might be used, although even for this distance 750 kV might serve the purpose. It is the duty of a design engineer to work out such alternatives in order that final decisions might be taken. For the sake of reliability, it is usual to have at least 2 circuits.

While the previous discussion is limited to ac lines, the dc alternatives must also be worked out based upon 2000 Amperes per pole. The usual voltages used are ± 400 kV (1600 MW/bipole), ± 500 kV (2000 MW) and ± 600 kV (2400 MW). These power-handling capacities do not depend on distances of transmission. It is left as an exercise at the end of the chapter for the reader to work out the dc alternatives for powers and distances given in Table 2.3.

2.5 COSTS OF TRANSMISSION LINES AND EQUIPMENT

It is universally accepted that cost of equipment all over the world is escalating every year. Therefore, a designer must ascertain current prices from manufacturer of equipment and line materials. These include conductors, hardware, towers, transformers, shunt reactors, capacitors, synchronous condensers, land for switchyards and line corridor, and so on. Generating station costs are not considered here, since we are only dealing with transmission in this book. In this section, some idea of costs of important equipment is given (which may be current in 2005) for comparison purposes only. These are not to be used for decision-making purposes.

(1US$ = Rs.50; 1 Lakh = 100, 000; 1 Crore = 100 Lakhs = 10 Million = 10^7).

(*a*) High Voltage DC ± 400 kV Bipole

Back-to-back terminals : Rs. 50 Lakhs/MVA for 150 MVA

Rs. 40 Lakhs/MVA for 300 MVA

Cost of 2 terminals :	Rs. 40 Lakhs/MVA
Transmission line:	Rs. 26.5 Lakhs/Circuit (cct) km
Switchyards :	Rs. 3000 Lakhs/bay

(*b*) 400 kV AC

Transformers : 400/220 kV Autotransformers

Rs. 3.7 Lakhs/MVA for 200 MVA 3-phase unit

to Rs. 3 Lakhs/MVA for 500 MVA 3-phase unit

400 kV/13.8 kV Generator Transformers

Rs. 2 Lakhs/MVA for 250 MVA 3-phase unit

to Rs. 1.5 Lakh/MVA for 550 MVA 3-phase unit.

(*c*) Shunt Reactors

Non-switchable	Rs. 2.6 Lakhs/MVA for 50 MVA unit to
	Rs. 2 Lakhs/MVA for 80 MVA unit
Switchable	Rs. 9 to 6.5 Lakhs/MVA for 50 to 80 MVA units.
Shunt Capacitors	Rs. 1 Lakh/MVA

Synchronous Condensers (Including transformers) :

Rs. 13 Lakhs/MVA for 70 MVA to

Rs. 7 Lakhs/MVA for 300 MVA

Transmission Line Cost:

400 kV Single Circuit: Rs. 25 Lakhs/cct km

220 kV: S/C: Rs. 13 Lakhs/cct km; D/C: Rs. 22 Lakhs/cct km.

Example 2.5. A power of 900 MW is to be transmitted over a length of 875 km. Estimate the cost difference when using ± 400 kV dc line and 400 kV ac lines.

Solution. Power carried by a single circuit dc line = 1600 MW. Therefore, 1 Circuit is sufficient and it allows for future expansion.

Power carried by ac line = $0.5\,E^2/xL = 0.5 \times 400^2/(0.32 \times 875) = 285$ MW/cct.

∴ 3 circuits will be necessary to carry 900 MW.

DC Alternative: cost of

(*a*)	Terminal Stations	Rs. 33.5×10^3 Lakhs
(*b*)	Transmission Line	Rs. 23×10^3 Lakhs
(*c*)	2 Switchyard Bays	Rs. 5.8×10^3 Lakhs
	Total	Rs. 62.3×10^3 Lakhs = Rs. 623 Crores

AC Alternative: Cost of

(*a*)	6 Switchyard Bays	Rs. 17.5×10^3 Lakhs
(*b*)	Shunt reactors 500 MVA	Rs. 1×10^3 Lakhs
(*c*)	Shunt capacitors 500 MVA	Rs. 0.5×10^3 Lakhs
(*d*)	Line cost: (3 × 875 × 25 Lakhs)	Rs. 65×10^3 Lakhs
	Total	Rs. 84×10^3 Lakhs = Rs. 840 Crores

Difference in cost = Rs. 217 Crores, dc being lower than ac.

(Certain items common to both dc and ac transmission have been omitted. Also, series capacitor compensation has not been considered).

Example 2.6. Repeat the above problem if the transmission distance is 600 km.

Solution. The reader can calculate that the dc alternative costs about 55 x 10^3 Lakhs or Rs. 550 Crores.

For the ac alternative, the power-handling capacity per circuit is increased to 285 × 875/600 = 420 MW. This requires 2 circuits for handling 900 MW.

The reactive powers will also be reduced to 120 MVA for each line in shunt reactors and switched capacitors. The cost estimate will then include:

(*a*)	4 Switchyard Bays	Rs. 11 × 10^3 Lakhs
(*b*)	Shunt reactors 240 MVA	Rs. 0.6 × 10^3 Lakhs
(*c*)	Shunt capacitors	Rs. 0.27 × 10^3 Lakhs
(*d*)	Line cost: 2 × 600 × 25 Lakhs	Rs. 30 × 10^3 Lakhs
	Total	Rs. 41. 87 × 10^3 Lakhs = 418.7 Crores.

The dc alternative has become more expensive than the ac alternative by about Rs.130 Crores. In between line lengths of 600 km and 875 km for transmitting the same power, the two alternatives will cost nearly equal. This is called the "Break Even Distance".

2.6 MECHANICAL CONSIDERATIONS IN LINE PERFORMANCE

2.6.1 Types of Vibrations and Oscillations

In this section a brief description will be given of the enormous importance which designers place on the problems created by vibrations and oscillations of the very heavy conductor arrangement required for e.h.v. transmission lines. As the number of sub-conductors used in a bundle increases, these vibrations and countermeasures and spacings of sub-conductors will also affect the electrical design, particularly the surface voltage gradient. The mechanical designer will recommend the tower dimensions, phase spacings, conductor height, sub-conductor spacings, etc. from which the electrical designer has to commence his calculations of resistance, inductance, capacitance, electrostatic field, corona effects, and all other performance characteristics. Thus, the two go hand in hand.

The sub-conductors in a bundle are separated by spacers of suitable type, which bring their own problems such as fatigue to themselves and to the outer strands of the conductor during vibrations. The design of spacers will not be described here but manufacturers' catalogues should be consulted for a variety of spacers available. These spacers are provided at intervals ranging from 60 to 75 metres between each span which is in the neighbourhood of 300 metres for e.h.v. lines. Thus, there may be two end spans and two or three subspans in the middle. The spacers prevent conductors from rubbing or colliding with each other in wind and ice storms, if any. However, under less severe wind conditions the bundle spacer can damage itself or cause damage to the conductor under certain critical vibration conditions. Electrically speaking, since the charges on the sub-conductors are of the same polarity, there exists electrostatic repulsion among them. On the other hand, since they carry currents in the same direction, there is electromagnetic attraction. This force is especially severe during short-circuit currents so that the spacer has a force exerted on it during normal or abnormal electrical operation.

Three types of vibration are recognized as being important for e.h.v. conductors, their degree of severity depending on many factors, chief among which are: (*a*) conductor tension, (*b*) span length, (*c*) conductor size, (*d*) type of conductor, (*e*) terrain of line, (*f*) direction of prevailing winds, (*g*) type of supporting clamp of conductor-insulator assemblies from the tower, (*h*) tower type, (*i*) height of tower, (*j*) type of spacers and dampers, and (*k*) the vegetation in the vicinity of line. In general, the most severe vibration conditions are created by winds without turbulence so that hills, buildings, and trees help in reducing the severity. The types of vibration are: (1) Aeolian Vibration, (2) Galloping, and (3) Wake-Induced Oscillations. The first two are present for both single-and multi-conductor bundles, while the wake-induced oscillation is confined to a bundle only. Standard forms of bundle conductors have sub-conductors ranging from 2.54 to 5 cm diameters with bundle spacing of 40 to 50 cm between adjacent conductors. For e.h.v. transmission, the number ranges from 2 to 8 sub-conductors for transmission voltages from 400 kV to 1200 kV, and up to 12 or even 18 for higher voltages which are not yet commercially in operation. We will briefly describe the mechanism causing these types of vibrations and the problems created by them.

2.6.2 Aeolian Vibration

When a conductor is under tension and a comparatively steady wind blows across it, small vortices are formed on the leeward side called Karman Vortices (which were first observed on aircraft wings). These vortices detach themselves and when they do alternately from the top and bottom they cause a minute vertical force on the conductor. The frequency of the forces is given by the accepted formula

$$F = 2.065\ v/d,\ \text{Hz} \qquad \text{...(2.5)}$$

where v = component of wind velocity normal to the conductor in km/ hour, and d = diameter of conductor in centimetres. [The constant factor of equation (2.5) becomes 3.26 when v is in mph and d in inches.]

The resulting oscillation or vibrational forces cause fatigue of conductor and supporting structure and are known as aeolian vibrations. The frequency of detachment of the Karman vortices might correspond to one of the natural mechanical frequencies of the span, which if not damped properly, can build up and destroy individual strands of the conductor at points of restraint such as at supports or at bundle spacers. They also give rise to wave effects in which the vibration travels along the conductor suffering reflection at discontinuities at points of different mechanical characteristics. Thus, there is associated with them a mechanical impedance. Dampers are designed on this property and provide suitable points of negative reflection to reduce the wave amplitudes. Aeolian vibrations are not observed at wind velocities in excess of 25 km/hour. They occur principally in terrains which do not disturb the wind so that turbulence helps to reduce aeolian vibrations.

In a bundle of 2 conductors, the amplitude of vibration is less than for a single conductor due to some cancellation effect through the bundle spacer. This occurs when the conductors are not located in a vertical plane which is normally the case in practice. The conductors are located in nearly a horizontal plane. But with more than 2 conductors in a bundle, conductors are located in both planes. Dampers such as the Stockbridge type or other types help to damp the vibrations in the subspans connected to them, namely the end sub-spans, but there are usually two or three sub-spans in the middle of the span which are not protected by these dampers provided only at the towers. Flexible spacers are generally provided which may or may not be designed to offer damping. In cases where they are purposely designed to damp the sub-span oscillations, they are known as spacer-dampers.

Since the aeolian vibration depends upon the power imparted by the wind to the conductor, measurements under controlled conditions in the laboratory are carried out in wind tunnels. The frequency of vibration is usually limited to 20 Hz and the amplitudes less than 2.5 cm.

2.6.3 Galloping

Galloping of a conductor is a very high amplitude, low-frequency type of conductor motion and occurs mainly in areas of relatively flat terrain under freezing rain and icing of conductors. The flat terrain provides winds that are uniform and of a low turbulence. When a conductor is iced, it presents an unsymmetrical corss-section with the windward side having less ice accumulation than the leeward side of the conductor. When the wind blows across such a surface, there is an aerodynamic lift as well as a drag force due to the direct pressure of the wind. the two forces give rise to torsional modes of oscillation and they combine to oscillate the conductor with very large amplitudes sufficient to cause contact of two adjacent phases, which may be 10 to 15 metres apart in the rest position. Galloping is induced by winds ranging from 15 to 50 km/hour, which may normally be higher than that required for aeolian vibrations but there could be an overlap. The conductor oscillates at frequencies between 0.1 and 1 Hz. Galloping is controlled by using "detuning pendulums" which take the form of weights applied at different locations on the span.

Galloping may not be a problem in a hot country like India where temperatures are normally above freezing in winter. But in hilly tracts in the North, the temperatures may dip to below the freezing point. When the ice loosens from the conductor, it brings another oscillatory motion called Whipping but is not present like galloping during only winds.

2.6.4 Wake-Induced Oscillation

The wake-induced oscillation is peculiar to a bundle conductor, and similar to aeolian vibration and galloping occurring principally in flat terrain with winds of steady velocity and low turbulence. The frequency of the oscillation does not exceed 3 Hz but may be of sufficient amplitude to cause clashing of adjacent sub-conductors, which are separated by about 50 cm. Wind speeds for causing wake-induced oscillation must be normally in the range 25 to 65 km/hour. As compared to this, aeolian vibration occurs at wind speeds less than 25 km/hour, has frequencies less than 20 Hz and amplitudes less than 2.5 cm. Galloping occurs at wind speeds between 15 and 50 km/hour, has a low frequency of less than 1 Hz, but amplitudes exceeding 10 metres. Fatigue failure to spacers is one of the chief causes for damage to insulators and conductors.

Wake-induced oscillation, also called "flutter instability", is caused when one conductor on the windward side aerodynamically shields the leeward conductor. To cause this type of oscillation, the leeward conductor must be positioned at rest towards the limits of the wake or windshadow of the windward conductor. The oscillation occurs when the bundle tilts 5 to 15° with respect to a flat ground surface. Therefore, a gently sloping ground with this angle can create conditions favourable to wake-induced oscillations. The conductor spacing to diameter ratio in the bundle is also critical. If the spacing B is less than $15d$, d being the conductor diameter, a tendency to oscillate is created while for $B/d > 15$ the bundle is found to be more stable. As mentioned earlier, the electrical design, such as calculating the surface voltage gradient on the conductors, will depend upon these mechanical considerations.

2.6.5 Dampers and Spacers

When the wind energy imparted to the conductor achieves a balance with the energy dissipated by the vibrating conductor, steady amplitudes for the oscillations occur. A damping device helps to achieve this balance at smaller amplitudes of aeolian vibrations than an undamped conductor. The damper controls the intensity of the wave-like properties of travel of the oscillation and provides an equivalent heavy mass which absorbs the energy in the wave. A sketch of a Stockbridge damper is shown in Fig. 2.2.

A simpler form of damper is called the Armour Rod, which is a set of wires twisted around the line conductor at the insulator supporting conductor and hardware, and extending for about 5 metres on either side. This is used for small conductors to provide a change in mechanical impedance. But for heavier conductors, weights must be used, such as the Stockbridge, which range from 5 kg for conductors of 2.5 cm diameter to 14 kg for 4.5 cm. Because of the steel strands inside them ACSR conductors have better built-in property against oscillations than ACAR conductors.

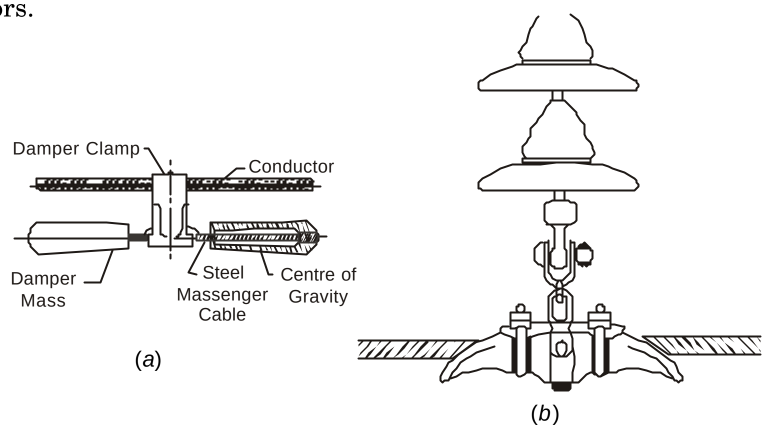

Fig. 2.2 (*a*) Stockbridge Damper; (*b*) Suspension Clamp (Courtesy: Electrical Manufacturing Co., Calcutta).

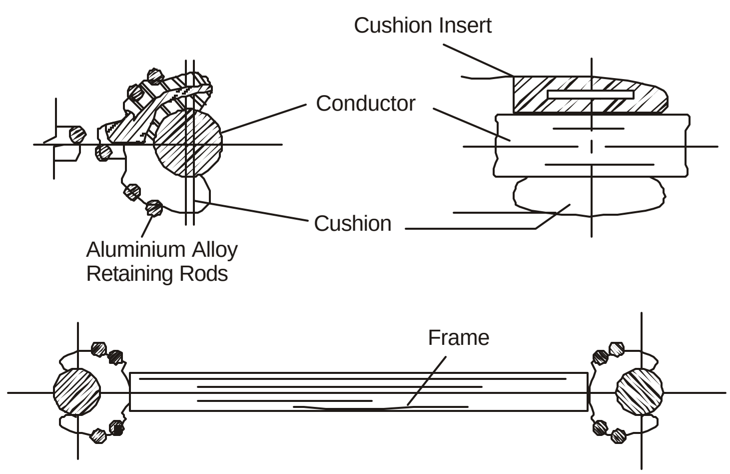

Fig. 2.3 Spacer for two-conductor bundle (Courtesy: EMC, Calcutta).

3

Calculation of Line and Ground Parameters

3.1 RESISTANCE OF CONDUCTORS

Conductors used for e.h.v. transmission lines are always stranded. Most common conductors use a steel core for reinforcement of the strength of aluminium, but recently high tensile strength aluminium is being increasingly used, replacing the steel. The former is known as ACSR (Aluminium Conductor Steel Reinforced) and the latter ACAR (Aluminium Conductor Alloy Reinforced). A recent development is the AAAC (All Aluminium Alloy Conductor) which consists of alloys of Al, Mg, Si. This has 10 to 15% less loss than ACSR. When a steel core is used, because of its high permeability and inductance, power-frequency current flows only in the aluminium strands. In ACAR and AAAC conductors, the cross-section is better utilized. Fig. 3.1 shows an example of a stranded conductor.

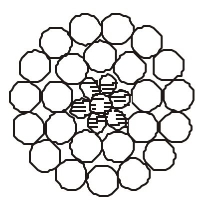

Fig 3.1 Cross-section of typical ACSR conductor.

If n_s = number of strands of aluminium, d_s = diameter of each strand in metre and ρ_a = specific resistance of Al, ohm-m, at temperature t, the resistance of the stranded conductor per km is

$$R = \rho_a \; 1.05 \times 10^3/(\pi d_s^2 n_s /4) = 1337 \; \rho_a / d_s^2 n_s \text{, ohms} \qquad ...(3.1)$$

The factor 1.05 accounts for the twist or lay whereby the strand length is increased by 5%.

Example 3.1. A Drake conductor of North-American manufacture has an outer diameter of 1.108 inches having an Al cross-sectional area of 795,000 circular mils. The stranding is 26 Al/7 Fe. Its resistance is given as 0.0215 ohm/1000′ at 20°C under dc, and 0.1284 ohm/mile at 50°C and 50/60 Hz. Calculate.

(*a*) diameter of each strand of Al and Fe in mils, inch, and metre units;

(*b*) check the values of resistances given above taking $\rho_a = 2.7 \times 10^{-8}$ ohm-metre at 20°C and temperature-resistance coefficient $\alpha = 4.46 \times 10^{-3}$/°C at 20°C.

(*c*) find increase in resistance due to skin effect.

Note. 1 inch = 1000 mils; 1 in^2 = $(4/\pi) \times 10^6$ cir-mils;

10^6 cir-mils = $(\pi/4) \times 2.54^2$ sq. cm. = 5.067 sq. cm.

Solution: Area of each strand of Al = 795,000/26 = 30,577 cm.

(*a*) Diameter of each strand, $d_s = \sqrt{30{,}577}$ = 175 mils = 0.175 inch

= 0.4444 cm = 0.00444 m

Referring to Fig. 3.1, there are 4 strands of Al along any diameter occupying 700 mils. The 3 diameters of Fe occupy 1108 – 700 = 408 mils since the overall dia. of the conductor is 1.108″ = 1108 mils.

Therefore, diameter of each steel strand = 408/3 = 136 mils = 0.136″ = 0.3454 cm

(*b*) Because of the high permeability of steel, the steel strands do not carry current. Then, for 1000 feet,

$$R_a = 2.7/10^{-8}\ (1000 \times 1.05/3.28)/\left[\frac{\pi}{4} \times (4.444 \times 10^{-3})^2 \times 26\right]$$

= 0.02144 ohm.

This is close to 0.0215 ohm/1000′

$$\text{At } 50°\text{C}, \ \rho_{50} = \frac{1 + 4.46 \times 10^{-3} \times 50}{1 + 4.46 \times 10^{-3} \times 20}\ \rho_{20} = 1.123\ \rho_{20}$$

$\therefore$ $R_{50} = 1.123 \times 0.0215 \times 5.28 = 0.1275$ ohm/mile.

(*c*) Increase in resistance due to skin effect at 50/60 Hz is

0.1284 – 0.1275 = 0.0009 ohm = 0.706%.

3.1.1 Effect of Resistance of Conductor

The effect of conductor resistance of e.h.v. lines is manifested in the following forms:

(1) Power loss in transmission caused by I^2R heating;

(2) Reduced current-carrying capacity of conductor in high ambient temperature regions. This problem is particularly severe in Northern India where summer temperatures in the plains reach 50°C. The combination of intense solar irradiation of conductor combined with the I^2R heating raises the temperature of Aluminium beyond the maximum allowable temperature which stands at 65°C as per Indian Standards. At an ambient of 48°C, even the solar irradiation is sufficient to raise the temperature to 65°C for 400 kV line, so that no current can be carried. If there is improvement in material and the maximum temperature raised to 75°C, it is estimated that a current of 600 amperes can be transmitted for the same ambient temperature of 48°C.

(3) The conductor resistance affects the attenuation of travelling waves due to lightning and switching operations, as well as radio-frequency energy generated by corona. In these cases, the resistance is computed at the following range of frequencies: Lightning—100 to 200 kHz; Switching—1000-5000 Hz; Radio frequency—0.5 to 2 MHz.

We shall consider the high-frequency resistance later on.

3.1.2 Power Loss in Transmission

In Chapter 2, average resistance values were given in Table 2.1. For various amounts of power transmitted at e.h.v. voltage levels, the I^2R heating loss in MW are shown in Table 3.1 below. The power factor is taken as unity. In every case the phase angle difference $\delta = 30°$ between E_s and E_r.

Table 3.1. I^2R Loss in MW of E.H.V. Lines

System kV	400	750	1000	1200
Resistance, ohm/km	0.031	0.0136	0.0036	0.0027
Power Transmitted		*I^2R Loss, MW*		
1,000 MW	48	25	7.8	5.84
2,000	96	50	15.6	11.68
5,000	240	125	39	29.2
10,000	480	250	78	58.4
20,000	960	500	156	116.8

We notice the vast reduction in MW loss occurring with increase in transmission voltage for transmitting the same power. The above calculations are based on the following equations:

(1) Current: $I = P/\sqrt{3}V$ ...(3.2)

(2) Loss: $p = 3I^2R = P^2R/V^2$ ...(3.3)

(3) Total resistance: $R = L.r$, ...(3.4)

where L = line length in km,

and r = resistance per phase in ohm/km.

(4) Total above holds for $\delta = 30°$. For any other power-angle the loss is

$$p = 3I^2rL = E^2r \sin^2 \delta /(L.x^2) \quad ...(3.5)$$

where x = positive-sequence reactance of line per phase.

3.1.3 Skin Effect Resistance in Round Conductors

It was mentioned earlier that the resistance of overhead line conductors must be evaluated at frequencies ranging from power frequency (50/60 Hz) to radio frequencies up to 2 MHz or more. With increase in frequency, the current tends to flow nearer the surface resulting in a decrease in area for current conduction. This gives rise to increase in effective resistance due to the 'Skin Effect'. The physical mechanism for this effect is based on the fact that the inner filaments of the conductors link larger amounts of flux as the centre is approached which causes an increase in reactance. The reactance is proportional to frequency so that the impedance to current flow is larger in the inside, thus preventing flow of current easily. The result is a crowding of current at the outer filaments of the conductor. The increase in resistance of a stranded conductor is more difficult to calculate than that of a single round solid conductor because of the close proximity of the strands which distort the magnetic field still further. It is easier to determine the resistance of a stranded conductor by experiment at the manufacturer's premises for all conductor sizes manufactured and at various frequencies.

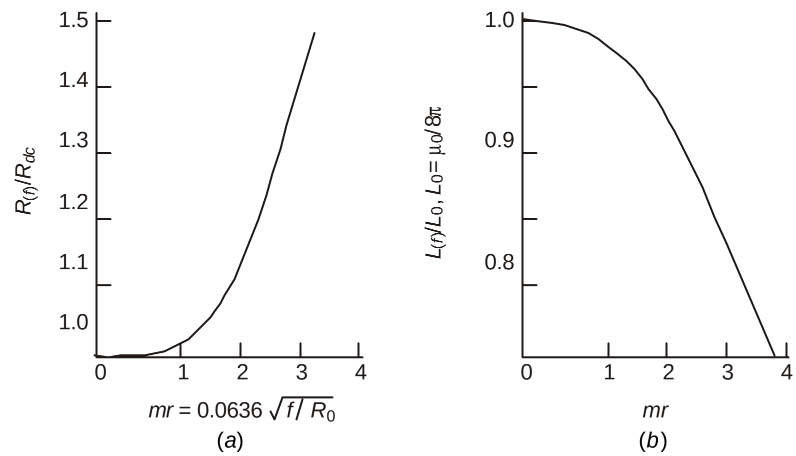

Fig. 3.2 Variation with frequency parameter (mr) of (a) skin effect resistance ratio $R_{ac}(f)/R_{dc}$ and (b) skin effect inductance $L(f)/L_0$, with $L_0 = \mu_0/8\pi$, the inductance with uniform current distribution in round conductor.

In this section, a method of estimating the ratio $R_{ac}(f)/R_{dc}$ will be described. The rigorous formulas involve the use of Bessel Functions and the resistance ratio has been tabulated or given in the form of curves by the National Bureau of Standards, Washington, several decades ago. Figure 3.2(a) shows some results where the ordinate is R_{ac}/R_{dc} at any frequency f and the abscissa is $X = mr = 0.0636\ \sqrt{f/R_0}$, where R_0 is the dc resistance of conductor in ohms/mile. When using SI units, $X = 1.59 \times 10^{-3}\ \sqrt{f/R_m}$, where R_m = dc resistance in ohm/metre.

Example 3.2. A Moose conductor has a resistance of 62 milli-ohm/km. Using Fig. 3.2(a), determine the highest frequency for which the graph is applicable for a round conductor.

Solution. Maximum value of X = 4 = $0.0636\ \sqrt{f/R_0}$.

Now, $R_0 = 62 \times 10^{-3} \times 1.609 = 0.1$

Therefore $f = (X/0.0636)^2 R_0 \approx 400$ Hz.

For other frequencies the functional relationship between $R_{ac}(f)/R_{dc}$ is as follows:

Let
$$\text{Ber}(X) = 1 - \frac{X^4}{2^2.4^2} + \frac{X^8}{2^2.4^2.6^2.8^2} \cdots$$

$$\text{Bei}(X) = \frac{X^2}{2^2} - \frac{X^6}{2^2.4^2.6^2} + \frac{X^{10}}{2^2.4^2.6^2.8^2.10^2} \cdots \qquad \text{...(3.6)}$$

$$\text{B}'\text{er}(X) = d\ \text{Ber}(X)/dX,\ \text{B}'\text{ei}(X) = d\ \text{Bei}(X)/dX$$

Then,
$$\frac{R_{ac}(f)}{R_{dc}} = \left(\frac{X}{2}\right)\frac{\text{Ber}(X).\text{B}'\text{ei}(X) - \text{Bei}(X).\text{B}'\text{er}(X)}{[\text{B}'\text{er}(X)]^2 + [\text{B}'\text{ei}(X)]^2} \qquad \text{...(3.7)}$$

The Bessel Functions are tabulated and values from there must be used [see H.B. Dwight: Mathematical Tables (Dover Publications) pages 194 onwards]. The following example will illustrate the increase in resistance of a round copper conductor up to a frequency of 100 kHz.

Example 3.3. A round 7/0 copper conductor 0.5″ (12.7 mm) in dia. has $\rho = 1.7 \times 10^{-8}$ ohm-m at 20°C. Calculate the variation of R_{ac}/R_{dc} as a function of frequency up to 10^5 Hz.

Solution. $R_0 = 1.7 \times 10^{-8} \times 1609/(\pi \times 12.7^2 \times 10^{-6}/4) = 0.216$ ohm/mile

$\therefore \quad 0.0636/\sqrt{R_0} = 0.0137.$

We will use a logarithmic increase for frequency;

f	100	300	600	1000	3000	6000	10^4	3×10^4	6×10^4	10^5
$X = 0.0137\sqrt{f}$	.137	.237	.335	.4326	.749	1.06	1.37	2.37	3.35	4.326
R_{ac}/R_{dc}	$1 + 0.37 \times 10^{-5}$	$1 + 0.4 \times 10^{-4}$	$1 + .8 \times 10^{-4}$	$1 + .8 \times 10^{-3}$	1.0017	1.0066	1.0182	1.148	1.35	1.8

1.0000037, 1.00004, 1.00008, 1.0008

[These values are taken from N.B.S. Tables and T. and D. Reference Book (Westinghouse)].

3.2 TEMPERATURE RISE OF CONDUCTORS AND CURRENT-CARRYING CAPACITY

When a conductor is carrying current and its temperature has reached a steady value, heat balance requires

$$\begin{pmatrix}\text{Internal Heat}\\ \text{Developed by } I^2R\end{pmatrix} + \begin{pmatrix}\text{External Heat Supplied}\\ \text{by Solar Irradiation}\end{pmatrix}$$

$$= \begin{pmatrix}\text{Heat Lost by}\\ \text{Convection to Air}\end{pmatrix} + \begin{pmatrix}\text{Heat Lost by}\\ \text{Radiation}\end{pmatrix} \quad \text{...(3.8)}$$

Let $W_i = I^2R$ heating in watts/metre length of conductor

W_s = solar irradiation ,, ,, ,, ,,

W_c = convection loss ,, ,, ,, ,,

and W_r = radiation loss ,, ,, ,, ,,

Then the heat balance equation becomes

$$W_i + W_s = W_c + W_r \quad \text{...(3.9)}$$

Each of these four terms depends upon several factors which must be written out in terms of temperature, conductor dimensions, wind velocity, atmospheric pressure, current, resistance, conductor surface condition, etc. It will then be possible to find a relation between the temperature rise and current. The maximum allowable temperature of an Al conductor is 65°C at present, but will be increased to 75°C . Many countries in the world have already specified the limit as 75°C above which the metal loses its tensile strength. The four quantities given above are as follows:

(1) I^2R *heating*. $W_i = I^2R_m$ watts/metre where, R_m = resistance of conductor per metre length at the maximum temperature.

$$R_m = \frac{1+\alpha t}{1+20\alpha} R_{20}.$$

with α = temperature resistance coefficient in ohm/°C and R_{20} = conductor resistance at 20°C.

(2) *Solar irradiation.*

$$W_s = s_a.I_s.d_m \text{ watts/metre}$$

where d_m = diametre of conductor in metre, s_a = solar absorption coefficient = 1 for black body or well-weathered conductor and 0.6 for new conductor, and I_s = solar irradiation intensity in watts/m^2.

At New Delhi in a summer's day at noon, I_s has a value of approximately 1000-1500 W/m^2.

[**Note:** 10^4 calories/sq. cm/day = 4860 watts/m^2]

(3) *Convection loss.*

$$w_c = 5.73 \sqrt{p\, v_m / d_m}.\Delta t, \text{ watts/m}^2$$

where p = pressure of air in atmospheres, v_m = wind velocity in metres/sec.,

and Δt = temperature rise in °C above ambient = $t - t_a$.

Since 1 metre length of conductor has an area of πd_m sq. m., the convection loss is

$$W_c = 18.\Delta t.\sqrt{p.v_m.d_m} \text{ , watts/metre}$$

(4) *Radiation loss.* This is given by Stefan-Boltzmann Law

$$W_r = 5.702 \times 10^{-8}\, e(T^4 - T_a^4), \text{ watts/m}^2$$

where e = relative emissivity of conductor-surface = 1 for black body and 0.5 for oxidized Al or Cu, T = conductor temperature in °K = 273 + t and T_a = ambient temperature in °K = 273 + t_a.

The radiation loss per metre length of conductor is

$$W_r = 17.9 \times 10^{-8}\, e(T^4 - T_a^4)\, d_m, \text{ watt/m.}$$

Equation (3.9) for the heat balance then becomes

$$I^2R_m + s_a I_s d_m = 18\ \Delta t\sqrt{p.v_m.d_m} + 17.9.e.d_m\left[\left(\frac{T}{100}\right)^4 - \left(\frac{T_a}{100}\right)^4\right] \quad ...(3.10)$$

Example 3.4. A 400-kV line in India uses a 2-conductor bundle with d_m = 0.0318 m for each conductor. The phase current is 1000 Amps (500 Amps per conductor). The area of each conductor is 515.7 mm^2, $\rho_a = 2.7 \times 10^{-8}$ ohm-m at 20°C, α = 0.0045 ohm/°C at 20°. Take the ambient temperature t_a = 40°C, atmospheric pressure p = 1, wind velocity v_m = 1 m/s, e = 0.5 and neglect solar irradiation. Calculate the final temperature of conductor due only to I^2R heating.

Solution. Let the final temperature = t°C.

Then, $$R_m = 2.7 \times 10^{-8}\ \frac{1+0.0045\times t}{1+0.0045\times 20}\ \frac{1.05}{515.7\times 10^{-6}}$$

$$= 0.5 \times 10^{-4}\ (1 + 0.0045t), \text{ ohm/m}$$

Therefore, $$W_t = I^2R_m = 12.5\ (1 + 0.0045t), \text{ watts/m}$$

$$W_c = 18\sqrt{1\times 0.0318}.(t-40) = 3.21(t-40), \text{watts/m}$$

$$W_r = 17.9 \times 0.5 \times 0.0318 \left[\left(\frac{273 + t}{100}\right)^4 - \left(\frac{273 + 40}{100}\right)^4\right]$$

$$= 0.2845 \{[(273 + t)/100]^4 - 95.95\}.$$

Using equation (3.9), the equation for t comes out as

$$12.5 (1 + 0.0045t) = 3.21t + 0.2845 \times 10^{-8} (273 + t)^4 - 155.7$$

or, $$(273 + t)^4 = (590 - 11.28t)\, 10^8.$$

A trial and error solution yields $t \approx 44°C$. (At this final temperature, we can calculate the values of the three heats which are $I^2R_m = 14.38$, $W_c = 12.84$, and $W_r = 1.54$, watts/m.).

Example. 3.5 In the previous example, calculate the final temperature (or temperature rise) if the solar irradiation adds (*a*) 10 watts/m, and (*b*) 1160 W/m^2 giving a contribution of 37 watts/m to the conductor.

Solution. By going through similar procedure, the answers turn out to be

(*a*) $t = 45.5°C$, $\Delta t = 5.5°C$;

(*b*) $t = 54.1°C$, $\Delta t = 14.1°C$.

We observe that had the ambient temperature been 50°C, the temperature rise would reach nearly the maximum. This is left as an exercise at the end of the chapter.

3.3 PROPERTIES OF BUNDLED CONDUCTORS

Bundled conductors are exclusively used for e.h.v. transmission lines. Only one line in the world, that of the Bonneville Power Administration in the U.S.A., has used a special expanded ACSR conductor of 2.5 inch diameter for their 525 kV line. Fig. 3.3 shows examples of conductor configurations used for each phase of ac lines or each pole of a dc line.

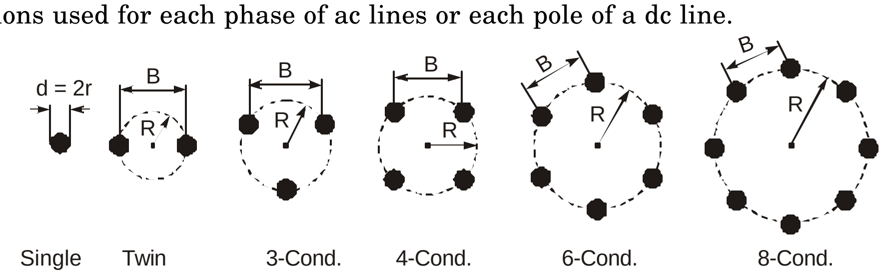

Fig. 3.3 Conductor configurations used for bundles in e.h.v. lines.

As of now a maximum of 18 sub-conductors have been tried on experimental lines but for commercial lines the largest number is 8 for 1150-1200 kV lines.

3.3.1 Bundle Spacing and Bundle Radius (or Diameter)

In almost all cases, the sub-conductors of a bundle are uniformly distributed on a circle of radius R. There are proposals to space them non-uniformly to lower the audible noise generated by the bundle conductor, but we will develop the relevant geometrical properties of an N-conductor bundle on the assumption of uniform spacing of the sub-conductors (Fig. 3.4). It is also reported that the flashover voltage of a long airgap is increased when a non-uniform spacing for sub-conductors is used for the phase conductor.

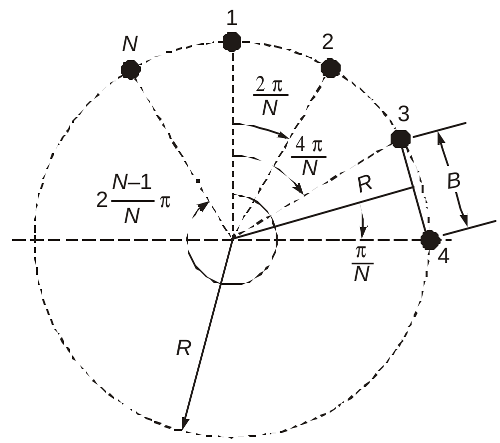

Fig. 3.4 Bundle spacing B, and bundle radius R.

The spacing between adjacent sub-conductors is termed 'Bundle Spacing' and denoted by B. The radius of the pitch circle on which the sub-conductors are located will be called the 'Bundle Radius', denoted as R. The radius of each sub-conductor is r with diameter d. The angle sub-tended at the centre by adjacent sub-conductors is (2π/N) radians, and it is readily seen that

$$\frac{B}{2} = R \sin(\pi/N) \text{ giving } R = B/2 \sin(\pi/N) \qquad ...(3.11)$$

For N = 2 to 18, the following table gives (R/B) and (B/R).

N =	2	3	4	6	8	12	18
R/B =	0.5	0.578	0.7071	1	1.308	1.874	2.884
B/R =	2	$\sqrt{3}$	$\sqrt{2}$	1	0.7654	0.5344	0.3472

3.3.2 Geometric Mean Radius of Bundle (Equivalent Radius)

Except for calculating the surface voltage gradient from the charge of each sub-conductor, for most other calculations the bundle of N-sub-conductors can be replaced by a single conductor having an equivalent radius. This is called the 'Geometric Mean Radius' or simply the 'Equivalent Radius.' It will be shown below that its value is

$$r_{eq} = (N.r.R^{N-1})^{1/N} = r[N.(R/r)^{N-1}]^{1/N} = R(N.r/R)^{1/N} \qquad ...(3.12)$$

It is the Nth root of the product of the sub-conductor radius r', and the distance of this sub-conductor from all the other (N – 1) companions in the bundle. Equation (3.12) is derived as follows:

Referring to Fig. 3.4, the product of (N – 1) mutual distances is

$$\left(2R\sin\frac{\pi}{N}\right)\left(2R\sin\frac{2\pi}{N}\right)\left(2R\sin\frac{3\pi}{N}\right)....\left(2R\sin\frac{N-1}{N}\pi\right)$$

$$= (2R)^{N-1}\left(\sin\frac{\pi}{N}\right)\left(\sin\frac{2\pi}{N}\right)....\left(\sin\frac{N-1}{N}\pi\right)$$

$$r_{eq} = \left[r.(2R)^{N-1} \sin\frac{\pi}{N}.\sin\frac{2\pi}{N} \cdots \sin\frac{N-1}{N}\pi\right]^{1/N} \quad ...(3.13)$$

For $N = 2,\ r_{eq} = (2rR)^{1/2}$

For $N = 3,\ r_{eq} = \left(2^2 R^2 .r.\sin\frac{\pi}{3}.\sin\frac{2\pi}{3}\right)^{1/3} = (3rR^2)^{1/3}$

For $N = 4,\ r_{eq} = \left(2^3 .R^3 .r.\sin\frac{\pi}{4}.\sin\frac{2\pi}{4}.\sin\frac{3\pi}{4}\right)^{1/4} = (4rR^3)^{1/4}$

For $N = 6,\ r_{eq} = \left(2^5 .R^5 .r.\sin\frac{\pi}{6}.\sin\frac{2\pi}{6} \cdots \sin\frac{5\pi}{6}\right)^{1/6} = (6.r.R^5)^{1/6}$

This is equation (3.12) where the general formula is $r_{eq} = (N.r.R^{N-1})^{1/N}$.

The reader should verify the result for N = 8, 12, 18.

Example 3.6 The configurations of some e.h.v. lines for 400 kV to 1200 kV are given. Calculate r_{eq} for each.

(*a*) 400 kV : $N = 2$, $d = 2r = 3.18$ cm, $B = 45$ cm

(*b*) 750 kV : $N = 4$, $d = 3.46$ cm, $B = 45$ cm

(*c*) 1000 kV : $N = 6$, $d = 4.6$ cm, $B = 12\ d$

(*d*) 1200 kV : $N = 8$, $d = 4.6$ cm, $R = 0.6$ m

Solution. The problem will be solved in different ways.

(*a*) $r_{eq} = \sqrt{r.B} = (1.59 \times 45)^{1/2} = 8.46$ cm = 0.0846 m

(*b*) $r_{eq} = [4 \times 1.73 \times (45/\sqrt{2})^3]^{1/4} = 21.73$ cm = 0.2173 m

(*c*) $r_{eq} = [6 \times 2.3 \times 55.2^5]^{1/6} = 43.81$ cm = 0.4381 m

Also, $r_{eq} = 55.2\ (6 \times 2.3/55.2)^{1/6} = 43.81$ cm

(*d*) $r_{eq} = 60\ (8 \times 2.3/60)^{1/8} = 51.74$ cm = 0.5174 m

We observe that as the number of sub-conductors increases, the equivalent radius of bundle is approaching the bundle radius. The ratio r_{eq}/R is $(Nr/R)^{1/N}$. The concept of equivalent bundle radius will be utilized for calculation of inductance, capacitance, charge, and several other line parameters in the sections to follow.

3.4 INDUCTANCE OF E.H.V. LINE CONFIGURATIONS

Fig. 3.5 shows several examples of line configuration used in various parts of the world. They range from single-circuit (S/C) 400 kV lines to proposed 1200 kV lines. Double-circuit (D/C) lines are not very common, but will come into practice to save land for the line corridor. As pointed out in chapter 2, one 750 kV circuit can transmit as much power as 4-400 kV circuits and in those countries where technology for 400 kV level exists there is a tendency to favour the four-circuit 400 kV line instead of using the higher voltage level. This will save on import of equipment from other countries and utilize the know-how of one's own country. This is a National Policy and will not be discussed further.

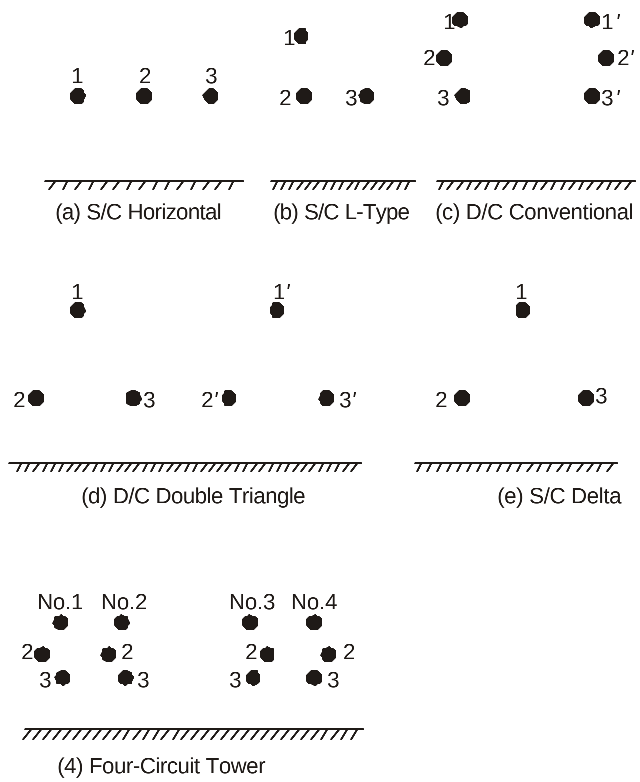

Fig. 3.5 E.h.v. line configurations used.

3.4.1 Inductance of Two Conductors

We shall very quickly consider the method of handling the calculation of inductance of two conductors each of external radius r and separated by a distance D which forms the basis for the calculation of the matrix of inductance of multi-conductor configurations.

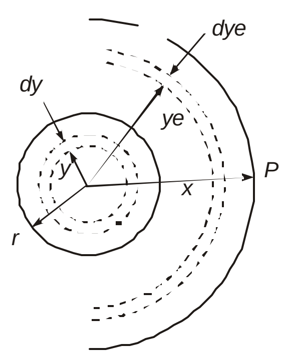

Fig. 3.6 Round conductor with internal and external flux linkages.

4

Voltage Gradients of Conductors

4.1 ELECTROSTATICS

Conductors used for e.h.v. transmission lines are thin long cylinders which are known as 'line charges'. Their charge is described in coulombs/unit length which was used for evaluating the capacitance matrix of a multiconductor line in Chapter 3. The problems created by charges on the conductors manifest themselves as high electrostatic field in the line vicinity from power frequency to *TV* frequencies through audio frequency, carrier frequency and radio frequency (*PF, AF, CF, TVF*). The attenuation of travelling waves is also governed in some measure by the increase in capacitance due to corona discharges which surround the space near the conductor with charges. When the macroscopic properties of the electric field are studied, the conductor charge is assumed to be concentrated at its centre, even though the charge is distributed on the surface. In certain problems where proximity of several conductors affects the field distribution, or where conducting surfaces have to be forced to become equipotential surfaces (in two dimensions) in the field of several charges it is important to replace the given set of charges on the conductors with an infinite set of charges. This method is known as the Method of Successive Images. In addition to the electric-field properties of long cylinders, there are other types of important electrode configurations useful for extra high voltage practice in the field and in laboratories. Examples of this type are sphere-plane gaps, sphere-to-sphere gaps, point-to-plane gaps, rod-to-plane gaps, rod-rod gaps, conductor-to-tower gaps, conductor-to-conductor gap above a ground plane, etc. Some of these types of gaps will also be dealt with in this chapter which may be used for e.h.v. measurement, protection, and other functions. The coaxial-cylindrical electrode will also be discussed in great detail because of its importance in corona studies where the bundle of *N* sub-conductors is strung inside a 'cage' to simulate the surface voltage gradient on the conductors in a setup which is smaller in dimensions than an actual outdoor transmission line.

4.1.1 Field of a Point Charge and Its Properties

The properties of electric field of almost all electrode geometries will ultimately depend on that of a point charge. The laws governing the behaviour of this field will form the basis for extending them to other geometries. Consider Figure 4.1 which shows the source point S_1 where a point charge + Q coulombs is located. A second point charge q coulomb is located at S_2 at a distance r metre from S_1. From Coulomb's Law, the force acting on either charge is

$$F = Q.q/4\pi e_0 e_r r^2, \text{ Newton} \qquad ...(4.1)$$

$$[e_0 = (\mu_0 g^2)^{-1} = 1000/36\pi\mu\mu F/m = 8.84194\ \mu\mu F/m$$

$$e_r = \text{relative permittivity of the medium = 1 in air]}$$

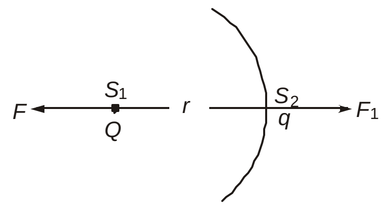

Fig. 4.1 Point charge Q and force on test charge q.

Where q is very small $(q \to 0)$, we define the electric field produced by Q at the location of q as

$$E = \lim_{q \to 0} (F/q) = Q/4\pi e_0 e_r r^2, \text{ Newton/Coulomb} \qquad ...(4.2)$$

The condition $q \to 0$ is necessary in order that q might not disturb the electric field of Q. Equation (4.2) may be re-written as

$$(4\pi r^2)(e_0 e_r E) = 4\pi r^2 D = Q \qquad ...(4.3)$$

Here we note that $4\pi r^2$ = surface are of a sphere of radius r drawn with centre at S_1. The quantity $D = e_0 e_r E$ is the dielectric flux density. Thus, we obtain Gauss's Law which states that 'the surface integral of the normal component of dielectric flux density over a closed surface equals the total charge in the volume enclosed by the surface'. This is a general relation and is valid for all types of electrode geometries.

Some important properties of the field of a point charge can be noted:

(*a*) The electric field intensity decreases rapidly with distance from the point charge inversely as the square of the distance, $(Q \propto 1/r^2)$.

(*b*) E is inversely proportional to $e_r.(E \propto 1/e_r)$.

(*c*) The potential of any point in the field of the point charge Q, defined as the work done against the force field of Q in bringing q from ∞ to S_2, is

$$\psi = \int_{\infty}^{r} -E dr = \frac{Q}{4\pi e_0 e_r} \int_{\infty}^{r} -\frac{dr}{r^2} = \frac{Q}{4\pi e_0 e_r} \frac{1}{r}, \text{ volt} \qquad ...(4.4)$$

(*d*) The potential difference between two points at distances r_1 and r_2 from S_1 will be

$$\psi_{12} = \frac{Q}{4\pi e_0 e_r}\left(\frac{1}{r_1} - \frac{1}{r_2}\right), \text{ volt} \qquad ...(4.5)$$

For a positive point charge, points closer to the charge will be at a higher positive potential than a further point.

(*e*) The capacitance of an isolated sphere is

$$C = Q/\psi = 4\pi e_0 e_r r, \text{ Farad} \qquad ...(4.6)$$

This is based on the assumption that the negative charge of – Q is at infinity.

These properties and concepts can be extended in a straightforward manner to apply to the field of a line charge and other electrode configurations.

Example 4.1. A point charge $Q = 10^{-6}$ coulomb (1 μC) is kept on the surface of a conducting sphere of radius r = 1 cm, which can be considered as a point charge located at the centre of the sphere. Calculate the field strength and potential at a distance of 0.5 cm from the surface of the sphere. Also find the capacitance of the sphere, $\varepsilon_r = 1$.

Solution. The distance of S_2 from the centre of the sphere S_1 is 1.5 cm.

$$E = 10^{-6} \bigg/ \left[4\pi \times \frac{1000}{36\pi} \times 10^{-12} \times 1.5^2 \times 10^{-4}\right]$$

$$= 10^{-6}/(0.25 \times 10^{-13})$$

$$= 40 \times 10^6 \text{ V/m} = 40 \text{ MV/m} = 400 \text{ kV/cm}$$

$$\Psi = E.r = 600 \text{ kV [using equations 4.2 and 4.4]}$$

$$C = 4\pi e_0 e_r r = 1.111\ \mu\mu F \text{ with } r = 0.01.$$

Example 4.2. The field strength on the surface of a sphere of 1 cm radius is equal to the corona-inception gradient in air of 30 kV/cm. Find the charge on the sphere.

Solution. 30 kV/cm = 3000 kV/m = 3×10^6 V/m.

$$3 \times 10^6 = Q_0 \bigg/ \left[4\pi \times \frac{1000}{36\pi} \times 10^{-12} \times 10^{-4}\right]$$

$$= 9 \times 10^{13} Q_0$$

giving $Q_0 = 3.33 \times 10^{-8}$ coulomb = 0.033 μC.

The potential of the sphere is

$$V = 3 \times 10^6 \times 10^{-2} = 30 \text{ kV.}$$

4.2 FIELD OF SPHERE GAP

A sphere-sphere gap is used in h.v. laboratories for measurement of extra high voltages and for calibrating other measuring apparatus. If the gap spacing is less than the sphere radius, the field is quite well determined and the sphere-gap breaks down consistently at the same voltage with a dispersion not exceeding ±3%. This is the accuracy of such a measuring gap, if other precautions are taken suitably such as no collection of dust or proximity of other grounded objects close by. The sphere-gap problem also illustrates the method of successive images used in electrostatics.

Figure 4.2 shows two spheres of radii R separated by a centre-centre distance of S, with one sphere at zero potential (usually grounded) and the other held at a potential V. Since both spheres are metallic, their surfaces are equipotentials. In order to achieve this, it requires a set of infinite number of charges, positive inside the left sphere at potential V and negative inside the right which is held at zero potential. The magnitude and position of these charges will be determined from which the voltage gradient resulting on the surfaces of the sphere on a line joining the centres can be determined. If this exceeds the critical disruptive voltage, a spark break-down will occur. The voltage required is the breakdown voltage.

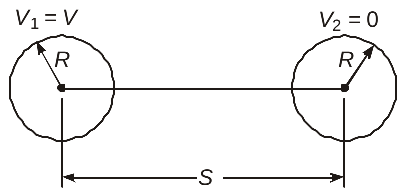

Fig. 4.2 The sphere gap.

Consider two point charges Q_1 and Q_2 located with a separation D, Figure 4.3. At a point $P(x, y)$ with coordinates measured from Q_1, the potentials are as follows:

Potential at P due to Q_1 $= \dfrac{Q_1}{4\pi e_0}\dfrac{1}{r_1}$ with $r_1 = \sqrt{x^2 + y^2}$

Potential at P due to Q_2 $= \dfrac{Q_2}{4\pi e_0}\dfrac{1}{r_2}$ with $r_2 = \sqrt{(D - x)^2 + y^2}$

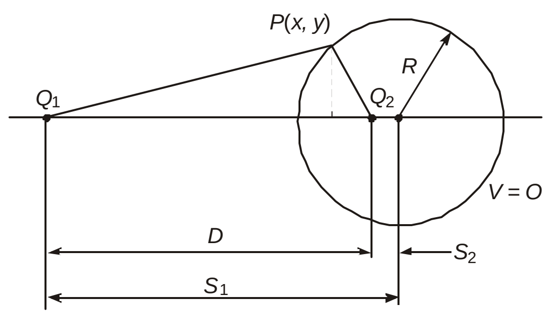

Fig. 4.3 Point charge Q_1 and sphere of radius R.

The total potential at P is $V_P = \dfrac{1}{4\pi e_0}(Q_1/r_1 + Q_2/r_2)$.

If this is to be zero, then $Q_2/Q_1 = -r_2/r_1$ ... (4.7)

This clearly shows that Q_1 and Q_2 must be of opposite polarity.

From (4.7), $r_2^2/r_1^2 = \dfrac{(D-x)^2 + y^2}{x^2 + y^2} = Q_2^2/Q_1^2$, giving

$$\left\{x - \frac{D}{1-(Q_2/Q_1)^2}\right\}^2 + y^2 = D^2(Q_2/Q_1)^2/\{1-(Q_2/Q_1)^2\}^2 \quad \text{...(4.8)}$$

This is an equation to a circle in the two-dimensional plane and is a sphere in three-dimensional space.

$$R = D(Q_2/Q_1)/\{1-(Q_2/Q_1)^2\} \quad \text{...(4.9)}$$

This requires Q_2 to be less than Q_1 if the denominator is to be positive. The centre of the zero-potential surface is located at $(S_1, 0)$, where

$$S_1 = D/\{1-(Q_2/Q_1)^2\} = \frac{Q_1}{Q_2}R \quad \text{...(4.10)}$$

This makes $$S_2 = S_1 - D = \frac{D(Q_2/Q_1)^2}{1-(Q_2/Q_1)^2} = \frac{Q_2}{Q_1}R \qquad ...(4.11)$$

Therefore, the magnitude of Q_2 in relation to Q_1 is

$$Q_2 = Q_1\frac{S_2}{R} = Q_1\frac{R}{S_1} \qquad ...(4.12)$$

Also, $$S_1S_2 = R^2 \qquad ...(4.13)$$

These relations give the following important property:

'Given a positive charge Q_1 and a sphere of radius R, with Q_1 located external to the sphere, whose centre is at a distance S_1 from Q_1, the sphere can be made to have a zero potential on its surface if a charge of opposite polarity and magnitude $Q_2 = (Q_1R/S_1)$ is placed at a distance $S_2 = R^2/S_1$ from the centre of the given sphere towards Q_1.'

Example 4.3. A charge of 10 μC is placed at a distance of 2 metres from the centre of a sphere of radius 0.5 metre (1-metre diameter sphere). Calculate the magnitude, polarity, and location of a point charge Q_2 which will make the sphere at zero potential.

Solution. $R = 0.5$, $S_1 = 2$ $\quad\therefore\quad S_2 = R^2/S_1 = 0.125$ m

$$Q_2 = Q_1R/S_1 = 10 \times 0.5/2 = 2.5\,\mu C$$

The charge Q_2 is of opposite sign to Q_1. Figure 4.4 shows the sphere, Q_1 and Q_2.

Example 4.4. An isolated sphere in air has a potential V and radius R. Calculate the charge to be placed at its centre to make the surface of the sphere an equipotential.

Solution. From equation (4.4), $Q = 4\pi e_0 VR$.

$S_2 = 0.125$ m $= R^2/S$

$Q_2 = -2.5$ μc $= Q_1R/S$

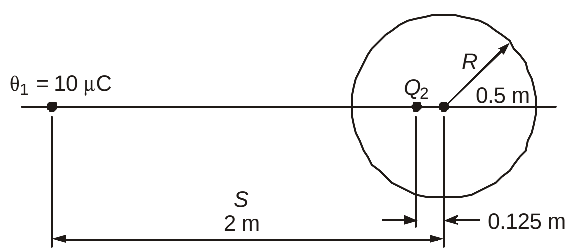

Fig. 4.4 Location of image charge Q_2 inside sphere to make sphere potential zero.

We now are in a position to analyze the system of charges required to make one sphere at potential V and a second sphere at zero potential as is the case in a sphere-sphere gap with one sphere grounded. Figure 4.5 shows the two spheres separated by the centre-centre distance S. The sphere 1 at left has potential V and that at right zero potential. Both spheres have equal radii R.

In order to hold sphere 1 at potential V, a charge $Q_1 = 4\pi e_0 VR$ must be placed at its centre. In the field of this charge, sphere 2 at right can be made a zero potential surface if an image charge Q_2 is placed inside this sphere. From the discussion presented earlier,

$Q_2 = -Q_1R/S$ and $S_2 = R^2/S$, as shown in Figure 4.5. However, locating Q_2 will disturb the potential of sphere 1. In order to keep the potential of sphere 1 undisturbed, we must locate an image charge $Q_1' = -Q_2R/(S - S_2)$ inside sphere 1 so that in the field of Q_2 and Q_1' the potential of sphere 1 is zero leaving its potential equal to V due to Q_1. The charge Q_1' is located at $S_1' = R^2/(S - S_2)$ from Q_1 (centre of sphere 1). It is now easy to see that the presence of Q_1' will disturb the potential of sphere 2. An image charge $Q_2' = -Q_1'R/(S - S_1')$ is called for inside sphere 2 located at $S_2' = R^2/(S - S_1')$ from the centre of sphere 2.

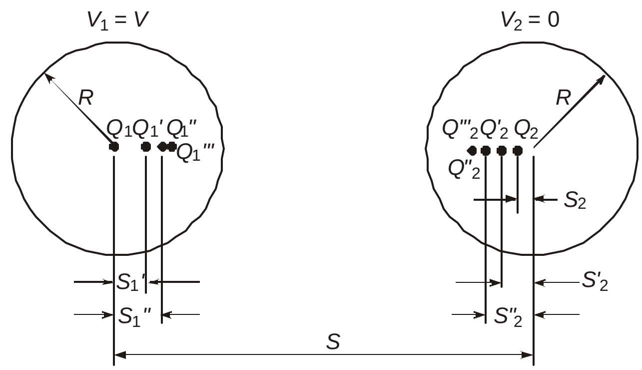

Fig. 4.5. Location of successive image charges to maintain spheres at potentials V and zero.

Successive image charges will have to be suitably located inside both spheres.

The sequence of charges and their locations can be tracked in a tabular form.

$$\left.\begin{aligned}
& Q_1 = 4\pi e_0 VR, Q_1' = -Q_2R/(S - S_2), Q_1'' = -Q_2'R/(S - S_2'). \\
& \qquad\qquad Q_1''' = -Q_2''R/(S - S_2''), \text{etc.} \\
& \text{(From centre of sphere 1)} \\
& S_1' = R^2/(S - S_2), S_1'' = R^2/(S - S_2'), S_1''' = R^2/(S - S_2''), \text{etc.} \\
& Q_2 = -Q_1R/S, Q_2' = -Q_1'R/(S - S_1'), Q_2'' = -Q_1''R/(S - S_1''), \\
& \qquad\qquad Q_2''' = -Q_1'''R/(S - S_1'''), \text{etc.} \\
& \text{(From centre of sphere 2)} \\
& S_2 = R^2/S, S_2' = R^2/(S - S_1'), S_2'' = R^2/(S - S_1''), \\
& \qquad\qquad S_2''' = R^2/(S - S_1''') \text{etc.}
\end{aligned}\right\} \qquad ...(4.14)$$

Example 4.5. A sphere gap consists of two spheres with $R = 0.25$ m each. The gap between their surfaces is 0.5 m. Calculate the charges and their locations to make the potentials 1 and 0.

Solution. The distance S between centres of the spheres = 1 m.

$$R^2/S = 0.25^2/1 = 0.0625 \text{ m}$$

Charges inside sphere 1		*Charges inside sphere* 2	
$V = 1$		$V = 0$	
Magnitude	*Distance from centre of sphere* 1	*Magnitude*	*Distance from centre of sphere* 2
$Q_1 = \pi e_0$	$S_1 = 0$	$Q_2 = -0.25\,Q_1$	$S_2 = 0.0625$ m
$Q_1' = \dfrac{0.25^2 Q_1}{1-.0625} = .0667Q_1$	$S_1' = \dfrac{0.25^2}{1-.0625} = 0.06667$	$Q_2' = \dfrac{-.0667Q_1 \times 0.25}{1-.067} = -0.01786Q_1$	$S_2' = \dfrac{0.25^2}{1-.0667} = 0.067$
$Q_1'' = \dfrac{0.01786\,Q_1 \times 0.25}{1-.067} = 0.00478Q_1$	$S_1'' = \dfrac{0.25^2}{1-.067} = 0.067$	$Q_2'' = \dfrac{-0.0487\,Q_1 \times 0.25}{1-.067} = -0.00128Q_1$	$S_2'' = 0.067$
$Q_1''' = 0.000344Q_1$	$S_1''' = 0.067.$		

Note that further calculations will yield extremely small values for the image charges. Furthermore, they are all located almost at the same points. The charges reduce successively in the ratio 0.25/0.933 = 0.268; i.e. $Q_2^n = -0.268Q_1^n$ and $Q_1^{n+1} = -0.268\,Q_2^n$. The electric field at any point X along the line joining the centres of the two spheres is now found from the expression

$$E = \frac{Q_1}{4\pi e_0}\frac{1}{X^2} + \frac{Q_1'}{4\pi e_0}\frac{1}{(X - S_1')^2} + \frac{Q_1''}{4\pi e_0}\frac{1}{(X - S_1'')^2} + $$

$$- \frac{Q_2}{4\pi e_0}\frac{1}{(S - X - S_2)^2} - \frac{Q_2'}{4\pi e_0}\frac{1}{(S - X - S_2')^2} - \frac{Q_2''}{4\pi e_0}\frac{1}{(S - X - S_2'')^2} \cdots \quad ...(4.15)$$

Since Q_2, Q_2', Q_2'' etc., are opposite in polarity to Q_1, Q_1', Q_1'' etc., the force on a unit test charge placed at X will be in the same direction due to all charges. The most important value of X is $X = R$ on the surface of sphere 1. If the value of E at $X = R$ exceeds the critical gradient for breakdown of air (usually 30 kV/cm peak at an air density factor $\delta = 1$), the gap breakdown commences.

Example 4.6. Calculate the voltage gradient at X = 0.25 m for the sphere gap in Example 4.5.

Solution. S = 1 m, $X = R$ = 0.25 m, $S - X$ = 0.75 m

$$E = \frac{Q_1}{4\pi e_0}\left[\frac{1}{0.25^2} + \frac{0.0667}{(0.25-0.067)^2} + \frac{0.00478}{(0.25-0.067)^2} + \ldots\right]$$

$$+ \frac{Q_1}{4\pi e_0}\left[\frac{0.25}{(0.75-0.065)^2} + \frac{0.01786}{(0.75-0.067)^2} + \frac{0.00128}{(0.75-0.067)^2} + \ldots\right]$$

$$= \frac{Q_1}{4\pi e_0}[18.12 + 0.573] = 18.693\,\frac{Q_1}{4\pi e_0}, \text{with } Q_1 = \pi e_0$$

= 4.673 V/m per volt

The contribution of charges inside the grounded sphere amount to

$$\frac{0.573}{18.693} \times 100 = 3.06\%$$

Example 4.7. In the previous example calculate the potential difference between the spheres for E = 30 kV/cm = 3000 kV/m, peak.

Solution. V = 3000/4.673 kV = 642 kV

Thus, the 0.5 metre diameter spheres with a gap spacing of 0.5 metre experience disruption at 642 kV, peak. The breakdown voltage is much higher than this value.

Sphere-Plane Gap

When a sphere of radius R and potential V is placed above a ground plane at zero potential, the problem is similar to the sphere-to-sphere gap problem. It is clear that in order to place zero potential on the plane, an image sphere with potential – V is necessary. The problem is first solved with the given sphere at + V and the image sphere at 0 potential, then keeping the image sphere at – V and the given sphere at 0 potential. The system of charges required will now be the same as with the sphere-to-sphere gap but the total charge inside the given sphere and its image are equal and amount to the sum of the charges $Q_1, Q_1', Q_1'', Q_2, Q_2', Q_2'' \ldots$ with all charges having the same sign. Their locations are also the same as before. Charges inside the given sphere have positive polarity and those inside the image sphere are negative.

4.3 FIELD OF LINE CHARGES AND THEIR PROPERTIES

Figure 4.6 shows a line charge of q coulomb/metre and we will calculate the electric field strength, potential, etc., in the vicinity of the conductor. First, enclose the line charge by a Gaussian cylinder, a cylinder of radius r and length 1 metre. On the flat surfaces the field will not have an outward normal component since for an element of charge dq located at S, there can be found a corresponding charge located at S' whose fields (force exerted on a positive test charge) on the flat surface F will yield only a radial component. The components parallel to the line charge will cancel each other out. Then, by Gauss's Law, if E_p = field strength normal to the curved surface at distance r from the conductor,

$$(2\pi r)(e_0 e_r E_p) = q \qquad \ldots(4.16)$$

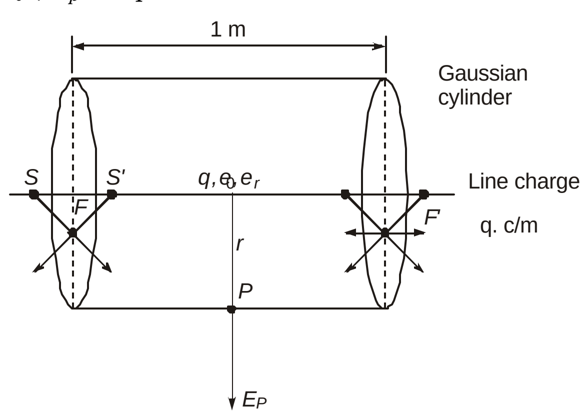

Fig. 4.6 Line charge with Gaussian cylinder.

The field strength at a distance r from the conductor is

$$E_p = (q/2\pi e_0 e_r)(1/r), \text{ Volts/metre} \qquad \ldots(4.17)$$

This is called the $(1/r)$-field as compared to the $(1/r^2)$-field of a point charge.

Let a reference distance r_0 be chosen in the field. Then the potential difference between any point at distance r and the reference is the work done on a unit test charge from r_0 to r.

Thus,
$$V_r = \frac{q}{2\pi e_0 e_r}\int_{r_0}^{r} -\frac{1}{\rho}d\rho = \frac{q}{2\pi e_0 e_r}(\ln r_0 - \ln r) \qquad ...(4.18)$$

In the case of a line charge, the potential of a point in the field with respect to infinity cannot be defined as was done for a point charge because of logarithmic term. However, we can find the p.d. between two points at distances r_1 and r_2, since

(p.d. between r_1 and r_2) = (p.d. between r_1 and r_0) – (p.d. between r_2 and r_0)

i.e.
$$V_{12} = \frac{q}{2\pi e_0 e_r}(\ln r_2 - \ln r_1) = \frac{q}{2\pi e_0 e_r}\ln\frac{r_2}{r_1} \qquad ...(4.19)$$

In the field of a positive line charge, points nearer the charge will be at a higher positive potential than points farther away ($r_2 > r_1$).

The potential (p.d. between two points, one of them being taken as reference r_0) in the field of a line charge is logarithmic. Equipotential lines are circles. In a practical situation, the charge distribution of a transmission line is closed, there being as much positive charge as negative.

4.3.1 2-Conductor Line: Charges + *q* and – *q*

Consider a single-phase line, Figure 4.7, showing two parallel conductors each of radius ρ separated by centre-to-centre distance of $2d$ with each conductor carrying a charge of q coulombs/metre but of opposite polarities. Place a unit test charge at point P at a distance X from the centre of one of the conductors. Then the force acting on it is the field strength at X, which is

$$E_p = \frac{q}{2\pi e_0 e_r}\left(\frac{1}{X} + \frac{1}{2d - X}\right) \text{ Newton/coulomb or V/m} \qquad ...(4.20)$$

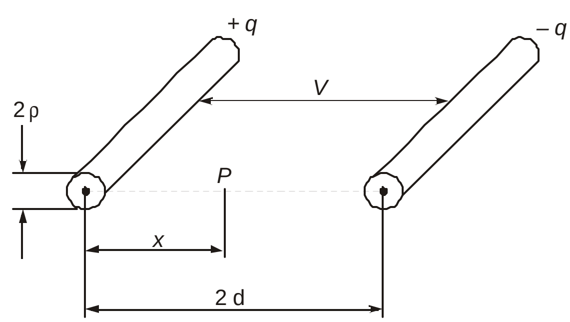

Fig. 4.7 Single-phase line.

The potential difference between the conductors is

$$V = \frac{q}{2\pi e_0 e_r}\int_{\rho}^{2d-\rho}\left(\frac{1}{X} + \frac{1}{2d - X}\right)dX$$

$$= \frac{q}{\pi e_0 e_r}\ln\frac{2d - \rho}{\rho} \approx \frac{q}{\pi e_0 e_r}\ln\frac{2d}{\rho}, \text{ if } 2d \gg \rho \qquad ...(4.21)$$

Hence, the capacitance of 1 metre length of both conductors is

$$C = q/V = \pi e_0 e_r / \ln(2d/\rho) \qquad ...(4.22)$$

On the surface of any one of the conductors, the voltage gradient is, from equations (4.20) and (4.21)

$$E = \frac{q}{2\pi e_0 e_r}\left(\frac{1}{\rho} + \frac{1}{2d-\rho}\right) \approx \frac{V}{2\rho \ln(2d/\rho)} \qquad ...(4.23)$$

This is true on the basis of neglecting the effect of the charge of the other conductor if it is far away to make the separation between conductors much greater than their radii.

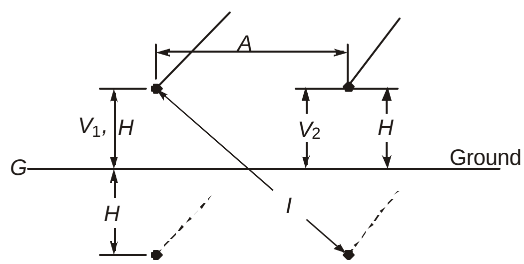

Fig. 4.8 Two-conductor line above ground plane and image conductors.

A transmission line in practice is strung above a ground plane and we observed in Chapter 3 that its effect can be taken into account by placing image charges, as shown in Figure 4.8. The charges on the aerial conductors are q_1 and q_2 coulombs/metre and their potentials with respect to ground are V_1 and V_2. Then,

$$\left.\begin{aligned} V_1 &= \frac{q_1}{2\pi e_0 e_r}\ln(2H_1/\rho_1) + \frac{q_2}{2\pi e_0 e_1}\ln(I_{12}/A_{12}) \\ V_2 &= \frac{q_1}{2\pi e_0 e_r}\ln(I_{12}/A_{12}) + \frac{q_2}{2\pi e_0 e_r}\ln(2H_2/\rho_2) \end{aligned}\right\} \qquad ...(4.24a)$$

In matrix form,

$$\begin{bmatrix} V_1 \\ V_2 \end{bmatrix} = \begin{bmatrix} \ln(2H_1/\rho_1), \ln(I_{12}/A_{12}) \\ \ln(I_{12}/A_{12}), \ln(2H_2/\rho_2) \end{bmatrix} \begin{bmatrix} q_1/2\pi e_0 e_r \\ q_2/2\pi e_0 e_r \end{bmatrix} \qquad ...(4.24b)$$

or $$[V] = [P][q/2\pi e_0 e_r] \qquad ...(4.24c)$$

The elements of [*P*] are Maxwell's Potential Coefficients which we have encountered in Chapter 3. For a single-phase line above ground, $V_1 = -V_2 = V$. Also, let $H_1 = H_2 = H$ and $\rho_1 = \rho_2 = \rho$. Then obviously, $q_1 = -q_2 = q$. Let $A_{12} = A$.

$$V = \frac{q}{2\pi e_0 e_r}[\ln(2H/\rho) - \ln(\sqrt{4H^2 + A^2}/A)]$$

$$= \frac{q}{2\pi e_0 e_r}\ln[2HA/\rho\sqrt{4H^2 + A^2}], \text{Volts} \qquad ...(4.25)$$

This gives the capacitance per unit length of each conductor to ground to be

$$C_g = q/V = 2\pi e_0 e_r / [\ln(A/\rho) - \ln(\sqrt{4H^2 + A^2}/2H)], \text{Farads} \qquad ...(4.26)$$

The capacitance between the two conductors is one-half of this since the two capacitances to ground are in series. Comparing equations (4.26) and (4.22) with $2d = A$, we observe that in the presence of ground, the capacitance of the system has been increased slightly because the denominator of (4.26) is smaller than that in (4.22).

The charging current of each conductor is

$$I_c = 2\pi f C_g V, \text{Amperes} \qquad ...(4.27)$$

and the charging reactive power is

$$Q_c = 2\pi f C_g V^2, \text{Vars} \qquad ...(4.28)$$

Example 4.8. A single-conductor e.h.v. transmission line strung above ground is used for experimental purposes to investigate high-voltage effects. The conductor is expanded ACSR with diameter of 2.5 inches (0.0635 m) and the line height is 21 metres above ground.

(*a*) Calculate the voltage to ground which will make its surface voltage gradient equal to corona-inception gradient given by Peek's Formula:

$$E_{or} = \frac{30}{\sqrt{2}}\frac{1}{m}\left(1+\frac{0.301}{\sqrt{\rho}}\right),$$ kV/cm, r.m.s., where m = 1.3 required for stranding effect, and the conductor radius is in cm.

(*b*) Find the charging current and MVAR of the single-phase transformer for exciting 1 km length of the experimental line.

Solution. Refer to Figure 4.9. ρ = 0.03175 m = 3.175 cm.

From equation (4.24) and in the absence of a second conductor,

$$V = \frac{q}{2\pi e_0}\ln(2H/\rho) \text{ and } E = \frac{q}{2\pi e_0}\frac{1}{\rho}$$

Now, $$E_{or} = \frac{30\times 10^2}{1.3\sqrt{2}}\left(1+\frac{0.301}{\sqrt{3.175}}\right) = 1907.4 \text{ kV/m}$$

(*a*) V = 1907.4 × 0.03175 × ln (42/0.03175) = 435.4 kV, r.m.s.

(*b*) Capacitance $C_g = qL/V = 2\pi e_0 L/\ln(2H/\rho)$ = 7.747 nF/km

Charging current at 50 Hz is

$$I_c = 2\pi \times 50 \times 7.747 \times 10^{-9} \times 435.4 \times 10^3 \, A$$
$$= 1.06 \text{ Ampere}$$

Charging kVAR Q_c = 1.06 × 435.4 = 461.5.

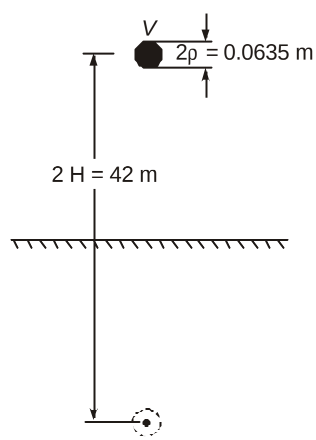

Fig. 4.9 Single-phase experimental line above ground for Example 4.8

The design of such an experimental 1 km line with 2.5 inch diameter conductor strung at an average height of 21 m above ground will need a 500 kV single-phase transformer rated for 1.1 A and 550 kVAR. In all such experimental projects, a research factor of 1.3 may be required so that the actual rating may be 565 kV at 1.38 A giving nearly 750 kVA.

4.4 CHARGE-POTENTIAL RELATIONS FOR MULTI-CONDUCTOR LINES

Section 3.5 in the last Chapter 3, equations (3.38) to (3.40) describe the charge-potential relations of a transmission line with n conductors on a tower. The effect of a ground plane considered as an equipotential surface gave rise to Maxwell's Potential coefficients and the general equations are

$$[V] = [P][Q/2\pi e_0] \qquad ...(4.29)$$

where the elements of the three matrices are, for $i, j = 1, 2, ..., n$

$$\left.\begin{aligned} &[V] = [V_1, V_2, V_3, ..., V_n]_t \\ &[Q/2\pi e_0] = (1/2\pi e_0)[Q_1, Q_2, ..., Q_n]_t \\ &P_{ii} = \ln(2H_i/r_{eq}(i)), P_{ij} = \ln(I_{ij}/A_{ij}), i \neq j \end{aligned}\right\} \qquad ...(4.30)$$

The equivalent radius or geometric mean radius of a bundled conductor has already been discussed and is

$$r_{eq} = R(N.\ r/R)^{1/N} \qquad ...(4.31)$$

where R = bundle radius = $B/2 \sin(\pi/N)$,

B = bundle spacing (spacing between adjacent conductors)

r = radius of each sub-conductor,

and N = number of conductors in the bundle.

The elements of Maxwell's potential coefficients are all known since they depend only on the given dimensions of the line-conductor configuration on the tower. In all problems of interest in e.h.v. transmission, it is required to find the charge matrix from the voltage since this is also known. The charge-coefficient matrix is evaluated as

$$[Q/2\pi e_0] = [P]^{-1}[V] = [M][V] \qquad ...(4.32)$$

or, if the charges themselves are necessary,

$$[Q] = 2\pi e_0[M][V] \qquad ...(4.33)$$

In normal transmission work, the quantity $Q/2\pi e_0$ occurs most of the time and hence equation (4.32) is more useful than (4.33). The quantity $Q/2\pi e_0$ has units of volts and the elements of both $[P]$ and $[M] = [P]^{-1}$ are dimensionless numbers.

On a transmission tower, there are p phase conductors or poles and one or two ground wires which are usually at or near ground potential. Therefore, inversion of $[P]$ becomes easier and more meaningful if the suitable rows and columns belonging to the ground wires are eliminated. An example in the Appendix illustrates the procedure to observe the effect of ground wires on the line-conductor charges, voltage gradients, etc. On a 3-phase ac line, the phase voltages are varying in time so that the charges are also varying at 50 Hz or power frequency. This will be necessary in order to evaluate the electrostatic field in the line vicinity. But for Radio Noise and Audible Noise calculations, high-frequency effects must be considered under suitable types of excitation of the multiconductors. Similarly, lightning and switching-surge studies also require unbalanced excitation of the phase and ground conductors.

4.4.1 Maximum Charge Condition on a 3-Phase Line

E.H.V. transmission lines are mostly single-circuit lines on a tower with one or two ground wires. For preliminary consolidation of ideas, we will restrict our attention here to 3 conductors excited by a balanced set of positive-sequence voltages under steady state. This can be extended to other line configurations and other types of excitation later on. The equation for the charges is,

$$\frac{1}{2\pi e_0}\begin{bmatrix} Q_1 \\ Q_2 \\ Q_3 \end{bmatrix} = \begin{bmatrix} M_{11}, & M_{12}, & M_{13} \\ M_{21}, & M_{22}, & M_{23} \\ M_{31}, & M_{32}, & M_{33} \end{bmatrix}\begin{bmatrix} V_1 \\ V_2 \\ V_3 \end{bmatrix} \quad ...(4.34)$$

For a 3-phase ac line, we have

$$V_1 = \sqrt{2}V \sin(wt + \phi),$$

$$V_2 = \sqrt{2}V \sin(wt + \phi - 120°)$$

and $V_3 = \sqrt{2}V \sin(wt + \phi + 120°)$ with

V = r.m.s. value of line-to-ground voltage and $w = 2\pi f$,

f = power frequency in Hz. The angle ϕ denotes the instant on V_1 where $t = 0$. If $wt + \phi$ is denoted as θ, there results

$$Q_1/2\pi e_0 = \sqrt{2}V[M_{11}\sin\theta + M_{12}\sin(\theta - 120°) + M_{13}\sin(\theta + 120°)]$$

$$= \sqrt{2V}[\{M_{11} - 0.5(M_{12} + M_{13})\}\sin\theta + 0.866(M_{13} - M_{12})\cos\theta] \quad ...(4.35)$$

Differentiating with respect to θ and equating to zero gives

$$\frac{d}{d\theta}(Q_1/2\pi e_0) = 0$$

$$= \sqrt{2}V[(M_{11} - 0.5M_{12} - 0.5M_{13})\cos\theta - \frac{\sqrt{3}}{2}(M_{13} - M_{12})\sin\theta]$$

This gives the value of $\theta = \theta_m$ at which Q_1 reaches its maximum or peak value. Thus,

$$\theta_m = \arctan[\sqrt{3}(M_{13} - M_{12})/(2M_{11} - M_{12} - M_{13})]^{-1} \quad ...(4.36)$$

Substituting this value of θ in equation (4.35) yields the maximum value of Q_1.

An alternative procedure using phasor algebra can be devised. Expand equation (4.35) as

$$Q_1/2\pi e_0 = \sqrt{2}V\sqrt{(M_{11} - .5M_{12} - .5M_{13})^2 + 0.75(M_{13} - M_{12})^2}\sin(\theta + \psi) \quad ...(4.37)$$

The amplitude or peak value of $Q_1/2\pi e_0$ is

$$(Q_1/2\pi e_0)_{\max} = \sqrt{2}V[M_{11}^2 + M_{12}^2 + M_{13}^2 - (M_{11}M_{12} + M_{12}M_{13} + M_{13}M_{11})]^{1/2} \quad ...(4.38)$$

It is left as an exercise to the reader to prove that substituting θ_m from equation (4.36) in equation (4.35) gives the amplitude of $(Q_1/2\pi e_0)_{\max}$ in equation (4.38).

Similarly for Q_2 we take the elements of 2nd row of [M].

$$(Q_2/2\pi e_0)_{\max} = \sqrt{2}V[M_{22}^2 + M_{21}^2 + M_{23}^2 - (M_{21}M_{22} + M_{22}M_{23} + M_{23}M_{21})]^{1/2} \quad ...(4.39)$$

For Q_3 we take the elements of the 3rd row of [M].

$$(Q_3/2\pi e_0)_{\max} = \sqrt{2}V[M_{33}^2 + M_{31}^2 + M_{32}^2 - (M_{31}M_{32} + M_{31}M_{33} + M_{33}M_{31})]^{1/2} \quad ...(4.40)$$

The general expression for any conductor is, for i = 1, 2, 3,

$$(Q_i/2\pi e_0)_{\max} = \sqrt{2}V[M_{i1}^2 + M_{i2}^2 + M_{i3}^2 - (M_{i1}M_{i2} + M_{i2}M_{i3} + M_{i3}M_{i1})]^{1/2} \quad ...(4.41)$$

4.4.2 Numerical Values of Potential Coefficients and Charge of Lines

In this section, we discuss results of numerical computation of potential coefficients and charges present on conductors of typical dimensions from 400 kV to 1200 kV whose configurations are given in Chapter 3, Figure 3.5. For one line, the effect of considering or neglecting the presence of ground wires on the charge coefficient will be discussed, but in a digital-computer programme the ground wires can be easily accommodated without difficulty. In making all calculations we must remember that the height H_i of conductor i is to be taken as the average height. It will be quite adequate to use the relation, as proved later,

$$H_{av} = H_{\min} + \text{Sag}/3 \quad ...(4.42)$$

*Average Line Height for Inductance Calculation**

The shape assumed by a freely hanging cable of length L_c over a horizontal span S between supports is a catenary. We will approximate the shape to a parabola for deriving the average height which holds for small sags. Figure 4.10 shows the dimensions required. In this figure,

H = minimum height of conductor at midspan

S = horizontal span,

and d = sag at midspan.

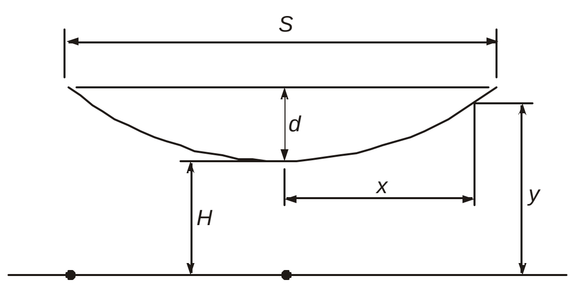

Fig. 4.10 Calculation of average height over a span S with sag d.

The equation to the parabolic shape assumed is

$$y = H + (4d/S^2)\,x^2 \quad ...(4.43)$$

The inductance per unit length at distance x from the point of minimum height is

$$L = 0.2 \ln (2y/r) = 0.2\,[\ln 2y - \ln r] \quad ...(4.44)$$

Since the height of conductor is varying, the inductance also varies with it.

The average inductance over the span is

$$L_{av} = \frac{1}{S}\int_{-S/2}^{S/2} 0.2(\ln 2y - \ln r)\,dx$$

*The author is indebted to Ms. S. Ganga for help in making this analysis.

$$= \frac{0.4}{S}\int_0^{S/2}(\ln 2y - \ln r)dx \quad \text{...(4.45)}$$

Now, $\ln 2y = \ln (2H + 8dx^2/S^2) = \ln (8d/S^2) + \ln (x^2 + S^2H/4d)$ ...(4.46)

Let $a^2 = S^2H/4d$. Then,

$$\ln(8d/S^2) + \frac{2}{S}\int_0^{S/2}\ln(x^2 + a^2)dx = \ln[(1 + H/d)\,S^2/4]$$

$$-2 + 2\sqrt{H/d}\tan^{-1}\sqrt{d/H} + \ln(8d/S^2)$$

$$= \ln 2d + \ln(1 + H/d) - 2 + 2\sqrt{H/d}\tan^{-1}\sqrt{d/H} \quad \text{...(4.47)}$$

If the right-hand side can be expressed as $\ln (2\,H_{av})$, then this gives the average height for inductance calculation. We now use some numerical values to show that H_{av} is approximately equal to

$$\left(H + \frac{1}{3}d\right) = H_{min} + \frac{1}{3}\text{Sag}$$

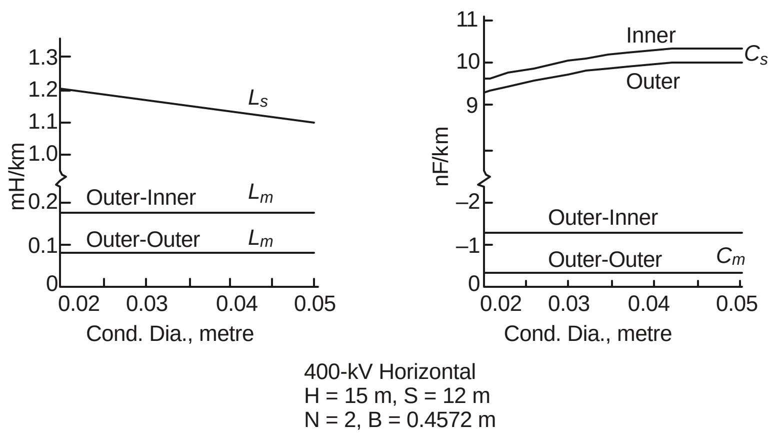

Fig. 4.11 Inductances and capacitances of 400 kV horizontal line.

(*a*) Consider $H = 10$, $d = 10$. Using these in equation (4.47) give

$\ln 20 + \ln (1 + 1) - 2 + 2 \tan^{-1} 1 = 3 + 0.6931 - 2 + \pi/2 = 3.259 = \ln 26 = \ln(2\,H_{av})$

$H_{av} = 26/2 = 13 = 10 + 3 = H + 0.3d$

(*b*) $H = 10$, $d = 8$. $\ln 16 + \ln 2.25 - 2 + 2\sqrt{1.25}\tan^{-1}\sqrt{0.8} = \ln 24.9$

$H_{av} = 12.45 = H + 2.45 = H + 0.306d$

(*c*) $H = 14$, $d = 10$. $H_{av} = 17.1 = 14 + 3.1 = H + 0.3d$

These examples appear to show that a reasonable value for average height is $H_{av} = H_{min} +$ sag/3. A rigorous formulation of the problem is not attempted here.

Figure 4.11, 4.12 and 4.13 show inductances and capacitances of conductors for typical 400 kV, 750 kV and 1200 kV lines.

4.5 SURFACE VOLTAGE GRADIENT ON CONDUCTORS

The surface voltage gradient on conductors in a bundle governs generation of corona on the line which have serious consequences causing audible noise and radio interference. They also affect carrier communication and signalling on the line and cause interference to television reception. The designer of a line must eliminate these nuisances or reduce them to tolerable limits specified by standards, if any exist. These limits will be discussed at appropriate places where AN, RI and other interferring fields are discussed in the next two chapters. Since corona generation depends on the voltage gradient on conductor surfaces, this will be taken up now for e.h.v. conductors with number of sub-conductors in a bundle ranging from 1 to N. The maximum value of N is 8 at present but a general derivation is not difficult.

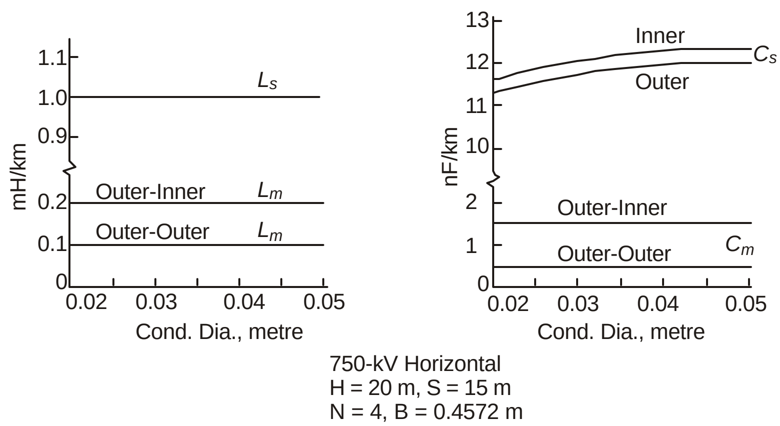

Fig. 4.12. L and C of 750 kV horizontal line.

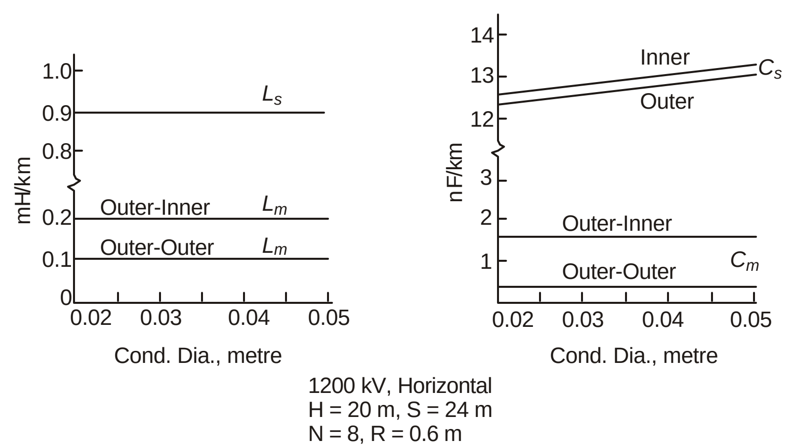

Fig. 4.13 L and C of 1200 kV horizontal line.

4.5.1 Single Conductor

Figure 4.9 can be used for a single conductor whose charge is q coulomb/metre. We have already found the line charges or the terms $(Q_i/2\pi e_0)$ in terms of the voltages V_i and the Maxwell's Potential Coefficient matrix $[P]$ and its inverse $[M]$, where $i = 1, 2, ..., n$, the number of conductors on a tower. For the single conductor per phase or pole, the surface voltage gradient is

$$E_c = \frac{q}{2\pi e_0}\frac{1}{r} \text{ volts/metre} \quad \text{...(4.48)}$$

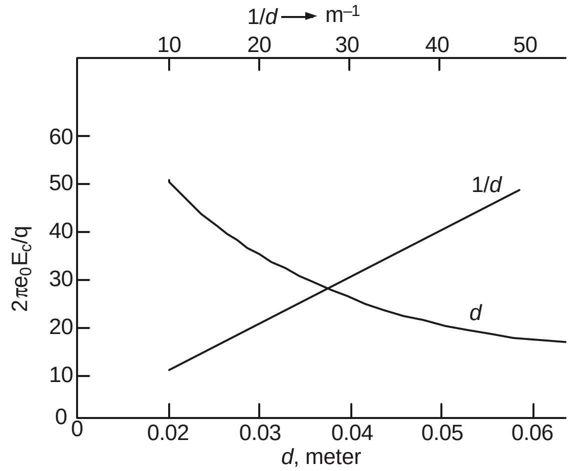

Fig. 4.14 Voltage gradient of single conductor.

This is plotted in Figure 4.14 as a function of conductor diameters ranging from 0.02 to 0.065 m. The largest single conductor manufactured is 2.5 inches (0.0635 m) in diameter for the B.P.A. 525 kV line in the U.S.A. In terms of voltage to ground, $V = \frac{q}{2\pi e_0}\ln(2H/r)$ so that

$$E_c = \frac{V}{r.\ln(2H/r)} \text{ volts/metre} \quad \text{...(4.49)}$$

The factor $E_c/(q/2\pi e_0)$ is also plotted against the reciprocal of diameter and yields approximately a straight line.

4.5.2 2-Conductor Bundle (Figure 4.15)

In this case, the charge Q obtained from equation (4.33) is that of the total bundle so that the charge of each sub-conductor per unit length is $q = Q/2$. This will form one phase of an ac line or a pole of a dc line. In calculating the voltage gradient on the surface of a sub-conductor, we will make the following assumptions:

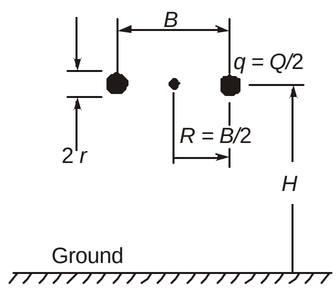

Fig. 4.15 2-conductor bundle above ground for voltage gradient calculation.

(1) The conductors of the other phases or poles are very far from the bundled conductor under examination, *i.e.* $S \gg B$ or $2R$.

(2) The image conductors are also very far, i.e. $2H \gg B$ or $2R$.

This allows us to ignore all other charges except that of the conductors in the bundle. Now, by definition, the electric field intensity is the force exerted on a unit positive test charge placed at the point where the field intensity is to be evaluated, which in this case is a point on the sub-conductor surface. Consider point P_i on the inside of the bundle, Figure 4.16. The force on a test charge is

E_i = Force due to conductor charge – Force due to the charge on second conductor of bundle.

At the point P_0 on the outside of the bundle, the two forces are directed in the same sense. It is clear that it is here that the maximum surface voltage gradient occurs.

Now, the force due to conductor charge = $\dfrac{q}{2\pi e_0}\dfrac{1}{r}$. In computing the force due to the charge of the other sub-conductor there is the important point that the conductors are metallic. When a conducting cylinder is located in the field of a charge, it distorts the field and the field intensity is higher than when it is absent. If the conducting cylinder is placed in a uniform field of a charge q, electrostatic theory shows that stress-doubling occurs on the surface of the metallic cylinder. In the present case, the left cylinder is placed at a distance B from its companion at right. Unless $B \gg r$, the field is non-uniform. However, for the sake of calculation of surface voltage gradients on sub-conductors in a multi-conductor bundle, we will assume that the field is uniform and stress-doubling takes place. Once again, this is a problem in successive images but will not be pursued here.

Therefore, $E_i = \dfrac{q}{2\pi e_0}\left(\dfrac{1}{r} - \dfrac{2}{B}\right) = \dfrac{q}{2\pi e_0}.\dfrac{1}{r}(1 - r/R)$

$$= \frac{Q}{2\pi e_0}\frac{1}{2}.\frac{1}{r}(1 - r/R) \qquad \text{...(4.50)}$$

where Q = total bundle charge.

On the other hand, at point P_0 on the outside of bundle

$$E_0 = \frac{Q}{2\pi e_0}\frac{1}{2}\frac{1}{r}(1 + r/R) \qquad \text{...(4.51)}$$

These are the minimum and maximum values, and they occur at $\theta = \pi$ and $\theta = 0$. The average is $E_{av} = \dfrac{Q}{2\pi e_0}\dfrac{1}{2}\dfrac{1}{r}$. The variation of surface voltage gradient on the periphery can be approximated to a cosine curve

$$E(\theta) = \frac{Q}{2\pi e_0}\frac{1}{2}\frac{1}{r}\left(1 + \frac{r}{R}\cos\theta\right) = E_{av}\left(1 + \frac{r}{R}\cos\theta\right) \qquad \text{...(4.52)}$$

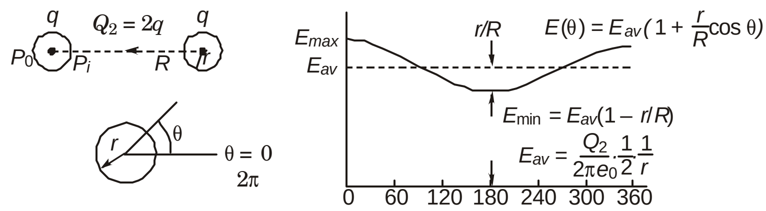

Fig. 4.16 Distribution of voltage gradient on 2-conductor bundle illustrating the cosine law.

This is shown in Figure 4.16. This is called the "cosine law" of variation of E with θ. We are now encountering three terms: Maximum gradient, Minimum gradient and Average gradient. Since we have neglected the charges on the other phases and the image conductors, the surface voltage gradient distribution on both sub-conductors of the bundle is identical. The concepts given above can be easily extended to bundles with more sub-conductors and we will consider N from 3 to 8.

Example 4.9. The dimensions of a ± 400 kV dc line are shown in Figure 417. Calculate

(*a*) the charge coefficient $Q/2\pi e_0$ for each bundle,

(*b*) the maximum and minimum surface gradient on the conductors by

(*i*) omitting the charges of the second pole and image conductors,

(*ii*) considering the charge of the second pole but omitting the charge of the image conductors,

(*c*) the average maximum surface voltage gradient of the bundle under case *b* (*ii*).

Solution. The potential coefficients are first calculated.

$$r_{eq} = \sqrt{0.0175 \times 0.45} = 0.08874 \text{ m}$$

$$P_{11} = P_{22} = \ln (24/0.08874) = 5.6$$

$$P_{12} = P_{21} = \ln (\sqrt{24^2 + 9^2}/9) = 1.047.$$

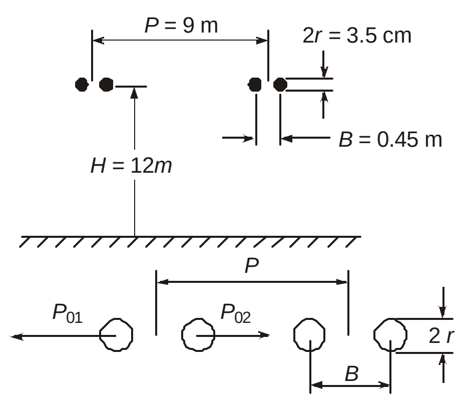

Fig. 4.17 Maximum and minimum values of voltage gradients on 2-conductor bundles.

$$[P] = \begin{bmatrix} 5.6, & 1.047 \\ 1.047, & 5.6 \end{bmatrix} \text{giving} [M] = [P]^{-1} = \begin{bmatrix} 0.185, & -0.0346 \\ -0.0346, & 0.185 \end{bmatrix}$$

(*a*)
$$\frac{1}{2\pi e_0}\begin{bmatrix} Q_1 \\ Q_2 \end{bmatrix} = \begin{bmatrix} 0.185, & -0.0346 \\ -0.0346, & 0.185 \end{bmatrix}\begin{bmatrix} 400 \\ -400 \end{bmatrix} \times 10^3$$

$$= \begin{bmatrix} 1 \\ -1 \end{bmatrix} 87.84 \times 10^3$$

The charge of each bundle is $2\pi e_0 \times 87.84 \times 10^3 = \frac{87.84}{18}$ μc/m

$= 4.88$ μc/m.

The charge of each sub-conductor is $q = 2.44$ μc/m length.

(*b*) (*i*) Maximum and minimum gradient = $\frac{q}{2\pi e_0}\frac{1}{r}(1 \pm r/R)$

Maximum $E_0 = 87.84 \times 10^3 \frac{1}{2}\frac{1}{0.0175}(1 + 0.0175/0.225)$

$= 2705$ kV/m $= 27.05$ kV/cm

Minimum $E_i = 23.15$ kV/cm $= 2315$ kV/m

Average gradient $= \frac{q}{2\pi e_0}\frac{1}{r} = \frac{87.84}{2}\frac{1}{.0175} = 2510$ kV/m

$= 25.1$ kV/cm

(*ii*) Consider the 2 sub-conductors on the left.

At P_{01}, the forces on a positive test charge are as shown in Figure 4.17.

$$E_{01} = \frac{q}{2\pi e_0}\frac{1}{r}(1 + r/R) - \frac{q}{2\pi e_0}\left(\frac{2}{9.0175} + \frac{2}{9.4675}\right)$$

$= 2705 - 19 = 2686$ kV/m $= 26.86$ kV/cm

$$E_{02} = \frac{q}{2\pi e_0}\frac{1}{r}(1 + r/R) + \frac{q}{2\pi e_0}\left(\frac{2}{8.4825} + \frac{2}{8.9325}\right)$$

$= 2705 + 20.2 = 2725.2$ kV/m $= 27.25$ kV/cm

$$E_{i_1} = \frac{q}{2\pi e_0}\frac{1}{r}(1 - r/R) + \frac{q}{2\pi e_0}\left(\frac{2}{8.9825} + \frac{2}{9.4325}\right)$$

$= 2315 + 19.1 = 2334$ kV/m $= 23.34$ kV/cm

$$E_{i_2} = \frac{q}{2\pi e_0}\frac{1}{r}(1 - r/R) - \frac{q}{2\pi e_0}\left(\frac{2}{8.5725} + \frac{2}{9.0225}\right)$$

$= 2315 - 20 = 2295$ kV/m $= 22.95$ kV/cm.

The maximum gradients on the two sub-conductors have now become 26.86 kV/cm and 27.25 kV/cm instead of 27.05 kV/cm calculated on the basis of omitting the charges of other pole.

(*c*) The average maximum gradient is defined as the arithmetic average of the two maximum gradients.

$$E_{\text{avm}} = \frac{1}{2}(26.86 + 27.25) = 27.055 \text{ kV/cm}$$

This is almost equal to the maximum gradient obtained by omitting the charges of the other pole.

For a 3-phase ac line, the effect of charges on other phases can usually be ignored because when the charge on the conductor of one phase is at peak value, the charge on the other phases are passing through 50% of their peak values but of opposite polarity. This has an even less effect than that has been shown for the bipolar dc line where the charge of the second pole is equal and opposite to the charge of the conductor under consideration. However, in a digital computer programme, all these could be incorporated. It is well to remember that all calculations are based on the basic assumption that ground is an equipotential surface and that the sub-conductor charges are concentrated at their centres. Both these assumptions are approximate. But a more rigorous analysis is not attempted here.

4.5.3 Maximum Surface Voltage Gradients for $N \geq 3$

The method described before for calculating voltage gradients for a twin-bundle conductor, N = 2, can now be extended for bundles with more than 2 sub-conductors. A general formula will be obtained under the assumption that the surface voltage gradients are only due to the charges of the N sub-conductors of the bundle, ignoring the charges of other phases or poles and those on the image conductors. Also, the sub-conductors are taken to be spaced far enough from each other so as to yield a uniform field at the location of the sub-conductor and hence the concept of stress-doubling will be used.

Figure 4.18 shows bundles with N = 3, 4, 6, 8 sub-conductors and the point P where the maximum surface voltage gradient occurs. The forces exerted on a unit positive test charge at P due to all N conductor-charges q are also shown as vectors. The components of these forces along the vector force due to conductor charge will yield the maximum surface voltage gradient. Due to symmetry, the components at right angles to this force will cancel each other, as shown on the figures.

N = 3. $B = \sqrt{3}R$ for equilateral spacing.

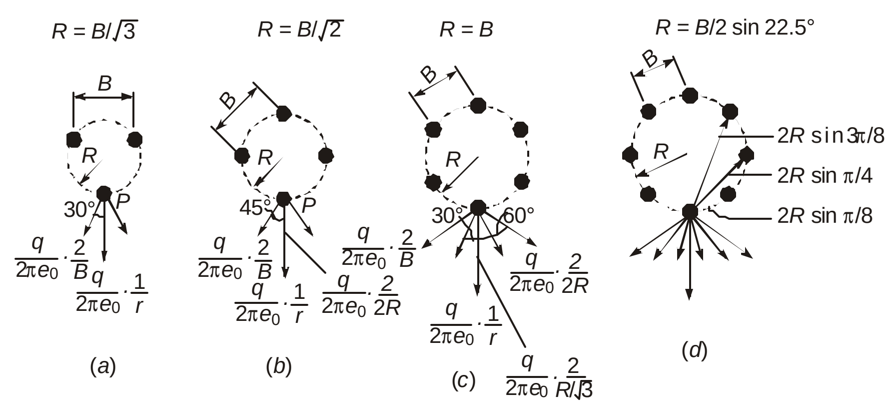

Fig. 4.18 Distribution of surface voltage gradients on 3-, 4-, 6-, and 8-conductor bundles.

$$E_P = \frac{q}{2\pi e_0}\frac{1}{r}\left(1+2\times r.\frac{2}{B}\cos 30^\circ\right) = \frac{q}{2\pi e_0}\frac{1}{r}(1+2r/R) \quad ...(4.53)$$

The sub-conductor charge is $q = Q/3$ where Q is obtained from equation (4.32), $[Q/2\pi e_0] = [M][V]$ as discussed earlier.

$N = 4. B = \sqrt{2}R$ for quadrilateral spacing.

$$E_P = \frac{q}{2\pi e_0}\left(\frac{1}{r}+\frac{2}{2R}+2\times\frac{2}{R\sqrt{2}}\cos 45^\circ\right)$$

$$= \frac{q}{2\pi e_0}\frac{1}{r}(1+3r/R) \quad ...(4.54)$$

Note the emergence of a general formula

$$E_P = \frac{q}{2\pi e_0}\frac{1}{r}[1+(N-1)r/R] \quad ...(4.55)$$

$N = 6$. $B = R$ for hexagonal spacing.

$$E_P = \frac{q}{2\pi e_0}\left[\frac{1}{r}+\frac{2}{2R}+2\times\frac{2}{R}\cos 60^\circ+2\times\frac{2}{R\sqrt{3}}\cos 30^\circ\right]$$

$$= \frac{q}{2\pi e_0}\frac{1}{r}(1+5r/R) = \frac{q}{2\pi e_0}\frac{1}{r}[1+(N-1)r/R] \quad ...(4.56)$$

$N = 8$, $B = 2R \sin 22^\circ.5$ for octagonal spacing

$$E_P = \frac{q}{2\pi e_0}\left[\frac{1}{r}+\frac{2}{2R}+2\times\frac{2}{2R\sin\pi/8}\cos\frac{3\pi}{8}+2\times\frac{2}{2R\sin\pi/4}\times\cos\frac{\pi}{4}+ 2\frac{2}{2R\sin 3\pi/8}\cos\frac{\pi}{8}\right]$$

$$= \frac{q}{2\pi e_0}\left(\frac{1}{r}+\frac{1}{R}+\frac{2}{R}+\frac{2}{R}+\frac{2}{R}\right) = \frac{q}{2\pi e_0}\frac{1}{r}(1+7r/R)$$

$$= \frac{q}{2\pi e_0}\frac{1}{r}[1+(N-1)r/R] \quad ...(4.57)$$

From the above analysis, we observe that the contributions to the gradient at P from each of the $(N-1)$ sub-conductors are all equal to $\frac{q}{2\pi e_0}\frac{1}{R}$. In general, for an N-conductor bundle,

$$E_P = \frac{q}{2\pi e_0}\left[\frac{1}{r}+\frac{2}{2R}+2\times\frac{2}{2R\sin\pi/N}\cos\left(\frac{\pi}{2}-\frac{\pi}{N}\right)+2\times\frac{2}{2R\sin 2\pi/N}\cos\left(\frac{\pi}{2}-\frac{2\pi}{N}\right)+\ldots+2\times\frac{2}{2R\sin(N-1)\pi/N}\cos\left(\frac{\pi}{2}-\frac{N-1}{N}\pi\right)\right]$$

$$= \frac{q}{2\pi e_0}\left[\frac{1}{r}+\frac{1}{R}+\frac{(N-2)}{R}\right] = \frac{q}{2\pi e_0}\frac{1}{r}[1+(N-1)r/R] \quad ...(4.58)$$

Figures 4.19, 4.20, and 4.21 show typical results of maximum surface voltage gradients for 400 kV, 750 kV, and 1200 kV lines whose dimensions are shown in Figure 3.5 [See S. Ganga, Ref. 17, "Other Journals"]

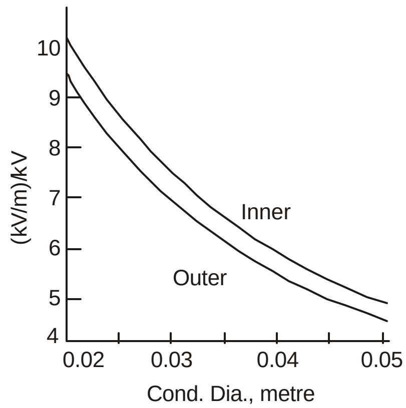

400 kV, Horizontal
H = 15 m, S = 12 m, N = 2,
B = 0.4572

Fig. 4.19 Surface voltage gradient on conductors of 400 kV line. See Figure 4.11 for dimensions.

4.5.4 Mangoldt (Markt-Mengele) Formula

In the case of a 3-phase ac line with horizontal configuration of phases, a convenient formula due to Mangoldt can be derived. This is also known as the Markt-Mengele Formula by some others.

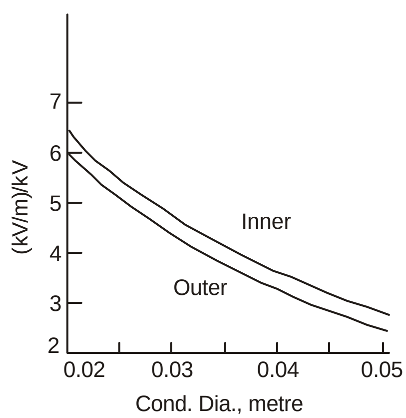

750 kV, Horizontal
H = 20 m, S = 15 m, N = 4
B = 0.4572 m

Fig. 4.20 Surface voltage gradient on conductors of 750 kV line. See Figure 4.12 for dimensions.

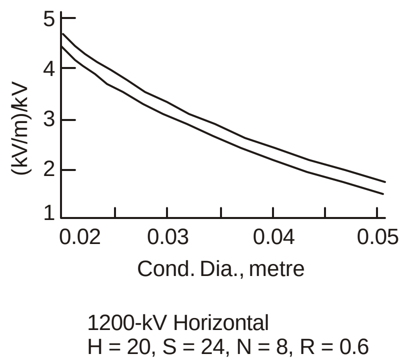

Fig. 4.21 Surface voltage gradients on 1200 kV lines. See Figure 4.13 for dimensions.

Referring to Figure 4.22, let Q_1, Q_2, Q_3 be the instantaneous charges on the bundles. The Maxwell's Potential coefficients are

$$\left.\begin{aligned} P_{11} &= P_{22} = P_{33} = \ln(2H/r_{eq}), \text{ where } r_{eq} = R(Nr/R)^{1/N} \\ P_{12} &= P_{21} = P_{23} = P_{32} = \ln(\sqrt{4H^2+S^2}/S) = \ln\sqrt{1+(2H/S)^2} \\ P_{13} &= P_{31} = \ln(\sqrt{4H^2+4S^2}/2S) = \ln\sqrt{1+(H/S)^2} \end{aligned}\right\} \quad \text{...(4.59)}$$

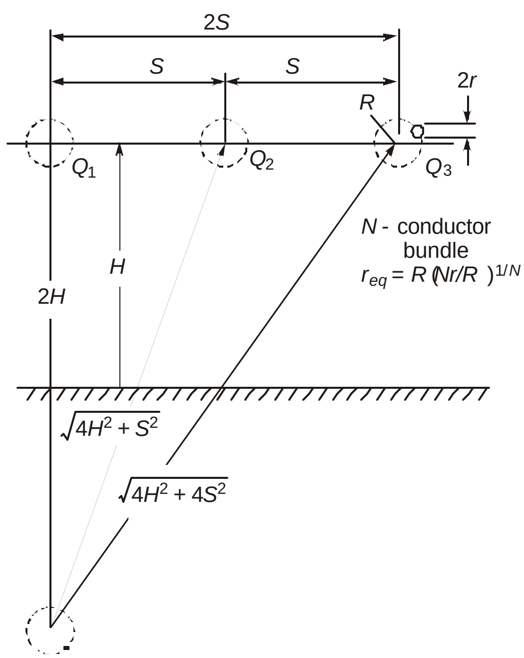

Fig. 4.22 3-phase horizontal configuration of line for derivation of Mangoldt Formula.

The voltage-charge relations are

$$\left.\begin{aligned} V_1 &= P_{11}.Q_1/2\pi e_0 + P_{12}.Q_2/2\pi e_0 + P_{13}.Q_3/2\pi e_0 \\ V_2 &= P_{21}.Q_1/2\pi e_0 + P_{22}.Q_2/2\pi e_0 + P_{23}.Q_3/2\pi e_0 \\ V_3 &= P_{31}.Q_1/2\pi e_0 + P_{32}.Q_2/2\pi e_0 + P_{33}.Q_3/2\pi e_0 \end{aligned}\right\} \quad \text{...(4.60)}$$

Both the voltages and the charges are sinusoidally varying at power frequency and at every instant of time, $V_1 + V_2 + V_3 = 0$ and $Q_1 + Q_2 + Q_3 = 0$. When the charge of any phase is passing through its peak value, the charges of the remaining two phases are negative but of magnitude 0.5 peak. From symmetry, the peak values of charges on the two outer phases will be equal. If we assume the peak values of Q_1, Q_2, Q_3 to be approximately equal, then, combining equations (4.59) and (4.60) we obtain the following equations:

For the Outer Phases

$$V_1 = \frac{Q_1}{2\pi e_0}(P_{11} - 0.5P_{12} - 0.5P_{13})$$

$$= \frac{Q_1}{2\pi e_0} \ln\frac{2H}{r_{eq}} \frac{1}{\left[\left\{1+\left(\frac{2H}{S}\right)^2\right\}\left\{1+\left(\frac{H}{S}\right)^2\right\}\right]^{1/4}} \quad \text{...(4.61)}$$

Therefore, $\dfrac{Q_1}{2\pi e_0}$ is found from the given voltage. If the r.m.s. value of phase voltage to ground is used, $\dfrac{Q_1}{2\pi e_0}$ is also the r.m.s. value of the charge coefficient and the resulting surface voltage gradient will also be in kV (r.m.s.)/metre, if V is in kV. The maximum surface voltage gradient will then be according to equation (4.58).

$$E_{0m} = \frac{Q_1}{2\pi e_0}\frac{1}{N}\frac{1}{r}\left[1+(N-1)\frac{r}{R}\right]$$

$$= \frac{1+(N-1)r/R}{N.r.\ln\dfrac{2H}{r_{eq}}\dfrac{1}{[\{1+(2H/S)^2\}\{1+(H/S)^2\}]^{1/4}}}V, \quad \text{...(4.62)}$$

Similarly, for the centre phase,

$$\frac{Q_2}{2\pi e_0} = [P_{22} - 0.5(P_{21} + P_{23})]^{-1}.V$$

and

$$E_{cm} = \frac{1+(N-1)r/R}{N r.\ln\dfrac{2H}{r_{eq}}\dfrac{1}{[1+(2H/S)^2]^{1/2}}}V \quad \text{...(4.63)}$$

Equations (4.62) and (4.63) are known as Mangoldt or Markt-Mengele Formulas. They were first derived only for the centre phase which gives a higher maximum voltage gradient than the outer phases. With corona assuming lot more importance since this formula was derived, we have extended their thinking to the outer phases also.

Example 4.10. For a 400-kV line, calculate the maximum surface voltage gradients on the centre and outer phases in horizontal configuration at the maximum operating voltage of 420 kV, r.m.s. line-to-line. The other dimensions are

$$H = 13 \text{ m}, S = 11 \text{ m}, N = 2, r = 0.0159 \text{ m}, B = 0.45 \text{ m}.$$

Solution. $2H/S = 26/11 = 2.364$ and $H/S = 1.182$

$$[\{1+(2H/S)^2\}\{1+(H/S)^2\}]^{1/4} = 1.982; \sqrt{1+(H/S)^2} = 2.567$$

$$r_{eq} = R(N.r/R)^{1/N} = 0.225\ (2 \times 0.0159/0.225)^{1/2} = 0.0846 \text{ m}$$

Also, $$r_{eq} = \sqrt{0.0159 \times 0.45} = 0.0846 \text{ m}, 2H/r_{eq} = 307.3$$

(*a*) Outer Phases

$$E_{0m} = \frac{(1+0.0159/0.225)420/\sqrt{3}}{2 \times 0.0159 \ln(307.3/1.982)} = 1619 \text{ kV/m} = 16.19 \text{ kV/cm}$$

(*b*) Centre Phase.

$$E_{cm} = \frac{(1+0.0159/0.225)420/\sqrt{3}}{2 \times 0.0159 \ln(307.3/2.567)} = 1707 \text{ kV/m} = 17.07 \text{ kV/cm}$$

The centre phase gradient is higher than that on the outer phases by

$$\frac{17.07 - 16.19}{16.19} \times 100 = 5.44\%$$

For a bipolar dc line, it is easy to show that the maximum surface voltage gradient on the sub-conductor of a bundle is

$$E_m = \frac{1+(N-1)r/R}{N.r.\ln\left[\dfrac{2H}{r_{eq}} \dfrac{1}{\sqrt{1+(2H/P)^2}}\right]} V \quad \text{...(4.64)}$$

where H = height of each pole above ground

P = pole spacing

and V = voltage to ground

Example 4.11. Using the data of Example 4.9, and using equation (4.64), calculate the maximum surface voltage gradient on the 2-conductor bundle for ± 400 kV dc line.

Solution. $H = 12$, $P = 9$, $r = 0.0175$, $N = 2$, $R = 0.225$

$r_{eq} = 0.08874$,

$$E_m = \frac{(1+0.0175/0.225)400}{2\times 0.0175\ \ln\left[\frac{24}{.08874}\frac{1}{\sqrt{1+(24/9)^2}}\right]}$$

$$= 2705 \text{ kV/m} = 27.05 \text{ kV/cm}$$

4.6 EXAMPLES OF CONDUCTORS AND MAXIMUM GRADIENTS ON ACTUAL LINES

Several examples of conductor configurations used on transmission lines following world-wide practice are given in the Table 4.1. The maximum surface voltage gradients are also indicated. These are only examples and the reader should consult the vast literature (CIGRE Proceedings, etc.) for more details. Most conductor manufacturers use British units for conductor sizes and the SI units are given only for calculation purposes. These details are gathered from a large number of sources listed in the bibliography at the end of the book.

The conductor sizes given in the table are not the only ones used. For example, the following range of conductor sizes is found on the North American continent.

345 *kV*. Single conductor— 1.424, 1.602, 1.737, 1.75, 1.762 inches dia

2-conductor bundle—1.108, 1.165, 1.196, 1.246 inches dia.

500 kV. Single conductor — 2.5 inches dia

2-bundle—1.602, 1.7, 1.75, 1.762, 1.82 inches dia (ACAR).

3-bundle—1.165 inches dia.

4-bundle—0.85, 0.9, 0.93 inches dia.

735-765 kV 4-bundle—1.165, 1.2, 1.382 inches dia.

4.7 GRADIENT FACTORS AND THEIR USE

From the Mangoldt (Markt-Mengele) formula given in Section 4.5, it is observed that the maximum surface voltage gradient in the centre phase of a horizontal 3-phase ac line is a function of the geometrical dimensions and the maximum operating voltage V. As shown in Table 4.1, the maximum operating voltages show a wide variation. It is therefore advantageous to have a table or graph of the normalized value called the 'gradient factor' in kV/cm per kV or V/m per volt or other units which will be independent of the voltage. The gradient factor is denoted by $g_f = E_{\text{cm}}/V$ and its value is

$$g_f = E_{\text{cm}}/V = \frac{1+(N-1)r/R}{N.r.\ln\left[\frac{2H}{r_{eq}}\frac{1}{\sqrt{1+(2H/S)^2}}\right]} \qquad ...(4.65)$$

Table 4.1. Conductor Details and Maximum Surface Voltage Gradients Used in EHV Lines

	Country	*Maximum Operating Voltage kV, RMS*	*Conductor Details No. × dia in inches (cm)*	*Maximum Gradient kv/cm, RMS*
(1)	India	420	2 × 1.258 (3.18)	17.0
(2)	Canada	315	2 × 1.382 (3.51)	17.4
		380	2 × 1.108 (2.814)	17.5 – 18.0
		525	4 × 0.93 (2.362)	18.8
		735	4 × 1.2, 1.382 (3.05, 3.51)	17.7–20.4
		1200	6 × 1.84, 2.0 (4.674, 5.08)	–
			8 × 1.65, 1.84 (4.19, 4.674)	–
(3)	U.S.A.	355 – 362	1 × 1.602 (4.07)	16.6
			2 × 1.175, 1.196 (2.985, 3.04)	15–16
		500	2 × 1.65 (4.19)	16.9
			3 × 1.19 (3.02)	16.4
		550	2 × 1.6 (4.07)	16.9
			1 × 2.5 (6.35)	16.7
		765	4 × 1.165 (2.96)	20.4
		1200	8 × 1.602 (4.07)	13.5
(4)	U.S.S.R.	400	3 × 1.19 (3.02)	13.6
		525	3 × 1.19 (3.02)	18.0
		1200	8 × 0.96 (2.438)	21.4
(5)	U.K.	420	2 × 1.09 (2.77)	19.6
			4 × 1.09 (2.77)	13.5
(6)	France	420	2 × 1.04 (2.64)	19.0
(7)	Germany	380	4 × 0.827 (2.1)	15.7
		420	4 × 0.854 (2.17)	16.7
(8)	Italy	380	2 × 1.168 (2.97)	15.0
		1050	4 × 1.76, 1.87 (4.47, 4.75)	17.1 – 19.8
			6 × 1.5 (3.81)	–
(9)	Sweden	380	3 × 1.25 (3.18)	12.5
		400	2 × 1.25 (3.18)	16.5
		800	4 × 1.6 (4.06)	17.6

By varying the parameters (r, N, R, H and S) over a large range curves can be plotted for g_f against the desired variable. From product of g_f and the maximum operating line-to-ground voltage of the line, the maximum surface voltage gradient is readily obtained. Such curves are shown in Figure 4.23 for N = 1, 2, 4 and for conductor diameters ranging from 0.7" to 2.5" (1.78 cm to 6.35 cm). The height H in all cases has been fixed at H = 50' (15 m) and the phase spacing S ranging from 20' to 50' (6 to 15 m). Calculations have shown that a variation of height H from 10 to 30 metres does not change g_f by more than 1%. The abscissa has been chosen as the reciprocal of the diameter and the resulting variation of gradient factor with $(1/d)$ is nearly a straight line, which is very convenient. In equation (4.65) it is observed that the conductor radius occurs in the denominator and this property has been used in plotting Figure 4.23. [Also see G. Veena, Ref. 16, "Other Journals"].

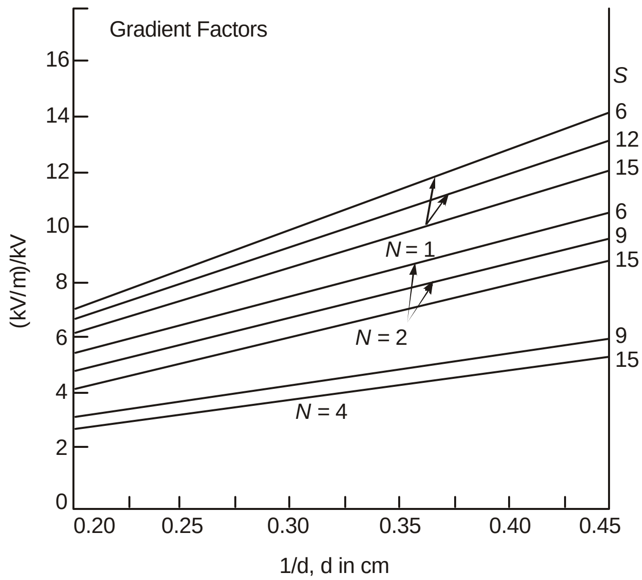

Fig. 4.23 Gradient factors of conductors (g_f in V/m/Volt).

Such graphs can also be prepared for the maximum surface voltage gradient factors for the outer phases or bipolar dc lines, etc., in a design office.

4.8 DISTRIBUTION OF VOLTAGE GRADIENT ON SUB-CONDUCTORS OF BUNDLE

While discussing the variation of surface voltage gradient on a 2-conductor bundle in section 4.5.2, it was pointed out that the gradient distribution follows nearly a cosine law, equation (4.52). We will derive rigorous expressions for the gradient distribution and discuss the approximations to be made which yields the cosine law. The cosine law has been verified to hold for bundled conductors with up to 8 sub-conductors. Only the guiding principles will be indicated here through an example of a 2-conductor bundle and a general outline for $N \geq 3$ will be given which can be incorporated in a digital-computer programme.

Figure 4.24 shows detailed view of a 2-conductor bundle where the charges q on the two sub-conductors are assumed to be concentrated at the conductor centres. At a point P on the surface of a conductor at angle θ from the reference direction, the field intensities due to the two conductor charges are, using stress-doubling effect,

$$E_1 = \frac{q}{2\pi e_0}\frac{1}{r} \text{ and } E_2 = \frac{q}{2\pi e_0}\frac{2}{B'} \quad \text{...(4.66)}$$

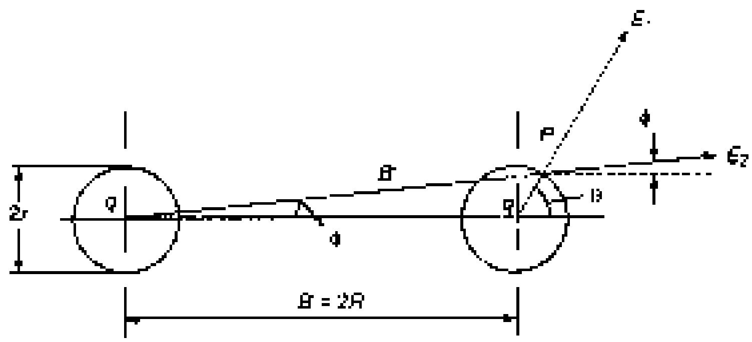

Fig. 4.24 Gradient distribution calculation on 2-conductor bundle

The total horizontal and vertical components of E_1 and E_2 at P will be

$$E_h = E_1\cos\theta + E_2\cos\phi, \text{ and } E_v = E_1\sin\theta + E_2\sin\phi \qquad ...(4.67)$$

The total field-intensity is $E_p = \sqrt{E_h^2 + E_v^2}$ ...(4.68)

$$\left.\begin{aligned} \text{Now, } B' &= \sqrt{(B + r\cos\theta)^2 + (r\sin\theta)^2}, \text{ with } B = 2R, \\ \sin\phi &= r\sin\theta / B' \text{ and } \cos\phi = (B + r\cos\theta)/B' \end{aligned}\right\} \qquad ...(4.69)$$

$$\therefore \quad E_p^2 = \left(\frac{q}{2\pi\epsilon_0}\right)^2 \frac{1}{r^2}[1 + 8r^2/(B')^2 + 4rB\cos\theta/(B')^2] \qquad ...(4.70)$$

Now $\quad (B')^2 = B^2\,[1 + (r^2 + 2Br\cos\theta)/B^2]^2$

and if $\quad r \ll B, B' \approx B + r\cos\theta$ and $(B')^2 \approx B^2$

Then, $\quad E_p^2 = \left(\frac{q}{2\pi\epsilon_0}\right)^2 \frac{1}{r^2}[(1 + 8r^2/B^2 + 4r\cos\theta/B)]$

$$\approx \left(\frac{q}{2\pi\epsilon_0}\right)^2 \frac{1}{r^2}[(1 + 4r\cos\theta/B)]$$

$$\therefore \quad E_p \approx \frac{q}{2\pi\epsilon_0}\cdot\frac{1}{r}\left(1 + \frac{2r}{B}\cos\theta\right) = \frac{q}{2\pi\epsilon_0}\cdot\frac{1}{r}\left(1 + \frac{r}{R}\cos\theta\right) \qquad ...(4.71)$$

where, for $X \ll 1$, $(1 + X)^{1/2} \approx 1 + X/2$.

For $N \geq 3$, the general expressions become very lengthy and it is best to write a programme for a digital computer. The procedure is illustrated here for a 6-conductor bundle whose dimensions are shown in Figure 4.25 with all relevant parameters for the calculation.

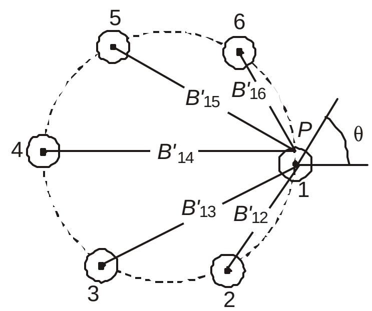

Fig. 4.25 Six-conductor bundle and gradient on sub-conductor.

We first evaluate the distances B'_{12} to B'_{16}.

$$\left.\begin{aligned}
B'_{12} &= \sqrt{[(R\sin 60^\circ + r\sin\theta)^2 + (R\cos 60^\circ + r\cos\theta)^2]}\\
B'_{13} &= \sqrt{[(\sqrt{3}R\sin 30^\circ + r\sin\theta)^2 + (\sqrt{3}R\cos 30^\circ + r\cos\theta)^2]}\\
B'_{14} &= \sqrt{[(r\sin\theta)^2 + (2R + r\cos\theta)^2]}\\
B'_{15} &= \sqrt{[(\sqrt{3}R\sin 30^\circ - r\sin\theta)^2 + (\sqrt{3}R\cos 30^\circ + r\cos\theta)^2]}\\
B'_{16} &= \sqrt{[(R\sin 60^\circ - r\sin\theta)^2 + (R\cos 60^\circ + r\cos\theta)^2]}
\end{aligned}\right\} \quad ...(4.72)$$

Next the horizontal and vertical components of the field intensity at P are evaluated. The factor $(q/2\pi e_0)$ is omitted in writing for the present but will be included at the end.

Conductor i (i = 1, 2, 3 4, 5, 6)	*Horizontal component* $E_h(i)$	*Vertical component* $E_v(i)$
1.	$\frac{1}{r}\cos\theta$	$\frac{1}{r}\sin\theta$
2.	$2(R\cos 60^\circ + r\cos\theta)/(B'_{12})^2$	$2(R\sin 60^\circ + r\sin\theta)/(B'_{12})^2$
3.	$2(\sqrt{3}R\cos 30^\circ + r\cos\theta)/(B'_{13})^2$	$2(\sqrt{3}R\sin 30^\circ + r\sin\theta)/(B'_{13})^2$
4.	$2(2R + r\cos\theta)/(B'_{14})^2$	$2r\sin\theta/(B'_{14})^2$
5.	$2(\sqrt{3}R\cos 30^\circ + r\cos\theta)/(B'_{15})^2$	$-2(\sqrt{3}R\sin 30^\circ - r\sin\theta)/(B'_{15})^2$
6.	$2(R\cos 60^\circ + r\cos\theta)/(B'_{16})^2$	$-2(R\sin 60^\circ - r\sin\theta)/(B'_{16})^2$

Total field intensity

$$E_P(\theta) = \frac{q}{2\pi e_0}\left[\left\{\sum_{i=1}^{6} E_h(i)\right\}^2 + \left\{\sum_{i=1}^{6} E_v(i)\right\}^2\right]^{1/2}$$

Figure 4.26 shows examples of surface voltage gradient distributions on bundled conductors with N = 2, 4, 6 subconductors.

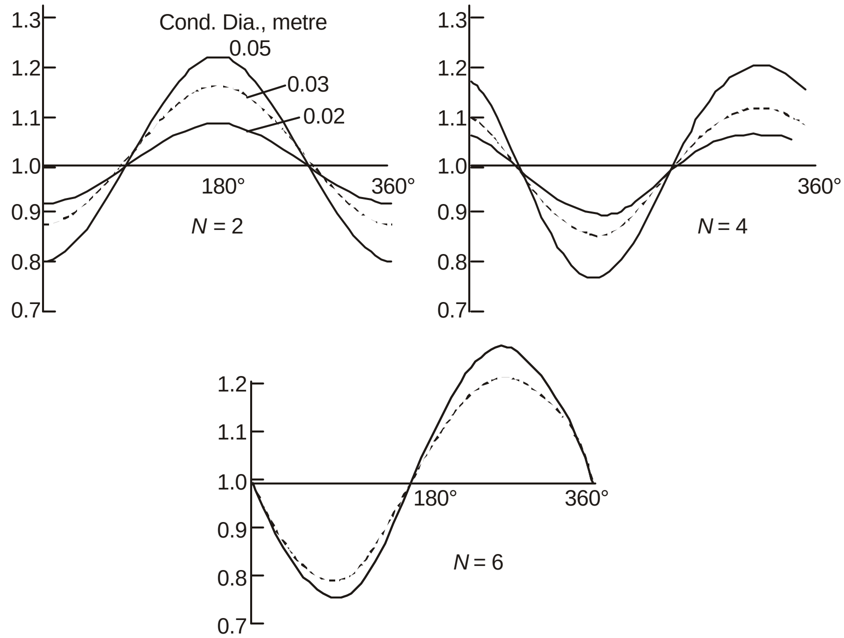

Fig. 4.26 Distribution of voltage gradient on bundle conductors for N = 2, 4, 6. Variation with conductor diameter.

4.9 DESIGN OF CYLINDRICAL CAGES FOR CORONA EXPERIMENTS

The effects of high voltage-gradients on bundled conductors are evaluated all over the world by "cages". In the simplest of these arrangements a large metallic cylinder at ground or near ground potential forms the outer cage with the bundled conductor strung inside. The centres of the cylinder and the bundle are coincident while the subconductors themselves are displaced off-centre, except for N = 1, a single conductor. Several examples are shown in Figure 4.27, in which a square cage is also included. When the dimensions of the outer cage become very large or where the length of conductor and weight are large with a resulting sag, a square cage made with mesh can be contoured to follow the sag. The cage arrangement requires lower voltage for creating the required surface voltage gradient on the conductors than in an overhead line above ground. Also artificial rain equipment can be used if necessary to obtain quick results. Measuring instruments are connected to ground both from the conductor at high voltage and the cage at near ground potential where necessary for Radio Interference, Corona Loss, charge, etc., measurements. Audible noise is usually measured as radiation into a microphone placed away from the test setup. Normally, the cage consists of three sections, a long middle section which is the principal cage which could extend up to 60 metres, with two short guard cages at either end grounded in order to minimize edge effects.

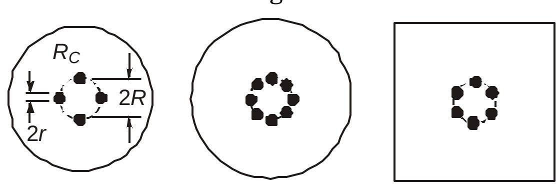

Fig. 4.27 Configuration of 'cages' used for corona studies.

5

Corona Effects-I: Power Loss and Audible Noise

5.1 I^2R LOSS AND CORONA LOSS

In Chapter 2, the average power-handling capacity of a 3-phase e.h.v. line and percentage loss due to I^2R heating were discussed. Representative values are given below for comparison purposes.

System kV	400		750		1000		1150	
Line Length, km	400	800	400	800	400	800	400	800
3-Phase MW/circuit ($P = 0.5\ V^2/xL$)	640	320	2860	1430	6000	3000	8640	4320
% Power Loss = 50 r/x	4.98%		2.4%		0.8%		0.6%	
kW/km Loss, 3-phase	80	20	170	42.5	120	30	130	32.5

When compared to the I^2R heating loss, the average corona losses on several lines from 345 kV to 750 kV gave 1 to 20 kW/km in fair weather, the higher values referring to higher voltages. In foul-weather, the losses can go up to 300 kW/km. Since, however, rain does not fall all through the year (an average is 3 months of precipitation in any given locality) and precipitation does not cover the entire line length, the corona loss in kW/km cannot be compared to I^2R loss directly. A reasonable estimate is the yearly average loss which amounts to roughly 2 kW/km to 10 kW/km for 400 km lines, and 20-40 kW/km for 800 km range since usually higher voltages are necessary for the longer lines. Therefore, cumulative annual average corona loss amounts only to 10% of I^2R loss, on the assumption of continuous full load carried. With load factors of 60 to 70%, the corona loss will be a slightly higher percentage. Nonetheless, during rainy months, the generating station has to supply the heavy corona loss and in some cases it has been the experience that generating stations have been unable to supply full rated load to the transmission line. Thus, corona loss is a very serious aspect to be considered in line design.

When a line is energized and no corona is present, the current is a pure sine wave and capacitive. It leads the voltage by 90°, as shown in Figure 5.1(*a*). However, when corona is present, it calls for a loss component and a typical waveform of the total current is as shown in Figure 5.1 (*b*). When the two components are separated, the resulting inphase component has a waveform which is not purely sinusoidal, Figure 5.1 (*c*). It is still a current at power frequency, but only the fundamental component of this distorted current can result in power loss.

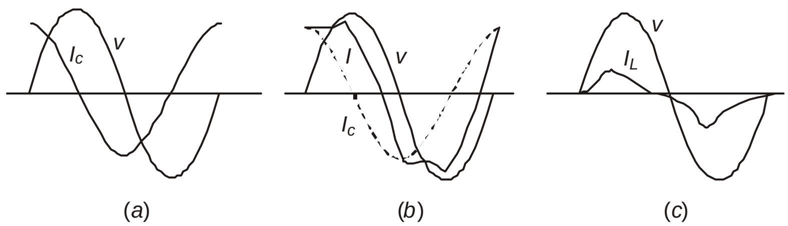

Fig. 5.1 Corona current waveform.

The mechanism of corona generation and its properties have been very extensively investigated and the reader is referred to the bibliography at the end of the book. Of vital importance is the generation of pulses which causes interference to radio, carrier communication, and gives rise to TV interference. These aspects will be discussed in the next chapter. In this chapter, engineering aspects of corona loss and audible noise will be described and data useful for design of lines based on these two phenomena will be discussed.

5.2 CORONA-LOSS FORMULAE

5.2.1 List of Formulae

Corona-loss formulae were initiated by F.W. Peek Jr. in 1911 derived empirically from most difficult and painstaking experimental work. Since then a horde of formulae have been derived by others, both from experiments and theoretical analysis. They all yield the power loss as a function of (*a*) the corona-inception voltage, V_o; (*b*) the actual voltage of conductor, V; (*c*) the excess voltage ($V — V_o$) above V_o; (*d*) conductor surface voltage gradient, E; (*e*) corona-inception gradient, E_o; (*f*) frequency, f; (*g*) conductor size, d, and number of conductors in bundle, N, as well as line configuration; (*h*) atmospheric condition, chiefly rate of rainfall, ρ, and (*i*) conductor surface condition.

The available formulae can be classified as follows: (see Bewley and *EHV* Reference Books in Bibliography)

A. Those Based on Voltages

(*i*) *Linear relationship* : Skilling's formula (1931):

$$P_c \propto V - V_o \quad ...(5.1)$$

(*ii*) *Quadratic relationship*

(*a*) Peek's formula (1911):

$$P_c \propto (V - V_o)^2 \quad ...(5.2)$$

(*b*) Ryan and Henline formula (1924):

$$P_c \propto V(V - V_o) \quad ...(5.3)$$

(*c*) Peterson′s formula (1933) :

$$P_c \propto V^2 . F(V/V_o) \quad ...(5.4)$$

where F is an experimental factor.

(*iii*) *Cubic Relationship*

(*a*) Foust and Menger formula (1928):

$$P_c \propto V^3 \quad ...(5.5)$$

(*b*) Prinz's formula (1940):

$$P_c \propto V^2 (V - V_o) \quad ...(5.6)$$

B. Those Based on Voltage Gradients

(*a*) Nigol and Cassan formula (1961):

$$P_c \propto E^2 \text{ In } (E/E_o) \quad ...(5.7)$$

(*b*) Project *EHV* formula (1966):

$$P_c \propto V.\ E^m,\ \text{m} = 5 \quad ...(5.8)$$

In order to obtain corona-loss figures from e.h.v. conductor configurations, outdoor experimental projects are established in countries where such lines will be strung. The resulting measured values pertain to individual cases which depend on local climatic conditions existing at the projects. It is therefore difficult to make a general statement concerning which formula or loss figures fit coronal losses universally. In addition to equations (5.1) to (5.8), the reader is referred to the work carried out in Germany at the Rheinau 400 kV Research Project, in France at the Les Renardieres Laboratory, in Russia published in the CIGRE Proceedings from 1956–1966, in Japan at the CRIEPI, in Sweden at Uppsala, and in Canada by the IREQ and Ontario Hydro.

We will here quote some formulas useful for evaluating 3-phase corona loss in kW/km, which are particularly adopted for e.h.v. lines, and some which are classic but cannot be used for e.h.v. lines since they apply only to single conductors and not to bundles. There is no convincing evidence that the total corona loss of a bundled conductor with N conductors is N times that of a single conductor.

(1) *Nigol and Cassan Formula* (Ontario Hydro, Canada).

$$P_c = K.f.r^3.\ \theta\ .E^2.\ \ln\ (E/E_0),\ \text{kW/km, 3-ph} \quad ...(5.9)$$

where f = frequency in Hz, r = conductor radius in cm.,

θ = angular portion in radians of conductor surface where the voltage gradient exceeds the critical corona-inception gradient,

E = effective surface gradient at operating voltage V, kV/cm, r.m.s.

E_0 = corona-inception gradient for given weather and conductor surface condition, kV/cm, r.m.s.

and K = a constant which depends upon weather and conductor surface condition.

Many factors are not taken into account in this formula such as the number of sub-conductors in bundle, etc.

(2) *Anderson, Baretsky, McCarthy Formula* (Project EHV, USA)

An equation for corona loss in rain giving the excess loss above the fair-weather loss in kW/3-phase km is:

$$P_c = P_{FW} + 0.3606\ K.V.r^2.\ln\ (1 + 10\rho).\ \sum_1^{3N} E^5 \quad ...(5.10)$$

Here, P_{FW} = total fair-weather loss in kW/km,
= 1 to 5 kW/km for 500 kV, and 3 to 20 kW/km for 700 kV,
$K = 5.35 \times 10^{-10}$ for 500 to 700 kV lines,
$= 7.04 \times 10^{-10}$ for 400 kV lines (based on Rheinau results),
V = conductor voltage in kV, line-line, r.m.s.,
E = surface voltage gradient on the underside of the conductor, kV/cm, peak,
ρ = rain rate in mm/hour,
r = conductor radius in cm,
and N = number of conductors in bundle of each phase [The factor 0.3606 = $1/1.609\sqrt{3}$].

Formulae are not available for (*a*) snow, and (*b*) hoar frost which are typical of Canadian and Russian latitudes. The EHV Project suggests $K = 1.27 \times 10^{-9}$ for snow, but this is a highly variable weather condition ranging from heavy to light snow. Also, the conductor temperature governs in a large measure the condition immediately local to it and it will be vastly different from ground-level observation of snow.

The value of ρ to convert snowfall into equivalent rainfall rate is given as follows :

Heavy snow : ρ = 10% of snowfall rate;

Medium snow : ρ = 2.5% of snowfall rate;

Light snow : ρ = 0.5% of snowfall rate.

The chief disadvantage in using formulae based upon voltage gradients is the lack of difinition by the authors of the formulae regarding the type of gradient to be used. As pointed out in Chapter 4, there are several types of voltage gradients on conductor surfaces in a bundle, such as nominal smooth-conductor gradient present on a conductor of the same outer radius as the line conductor but with a smooth surface, or the gradient with surface roughness taken into account, or the average gradient, or the average maximum gradient, and so on. It is therefore evident that for Indian conditions, an outdoor e.h.v. project is the only way of obtaining meaningful formulae or corona-loss figures applicable to local conditions.

Later on in Section 5.3, we will derive a formula based upon charge voltage relations during the presence of a corona discharge.

5.2.2 The Corona Current

The corona loss P_c is expressed as

$P_c = 3 \times$ line-to-ground voltage $\times$ in-phase component of current.

From the previously mentioned expressions for P_c, we observe that different investigators have different formulas for the corona current. But in reality the current is generated by the movement of charge carriers inside the envelope of partial discharge around the conductor. It should therefore be very surprising to a discerning reader that the basic mechanism, being the same all over the world, has not been unified into one formula for this phenomenon. We can observe the expressions for current according to different investigators below.

1. *Peek's Law*. F.W. Peek, Jr., was the forerunner in setting an example for others to follow by giving an empirical formula relating the loss in watts per unit length of conductor

with nearly all variables affecting the loss. For a conductor of radius r at a height H above ground,

$$P_c = 5.16\times10^{-3} f\sqrt{r/2H}\, V^2(1-V_o/V)^2, \text{kW/km} \quad ...(5.11)$$

where V, V_o are in kV, r.m.s., and r and H are in metres. The voltage gradients are, at an air density of δ, for a smooth conductor,

$$E = V/r \ln(2H/r) \text{ and } E_o = 21.4\ \delta(1+0.0301/\sqrt{r\delta}) \quad ...(5.12)$$

Example 5.1. For r = 1 cm, H = 5m, f = 50 Hz, calculate corona loss P_c according to Peek's formula when E = 1.1 E_o, and δ = 1.

Solution. $E_0 = 21.4(1+0.0301/\sqrt{0.01}) = 27.84\,\text{kV/cm, r.ms.}$

$\therefore$ $E = 1.1E_0 = 30.624\,\text{kV/cm}. \sqrt{r/2H} = 0.0316$

V = 30.624 ln (10/0.01) = 211.4 kV. (line-to-line voltage

$= 211.4\sqrt{3}$ = 366 kV)

$P_c = 5.16 \times 10^{-3} \times 50 \times 0.0316 \times 211.4^2(1 - 1/1.1)^2 = 2.954$ kW/km

$\cong$ 3 kW/km.

The expression for the corona-loss current is

$$i_c = P_c/V = 5.16 \times 10^{-2} f \sqrt{r/2H}\, V(1 - V_o/V)^2, \text{Amp/km} \quad ...(5.13)$$

For this example, i_c = 3000 watts/211.4 kV = 14 mA/km.

2. *Ryan-Henline Formula*

$$P_c = 4 fCV(V - V_0).10^6, \text{kW/km} \quad ...(5.14)$$

Here C = capacitance of conductor to ground, Farad/m

$= 2\pi e_0/\ln(2H/r)$

and V, V_0 are in kV, r.ms.

We can observe that the quantity (CV) is the charge of conductor per unit length. The corona-loss current is

$$i_c = 4 fC(V - V_0).\ 10^6, \text{Amp/km} \quad ...(5.15)$$

Example 5.2. For the previous example 5.1, compute the corona loss P_c and current i_c using Ryan-Henline formulae, equations (5.14) and (5.15).

Solution. $P_c = 4 \times 50 \times 211.4^2 (1 - 1/1.1) \times 10^{-3}/18 \ln(1000)$

= 6.47 kW/km

$i_c = 6.47/211.4 = 3.06 \times 10^{-2}$ Amp/km = 30.6 mA/km

3. *Project EHV Formula.* Equation (5.10).

Example 5.3. The following data for a 750 kV line are given. Calculate the corona loss per kilometre and the corona loss current.

Rate of rainfall ρ = 5 mm/hr. $K = 5.35 \times 10^{-10}$, P_{FW} = 5 kW/km

V = 750 kV, line-to-line. H = 18 m, S = 15 m phase spacing

$N = 4$ sub-conductors each of $r = 0.0175$ m with bundle spacing

$B = 0.4572$ m. (Bundle radius $R = B/\sqrt{2} = 0.3182$ m). Use surface voltage gradient on centre phase for calculation.

Solution. From Mangoldt Formula, the gradient on the centre phase conductor will be

$$E = V.[1 + (N-1)\, r/R]/[\text{N.r. ln } \{2H/r_{eq}\sqrt{(2H/S)^2+1}\,\}]$$

where $r_{eq} = R\,(N.r/R)^{1/N}$. Using the values given,

$E = 18.1$ kV/cm, r.m.s., $= 18.1\sqrt{2}$ peak = 25.456

$P_c = 5 + 0.3606 \times 5.35 \times 10^{-10} \times 750 \times 0.175^2 \times \ln(1 + 50) \times 12 \times (25.456)^5$

$= 5 + 229 = 234$ kW/km, 3-phase

The current is

$$i_c = P_c/\sqrt{3}V = 234/750\sqrt{3} = 0.54 \text{ A/km}.$$

Note that the increase in loss under rain is nearly 46 times that under fair weather. Comparing with Table on page 127 the corona loss is much higher than the I^2R heating loss.

5.3 CHARGE-VOLTAGE (*q – V*) DIAGRAM AND CORONA LOSS

5.3.1 Increase in Effective Radius of Conductor and Coupling Factors

The partial discharge of air around a line conductor is the process of creation and movement of charged particles and ions in the vicinity of a conductor under the applied voltage and field. We shall consider a simplified picture for conditions occurring when first the voltage is passing through the negative half-cycle and next the positive half-cycle, as shown in Figure 5.2.

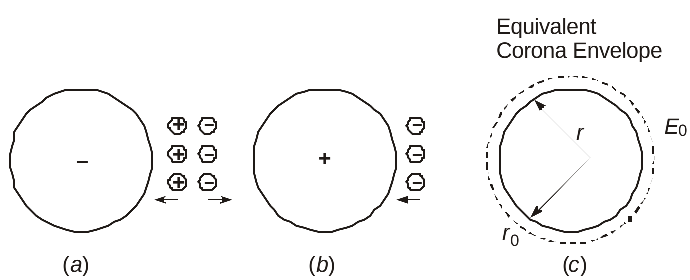

Fig. 5.2 Space-charge distribution in corona and increase in effective radius of conductor

In Figure 5.2(*a*), free electrons near the negative conductor when repelled can acquire sufficient energy to form an electron avalanche. The positive ions (a neutral molecule which has lost an electron) are attracted towards the negative conductor while the electrons drift into lower fields to attach themselves to neutral atoms or molecules of Nitrogen and Oxygen to form negative ions. Some recombination could also take place. The energy imparted for causing initial ionization by collision is supplied by the electric field. During the positive half cycle, the negative ions are attracted towards the conductor, but because of local conditions not all ions drift back to the conductor. A space charge is left behind and the hysteresis effect gives rise to the energy loss. Furthermore, because of the presence of charged particles, the effective charge of the conductor ground electrode system is increased giving rise to an increase in effective capacitance. This can be interpreted in an alternative manner by assuming that the conductor diameter is effectively increased by the conducting channel up to a certain extent where the electric field intensity decreases to a value equal to that required for further ionization, namely, the corona-inception gradient, Figure 5.2(*c*).

Example 5.4. A single smooth conductor 1 cm in radius is strung 5 metres above ground; using Peek's formula for corona-inception gradient, find

(*a*) the corona-inception voltage,

(*b*) the equivalent radius of conductor to the outside of the corona envelope at 20% overvoltage. Take $\delta = 1$.

Solution.

(*a*) $E_0 = 21.4(1 + 0.0301/\sqrt{r}) = 27.84 \text{ kV/cm} = 2784 \text{ kV/m}.$

$\therefore$ $V_0 = E_0 . r . \ln(2H/r) = 2784 \times 0.01 \times \ln(10/0.01)$

$= 192.3$ kV, r.m.s.

(*b*) Let r_0 = effective radius of the corona envelope

Then, $E_{0c} = 2140(1 + 0.0301)/\sqrt{r_0})$, and

$1.2 \times 192.3 = E_{0c}.r_o.\ln(2H/r_o)$ giving

$230.8 = 2140\,(1 + 0.0301/\sqrt{r_0}).r_0.\ln(10/r_0).$

A trial solution yields $r_0 = 0.0126$ m = 1.26 cm.

So far we have considered power-frequency excitation and worked with effective or r.m.s. values of voltage and voltage gradient. There are two other very important types of volltage, namely the lightning impulse and switching surge, which give rise to intense corona on the conductors. The resulting energy loss helps to attenuate the voltage magnitudes during travel from a source point to other points far away along the overhead line. The resulting attenuation or decrease in amplitude, and the distortion or waveshape will be discussed in detail in the next section. We mention here that at power frequency, the corona-inception gradient and voltage are usually higher by 10 to 30% of the operating voltage in fair weather so that a line is not normally designed to generate corona. However, local conditions such as dirt particles etc., do give rise to some corona. On the other hand, under a lightning stroke or a switching operation, the voltage exceeds twice the peak value of corona-inception voltage. Corona plumes have been photographed from actual lines which extend up to 1.2 metres from the surface of the conductor. Therefore, there is evidence of a very large increase in effective diameter of a conductor under these conditions.

Corona-inception gradients on conductors under impulse conditions on cylindrical conductors above a ground plane are equal to those under power frequency but crest values have to be used in Peek's formula. The increase in effective radius will in turn change the capacitance of the conductor which has an influence on the voltage coupled to the other phase-conductors located on the same tower. The increased coupling factor on mutually-coupled travelling waves was recognized in the 1930's and 40's under lightning conditions. At present, switching surges are of great concern in determining insulation clearance between conductor and ground, and conductor to conductor. We will consider the increase in diameter and the resulting coupling factors under both types of impulses.

Example 5.5. A single conductor 2.5 inch in diameter of a 525-kV line (line-to-line voltage) is strung 13 m above ground. Calculate (*a*) the corona-inception voltage and (*b*) the effective radius of conductor at an overvoltage of 2.5 p.u. Consider a stranding factor m = 1.25 for roughness. (*c*) Calculate the capacitance of conductor to ground with and without corona. (*d*) If a second conductor is strung 10 m away at the same height, calculate the coupling factors in the two cases. Take $\delta = 1$.

Solution. r = 0.03176 m, H = 13.

(*a*) $E_{0r} = 2140 \times 0.8\ (1 + 0.0301/\sqrt{0.03176})$

$= 2001$ kV/m = 20 kV/cm.

$V_0 = E_0.r.\ \ln\ (2H/r) = 532.73$ kV r.m.s., line-to-ground,

$= 753.4$ kV peak.

At 525 kV, r.m.s., line-to-line, there is no corona present.

(*b*) 2.5 p.u. voltage = $2.5 \times 525\sqrt{2/3}$ = 1071.65 kV, crest.

Therefore, corona is present since the corona-onset voltage is 753.4 kV, crest.

When considering the effective radius, we assume a smooth surface for the envelope so that

$$1071.65 = 3000\ (1 + 0.0301/\sqrt{r_0}).r_0.\ln(26/r_0).$$

A trial and error solution yields r_0 = 0.05 metre. This is an increase in radius of 0.05 – 0.03176 = 0.01824 metre or 57.43%.

(*c*) $C = 2\pi e_0/\ln(2H/r)$.

Without corona, C = 8.282 nF/km;

With corona, C = 8.88 nF/km,

(*d*) The potential coefficient matrix is

$$[P] = \begin{bmatrix} P_{11}, & P_{12} \\ P_{21}, & P_{22} \end{bmatrix} \text{and}\,[M] = [P]^{-1} = \begin{bmatrix} P_{22}, & -P_{12} \\ -P_{21}, & P_{11} \end{bmatrix} \frac{1}{\Delta}$$

where $\Delta = |[P]|$, the determinant.

The self-capacitance is $2\pi e_0 P_{11}/\Delta$ while the mutual capacitance is – $2\pi e_o P_{12}/\Delta$. The coupling factor is $K_{12} = -P_{12}/P_{11}$.

Without corona $K_{12} = -\ln\ (\sqrt{26^2 + 10^2}/10)/\ln(26/0.03176)$

$= -1.0245/6.7076 = -0.15274$

With corona, $K_{12} = -1.0245/\ln\ (26/.05) = -0.1638$.

This is an increase of 7.135%.

For bundled conductors, coupling factors between 15% to 25% are found in practice. Note that with a switching surge of 1000 kV crest, the second conductor experiences a voltage of nearly 152 kV crest to ground so that the voltage between the conductors could reach 850 kV crest.

5.3.2 Charge-Voltage Diagram with Corona

When corona is absent the capacitance of a conductor is based on the physical radius of the metallic conductor. The charge-voltage relation is a straight line *OA* as shown in Figure 5.3 and $C = q_0/V_0$, where V_0 = the corona-inception voltage and q_0 the corresponding charge. However, beyond this voltage there is an increase in charge which is more rapid than given by the slope C of the straight-line $q_0 — V_0$ relation. This is shown as the portion *AB* which is nearly straight. When the voltage is decreased after reaching a maximum V_m there is a hysteresis effect and the $q – V$ relation follows the path *BD*. The slope of *BD* almost equals C showing that the space-charge cloud near the conductor has been absorbed into the conductor and charges far enough away from the conductor are not entirely pulled back. The essential properties of the $q – V$ diagram for one half-cycle of an ac voltage or the unipolar lightning and switching impulses can be obtained from the trapezoidal area *OABD* which represents the energy loss.

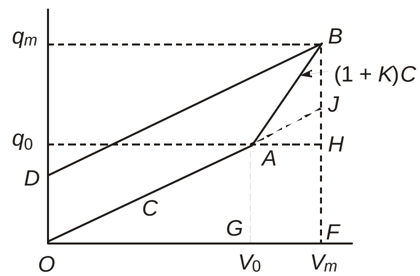

Fig. 5.3 Charge-Voltage diagram of corona.

Let the slope of *AB* equal $(1 + K)\,C$ where K is an experimental factor which lies between 0.6 and 0.8 having an average value of 0.7. The maximum charge correspondihg to V_m is denoted as q_m. The area of *OABD* equals $\frac{1}{2}KC(V_m^2 - V_0^2)$ as shown below:

$$\text{Area } OABD = (\text{Area } DOFB) - (\text{Area } OAG) - \text{Area } (GAHF) - \text{Area } (AHB)$$

$$= (\text{Area } DOFB) - \frac{1}{2}q_0V_0 - q_0(V_m - V_0) - \frac{1}{2}(q_m - q_0)(V_m - V_0)$$

$$= \text{Area DOFB} - \frac{1}{2}\{q_0V_m + q_m(V_m - V_0)\} \quad ...(5.16)$$

Now, $\quad BH = q_m - q_0 = (1+K)q_0(V_m - V_0)/V_0,$

$\quad JH = q_0(V_m - V_0)/V_0,$

and $\quad BF = q_m = q_0 + (1+K)q_0(V_m - V_0)/V_0,$

$\therefore \quad DO = BJ = BH - JH = Kq_0(V_m - V_0)/V_0. \quad ...(5.17)$

$$\text{Area } DOFB = \frac{1}{2}(DO + BF)V_m = Kq_0(V_m - V_0)V_m/V_0 + \frac{1}{2}q_0V_m^2/V_0 \quad ...(5.18)$$

$$\text{Area } OAG = \frac{1}{2}q_0V_0; \text{Area } AGFH = q_0(V_m - V_0).$$

$$\text{Area } AHB = \frac{1}{2}(q_m - q_0)(V_m - V_0) = \frac{1}{2}q_0(V_m^2 - V_0^2)/V_0 + \frac{1}{2}Kq_0(V_m - V_0)^2/V_0 \quad ...(5.19)$$

$$\therefore \qquad \text{Areas } (OAG + AGFH + AHB) = \frac{1}{2}(q_0/V_0)[V_m^2 + K(V_m - V_0)^2], \qquad ...(5.20)$$

Finally,

$$\text{Area } OABD = \frac{1}{2}K.q_0(V_m - V_0)(V_m + V_0)/V_0$$

$$= \frac{1}{2}KC(V_m^2 - V_0^2) \qquad ...(5.21)$$

For a unipolar waveform of voltage the energy loss is equal to equation (5.21). For an ac voltage for one cycle, the energy loss is twice this value.

$$\therefore \; W_{ac} = KC(V_m^2 - V_0^2) \qquad ...(5.22)$$

The corresponding power loss will be

$$P_c = f\,W_{ac} = fKC(V_m^2 - V_0^2) \qquad ...(5.23)$$

If the maximum voltage is very close to the corona-inception voltage V_0, we can write

$$V_m^2 - V_0^2 = (V_m + V_0)(V_m - V_0) = 2V_m(V_m - V_0), \text{ so that}$$

$$P_c = 2f\,KCV_m(V_m - V_0) \qquad ...(5.24)$$

where all voltages are crest values. When effective values for V_m and V_0 are used.

$$P_c = 4f\,KCV(V - V_0) \qquad ...(5.25)$$

This is very close to the Ryan-Henline formula, equation (5.14) with $K = 1$. For lightning and switching impulses the energy loss is equation (5.21) which is $W = \frac{1}{2}KC(V_m^2 - V_0^2)$ where all voltages are crest values.

Example 5.6. An overhead conductor of 1.6 cm radius is 10 m above ground. The normal voltage is 133 kV r.m.s. to ground (230 kV, line-to-line). The switching surge experienced is 3.5 p.u. Taking $K = 0.7$, calculate the energy loss per km of line. Assume smooth conductor.

Solution.

$$C = 2\pi e_0 / \ln(2H/r) = 7.79 \text{ nF/km}$$

$$E_0 = 30(1 + 0.0301/\sqrt{0.016}) = 37.14 \text{ kV/cm, crest}$$

$$\therefore \qquad V_0 = E_0.r. \ln(2H/r) = 423.8 \text{ kV, crest}$$

$$V_m = 3.5 \times 133\sqrt{2} = 658.3 \text{ kV, crest}$$

$$\therefore \qquad W = 0.5 \times 0.7 \times 7.79 \times 10^{-9}(658.3^2 - 423.8^2) \times 10^6 \text{ Joule/km}$$

$$= 0.7 \text{ kJ/km.}$$

This property will be used in deriving attenuation of travelling waves caused by lightning and switching in Chapter 8.

5.4 ATTENUATION OF TRAVELLING WAVES DUE TO CORONA LOSS

A voltage wave incident on a transmission line at an initial point $x = 0$ will travel with a velocity v such that at a later time t the voltage reaches a point $x = vt$ from the point of incidence, as shown in Figure 5.4 In so doing if the crest value of voltage is higher than the corona-disruptive voltage for the conductor, it loses energy while it travels and its amplitude decreases corresponding to the lower energy content. In addition to the attenuation or decrease in amplitude, the waveshape also shows distortion. In this section, we will discuss only attenuation since distortion must include complete equations of travelling waves caused by inductance and capacitance as well as conductor and ground-return resistance. This is dealt with in Chapter 8.

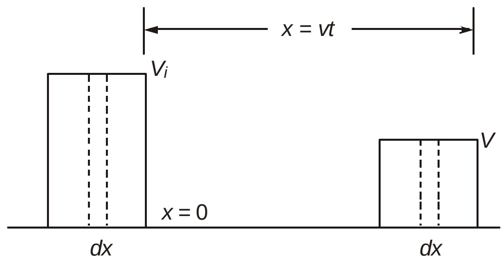

Fig. 5.4 Attenuation of voltage on a transmission line.

The energy of the wave is stored in both electromagnetic form and electrostatic form. The time rate of loss of stored energy is equal to the power loss due to corona, whose functional relationship with voltage has been given in Section 5.2. The total energy in a differential length dx of the wave will be.

$$dw = \frac{1}{2}(C.dx)V^2 + \frac{1}{2}(L.dx)I^2 \qquad ...(5.26)$$

where L and C are inductance and capacitance per unit length of line. For a travelling wave, the voltage V and current I are related by the surge impedance $Z = \sqrt{L/C},$ and the wave velocity is $v = 1/\sqrt{LC}$ Consequently, $I^2 = V^2/Z^2 = V^2C/L$. Thus, equation (5.26) becomes.

$$dw = C.dx.V^2. \qquad ...(5.27)$$

The rate of dissipation of energy, assuming the capacitance does not change with voltage for the present analysis, is

$$dw/dt = d\,(CV^2.dx)/dt = 2CV.dx.dV/dt. \qquad ...(5.28)$$

Now, the power loss over the differential length dx is

$$P_c = f(V).dx, \text{so that } 2CV.dV/dt = -P_c = -f(V). \qquad ...(5.29)$$

For different functional relations $P_c = f(V)$, equation (5.29) can be solved and the magnitude of voltage after a time of travel t (or distance $x = vt$) can be determined. We will illustrate the procedure for a few typical values of $f(V)$, but will consider the problem later on by using equation (5.21) in Chapter 8.

(*a*) *Linear Relationship*

Let $f(V) = K_s(V - V_0)$. Then, with V_i = initial voltage, $2\,CV\,dV/dt = -K_s(V - V_0)$. By separating variables and using the initial condition $V = V_i$ at $t = 0$ yields

$$(V - V_0).e^{V/V_0} = (V_i - V_0).e^{(V_i \propto t)/V_0}, \qquad ...(5.30)$$

where $\alpha = K_s/2C$ and V_0 = corona-inception voltage.

Also, the voltages in excess of the corona-inception voltage at any time t or distance $x = vt$ will be

$$(V - V_0)/V_i - V_0) = e^{(V_i - V - \propto t)/V_0}. \qquad ...(5.31)$$

This expression yields an indirect method of determining $\alpha = K_s/2C$ by experiment, if distortion is not too great. It requires measuring the incident wave magnitude V_i and the magnitude V after a time lapse of t or distance $x = vt$ at a different point on the line, whose corona-inception voltage V_0 is known. When C is also known, the constant K_s is calculated.

Example 5.7. A voltage with magnitude of 500 kV crest is incident on a conductor whose corona-inception voltage is 100 kV crest, and capacitance C = 10 nF/km. After a lapse of 120 μs (36 km of travel at light velocity) the measured amplitude is 110 kV. Calculate α and K_s.

Solution. $V_i/V_0 = 5, V - V_0 = 10, V_i - V_0 = 400.$

$$V_0 = 100\text{kV} = 10^5 \text{ volts}$$

$$\therefore \quad 10/400 = [\exp(500-110)/100] \exp(-120\times10^{-6}\times a/10^5)$$

This gives $\alpha = K_s/2C = 6.325\times10^9$ volt$-$sec^{-1}.

$$\therefore \quad K_s = 2\times6.325\times10^9\times10\times10^{-9} = 126.5 \text{ watts/km-volt or Amp/km.}$$

(*b*) *Quadratic Formula*

(*i*) Let the loss be assumed to vary as

$$f(V) = K_R\, V(V - V_0) \quad \text{...(5.32)}$$

So that

$$2CV\,(dV/dt) = -K_R\, V(V - V_0).$$

With $V = V_i$ at $t = 0$, integration gives

$$\frac{V - V_0}{V_i - V_0} = \exp[-(K_R/2C)t] \quad \text{...(5.33)}$$

The voltage in excess of corona-inception value behaves as if it is attenuated by a resistance of R per unit length as given by the formula

$$(V - V_0) = (V_i - V_0).\ \exp[-(R/2L)t]$$

$$\therefore \quad K_R = RC/L = R/Z^2.$$

For the previous example.

$$K_R = \frac{2\times10^{-9}}{120\times10^{-6}}.\ \ln\frac{400}{10} = 61.5\times10^{-6}.$$

The units are watts/km-volt^2.

(*ii*) If the loos is assumed to vary as

$$f(V) = K_Q(V^2 - V_0^2) \quad \text{...(5.34)}$$

then $2CV\,(dV/dt) = -K_Q(V^2 - V_0^2)$ with $V = V_i$ *at* $t = 0$.

$$\therefore \quad \frac{V^2 - V_0^2}{V_i^2 - V_0^2} = \exp[-(K_Q/C)t]$$

For the previous example,

$$K_Q = \frac{10\times10^{-9}}{120\times10^{-6}}.\ln\frac{500^2 - 100^2}{110^2 - 100^2} = 395\times10^{-6}.$$

(*iii*) Let $f(V) = K_P(V - V_0)^2$. Then,

$$2CV.(dV/dt) = -K_P(V - V_0)^2 \text{ with } V = V_i \text{ at } t = 0.$$

This gives

$$\ln \frac{V_i - V_0}{V - V_0} + \frac{V_0(V_i - V)}{(V_i - V_0)(V - V_0)} = (K_P/2C)t \quad ...(5.35)$$

For $V_0 = 100$ kV, $V_i = 500$ kV, $V = 110$ kV, $C = 10 \times 10^{-9}$ F/km, and $t = 120 \times 10^{-6}$ sec, there results $K_p = 224 \times 10^{-6}$.

(*c*) *Cubic Relation*

$$\text{If } f(V) = K_c.V^3, 2CV(dV/dt) = -K_cV^3$$

giving $$V_i/V = 1 + (K_c/2C)V_it. \quad ...(5.36)$$

For the previous example, $K_c = 1.182 \times 10^{-9}$ watts/km-volt^3.

5.5 AUDIBLE NOISE: GENERATION AND CHARACTERISTICS

When corona is present on the conductors, e.h.v. lines generate audible noise which is especially high during foul weather. The noise is broadband, which extends from very low frequency to about 20 kHz. Corona discharges generate positive and negative ions which are alternately attracted and repelled by the periodic reversal of polarity of the ac excitation. Their movement gives rise to sound-pressure waves at frequencies of twice the power frequency and its multiples, in addition to the broadband spectrum which is the result of random motions of the ions, as shown in Figure 5.5. The noise has a pure tone superimposed on the broadband noise. Due to differences in ionic motion between ac and dc excitations, dc lines exhibit only a broadband noise, and furthermore, unlike for ac lines, the noise generated from a dc line is nearly equal in both fair and foul weather conditions. Since audible noise (AN) is man-made, it is measured in the same manner as other types of man-made noise such as aircraft noise, automobile ignition noise, transformer hum, etc. We will describe meters used and methods of AN measurements in a subsequent section 5.7.

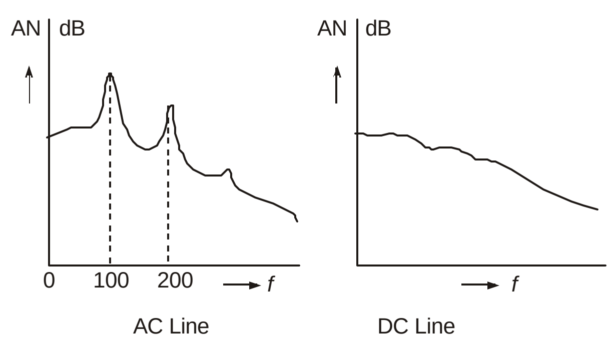

Fig. 5.5 Audible Noise frequency spectra from ac and dc transmission lines.

Audible noise can become a serious problem from 'psycho-acoustics' point of view, leading to insanity due to loss of sleep at night to inhabitants residing close to an e.h.v. line. This problem came into focus in the 1960's with the energization of 500 kV lines in the USA. Regulatory bodies have not as yet fixed limits to AN from power transmission lines since such regulations do not exist for other man-made sources of noise. The problem is left as a social one which has to be settled by public opinion. The proposed limits for AN are discussed in the next section.

5.6 LIMITS FOR AUDIBLE NOISE

Since no legislation exists setting limits for AN for man-made sources, power companies and environmentalists have fixed limits from public-relations point of view which power companies have accepted from a moral point of view. In doing so, like other kinds of interference, human beings must be subjected to listening tests. Such objective tests are performed by every civic-minded power utility organization. The first such series of tests performed from a 500-kV line of the Bonneville Power Administration in the U.S.A. is known as Perry Criterion. The AN limits are as follows:

No complaints : Less than 52.5 dB (*A*),

Few complaints : 52.5 dB (A) to 59 dB (*A*),

Many complaints : Greater than 59 dB (*A*),

The reference level for audible noise and the dB relation will be explained later. The notation (*A*) denotes that the noise is measured on a meter on a filter designated as *A*-weighting network. There are several such networks in a meter.

Design of line dimensions at e.h.v. levels is now governed more by the need to limit AN levels to the above values. The selection of width of line corridor or right-of-way (R-O-W), where the nearest house can be permitted to be located, if fixed from AN limit of 52.5 dB(*A*), will be found adequate from other points of view at 1000 to 1200 kV levels. The design aspect will be considered in Section 5.8. The audible noise generated by a line is a function of the following factors:

(*a*) the surface voltage gradient on conductors,

(*b*) the number of sub-conductors in the bundle,

(*c*) conductor diameter,

(*d*) atmospheric conditions, and

(*e*) the lateral distance (or aerial distance) from the line conductors to the point where noise is to be evaluated.

The entire phenomenon is statistical in nature, as in all problems related to e.h.v. line designs, because of atmospheric conditions.

While the Perry criterion is based upon actual listening experiences on test groups of human beings, and guidelines are given for limits for AN from an e.h.v. line at the location of inhabited places, other man-made sources of noise do not follow such limits. A second criterion for setting limits and which evaluates the nuisance value from man-made sources of AN is called the 'Day-Night Equivalent' level of noise. This is based not only upon the variation of AN with atmospheric conditions but also with the hours of the day and night during a 24-hour period. The reason is that a certain noise level which can be tolerated during the waking hours of the day, when ambient noise is high, cannot be tolerated during sleeping hours of the night when little or no ambient noises are present. This will be elaborated upon in Section 5.9. According to the Day-Night Criterion, a noise level of 55 dB(*A*) can be taken as the limit instead of 52.5 dB(A) according to the Perry Criterion. From a statistical point of view, these levels are considered to exist for 50% of the time during precipitation hours. These are designated as L_{50} levels.

5.7 AN MEASUREMENT AND METERS

5.7.1 Decibel Values in AN and Addition of Sources

Audible noise is caused by changes in air pressure or other transmission medium so that it is described by Sound Pressure Level (SPL). Alexander Graham Bell established the basic unit for SPL as 20×10^{-6} Newton/m^2 or 20 micro Pascals [2×10^{-5} micro bar]. All decibel values are referred to this basic unit. In telephone work there is a flow of current in a set of head-phones or receiver. Here the basic units are 1 milliwatt across 600 ohms yielding a voltage of 775 mV and a current of 1.29 mA. For any other SPL, the decibel value is

$$\text{SPL(dB)} = 10 \text{ Log}_{10} (\text{SPL}/20 \times 10^{-6}) \text{ Pascals} \quad ...(5.37)$$

This is also termed the 'Acoustic Power Level', denoted by PWL, or simply the audible noise level, AN.

Example 5.8. The AN level of one phase of a 3-phase transmission line at a point is 50 dB. Calculate (*a*) the SPL in Pascals; (*b*) if a second source of noise contributes 48*dB* at the same location, calculate the combined AN level due to the two sources.

Solution.

(*a*) $10 \text{ Log}_{10} (\text{SPL}_1/2 \times 10^{-5}) = 50$, which gives

$\text{SPL}_1 = 2 \times 10^{-5} \times 10^{50/10} = 2$ Pascals

(*b*) Similarly, $\text{SPL}_2 = 2 \times 10^{-5} \times 10^{48/10} = 1.262$ Pascals

$\therefore$ Total SPL = $\text{SPL}_1 + \text{SPL}_2 = 3.262$ Pascals.

The decibel value will be

$\text{AN} = 10 \text{ Log}_{10} (\text{SPL}/2 \times 10^{-5}) = 52.125$ dB.

Consider N sources whose decibel values, at a given point where AN level is to be evaluated, are $\text{AN}_1, \text{AN}_2, ..., \text{AN}_N$. In order to add these sources and evaluate the resultant SPL and dB values, the procedure is as follows:

The individual sound pressure levels are

$$\text{SPL}_1 = 20 \times 10^{-6} \times 10^{\text{AN}_1/10}, \text{SPL}_2 = 20 \times 10^{-6} \times 10^{\text{AN}_2/10} \text{ etc.}$$

$$\therefore \text{ The total SPL} = \text{SPL}_1 + \text{SPL}_2 + \ldots = 2 \times 10^{-5} \sum_{i=1}^{N} 10^{\text{AN}_i/10} \quad ...(5.38)$$

The decibel value of the combined sound pressure level is

$$\text{AN} = 10 \text{ Log}_{10} (\text{SPL}/2 \times 10^{-5}) = 10 \text{ Log}_{10} \sum_{i=1}^{N} 10^{0.1\text{AN}_i} \quad ...(5.39)$$

Example 5.9. A 3-phase line yields AN levels from individual phases to be 55 dB, 52 dB, and 48 dB. Find the resulting AN level of the line.

Solution. $10^{0.1\text{AN}_1} + 10^{0.1\text{AN}_2} + 10^{0.1\text{AN}_3} = 10^{5.5} + 10^{5.2} + 10^{4.8} = 5.382 \times 10^5$

$\therefore$ $\text{AN} = 10 \text{ Log}_{10}(5.382 \times 10^5) = 57.31 \text{ dB}.$

5.7.2 Microphones

Instruments for measurement of audible noise are very simple in construction in so far as their principles are concerned. They would conform to standard specifications of each country, as for example, ANSI, ISI or I.E.C., etc. The input end of the AN measuring system consists of a microphone as shown in the block diagram, Figure 5.6. There are three types of microphones used in AN measurement from e.h.v. lines and equipment. They are (*i*) air-condenser type; (*ii*) ceramic; and (*iii*) electret microphones. Air condenser microphones are very stable and exhibit highest frequency response. Ceramic ones are the most rugged of the three types. Since AN is primarily a foul-weather phenomenon, adequate protection of microphone from weather is necessary. In addition, the electret microphone requires a polarization voltage so that a power supply (usually battery) will also be exposed to rain and must be protected suitably.

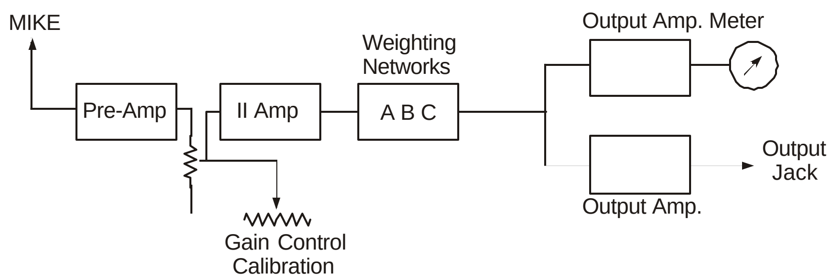

Fig. 5.6 Block diagram of AN Measuring Circuit.

Some of the microphones used in AN measurement from e.h.v. lines are General Radio Type 1560-P, or 1971-9601, or Bruel and Kjor type 4145 or 4165, and so on. The GR type has a weather protection. Since AN level form a transmission line is much lower than, say, aircraft or ignition noise, 1″ (2.54 cm) diameter microphones are used although some have used $\frac{1}{2}$″ ones, since these have more sensitivity than 1" microphones. Therefore, size is not the determining factor.

The most important characteristic of a microphone is its frequency response. In making AN measurements, it is evident that the angle between the microphone and the source is not always 90° so that the grazing angle determines the frequency response. Some typical characteristics are as shown in Figure 5.7.

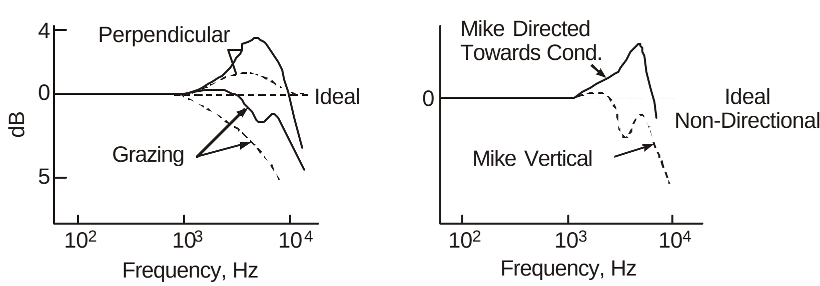

Fig. 5.7 Response of microphone for grazing and perpendicular incidence.

AN levels are statistical in nature and long-term measurements are carried out by protecting the microphone from rain, wind, animals, and birds. Some types of shelters use wind-screens with a coating of silicone grease. Foam rubber wind-covers have also been used which have negligible attenuation effect on the sound, particularly on the *A*-weighted network which will be described below. Every wind-cover must also be calibrated and manufacturers supply this data. Foam-rubber soaks up rain and must be squeezed out periodically and silicone grease applied.

5.7.3 Weighting Networks

There are 5 weighting networks designated as *A* to *E* in Sound Pressure Level Meters. The '*A*' weighted network has been designed particularly to have nearly the same response as the human ear, while the '*C*' weighted network has a flat response up to 16 kHz. The '*A*' network is also least susceptible to wind gusts. It is also preferred by Labour Relations Departments for assessing the adversity of noise-created psychological and physiological effects in noisy environments such as factories, power stations, etc.

Typical frequency response of the *A, B, C* weighting networks are sketched in Figure 5.8(*a*) while 5.8(*b*) compares the responses of *A, D* networks. The *A*-weighting network is widely used for relatively nondirectional sources. From these curves it is seen that the *C*-network provides essentially flat response from 20 Hz to 10 kHz. The human ear exhibits such flat response for sound pressure levels up to 85 dB or more. At lower SPL, the human ear does not have a flat response with frequency and the *A* and *B* networks are preferred. The *A* network is used for SPL up to 40 dB and the *B* for SPL up to 70 dB. Sometimes, the *A*-weighted network is known as the 40 dB network. It is also used for transformer noise measurements.

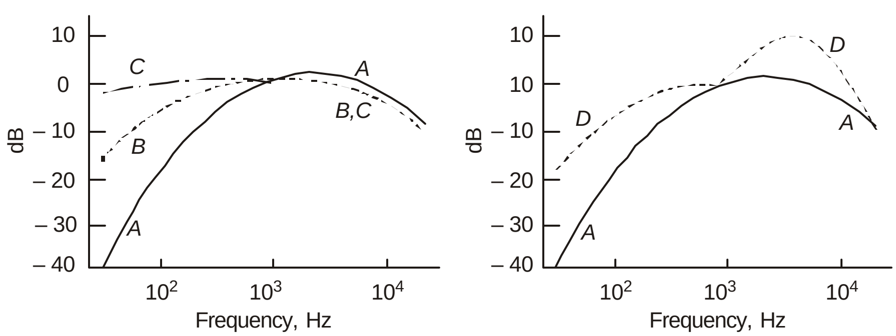

Fig. 5.8 Frequency responses of (*a*) *A, B, C* weighting networks, (*b*) *A, D* weighting networks.

5.7.4 Octave Band and Third Octave Band

It was mentioned earlier that in addition to the broadband noise generated by corona, pure tones at double the power frequency and its multiples exist. These discrete-frequency components or line spectra are measured on octave bands by selective filters. Figure 5.9 shows a schematic diagram of the switching arrangement for use with a 50-Hz line.

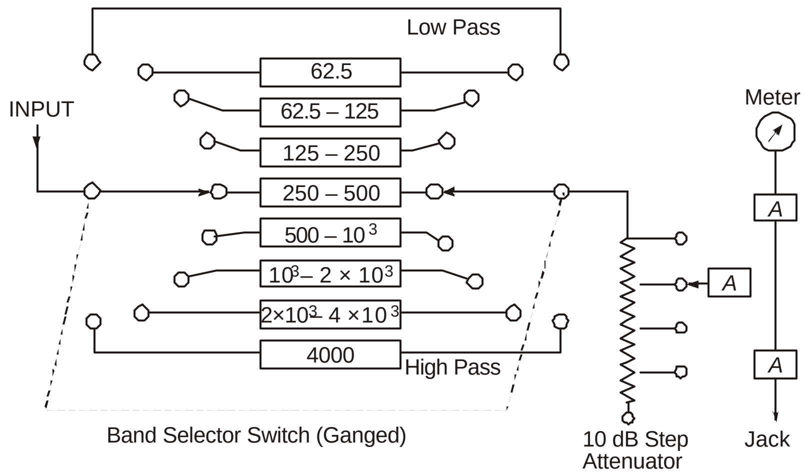

Fig. 5.9 Octave band AN meter circuit.

The octave band consists of a centre frequency f_0. Let f_1 and f_2 be the upper and lower frequencies of the bands. Then $f_0 = \sqrt{f_1 f_2}$. An octave band extends from the lower frequency $f_2 = f_0/\sqrt{2}$ to the upper frequency $f_1 = \sqrt{2}f_0 = 2f_2$.

A third-octave band extends from the lower frequency $f_3 = f_0/(2)^{1/6} = 0.891\ f_0$ to an upper frequency $f_4 = (2)^{1/6}.f_0 = 1.1225f_0 = (2)^{1/3}f_3$. The octave and third-octave band SPL is the integrated SPL of all the frequency components in the band.

Example 5.10. An octave band has a centre frequency of 1000 Hz. (*a*) Calculate the upper and lower frequencies of the band. (*b*) Calculate the same for third-octave band.

Solution. (*a*) $f_0 = 1000$. $\therefore$ $f_1 = \sqrt{2}f_0 = 1414$ Hz, $f_2 = 707$ Hz.

(*b*) $f_4 = (2)^{1/6}f_0 = 1122\,\text{Hz}, f_3 = 1000/(2)^{1/6} = 891\,\text{Hz}$.

All frequency components radiated by a transmission line have to propagate from the conductor to the meter and therefore intervening media play an important role, particularly reflections from the ground surface. The lowest-frequency octave band is most sensitive to such disturbances while the *A*-weighted network and higher frequency octave bands give a flat overall response. Examples are shown in Figure 5.10.

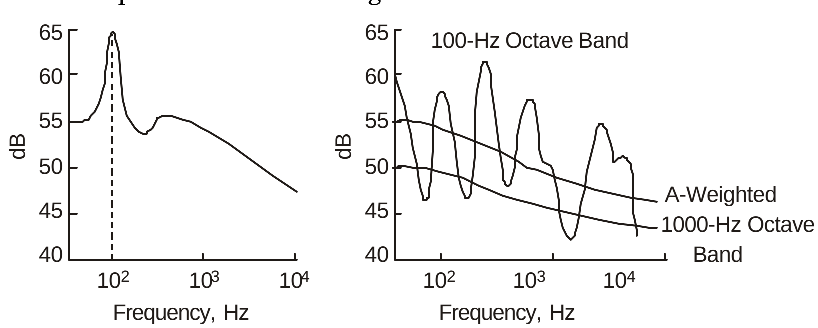

Fig. 5.10 Octave band response for line AN.
(*a*) Frequency spectrum, (*b*) Lateral profile for 100-Hz Octave band.

Thus, displacing the microphone even a few metres can give erroneous results on a 100-Hz octave band. The curve is caused by standing waves and reflections from the ground surface.

5.8 FORMULAE FOR AUDIBLE NOISE AND USE IN DESIGN

Audible noise from a line is subject to variation with atmospheric condition. This means that there is no one quantity or AN level that can be considered as the audible noise level of a line. All designers accept two levels–the L_{50} level and the L_5 level. These are defined as follows:

L_{50} *Level:* This is the AN level as measured on the A-weighted network which is exceeded 50% of the time during periods of rain, usually extending over an entire year.

L_5 *Level*: Similar to L_{50}, but exceeded only 5% of the total time.

The L_5 level is used for describing the noise levels in heavy rain which are generated in artificial rain tests. These are carried out in 'cage tests' where artificial rain apparatus is used, as well as from short outdoor experimental lines equipped with such apparatus. Many empirical formulas exist for calculating the AN level of an e.h.v. line [see IEEE Task Force paper, October 1982]. However, we will discuss the use of the formula developed by the B.P.A. of the USA. It is applicable for the following conditions:

(*a*) All line geometries with bundles having up to 16 sub-conductors.

(*b*) Sub-conductor diameters in the range 2 cm to 6.5 cm.

(*c*) The AN calculated is the L_{50} level in rain.

(*d*) Transmission voltages are 230 kV to 1500 kV, 3-phase ac.

Referring to Figure 5.11, the AN level of each phase at the measuring point M is, with i = 1, 2, 3,

$$\text{AN}(i) = 120 \log_{10} E_{am}(i) + 55 \log_{10} d - 11.4 \log_{10} D(i) - 115.4, \text{ dB}(A) \quad (5.40)$$

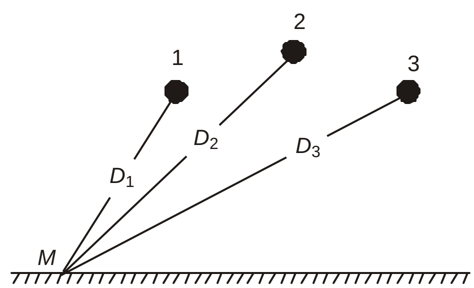

Fig. 5.11 Calculation of AN level of line by B.P.A. Formula.

It applies for $N < 3$ sub-conductors in the bundles. For $N \geq 3$, the formula becomes

$$\text{AN}(i) = 120 \log_{10} E_{am}(i) + 55 \log_{10} d - 11.4 \log_{10} D(i) + 26.4 \log_{10} N - 128.4, \text{ dB}(A) \quad ...(5.41)$$

Here, $E_{am}(i)$ = average maximum surface voltage gradient on bundle belonging to phase i in kV/cm, r.m.s.

d = diameter of sub-conductor in cm.,

N = number of sub-conductors in bundle,

and $D(i)$ = aerial distance from phase i to the location of the microphone in metres.

When all dimensions are in metre units, the above give

$$N < 3 : \text{AN}(i) = 120 \log E_m(i) + 55 \log d_m - 11.4 \log D(i) + 234.6, \text{ dB}(A) \quad ...(5.42)$$

$$N \geq 3 : \text{AN}(i) = 120 \log E_m(i) + 55 \log d_m - 11.4 \log D(i) + 26.4 \log N + 221.6, \text{ dB}(A) \quad ...(5.43)$$

Having calculated the AN level of each phase, the rule for addition of the three levels follows equation (5.39),

$$\text{AN} = 10 \log_{10} \sum_{i=1}^{3} 10^{0.1AN(i)}, \text{dB}(A) \quad ...(5.44)$$

For a double-circuit line, the value of i extends from 1 to 6.

We observe that the AN level depends on the following four quantities:

(*i*) the surface voltage gradient on conductor,

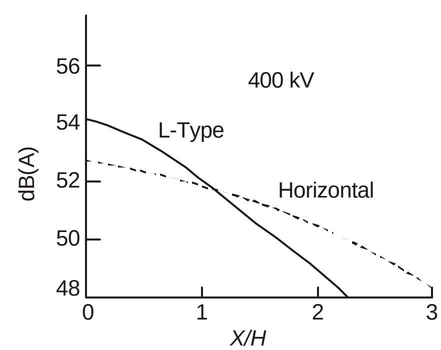

Fig. 5.12 AN level of 400 kV line (calculated).

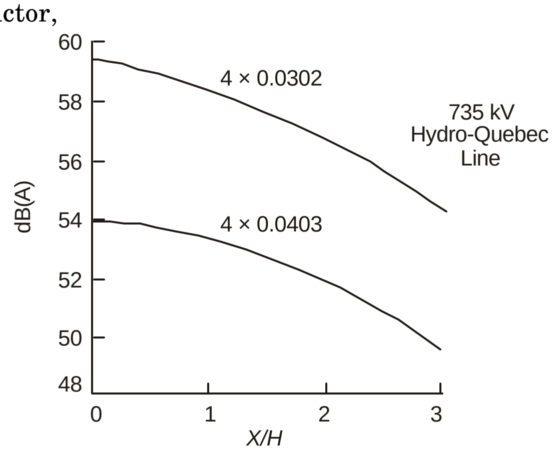

Fig. 5.13 AN level of 735 kV line (calculated).

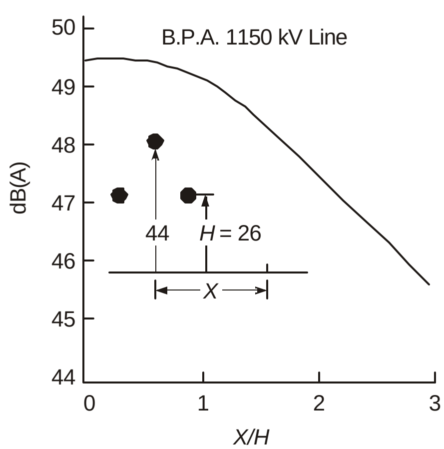

Fig. 5.14 AN level of 1150 kV line (calculated).

(*ii*) the conductor diameter,

(*iii*) the number of sub-conductors in bundle, and (*iv*) the aerial distance to the point of measurement from the phase conductor under consideration. Atmospheric condition is included in having prescribed this as the L_{50}-level while the weighting network is described by the notation dB(*A*) on a Sound Level Meter.

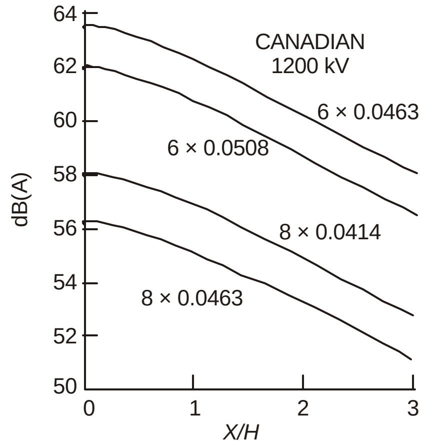

Fig. 5.15 AN level of 1200 kV horizontal line (calculated).

A model for the generation of AN under rain has been developed very recently by Kirkham and Gajda to which the reader is referred for very thoughtful ideas on the basic mechanisms involved in AN generation.

L_{50} levels of AN from several representative lines from 400 kV to 1200 kV are plotted in Figs. 5.12 to 5.15, calculated according to the B.P.A. formula, equations (5.40) to (5.44). In all cases, the average maximum gradient does not differ from the maximum gradient in the bundle by more than 4%, so that only the maximum surface voltage gradient is used in the above figures. This is as described in Chapter 4.

$$E_{max} = \frac{q}{2\pi e_0}\frac{1}{N}\frac{1}{r}[1+(N-1)r/R] \quad ...(5.45)$$

Example 5.11. A 735 kV line has the following details: $N = 4$, $d = 3.05$ cm, B = bundle spacing = 45.72 cm, height $H = 20$ m, phase separation $S = 14$ m in horizontal configuration. By the Mangoldt formula, the maximum conductor surface voltage gradients are 20kV/cm and 18.4 kV/cm for the centre and outer phases, respectively. Calculate the SPL or AN in dB(*A*) at a distance of 30 m along ground from the centre phase (line centre). Assume that the microphone is kept at ground level. See Figure 5.16.

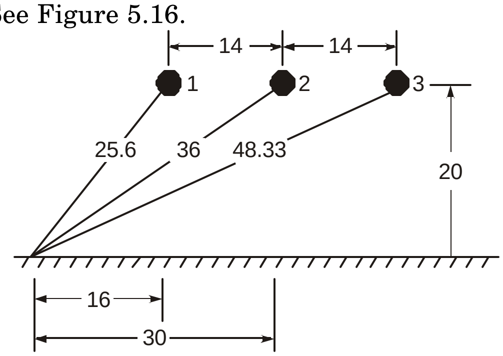

Fig. 5.16 735 kV line configuration for Example 5.11.

Solution.

Phase 1. $E_m = 18.4, D_1 = 25.6$

$AN_1 = 120 \log_{10} 18.4 + 55 \log_{10} 3.05 - 11.4 \log_{10} 25.6 + 26.4 \log_{10} 4 - 128.4$

$= 120 \log 18.4 - 11.4 \log 25.6 - 85.87$

$= 151.78 - 16.05 - 85.87 = 49.86$ dB(A)

Phase 2. $E_m = 20, D_2 = 36$

$AN_2 = 120 \log 20 - 11.4 \log 36 - 85.87 = 52.5$ dB(A)

Phase 3. $E_m = 18.4, D_3 = 48.33$

$AN_3 = 120 \log 18.4 - 11.4 \log 48.33 - 85.87 = 46.71$ dB(A)

$\therefore$ Total $AN = 10 \log_{10} (10^{4.986} + 10^{5.25} + 10^{4.671}) = 10 \log (32.15 \times 10^4) = 55$ dB(A)

This is within the range of low-complaint region according to the Perry Criterion which is 52.5 to 59 dB(A).

5.9 RELATION BETWEEN SINGLE-PHASE AND 3-PHASE AN LEVELS

Obtaining data of AN and other quantities from e.h.v. lines involves great expense in setting up full-scale outdoor 3-phase experimental lines. Most of the design data can be obtained at less cost from a single-phase outdoor line or from cage experiments. The quantities of interest in so far as interference from e.h.v. lines are concerned are AN, Radio Interferecne and Electrostatic Field at 50 Hz. It is therefore worth the effort to consider what relation, if any, exists between experimental results obtained from 1-phase lines and an actual 3-phase line. If such a relation can be found, then 1-phase lines can be used for gathering data which can then be extrapolated to apply to 3-phase lines. We first consider a horizontal line.

The AN level from any phase at the measuring point M consists of a constant part and a variable part which can be seen from equations (5.40) to (5.43). They are written as, for $N \geq 3$,

$$AN_1 = (55 \log d + 26.4 \log N - 128.4) + 120 \log E_1 - 11.4 \log D_1$$
$$= K + 120 \log E_1 - 11.4 \log D_1$$

Similarly, $$AN_2 = K + 120 \log E_2 - 11.4 \log D_2$$

and $$AN_3 = K + 120 \log E_1 - 11.4 \log D_3$$

Let the centre-phase gradient be written as $E_2 = (1 + m) E_1$ and the ratios $k_2 = D_2/D_1$ and $k_3 = D_3/D_1$. Then, total AN level of the 3-phases obtained after combining the AN levels of the 3 individual phases is

$$AN_T = 10 \log_{10} \sum_{i=1}^{3} 10^{0.1\,AN(i)}$$
$$= 10 \log_{10}[10^{0.1K}.10^{12 \log E_1}\{10^{-1.14 \log D_1} + 10^{-1.14 \log D_3}$$
$$+ 10^{-1.14 \log D_2 + 12 \log(1+m)}\}]$$
$$= K + 120 \log E_1 - 11.4 \log D_1 + 10 \log [1 + k_3^{-1.14} + (1 + m)^{12}.k_2^{-1.14}] \quad ...(5.46)$$

For a single-phase line with the same surface voltage gradient E_2 as the centre-phase conductor of the 3-phase configuration, and at a distance D_2, the noise level is

$$AN_s = K + 120 \log E_1 - 11.4 \log D_1 + 10 \log_{10} [k_2^{-1.14} (1 + m)^{12}] \quad ...(5.47)$$

Therefore, the difference in AN levels of equation (5.46) and (5.47) is

$$\mathrm{AN}_T - \mathrm{AN}_s = 10 \log_{10} \frac{1 + k_3^{-1.14} + k_2^{-1.14}(1+m)^{12}}{k_2^{-1.14}(1+m)^{12}} \qquad ...(5.48)$$

This is the decibel adder which will convert the single-phase AN level to that of a 3-phase line.

Example 5.12. Using equation (5.46) compute AN_T for the 735 kV line of example 5.11.

Solution. $K = -85.87$, $1 + m = 20/18.4 = 1.087$.

$11.4 \log D_1 = 16.05$, $120 \log E_1 = 151.8$, $k_2 = 36/25.6 = 1.406$,

$k_3 = 48.33/25.6 = 1.888$

$$\therefore \quad 1 + k_3^{-1.14} + k_2^{-1.14}(1+m)^{12} = 3.33$$

$$\mathrm{AN}_T = -85.87 + 151.8 - 16.05 + 10 \log 3.33 = 55.1 \text{ dB}(A).$$

Example 5.13. Using equation (5.48). compute the decibel adder to convert the single-phase AN level of the centre phase to the three-phase AN level of examples 5.11 and 5.12.

Solution.

$$\frac{1 + k_3^{-1.14} + k_2^{-1.14}(1+m)^{12}}{k_2^{-1.14}(1+m)^{12}} = \frac{3.33}{1.8444} = 1.8054$$

$\therefore$ dB adder = 10 log 1.8054 = 2.566.

The AN level of the centre phase was 52.5 dB(A) at 30 m from the conductor along ground. This will be the level of a single-phase line with the same surface voltage gradient and distance to the location of microphone.

$\therefore$ $\mathrm{AN}_T = \mathrm{AN}_s +$ dB adder = 52.5 + 2.566 = 55.07 dB(A)

5.10 DAY-NIGHT EQUIVALENT NOISE LEVEL

In previous discussions the AN level of a transmission line has been chosen as the L_{50} value or the audible noise in decibels on the A-weighted network that is exceeded for 50% of the duration of precipitation. This has been assumed to give an indication of the nuisance value. However, another criterion which is actively followed and applied to man-made AN sources is called the Day-Night Equivalent Noise level. This has found acceptance to aircraft noise levels, heavy road traffic noise, ignition noise, etc., which has led to litigation among many aggrieved parties and the noise makers. According to this criterion, certain sound level might be acceptable during day-time hours when ambient noises will be high. But during the night-time hours the same noise level from a power line or other man-made sources could be found objectionable because of the absence of ambient noises. The equivalent annoyance during nights is estimated by adding 10 dB(A) to the day-time AN level, or, in other words, by imposing a 10 dB (A) penalty.

Consider an L_{50} level of a power line to be AN and the day-time to last for D hours. Then, the actual annoyance level for the entire 24 hours is computed as a day-night equivalent level as follows:

$$L_{dn} = 10 \log_{10} \left[\frac{1}{24} \{ D.10^{0.1\mathrm{AN}} + (24 - D).10^{0.1(\mathrm{AN}+10)} \} \right], \text{ dB}(A) \qquad ...(5.49)$$

This is under the assumption that the level AN is present throughout the 24 hours.

Example 5.14. The L_{50} level of a line is 55 dB(A). The day-light hours are 15 and night-time is 9 hours in duration. Calculate the day-night equivalent and the decibel adder to the day-time AN level.

Solution. $$L_{dn} = 10\,\text{Log}_{10}\left[\frac{1}{24}(15\times 10^{5.5} + 9\times 10^{6.5})\right] = 61.4\,\text{dB}(A)$$

The decibel adder is 61.4 – 55 = 6.4 dB(A).

An addition of 6.4 dB increases the SPL by 4.365 times [10 log 4.365 = 6.4]. The nuisance value of the line has been increased by 6.4 dB(A) by adding 10 dB(A) penalty for night hours.

If the day-night hours are different from 15 and 9, a different decibel adder will be necessary. The 10 dB(A) penalty added to night time contributes 6 times the AN value as the day-time level, since.

$$9\times 10^{6.5}/15\times 10^{5.5} = 90/15 = 6.$$

In evaluating the nuisance value of AN from an e.h.v. line, we are only concerned with the duration of rainfall during a day and not the total day-night hours or 24 hours. If rain is not present over the entire 24 hours but only for a certain percentage of the day and night, then the day-night equivalent value of AN is calculated as shown below. Let it be assumed that

p_d = % of duration of rainfall during the day time,

and p_n = % of duration of rainfall during the night.

Then, $$L_{dn} = 10\,Log_{10}\,[(1/24)\{(Dp_d/100).10^{0.1\text{AN}} + (24-D)(p_n/100)\,10^{0.1(\text{AN}+10)}\}] \quad ...(5.50)$$

Example 5.15. The following data are given for a line : L_{50} = 55 dB(A). D = 15, p_d = 20, p_n = 50. Calculate the day-night equivalent of AN and the dB-adder.

Solution. Duration of rain is 3 hours during the day and 4.5 hours during the night.

$$\therefore \quad L_{dn} = 10\,\text{Log}_{10}[(1/24)(15\times 0.2\times 10^{5.5} + 9\times 0.5\times 10^{6.5})]$$
$$= 58\ \text{dB}(A).$$

The decibel adder is 3 dB(A).

Now, the night-time contribution is 15 times that during the day time ($4.5 \times 10^{6.5}/3 \times 10^{5.5}$ = 45/3 = 15).

In the above equation (5.50), it was assumed that the L_{50} levels for both day and night were equal, or in other words, the precipitation characteristics were the same. If this is not the case, then the proper values must be used which are obtained by keeping very careful record of rainfall rates and AN levels. Such experiments are performed with short outdoor experimental lines strung over ground, or in 'cages'.

5.11 SOME EXAMPLES OF AN LEVELS FROM EHV LINES

It might prove informative to end this chapter with data on the performance of some e.h.v. line designs based upon AN limits from all over the world.

(1) The B.P.A. in the U.S.A. has fixed 50 dB(A) limit for the L_{50} noise level at 30 m from the line centre in rain for their 1150 kV line operating at 1200 kV.

(2) The A.E.P., U.H.V. Project of the E.P.R.I., and several other designs fall very close to the above values.

6

Corona Effects-II: Radio Interference

6.1 CORONA PULSES: THEIR GENERATION AND PROPERTIES

There are in general two types of corona discharge from transmission-line conductors: (i) Pulseless or Glow Corona; (ii) Pulse Type or Streamer Corona. Both these give rise to energy loss, but only the pulse-type of corona gives interference to radio broadcast in the range of 0.5 MHz to 1.6 MHz. In addition to corona generated on line conductors, there are spark discharges from chipped or broken insulators and loose guy wires which interfere with TV reception in the 80–200 MHz range. Audible noise has already been discussed in Chapter 5 which is caused by rain drops and high humidity conditions. Corona on conductors also causes interference to Carrier Communication and Signalling in the frequency range 30 kHz to 500 kHz.

In the case of Radio and TV interference the problem is one of locating the receivers far enough from the line in a lateral direction such that noise generated by the line is low enough at the receiver location in order to yield a satisfactory quality of reception. In the case of carrier interference, the problem is one of determining the transmitter and receiver powers to combat line-generated noise power.

In this section we discuss the mechanism of generation and salient characteristics of only pulse-type corona in so far as they affect radio reception. As in most gas discharge phenomena under high impressed electric fields, free electrons and charged particles (ions) are created in space which contain very few initial electrons. We can therefore expect a build up of resulting current in the conductor from a zero value to a maximum or peak caused by the avalanche mechanism and their motion towards the proper electrode. Once the peak value is reached there is a fall in current because of lowering of electric field due to the relatively heavy immobile space charge cloud which lowers the velocity of ions. We can therefore expect pulses to be generated with short crest times and relatively longer fall times. Measurements made of single pulses by the author in co-axial cylindrical arrangement are shown in Figure 6.1 under dc excitation. Similar pulses occur during the positive and negative half-cycles under ac excitation. The best equations that fit the observed wave shapes are also given on the figures. It will be assumed that positve corona pulses have the equation

$$i_+ = k_+ i_p (e^{-\alpha t} - e^{-\beta t}) \qquad ...(6.1)$$

while negative pulses can be best described by

$$i_- = k_- i_p t^{-3/2} . e^{-\gamma / t - \delta t} \qquad ...(6.2)$$

These equations have formed the basis for calculating the response of bandwidth-limited radio receivers (noise meters), and for formulating mathematical models of the radio-noise problem. In addition to the waveshape of a single pulse, their repetition rate in a train of pulses is also important.

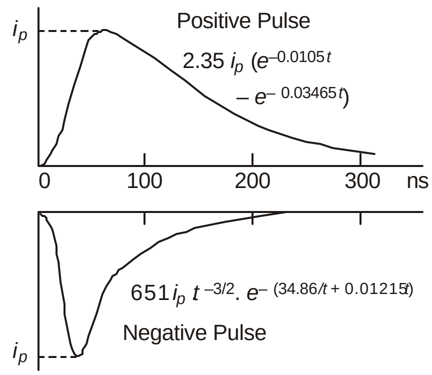

Fig. 6.1 Single positive and negative pulses

$$i_+ = k_+ i_p (e^{-\alpha t} - e^{-\beta t});\ i_- = k_- i_p . t^{-1.5} \cdot e^{(-\gamma/t - \delta t)}$$

Referring to Fig. 6.2, when a conductor is positive with respect to ground, an electron avalanche moves rapidly into the conductor leaving the heavy positive-ion charge cloud close to the conductor which drifts away. The rapid movement of electrons and motion of positive-ions gives the steep front of the pulse, while the further drift of the positive-ion cloud will form the tail of the pulse. It is clear that the presence of positive charges near the positive conductor lowers the field to an extent that the induced current in the conductor nearly vanishes. As soon as the positive-ions have drifted far enough due to wind or neutralized by other agencies such as free electrons by recombination, the electric field in the vicinity of the conductor regains sufficiently high value for pulse formation to repeat itself. Thus, a train of pulses results from a point in corona on the conductor. The repetition rate of pulses is governed by factors local to the conductor. It has been observed that only one pulse usually occurs during a positive half cycle in fair weather and could increase to about 10 in rain where the water sprays resulting from breaking raindrops under the applied field control electrical conditions local to the conductor.

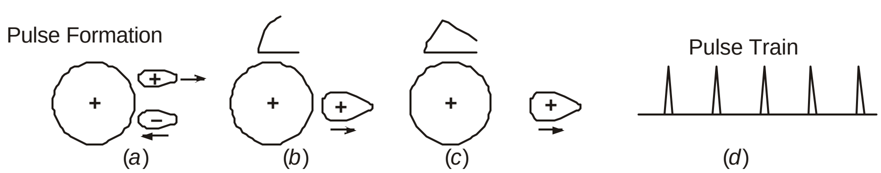

Fig. 6.2 Formation of pulse train from positive polarity conductor.

The situation when the conductor is negative with respect to ground is the reverse of that described above. The electron avalanche moves away from the conductor while the positive-ion cloud moves towards the negatively-charged conductor. However, since the heavy positive-ions are moving into progressively higher electric fields, their motion is very rapid which gives rise to a much sharper pulse than a positive pulse. Similarly, the lighter electrons move rapidly away from the conductor and the electric field near the conductor regains its original value for the next pulse generation quicker than for the positive case. Therefore, negative pulses are smaller in amplitude, have much smaller rise and fall times but much higher repetition rates than positive pulses. It must at once be evident that all the properties of positive and negative pulses are random in nature and can only be described through random variables.

Typical average values of pulse properties are as follows:

Type	*Time to Crest*	*Time to 50% on Tail*	*Peak Value of Current*	*Repetition Rate Pulses per Second*	
				A.C.	*D.C.*
Positive	50 ns	200 ns	100 mA	Power Freq.	1,000
Negative	20 ns	50 ns	10 mA	100 × P.F.	10,000

Pulses are larger as the diameter of conductor increases because the reduction in electric field strength as one moves away from the conductor is not as steep as for a smaller conductor so that conditions for longer pulse duration are more favourable. In very small wires, positive pulses can be absent and only a glow corona can result, although negative pulses are present when they are known as Trichel Pulses named after the first discoverer of the pulse-type discharge. Negative pulses are very rarely important from the point of view of radio interference as will be described under "Radio Noise Meter Response" to corona pulses in Section 6.2. Therefore, only positive polarity pulses are important because of their larger amplitudes even though their repetition rate is lower than negative pulses.

6.1.1 Frequency Spectrum

The frequency spectrum of radio noise measured from long lines usually corresponds to the Fourier Amplitude Spectrum (Bode Amplitude Plot) of single pulses. These are shown in Figure 6.3. The Fourier integral for a single double-exponential pulse is

$$F\,(jw) = \int_{-\infty}^{\infty} f(t).e^{-jwt}.dt = \int_{0}^{to} Ki_p\,(e^{-\alpha t} - e^{-\beta t}).e^{-jwt}.dt$$

$$= Ki_p[1/(\alpha + jw) - 1/(\beta + jw)]$$

$$= Ki_p(\beta - \alpha)/(\alpha + jw)(\beta + jw)$$

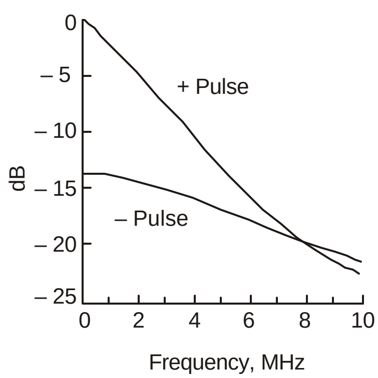

Fig. 6.3 Bode frequency plot of positive and negative corona pulses.

The amplitude is

$$A\,(w) = K.i_p.(\beta - \alpha)/\sqrt{(\alpha^2 + w^2)(\beta^2 + w^2)} \quad ...(6.4)$$

At low frequencies when $\omega \ll \alpha$ and β, the amplitude varies as $Ki_p(\beta - \alpha)/\alpha\beta$, showing that it is independent of frequency. At high frequencies when $\omega \gg \alpha$ and β, $A(\omega) = Ki_p(\beta - \alpha)/\omega^2$. On a log-log plot this has a slope of –2. Assuming that both the positive and negative pulses are double-exponential in shape with the timings 50/150 and 20/50 ns, the values of α and β are:

Positive Pulse : $\alpha = 10.5\times10^6$, $\beta = 34.65\times10^6$

Negative Pulse : $\alpha = 38.3\times10^6$, $\beta = 83\times10^6$

Table 6.1 shows details of calculation of amplitude vs. frequency from 0 to 10 MHz by taking the reference (0 dB) at $f = 0$ for the positive pulse. At $f = 0$, the amplitude of negative pulse frequency spectrum is 13.5 dB below that for positive pulse, for equal peak amplitudes.

Table 6.1 Amplitude-Frequency Spectrum of Pulses

f	0	0.5	1	1.5	2	4	6	8	10	MHz
Positive	0	–.4	–1.47	–2.9	–4.4	–10	–15	–19	–22	dB
Negative	–13.5	–13.54	–13.64	–13.8	–14	–15.4	–17.3	–19.2	–21.1	dB

These are plotted in Fig. 6.3. Evaluation of K, α and β values with given crest time and time to 50% value on tail is carried out in Chapter 13. The equations are however given here.

Let $x = \beta/\alpha$ and $y = t_t/t_p$ which is given.

Then. $$x(y-1).\ln(x) = (x-1).\ln[2(x^y-1)/(x-1)] \quad \ldots(6.5)$$

$$\alpha = \ln(x)/(x-1)\,t_p \quad \ldots(6.6)$$

and $$K = 1/[\exp(-\alpha t_p) - \exp(-\beta t_p)] \quad \ldots(6.7)$$

First, equation (6.5) is solved by trial and error for x, and α found from (6.6). Then $\beta = x\alpha$. Finally, K is determined from calculated values of α, β and the known value of crest time t_p.

Example 6.1. A double-exponential pulse has a crest time of $t_p = 50$ ns. and time to 50% value on tail equal to $t_t = 150$ ns. Calculate α, β and K, and write the equation to the pulse in terms of the peak value i_p.

Solution: $y = t_t/t_p = 3$. Hence the equation for $x = \beta/\alpha$ is

$$2x\ln(x) = (x-1)\ln[2(x^3-1)/(x-1)].$$

A trial and error solution yields $x = \beta/\alpha = 3.45$

$$\alpha = \ln(x)/t_p(x-1) = \ln(3.45)/2.45\times50\times10^{-9} = 10\times10^6.$$

$\therefore$ $$\beta = 34.5\times10^6.$$

Also, $\alpha t_p = 0.50546$ and $\beta t_p = 1.7438$.

Finally, $K = 1/(e^{-\alpha t_p} - e^{-\beta t_p}) = 2.3346$.

The equation to the pulse is $i(t) = 2.3346\, i_p(e^{-10^7 t} - e^{-3.45\times10^7 t})$.

If time is measured in nanoseconds,

$$i(t) = 2.3346 i_p(e^{-0.01t} - e^{-0.0345t}).$$

6.2 PROPERTIES OF PULSE TRAINS AND FILTER RESPONSE

Radio Interference (RI) level is governed not only by the amplitude and waveshape of a single pulse but also by the repetitive nature of pulses in a train. On an ac transmission line, as mentioned earlier, positive pulses from one single point in corona occur once in a cycle or at the most 2 or 3 pulses are generated near the peak of the voltage. In rain, the number of pulses in one positive half cycle shows an increase. Therefore, the number of pulses per second on a 50 Hz line from a single point in fair weather ranges from 50 to 150 and may reach 500 in rain. Since there exist a very large number of points in corona, and the pulses occur randomly in time without correlation, the frequency spectrum is band-type and not a line spectrum. It is also found that in fair weather there exists a certain shielding effect when one source in corona does not permit another within about 20 to 50 cm. This is verified by photographs taken at night when plumes of bluish discharges occur at discrete points. However, in rain, there is a continuous luminous envelope around a conductor. It is therefore a matter of some difficulty in actually ascertaining the repetition rate of pulses as seen by the input end of a noise meter, which is either a rod antenna or a loop antenna. Fortunately, this is not as serious as it looks, since the integrated response of a standard noise-meter circuit is practically independent of the pulse repetition rate if the number of pulses per second (pps) is less than the bandwidth frequency of the filter in the meter weighting circuit. This is discussed below for a simple case of rectangular pulses with periodic repetition. The analysis can be extended to include finally the actual case of randomly-occurring pulse trains with double-exponential shape. But this is a highly advanced topic suitable for experts involved in design of noise meters. [See Begamudre, Trans. Can. Eng. Inst., Oct. 1970].

Consider Figure 6.4 showing rectangular pulses of amplitude A and width τ having a periodic time T and repetition frequency $f = 1/T$ pulses per second. When this is an even function the Fourier Series for this type of pulse train contains only cosine terms. The amplitude of any harmonic is

$$F(k) = \frac{4}{T}\int_0^{\tau} A\cos 2\pi k f t\, dt = \frac{4A}{2\pi k}\sin\frac{2\pi k\tau}{T} \qquad \text{...(6.8)}$$

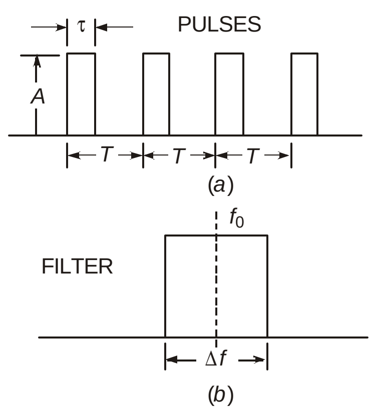

Fig. 6.4 (*a*) Pulse train: Amplitude A, width τ, period T.
(*b*) Ideal bandwidth-limited filter with centre frequency f_o and bandwidth Δf.

The Fourier Series is

$$F(w) = \sum_{k=1}^{\infty}\left(\frac{4A}{2\pi k}\sin\frac{2\pi k\tau}{T}\right)\cos kwt \qquad ...(6.9)$$

Let such a signal be passed through an ideal filter with bandwidth Δf and steep cut-off, as shown in Fig. 6.4(b). Then, the number of harmonics passed will be.

$$N = \Delta f / f = \Delta f.T. \qquad ...(6.10)$$

If the meter is tuned to a centre frequency $f_0 = nf$, the output will contain harmonic terms from $k = \left(n - \frac{1}{2}N\right)$ to $\left(n + \frac{1}{2}N\right)$. The output of the filter is then.

$$\left[\frac{4A}{2\pi}\,\frac{1}{n - \frac{1}{2}N}\sin 2\pi\left(n - \frac{N}{2}\right)f\tau\right] \text{ to } \left[\frac{4A}{2\pi}\,\frac{1}{n + \frac{1}{2}N}\sin 2\pi\left(n + \frac{N}{2}\right)f\tau\right]$$

Certain approximations can be made to obtain a workable expression when we consider what happens in an actual situation in practice. The tuned frequency is about f_0 = 1 MHz and the repetition frequency f can be considered as f = 1000 pps. The meter bandwidth is 5 kHz for ANSI meters and 9 kHz for CISPR meters of European design. Therefore.

$$n = f_0 / f = 10^6 / 10^3 = 1000.$$

Since the bandwidth is 5 kHz and the harmonics of the pulse train are separated by 1000 Hz, only 5 or 6 harmonic components will pass in the 5 kHz bandwidth. For Δf = 9 kHz, about 9 or 10 harmonic components will pass. Thus, (n – N/2) and (n + N/2) range from 997 to 1003 and we can approximate both these with a value of 1000 which is f_0/f. The output of the filter will then be the sum of harmonic terms such as

$$\frac{4A}{2\pi}\frac{f}{f_0}\left[\sin 2\pi\left(f_0 - \frac{\Delta f}{2}\right)\tau \text{ to } \sin 2\pi\left(f_0 + \frac{\Delta f}{2}\right)\tau\right]$$

where the pulse width τ is of the order of 100 ns = 10^{-7}.

Now, $$\sin\left(2\pi f_0\tau - 2\pi\frac{\Delta f}{2}\tau\right) = \sin 2\pi f_0\tau.\cos 2\pi\frac{\Delta f}{2}\tau - \cos 2\pi f_0\tau.\sin 2\pi\frac{\Delta f}{2}\tau. \qquad ...(6.11)$$

Since $2\pi\frac{\Delta f}{2}\tau \approx 2\pi \times 2500 \times 10^{-7} = 157 \times 10^{-5}$,

we can write $\cos 2\pi\frac{\Delta f}{2}\tau = 1$ and $\sin 2\pi\frac{\Delta f}{2}\tau = 0$. Then, the output of the filter will be nearly

$$\frac{4A}{2\pi}.\frac{f}{f_0}.N.\sin 2\pi f_0\tau.\cos 2\pi f_0 t \qquad ...(6.12)$$

where we have introduced the time function of equation (6.9). The final output can also be written as

$$\frac{4A}{2\pi}\frac{\Delta f}{f_0}.\sin 2\pi f_0\tau.\cos 2\pi f_0 t \qquad ...(6.13)$$

since $Nf = \Delta f$, the bandwidth, according to (6.10).

The output of the filter is a cosine wave at frequency f_0, the tuned frequency (1 MHz, say), and is modulated by the amplitude

$$\frac{2A}{\pi}.\frac{\Delta f}{f_0}.\sin 2\pi f_0\tau = \frac{2A}{\pi}.\Delta f.\frac{\sin 2\pi f_0\tau}{2\pi f_0\tau}(2\pi\tau) = 4(A\tau).(\Delta f).\frac{\sin 2\pi f_0\tau}{2\pi f_0\tau} \quad ...(6.14)$$

For low tuned frequencies, the sigma factor $\frac{\sin 2\pi f_0\tau}{2\pi f_0\tau}$ is nearly 1. Thus, at low frequencies f_0, the response of the filter is nearly flat and rolls off at higher frequency. The following salient properties can also be noted from equation (6.14).

(1) The response of the filter is directly proportional to $(A\tau) =$ area of the pulse.

(2) The response is proportional to $(\Delta f) =$ bandwidth, provided the number of harmonics passed is very low.

(3) The response is proportional to the Si-factor.

That the response of the filter is flat up to a certain repetition frequency of pulses is not surprising since as the repetition frequency increases, the tuned frequency becomes a lower order harmonic of the fundamental frequency with resulting higher amplitude. But there is a corresponding reduction in the number of harmonics passed in the bandwidth of the filter giving an output which is nearly equal to that obtained at a lower tuned frequency. Therefore, changes in repetition frequency of the pulses in a train affect the noise level only to a small degree.

Since the amplitude-duration product of the pulse determines the output, it is evident that a positive corona pulse yields much higher noise level than a negative corona pulse. In practice, we omit negative-corona generated radio interference.

6.3 LIMITS FOR RADIO INTERFERENCE FIELDS

Radio Interference (RI) resulting from a transmission line is a man-made phenomenon and as such its regulation should be similar to other man-made sources of noise as mentioned in Chapter 5, such as audible noise, automobile ignition noise, aircraft noise, interference from welding equipment, r–f heating equipment etc. Some of these are governed by *IS* 6842. Legislation for fixing limits to all these noise sources is now gaining widespread publicity and awareness in public in order to protect the environment from all types of pollution, including noise. Interference to communication systems is described through Signal-to-Noise Ratio designated as S/N Ratio, with both quantities measured on the same weighting circuit of a suitable standard meter. However, it has been the practice to designate the signal from a broadcast station in terms of the average signal strength called the Field Intensity (FI) setting of the field-strength meter, while the interference signal to a radio receiver due to line noise is measured on the Quasi-Peak (QP) detector circuit. The difference in weighting circuits will be discussed later on. There are proposals to change this custom and have both signal and noise measured on the same weighting circuit. This point is mentioned here in order that the reader may interpret S/N ratios given by public utility organizations in technical literature or elsewhere since interference problems result in expensive litigations between contesting parties.

As mentioned earlier, it is the duty or responsibility of a designer to keep noise level from a line below a limiting value at the edge of the right-of-way (R-O-W) of the line corridor. The value to be used for this RI limit is causing considerable discussion and, we shall describe two points of view currently used in the world. Some countries, particularly in Europe, have set definite limits for the RI field from power lines, while in north America only the minimum acceptable S/N ratio at the receiver location has been recommended. We will examine the rationale of the two points of view and the steps to be followed in line design.

When a country is small in size with numerous towns with each having its own broadcast station and a transmission line runs close by, it is easy on the design engineer of the line if a definite RI limit is set and station signal strengths are increased by increasing the transmitter power in order to yield satisfactory quality of radio reception to all receivers located along the line route. The following Table 6.2, gives limits set by certain European countries.

Table 6.2. RI Limits in Various Countries of the World (Loop Antenna)

Country	*Distance from Line*	*RI Limit*	*Frequency*	*Remarks*
(1) Switzerland	20 m from outermost phase	200 μV/m (46 dB above 1 μV/m)	500 kHz	Dry weather 10°C
(2) Poland	20 m from outerphase	750 μV/m (57.5 dB)	500 kHz ± 10 kHz	Air humidity <80% Temp. 5°C
(3) Czechoslovakia	*Voltage kV* / *Distance from line centre*: 220 – 50 m; 400 – 55; 750 – 70	40 dB	500 kHz	Air humidity = 70% Dry weather
(4) U.S.S.R.	100 m from outerphase	40 dB	500 kHz	For 80% of the year limit should not be exceeded

One immediate observation to make is that there is no uniformity even in a small area such as Europe, Excluding the U.S.S.R. In countries like France where a large rural population exists, no set RI limit is specified since broadcast stations are located far from farming communities who have to be assured satisfactory S/N ratio.

In North America the following practice is adopted in the U.S.A. and Canada.

U.S.A. Recommended practice is to guarantee a minimum S/N ratio of 24 dB at the receiver for broadcast signals having a minimum strength of 54 dB at the receiver.

Canada. For satisfactory reception, a S/N ratio of 22 dB or better must be provided in fair weather in suburban regions for stations with a mean signal strength of 54 dB (500 μV/m). In urban regions, this limit can be increased by 10 dB, and in rural areas lowered by 3 dB.

Based on these two points of view, namely, (1) setting a definite RI limit, and (2) providing a minimum S/N ratio at the receiver, the procedures required for line design will be different, which are outlined here.

(1) When RI limit in dB or μV/m is specified at a particular frequency and weather condition, it is only necessary to calculate the lateral decrement or profile of RI. This is the attenuation of the noise signal as one proceeds away from the line for an assumed line configuration. (The procedure for calculation of lateral profile will be outlined in Section 6.6 and following sections). By taking a large number of alternative line designs, a choice can be made of the most suitable conductor configuration.

(2) When line design is based upon S/N ratio, measurement of broadcast-station signals must be carried out all along a proposed line route of all stations received. This can also be calculated provided the station power, frequency, and distance to the receiver are known. The allowable noise from the line at these frequencies is then known from the S/N ratio value. The R-O-W can be specified at every receiver location for a chosen size of conductor and line configuration (line height and phase spacing). The procedural difficulties involved in this method are illustrated as follows. Consider that at a farming community where a future line may pass nearby, the station field strengths are recorded and a S/N ratio of 24 dB must be allowed. The table below shows an example of station strengths and allowable noise at the station frequencies.

Frequency of Station	0.5	0.8	1	1.1	1.3	1.52	MHz
Received Signal Strength	55	60	50	75	57	52	dB
Allowable Noise Level (*signal strength-24 dB*)	31	36	26	51	33	28	dB

If we assume that corona-generated noise has a frquency spectrum such as shown in Figure 6.3 which varies nearly as $f^{-1.5}$, then the noise level in realtion to that at 1 MHz taken as reference can also be tabulated. Since the allowable noise level at 1 MHz is 26 dB, the permissible noise at other frequencies are determined. When this is done, it will become clear that certain stations will not be guaranteed a minimum S/N ratio of 24 dB, as shown below.

Frequency, MHz	0.5	0.8	1.0	1.1	1.3	1.52	MHz
Corona Noise Adder	9	4	0	–1	–2	–3.6	dB
Allowed Noise	35	30	26	25	24	22.4	dB
S/N Ratio, dB	20	30	24	50	33	29.6	dB

Therefore, for the station broadcasting at 0.5 MHz, the recommended minimum S/N ratio of 24 dB cannot be guaranteed. The situation is represented pictorially in Figure 6.5. This leads to the conclusion that at any given receiver location, with a chosen line design, all stations received cannot be guaranteed satisfactory quality of reception with a given width of R-O-W. It is very uneconomical to increase the width of R-O-W to accommodate all radio stations. Therefore, regulatory bodies must also specify the number of stations (or percentage) received at a village or town for which satisfactory reception can be guaranteed. This may usually be 50% so that listeners have the choice of tuning into at least 50% of the stations for which satisfactory reception is guaranteed.

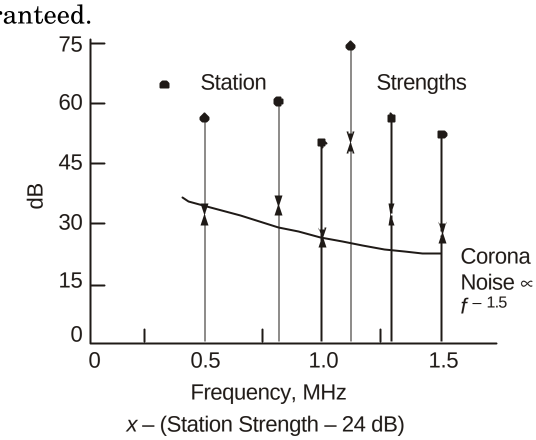

Fig. 6.5 Station signal strength (.), –24 dB (×), and corona-generated noise(–). Illustrating basis for design based upon minimum S/N ratio of 24 db.

This process has to be repeated at all villages and towns or other locations such as military establishments, etc., along the proposed line route and a best compromise for line design arrived at. Once a definite RI limit is set at a fixed lateral distance from the line as controlled by the S/N ratio, which in the above example was 26 dB at 1 MHz at the edge of R-O-W, the line design follows similar lines as for case (1) where the limit is specified to start with under legislation of the country.

Referring to Fig 6.5, any *X*-mark falling below the corona-generated noise curve represents a station for which the minimum S/N ratio of 24 dB cannot be obtained. Therefore, quality of reception for such a station at the receiver location will be unsatisfactory.

6.4 FREQUENCY SPECTRUM OF THE RI FIELD OF LINE

The frequency spectrum of radio noise refers to the variation of noise level in μV or μV/m (or their dB values referred to 1 μV or 1μV/m) with frequency of measurement. The frequency-spectrum of a single corona pulse of double-exponential shape was found in Section 6.1 to be

$$A(w) = K i_p.(\beta - \alpha)/\sqrt{(\alpha^2 + w^2)(\beta^2 + w^2)} \qquad ...(6.14)$$

On a long line, there exist a very large number of points in corona and a noise meter located in the vicinity of the line (usually at or near ground level) responds to a train of pulses originating from them. The width of a single pulse is about 200 ns (0.2 μs) while the separation of pulses as seen by the input end of the meter could be 1 μs or more. Therefore, it is unusual for positive pulses to overlap and the noise is considered as impulsive. When pulses overlap, the noise is random. Measurements indicate that from a long line, the RI frequency spectrum follows closely.

$$RI(w) \propto f^{-1} \text{ to } f^{-1.5} \qquad ...(6.15)$$

Thus, at 0.5 MHz the noise is 6-9 dB higher than at 1 MHz, while at 2 MHz it is 6–9 dB lower. In practice, these are the adders suggested to convert measured noise at any frequency to 1 MHz level. The frequency spectrum is therefore very important in order to convert noise levels measured at one frequency to another. This happens when powerful station signal interferes with noise measurements from a line so that measurements have to be carried out at a frequency at which no broadcast station is radiating. The frequency spectrum from corona-generated line noise is nearly fixed in its characteristic so that any deviation from it as measured on a noise meter is an indication of sources other than the line, which is termed "background noise". In case a strong source of noise is present nearby, which is usually a factory with motors that are sparking or a broken insulator on the tower, this can be easily recognized since these usually yield high noise levels up to 30 MHz and their frequency spectrum is relatively flat.

6.5 LATERAL PROFILE OF RI AND MODES OF PROPAGATION

The most important aspect of line design from interference point of view is the choice of conductor size, number of sub-conductors in bundle, line height, and phase spacing. Next in importance is the fixing of the width of line corridor for purchase of land for the right-of-way. The lateral decrement of radio noise measured at ground level as one moves away from the line has the profile sketched in Fig. 6.6. It exhibits a characteristic double hump within the space between the conductors and then decreases monotonically as the meter is moved away from the outer

6.8 MEASUREMENT OF RI, RIV, AND EXCITATION FUNCTION

The intereference to AM broadcast in the frequency range 0.5 MHz to 1.6 MHz is measured in terms of the three quantities : Radio Interference Field Intensity (RIFI or RI), the Radio Influence Voltage (RIV), and more recently through the Excitation Function. Their units are mV/m, mV, and mA/$\sqrt{\text{m}}$ or the decibel values above their reference values of 1 unit $(\mu\text{V}/\text{m}, \mu\text{V}, \mu\text{A}/\sqrt{\text{m}})$. The nuisance value for radio reception is governed by a quantity or level which is nearly equal to the peak value of the quantity and termed the Quasi Peak. A block diagram of a radio noise meter is shown in Fig. 6.17. The input to the meter is at radio frequency (r-f) which is amplified and fed to a mixer. The rest of the circuit works exactly the same as a highly sensitive super-heterodyne radio receiver, However, at the IF output stage, a filter with 5 kHz or 9 kHz bandwidth is present whose output is detected by the diode D. Its output charges a capacitance C through a low resistance R_c such that the charging time constant $T_c = R_c C = 1$ ms. A second resistance R_d is in parallel with C which is arranged to give a time constant $T_d = R_d C = 600$ ms in ANSI meters and 160 ms in CISPR or European standard meters. Field tests have shown that there is not considerable difference in the output when comparing both time constants for line-generated corona noise. The voltage across the capacitor can either be read as a current through the discharge resistor R_d or a micro-voltmeter connected across it.

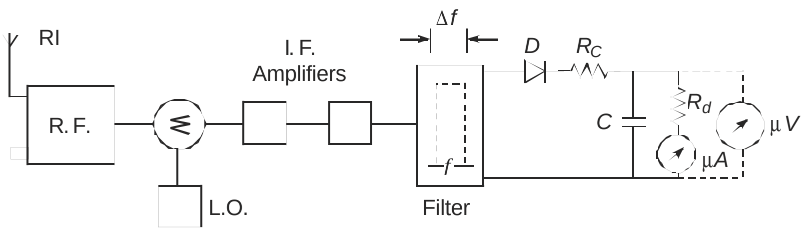

Fig. 6.17 Block diagram of Radio Noise Meter.

For radiated interference measurement RI, the front end of the meter is fitted with either a rod antenna of 0.5 to 2 metres in length or a loop antenna of this size of side. For conducted measurements, the interfering voltage RIV is fed through a jack. The input impedance of the meter is 50 ohms:

The following formulas due to Nigol apply to the various settings of the noise meter for repetitive pulses:

Peak Value: $V_p = \sqrt{2}.A.\tau.\Delta f$ ...(6.55)

Quasi Peak: $V_{qp} = KV_P$ ...(6.56)

Average: $V_{av} = \sqrt{2}.A.\tau.f_0$ ...(6.57)

R.M.S. Value: $V_{rms} = \sqrt{2}.A.\tau.\sqrt{f_0.\Delta f}$ ...(6.58)

where, A = amplitude of repetitive pulses,
τ = pulse duration,
Δf = bandwidth of meter,
f_0 = repetition frequency of pulses, $< \Delta f$,
and K = a constant $\approx 0.9 - 0.95$.

Relations can be found among these four quantities if necessary.

Conducted RIV is measured by a circuit shown schematically in Fig. 6.18. The object under test, which could be an insulator string with guard rings, is energized by a high voltage source at power frequency or impulse. A filter is interposed such that any r-f energy produced by partial discharge in the test object is prevented from flowing into the source and all r-f energy goes to the measuring circuit. This consists of a discharge-free h.v. coupling capacitor of about 500 to 2000 pF in series at the ground level with a small inductance L. At 50 Hz, the coupling capacitor has a reactance of 6.36 Megohms to 1.59 Megohms. The value of L is chosen such that the voltage drop is not more than 5 volts so that the measuring equipment does not experience a high power-frequency voltage.

Let V = applied power frequency voltage from line to ground,

V_L = voltage across L,

X_c = reactance of coupling capacitor

and $X_L = 2\pi fL$ = reactance of inductor.

Then, $$V_L = V.X_L/(X_c - X_L) \simeq VX_L/X_c = 4\pi^2 f^2 LC_c.V \quad ...(6.59)$$

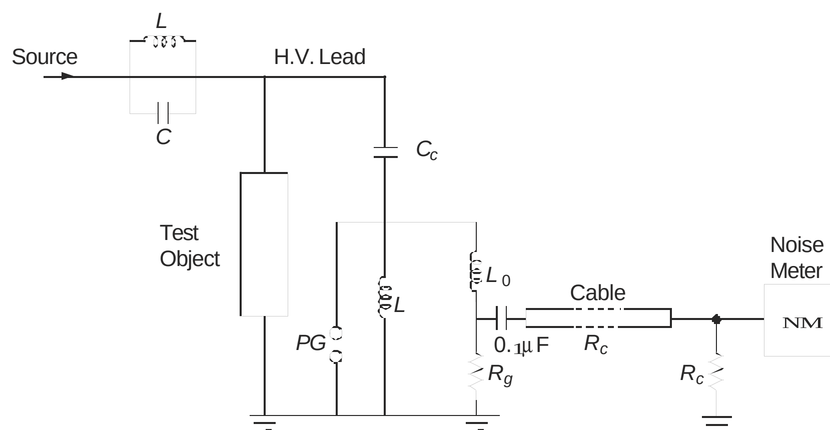

Fig. 6.18 Circuit for measuring Radio Influence Voltage (RIV).

Example 6.8. A test object for 400 kV is undergoing an RIV test. The coupling capacitor has 1000 pF and the voltage across the measuring system is to be 1 volt. Calculate the value of inductance required if

$$V = 420/\sqrt{3}\,\text{kV} = 243.5\,\text{kV}$$

Solution. $$L = X_L/2\pi f = V_L/4\pi^2 f^2 C_c V$$

$$L = 1/(4\pi^2 \times 50^2 \times 10^{-9} \times 242.5 \times 10^3) = 41.8\,\text{mH}.$$

[At 50 Hz, $X_L = 2\pi fL = 13.1$ ohm, $X_c = 3.185$ Megohm].

At radio frequencies, the inductance presents a very high impedance while the coupling capacitor has very low reactance. The capacitor is tuned at a fixed frequency, usually 1 MHz, with an r-f choke, L_0. There is a series R_g to ground. This r-f voltage is fed to the noise meter through a length of cable of 50 ohm characteristic impedance terminated in a 50 ohm resistance at the input end of the meter.

The value of L_0 is obtained from the equation.

$$f = 1/2\pi\sqrt{L_0C_c} \text{ or } L_0 = 1/4\pi^2f^2C_c \quad ...(6.60)$$

where f = measuring frequency.

Example 6.9. In the above example with C_c = 1000 pF, calculate

(*a*) the value of L_0 to tune the circuit to 1 MHz,

(*b*) the reactance of L = 41.8 mH at 1 MHz and

(*c*) that of the coupling capacitor C_c. Check with reactance of L_0.

Solution.

(*a*) $L_0 = 1/4\pi^2 \times 10^{12} \times 10^{-9} = 25.33\ \mu$H.

(*b*) $X_L = 2\pi \times 10^6 \times 41.8 \times 10^{-3} = 262.64$ kilohms.

(*c*) $X_c = 1/2\pi \times 10^6 \times 10^{-9} = 159$ ohms.

$X_{L0} = 2\pi \times 10^6 \times 25.33 \times 10^{-6} = 159$ ohms.

The *r-f* voltage developed across R_g is fed to the noise meter. Since transmission lines have a characteristic impedance in the range 300 to 600 ohms, standard specifications stipulated that the r-f voltage must be measured across 600 ohms. Thus, R_g is in the neighbourhood of 600 ohms. However, it was obvious that this could not be done since the presence of cable will lower the impedance to ground. In earlier days of RIV measurement at lower voltages (230 kV equipment) the noise meter was directly connected across R_g and its input end was open. The operator sat right underneath the pedestal supporting the coupling capacitor in order to read the meter or used a pair of binoculars from a distance. But with increase in test voltage, the need for maintaining a safe distance necessitates a cable of 10m to 20m. With its surge impedance R_c conected across R_g, which has a higher value, the combined parallel impedance is lower than R_c. No coaxial cables are manufactured for high surge impedance, so that standard specifications allow RIV to be measured across 150 ohm resistance made up of R_g and R_c in parallel. It is clear that the measuring cable must have R_c greater than 150 ohms. The highest impedance cable has R_c = 175 ohms on the market. The value of R_g can be selected such that

$R_cR_g/(R_c + R_g)$ = 150 ohms

giving $R_g = 150\ R_c/(R_c - 150)$ ...(6.61)

For R_c = 175 ohms, $R_g = 6\ R_c$ = 1050 ohms.

The meter reading is then multiplied by a factor of 4 in order to give the RIV measured across 600 ohms, or by a factor of 2 for 300 ohms surge impedance.

6.9 MEASUREMENT OF EXCITATION FUNCTION

The corona generating function or the excitation function caused by injected current at radio frequencies from a corona discharge is measured on short lengths of conductor strung inside "cages" as discussed earlier. The design of cages has been covered in great detail in Chapter 4, Some examples of measuring radio noise and injected current are shown in Fig. 6.19. In every case the measured quantity is RIV at a fixed frequency and the excitation function calculated as described later. The filter provides an attenuation of at least 25 dB so that the RI current is solely due to corona on conductor. The conductor is terminated in a capacitance C_c at one end in series with resistances R_1 and R_c, while the other end is left open. The conductor is strung with strain insulator at both ends which can be considered to offer a very high impedance at 1

7

Electrostatic and Magnetic Fields of EHV Lines

7.1 ELECTRIC SHOCK AND THRESHOLD CURRENTS

Electrostatic effects from overhead e.h.v. lines are caused by the extremely high voltage while electromagnetic effects are due to line loading current and short-circuit currents. Hazards exist due to both causes of various degree. These are, for example, potential drop in the earth's surface due to high fault currents, direct flashover from line conductors to human beings or animals. Electrostatic fields cause damage to human life, plants, animals, and metallic objects such as fences and buried pipe lines. Under certain adverse circumstances these give rise to shock currents of various intensities.

Shock currents can be classified as follows:

(*a*) *Primary Shock Currents*. These cause direct physiological harm when the current exceeds about 6-10 mA. The normal resistance of the human body is about 2-3 kilohms so that about 25 volts may be necessary to produce primary shock currents. The danger here arises due to ventricular fibrillation which affects the main pumping chambers of the heart. This results in immediate arrest of blood circulation. Loss of life may be due to (*a*) arrest of blood circulation when current flows through the heart, (*b*) permanent respiratory arrest when current flows in the brain, and (*c*) asphyxia due to flow of current across the chest preventing muscle contraction.

The 'electrocution equation' is $i^2t = K^2$, where $K = 165$ for a body weight of 50 kg, i is in mA and t is in seconds. On a probability basis death due to fibrillation condition occurs in 0.5% of cases. The primary shock current required varies directly as the body weight. For $i = 10$ mA, the current must flow for a time interval of 272 seconds before death occurs in a 50 kg human being.

(*b*) *Secondary Shock Currents.* These cannot cause direct physiological harm but may produce adverse reactions. They can be steady state 50 Hz or its harmonics or transient in nature. The latter occur when a human being comes into contact with a capacitively charged body such as a parked vehicle under a line. Steady state currents up to 1 mA cause a slight tingle on the fingers. Currents from 1 to 6 mA are classed as, 'let go' currents. At this level, a human being has control of muscles to let the conductor go as soon as a tingling sensation occurs. For a 50% probability that the let-to current may increase to primary shock current, the limit for men is 16 mA and for women 10 mA. At 0.5% probability, the currents are 9 mA for men, 6 mA for women, and 4.5 mA for children.

A human body has an average capacitance of 250 pF when standing on an insulated platform of 0.3 m above ground (1 ft.). In order to reach the let-go current value, this will require 1000 to 2000 volts. Human beings touching parked vehicles under the line may experience these transient currents, the larger the vehicle the more charge it will acquire and greater is the danger.

Construction crews are subject to hazards of electrostatic induction when erecting new lines adjacent to energized lines. An ungrounded conductor of about 100 metres in length can produce shock currents when a man touches it. But grounding both ends of the conductor brings the hazard of large current flow. A movable ground mat is generally necessary to protect men and machines. When stringing one circuit on a double-circuit tower which already has an energized circuit is another hazard and the men must use a proper ground. Accidents occur when placing or removing grounds and gloves must be worn. Hot-line techniques are not discussed here.

7.2 CAPACITANCE OF LONG OBJECT

Electrostatic induction to adjacent lines such as telephone lines can be determined by Maxwell's Potential Coefficients and their inverses. If ground resistance and inductance are to be considered, Carson's formulas given in Chapter 3 are used. However, for a long object such as a lorry or vehicle parked parallel to a line under it, an empirical formula for its

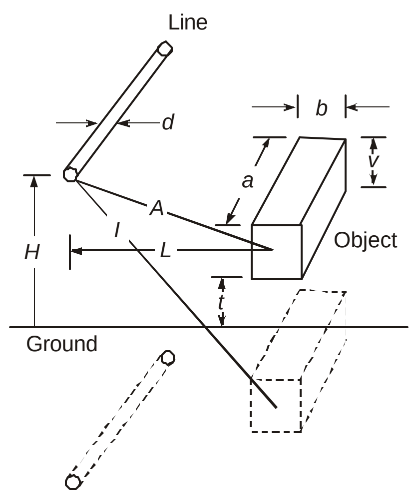

Fig. 7.1 Calculation of capacitance of long object located near an e.h.v. line.

capacitance due to Comsa and René is given here. The object is replaced by an equivalent cylinder of diameter D and height h above ground as shown below. Figure 7.1 gives the actual dimensions of the object where a = length of object, b = width, v = height, t = height of tyres. Then, $h = t + v - 0.5\ b$, and $D = b$. Other dimensions of line are shown on the figure. The capacitance of the vehicle, including end effects, is

$$C = a.C_1 + C_2 \qquad ...(7.1)$$

where $$C_1 = 2\pi e_0 \ln(I/A) \Big/ \left[\left(\ln\frac{4H}{d}\right).\left(\ln\frac{4h}{D}\right) + \ln(I/A)\right], \text{pF/m} \qquad ...(7.2)$$

and $$C_2 = 31.b, \text{ pF due to end effects.} \qquad ...(7.3)$$

Example 7.1. The following details of a truck parked parallel to a line are given. Find its capacitance. Length a = 8 m, height of body v = 3m, width b = 3m, t = 1.5 m. Height of line conductor H = 13m, dia. of conductor = 0.0406m, distance of parking L = 6m.

Solution. $h = t + v - 0.5b = 3,\quad D = b = 3, I = 17.1,\quad A = 11.66,$

$$\therefore \qquad C_1 = \frac{10^{-9}}{18} \times \ln(17.1/11.66) \Big/ \left[\ln \frac{52}{.0406} \ln \frac{12}{3} + \ln \frac{17.1}{11.66}\right]$$

= 2.065 pF/metre length of truck.

$C_2 = 31\, b = 93$ pF.

$\therefore \qquad C = 8 \times 2.065 + 93 = 109.5$ pF.

Note that the edge effect is considerable.

7.3 CALCULATION OF ELECTROSTATIC FIELD OF A.C. LINES

7.3.1 Power-Frequency Charge of Conductors

In Chapter 4, we described the method of calculating the electrostatic charges on the phase conductors from line dimensions and voltage. For n phases, this is, see Fig. 7.2, with q = total bundle charge and V = line to ground voltage.

$$\frac{1}{2\pi e_0}[q] = [P]^{-1}[V] = [M][V] \qquad ...(7.4)$$

where $[q] = [q_1, q_2, q_3, \ldots, q_n]_t$ ...(7.5)

$[V] = [V_1, V_2, V_3, \ldots, V_n]_t$

$[P] = n \times n$ matrix of Maxwell's Potential coefficients with

$$P_{ii} = \ln(2H_t / r_{eq}) \text{ and } P_{ij} = \ln(I_{ij} / A_{ij}), i \neq j \qquad ...(7.6)$$

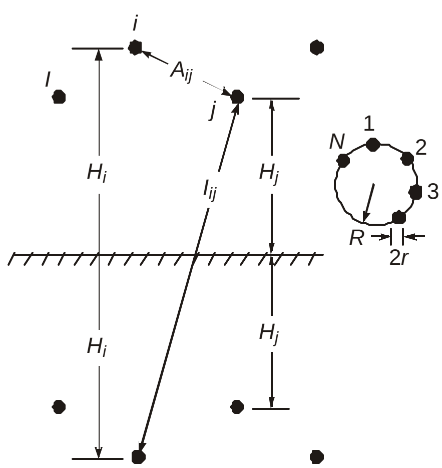

Fig. 7.2 n-phase line configuration for charge calculation.

Here, H_i = height of conductor i above ground = $H_{min} + \frac{1}{3}$ sag,

I_{ij} = distance between conductor i above ground and the image of conductor j below ground, $i \neq j$,

A_{ij} = aerial distance between conductors i and j, $i \neq j$,

$r_{eq} = R(N.r/R)^{1/N}$ = equivalent bundle radius,

R = bundle radius $= B/2\sin(\pi/N)$,

N = number of sub-conductors in bundle,

r = radius of each sub-conductor,

and $i, j = 1, 2, 3, \ldots, n$.

Since the line voltages are sinusoidally varying with time at power frequency, the bundle charges q_1 to q_n will also vary sinusoidally. Consequently, the induced electrostatic field in the vicinity of the line also varies at power frequency and phasor algebra can be used to combine several components in order to yield the amplitude of the required field, namely, the horizontal, vertical or total vectors.

7.3.2 Electrostatic Field of Single-Circuit 3-Phase Line

Let us consider first a 3-phase line with 3 bundles on a tower and excited by the voltages.

$$[V] = V_m[\sin(wt + \varphi), \sin(wt + \varphi - 120°), \sin(wt + \varphi + 120)°] \quad \ldots(7.7)$$

Select an origin O for a coordinate system at any convenient location. In general, this may be located on ground under the middle phase in a

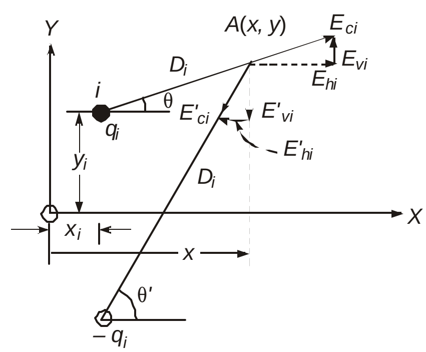

Fig. 7.3 Calculation of e.s. field components near the line.

symmetrical arrangement. The coordinates of the line conductors are (x_i, y_i). A point $A(x,y)$ is shown where the horizontal, vertical, and total e.s. field components are required to be evaluated, as shown in Fig. 7.3. The field vector at A due to the charge of the aerial conductor is with

$$D_i^2 = (x - x_i)^2 + (y - y_i)^2,$$

$$E_c = (q_i/2\pi e_0)(1/D_i) \quad \ldots(7.8)$$

Its horizontal and vertical components are

$$E_h = E_c \cos\theta = (q_i / 2\pi e_0)(x - x_i)/D_i^2 \quad ...(7.9)$$

and

$$E_v = E_c \sin\theta = (q_i / 2\pi e_0)(y - y_i)/D_i^2 \quad ...(7.10)$$

Similarly, due to image charge of conductor

$$E_c' = (q_i / 2\pi e_0)(1/D_i')$$

where

$$(D_i')^2 = (x - x_i)^2 + (y + y_i)^2,$$

$$\left.\begin{aligned} E_h' &= (q_i / 2\pi e_0)(x - x_i)/(D_i')^2 \\ E_v' &= (q_i / 2\pi e_0)(y + y_i)/(D_i')^2 \end{aligned}\right\} \quad ...(7.11)$$

We observe that the field components of E_c and E_c' are in opposite directions. Therefore, the total horizontal and vertical components at A due to both charges are

$$E_{hi} = (q_i / 2\pi e_0)(x - x_i)[1/D_i^2 - 1/(D_i')^2] \quad ...(7.12)$$

$$E_{vi} = (q_i / 2\pi e_0)[(y - y_i)/D_i^2 - (y + y_i)/(D_i')^2] \quad ...(7.13)$$

Consequently, due to all n phases, the sum of horizontal and vertical components of e.s. field at the point $A(x, y)$ will be

$$E_{hn} = \sum_{i=1}^{n} E_{hi}, \text{and} E_{vn} = \sum_{i=1}^{n} E_{vi} \quad ...(7.14)$$

The total electric field at A is

$$E_{in} = (E_{hn}^2 + E_{vn}^2)^{1/2} \quad ...(7.15)$$

We can write these out explicitly for a 3-phase line.

Let

$$J_i = (x - x_i)[1/D_i^2 - 1/(D_i')^2] \quad ...(7.16)$$

and

$$K_i = (y - y_i)/D_i^2 - (y + y_i)/(D_i')^2 \quad ...(7.17)$$

The bundle charges are calculated from equations (7.4), (7.5), and (7.6), so that from equations (7.12), (7.13), (7.16) and (7.17) there results.

$$\begin{aligned} E_{h1} &= (q_1 / 2\pi e_0)J_1 = V_m.J_1[M_{11} \sin(wt + \varphi) + M_{12} \sin(wt + \varphi - 120°) \\ &\quad + M_{13} \sin(wt + \varphi + 120°)] \\ E_{h2} &= (q_2 / 2\pi e_0)J_2 = V_m.J_2[M_{21} \sin(wt + \varphi) + M_{22} \sin(wt + \varphi - 120°) \\ &\quad + M_{23} \sin(wt + \varphi + 120°)] \\ E_{h3} &= (q_3 / 2\pi e_0)J_3 = V_m.J_3[M_{31} \sin(wt + \varphi) + M_{32} \sin(wt + \varphi - 120°)] \\ &\quad + M_{33} \sin(wt + \varphi + 120°)] \end{aligned}$$

$\therefore$ The total horizontal component is, adding vertically,

$$\begin{aligned} E_{hn} &= V_m[(J_1.M_{11} + J_2.M_{21} + J_3.M_{31})\sin(wt + \varphi) \\ &\quad + (J_1.M_{12} + J_2.M_{22} + J_3.M_{32})\sin(wt + \varphi - 120°) \\ &\quad + (J_1.M_{13} + J_2.M_{23} + J_3.M_{33})\sin(wt + \varphi + 120°)] \end{aligned}$$

$$= V_m[J_{h1}.\sin(wt+\varphi)+J_{h2}.\sin(wt+\varphi-120°)$$
$$+J_{h3}\sin(wt+\varphi+120°)]$$

and in phasor form,

$$E_{hn} = V_m[J_{h1}\angle\varphi + J_{h2}\angle\varphi-120^0 + J_{h3}\angle\varphi+120^0] \quad ...(7.18)$$

This is a simple addition of three phasors of amplitudes J_{h1}, J_{h2}, J_{h3} inclined at 120° to each other. Resolving them into horizontal and vertical components (real and j parts with $\varphi = 0$), we obtain

$$\left.\begin{aligned} \text{real part} &= J_{h1}-0.5J_{h2}-0.5J_{h3} \\ \text{and imaginary part} &= 0-0.866J_{h2}+0.866J_{h3} \end{aligned}\right\} \quad ...(7.19)$$

Consequently, the amplitude of electric field is

$$\hat{E}_{hn} = [(J_{h1}-0.5J_{h2}-0.5J_{h3})^2+0.75(J_{h3}-J_{h2})^2]^{1/2}V_m$$
$$= (J_{h1}^2+J_{h2}^2+J_{h3}^2-J_{h1}J_{h2}-J_{h2}J_{h3}-J_{h3}J_{h1})^{1/2}.C_m$$
$$= J_h.V_m.$$

The r.m.s. value of the total horizontal component at A (x, y) due to all 3 phases will be

$$E_{hn} = \hat{E}_{hn}/\sqrt{2} = J_h.V \quad ...(7.20)$$

where V = r.m.s. value of line to ground voltage.

In a similar manner, the r.m.s. value of toal vertical component of field at A due to all 3 phases is

$$E_{vn} = K_v.V = V(K_{v1}^2+K_{v2}^2+K_{v3}^2-K_{v1}K_{v2}-K_{v2}K_{v3}-K_{v3}K_{v1})^{1/2} \quad ...(7.21)$$

where
$$\left.\begin{aligned} K_{v1} &= K_1M_{11}+K_2.M_{21}+K_3.M_{31} \\ K_{v2} &= K_1M_{12}+K_2.M_{22}+K_3M_{32} \\ K_{v3} &= K_1.M_{13}+K_2.M_{23}+K_3.M_{33} \end{aligned}\right\} \quad ...(7.22)$$
and

where the values of K_1, K_2, K_3 are obtained from equation (7.17) for K_i with i = 1, 2, 3.

Example 7.2. Compute the r.m.s. values of ground-level electrostatic field of a 400-kV line at its maximum operating voltage of 420 kV (line-to-line) given the following details. Single circuit horizontal configuration. H = 13 m, S = 12 m, conductor 2 × 3.18 cm diameter, B = 45.72 cm. Vary the horizontal distance along ground from the line centre from 0 to 3 H. See Fig. 7.4.

Solution. At the ground level, the horizontal component of e.s. field is zero everywhere since the ground surface is assumed to be an equipotential. Also, for every point on ground, the distances from aerial conductor and its image are such that D_i and D_i' are equal.

Step 1. $P_{ii} = \ln(2H/r_{eq}), P_{ij} = \ln(I_{ij}/A_{ij}), r_{eq} = R(N.r/R)^{1/N}$

$N = 2$, $R = B/2$. Then the [P] and [M] matrices are

$$[P] = \begin{bmatrix} 5.64, & 0.87, & 0.39 \\ 0.87, & 5.64, & 0.87 \\ 0.39, & 0.87, & 5.64 \end{bmatrix} \text{and}$$

$$[M]=[P]^{-1}=\begin{bmatrix}172.8, & -25.6, & -8\\ -25.6, & 176.2, & -25.6\\ -8, & -25.6, & 172.8\end{bmatrix}10^{-3}$$

Step 2. Coordinates of conductors with origin placed on ground under the centre-phase, see Fig. 7.4, are $x_1=-12, x_2=0, x_3=+12, y_1=y_2=y_3=13. y=0$ on ground.

Step 3. At a point $A(x, 0)$ along ground, from equation (7.17),

$$K_1=-13/[(x+12)^2+(-13)^2]-13/[(x+12)^2+(+13)^2]$$
$$=-26/[(x+12)^2+169].$$

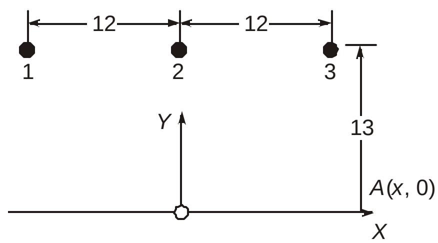

Fig. 7.4 Details of 400 kV line for evaluation of ground-level e.s. field at point *A*.

Similarly, $K_2=-26/(x^2+169)$ and $K_3=-26/[(x-12)^2+169]$.

Step 4.
$$K_{v1}=K_1M_{11}+K_2M_{21}+K_3M_{31}$$
$$=\frac{-4.493}{(x+12)^2+169}+\frac{0.666}{x^2+169}+\frac{0.208}{(x-12)^2+169}$$

$$K_{v2}=K_1M_{12}+K_2M_{22}+K_3M_{32}$$
$$=\frac{0.666}{(x+12)^2+169}-\frac{4.58}{x^2+169}+\frac{0.666}{(x-12)^2+169}$$

$$K_{v3}=K_1M_{13}+K_2M_{23}+K_3M_{33}$$
$$=\frac{0.208}{(x+12)^2+169}+\frac{0.666}{x^2+169}-\frac{4.493}{(x-12)^2+169}$$

Step 5.
$$K_v=(K_{v1}^2+K_{v2}^2+K_{v3}^2-K_{v1}K_{v2}-K_{v2}K_{v3}-K_{v3}K_{v1})^{1/2}$$

Step 6.
$$E_v=K_v.420/\sqrt{3}\text{ kV/metre.}$$

A computer programme written for x varying from 0 to 3 H = 39 m from the line centre has given the following results, which are also plotted in Fig. 7.5.

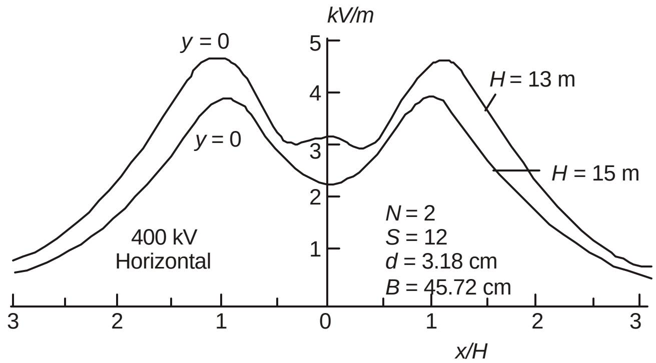

Fig. 7.5 Profile of E.S. field of 400 kV line at ground level.

x/H	0	0.1	0.2	0.3	0.4	0.5	0.6	0.7
E_v,kV/m	3.214	3.182	3.11	3.06	3.11	3.29	3.60	3.96
x/H	0.8	0.9	1.0	1.1	1.2	1.3	1.4	1.5
E_v	4.3	4.55	4.69	4.694	4.576	4.136	4.08	3.76
x/H	1.6	1.7	1.8	1.9	2.0	2.2	2.6	3.0
E_v	3.42	3.1	2.78	2.494	2.23	1.785	1.16	0.783

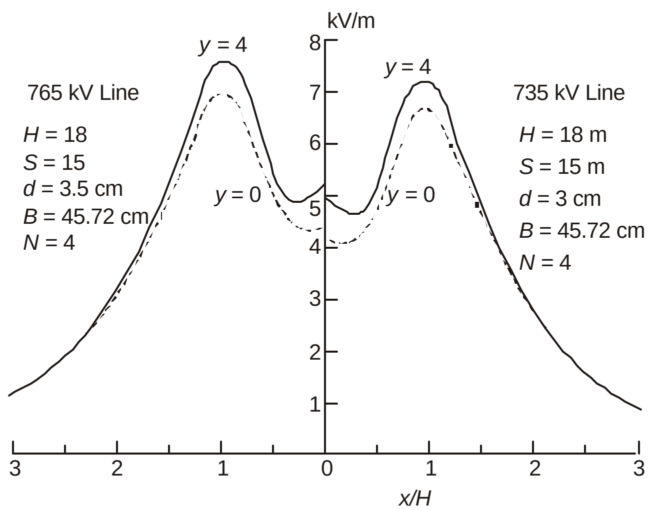

Fig. 7.6 E.S. field profile of 750 kV line (calculated).

We observe that the maximum value of ground-level field does not occur at the line centre but at $x/H = 1.1(x = 14.3\,\text{m})$. There is a double hump in the graph. Further examples for 750 kV, 1000 kV and 1200 kV lines are shown in Figs. 7.6 to 7.8 using typical dimensions. In all cases, the presence of overhead ground wires has been neglected. In a digital computer programme they can be included but their effect is negligible. The fields at $y = 4$ m above ground are also shown which a truck might experience.

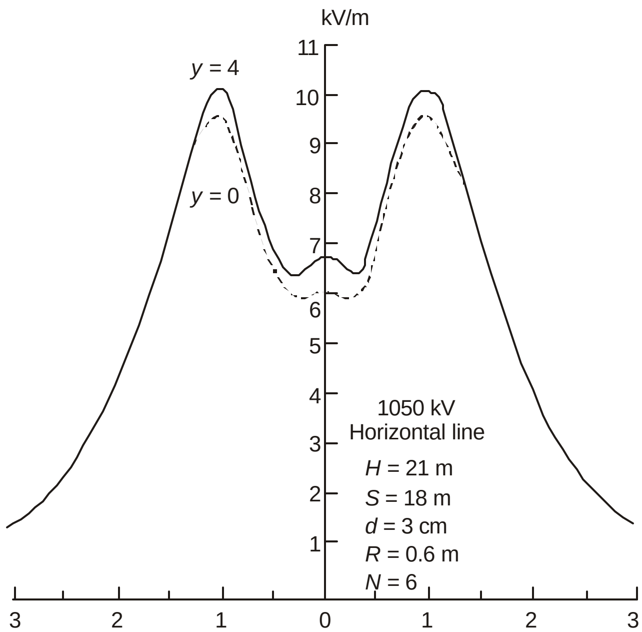

Fig. 7.7 E.S. field profile of 1000 kV line (calculated).

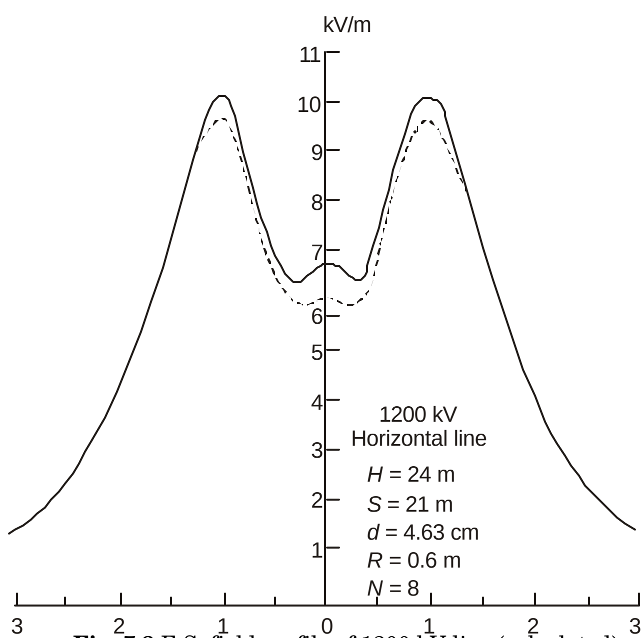

Fig. 7.8 E.S. field profile of 1200 kV line (calculated).

7.3.3 Electrostatic Field of Double-Circuit 3-phase A.C. Line

On a D/C line there are 6 conductors on a tower, neglecting ground wires above the line conductors. [Some proposals for using shielding wires under the line conductors are made, but such problems will not be discussed in this book]. The e.s. field will depend on the phase configuration of the two circuits and for illustrating the procedure, the arrangement shown in Fig. 7.9 will be used. The positions occupied by the phases are numbered 1 to 6 and it is evident that (a) conductors 1 and 4 have the voltage $V_m \sin(wt + \varphi)$, (b) conductors 2 and 5 have voltages $V_m \sin(wt + \varphi - 120°)$ and (c) conductors 3 and 6 have voltages $V_m \sin(wt + \varphi + 120°)$.

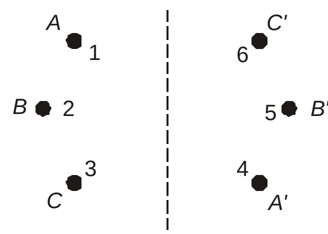

Fig.7.9 Configuration of a double-circuit (D/C) line.

Consequently, the horizontal and vertical components of e.s. field will consist of 6 quantities as follows:

$$E_{h1} = \frac{q_1}{2\pi e_0} J_1 = V_m . J_1 [(M_{11} + M_{14}) \sin(wt + \varphi) + (M_{12} + M_{15}) \sin(wt + \varphi - 120°) + (M_{13} + M_{16}) \sin(wt + \varphi + 120°)] \quad ...(7.23)$$

$$\vdots$$

$$E_{h6} = \frac{q_6}{2\pi e_0} J_6 = V_m . J_6 [(M_{61} + M_{64}) \sin(wt + \varphi) + (M_{62} + M_{65}) \sin(wt + \varphi - 120°) + (M_{63} + M_{66}) \sin(wt + \varphi + 120°)] \quad ...(7.24)$$

where the Maxwell's Potential coefficient matrix [P] and its inverse [M] are now of order 6 × 6, and the J_i values are given from equation (7.16) by using i = 1, 2, ..., 6 in turn. Once again, the total horizontal component of e.s. field at $A(x, y)$ is of the form

$E_{ht} = V_m [J_{h1} \sin (wt + \varphi) + J_{h2} \sin(wt + \varphi - 120°) + J_{h3} . \sin(wt + \varphi + 120°)]$ and in phasor form

$$E_{ht} = V_m (J_{h1} \angle\varphi + J_{h2} \angle\varphi - 120° + J_{h3} \angle\varphi + 120°) \quad ...(7.25)$$

The quantities J_{h1}, J_{h2}, J_{h3}, are obtained by adding equations (7.23) to (7.24) vertically and collecting the coefficients of sin $(wt + \varphi), \sin(wt + \varphi - 120°)$ and $\sin(wt + \varphi + 120°)$. This is of the same form as equation (7.19).

Similarly, the total vertical component of e.s. field can be obtained by using equation (7.17) for calculating K_1 to K_6. Then,

$$E_{vt} = K_v . V$$

$$\text{where} \quad K_v = K_{v1}^2 + K_{v2}^2 + K_{v3}^2 - K_{v1}K_{v2} - K_{v2}K_{v3} - K_{v3}K_{v1})^{1/2}$$

$$\text{with} \quad K_{v1} = K_1(M_{11} + M_{14}) + K_2(M_{21} + M_{24}) + K_3(M_{31} + M_{34})$$
$$+ K_4(M_{41} + M_{44}) + K_5(M_{51} + M_{54}) + K_6(M_{61} + M_{66}) \quad ...(7.27)$$

$$\vdots$$

$$K_{v3} = K_1(M_{13} + M_{16}) + K_2(M_{23} + M_{26}) + K_3(M_{33} + M_{36})$$
$$+ K_4(M_{43} + M_{46}) + K_5(M_{53} + M_{56}) + K_6(M_{63} + M_{66}) \quad ...(7.28)$$

The total e.s. field at every point $A(x, y)$ will be

$$E_t = [E_{ht}^2 + E_{vt}^2]^{1/2} \quad ...(7.29)$$

7.3.4 Six-Phase A.C. Line

A recent advancement in medium-voltage lines is the use of high phase order lines with more than 3 phases on the same tower. We will complete the problem of e.s. field calculation with a 6-phase line where the voltages are now.

$V_1 = V_m\angle 0°, V_2 = V_m\angle -60°, V_3 = V_m\angle -120°, V_4 = V_m\angle -180°, V_5 = V_m\angle -240°$ and $V_6 = V_m\angle -300°$. Thus, V_1 and V_4 are in phase opposition, which is also true of V_2 and V_5, and V_3 and V_6. The arrangement of phase positions is shown in Fig. 7.10. It is clear that the Maxwell's Potential coefficient matrix [P] and its inverse [M] are the same as for a double-circuit 3-phase line of the previous section. The values of J_i and K_i are also the same as were obtained from equations (7.16) and (7.17), for i = 1, 2, ..., 6.

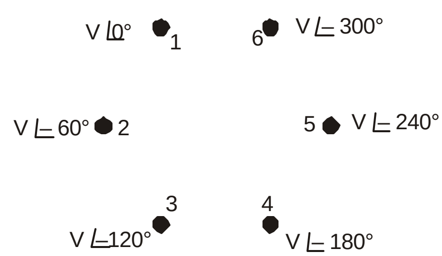

Fig. 7.10 Details of 6-phase line.

Equations are now written down for the horizontal and vertical components of the e.s. field at a point $A(x, y)$ due to the six voltages as follows:

$$E_{h1} = J_1 \cdot \frac{q}{2\pi e_0} = J_1 . V_m [M_{11} \sin(wt + \varphi) + M_{12} \sin(wt + \varphi - 60°)$$
$$+ M_{13} \sin(wt + \varphi - 120°) + M_{14} \sin(wt + \varphi - 180°)$$
$$+ M_{15} \sin(wt + \varphi - 240°) + M_{16} \sin(wt + \varphi - 300°)]$$
$$= V_m . J_1 [(M_{11} - M_{14}) \sin(wt + \varphi) + (M_{12} - M_{15}) \sin(wt + \varphi - 60°)$$
$$+ (M_{13} - M_{16}) \sin(wt + \varphi - 120°)] \quad ...(7.30)$$

Similarly for the remaining 5 conductors. For conductor 6,

$$E_{h6} = V_m.J_6[(M_{61} - M_{64})\sin(wt+\varphi) + (M_{62} - M_{65})\sin(wt+\varphi-60°)$$
$$+(M_{63} - M_{66})\sin(wt+\phi-120°)] \quad ...(7.31)$$

The total horizontal component of e.s. field at $A(x,y)$ will be of the form

$$E_{ht} = E_{h1} + E_{h2} + E_{h3} + E_{h4} + E_{h5} + E_{h6}$$
$$= V_m[J_{h1}\sin(wt+\varphi) + J_{h2}\sin(wt+\varphi-60°) + J_{h3}\sin(wt+\varphi-120°)]$$
$$= V_m(J_{h1}\angle 0° + J_{h2}\angle -60° + J_{h3}\angle -120°) \quad ...(7.32)$$

Its amplitude is obtained by separating the real part and *j*-part and taking the resulting vectroial sum.

The real part is $[J_{h1} + 0.5(J_{h2} - J_{h3})]$ and the *j*-part is $0.866\ (J_{h2} + J_{h3})$. The amplitude is

$$J_h = [\{J_{h1} + 0.5(J_{h2} - J_{h3})\}^2 + 0.75(J_{h2} + J_{h3})^2]^{1/2}$$
$$= (J_{h1}^2 + J_{h2}^2 + J_{h3}^2 + J_{h1}J_{h2} + J_{h2}J_{h3} - J_{h3}J_{h1})^{1/2} \quad ...(7.33)$$

The total horizontal component of e.s. field at the point $A(x, y)$ has the corresponding r.m.s. value.

$$E_h = J_h.V, \text{where } V = V_m/\sqrt{2} \quad ...(7.34)$$

Similarly, the total vertical component at $A(x, y)$ is

$$E_v = K_v.V \quad ...(7.35)$$

where
$$K_v = (K_{v1}^2 + K_{v2}^2 + K_{v3}^2 + K_{v1}K_{v2} + K_{v2}K_{v3} - K_{v3}K_{v1})^{1/2} \quad ...(7.36)$$

$$K_{v1} = K_1(M_{11} - M_{14}) + K_2(M_{21} - M_{24}) + K_3(M_{31} - M_{34}) + K_4(M_{41} - M_{44})$$
$$+K_5(K_{51} - K_{54}) + K_6(M_{61} - M_{64})$$

$$K_{v2} = K_1(M_{12} - M_{15}) + K_2(M_{22} - M_{25}) + K_3(M_{32} - M_{36}) + K_4(M_{42} - M_{45})$$
$$+K_5(M_{52} - M_{55}) + K_6(M_{62} - M_{65})$$

and
$$K_{v3} = K_1(M_{13} - M_{16}) + K_2(M_{23} - M_{26}) + K_3(M_{33} - M_{36}) + K_4(M_{43} - M_{46})$$
$$+K_5(M_{53} - M_{56}) + K_6(M_{63} - M_{66})$$

The quantities K_1 to K_6 are calculated from equation (7.17).

7.4 EFFECT OF HIGH E.S. FIELD ON HUMANS, ANIMALS, AND PLANTS

In section 7.1, a discussion of electric shock was sketched. The use of e.h.v. lines is increasing danger of the high e.s. field to (*a*) human beings, (*b*) animals, (*c*) plant life, (*d*) vehicles, (*e*) fences, and (*f*) buried pipe lines under and near these lines. It is clear from section 7.2 that when an object is located under or near a line, the field is disturbed, the degree of distortion depending upon the size of the object. It is a matter of some diffficulty to calculate the characteristics of the distorted field, but measurements and experience indicate that the effect of the distorted field can be related to the magnitude of the undistorted field. A case-by-case study must be made if great accuracy is needed to observe the effect of the distorted field. The limits for the undistorted field will be discussed here in relation to the danger it poses.

(*a*) *Human Beings*

The effect of high e.s. field on human beings has been studied to a much greater extent than on any other animals or objects because of its grave and shocking effects which has resulted in loss of life. A farmer ploughing his field by a tractor and having an umbrella over his head for shade will be charged by corona resulting from pointed spikes. The vehicle is also charged when it is stopped under a transmission line traversing his field. When he gets off the vehicle and touches a grounded object, he will discharge himself through his body which is a pure resistance of about 2000 ohms. The discharge current when more than the let-go current can cause a shock and damage to brain.

It has been ascertained experimentally that the limit for the undisturbed field is 15 kV/m, r.m.s., for human beings to experience possible shock. An e.h.v. or u.h.v. line must be designed such that this limit is not exceeded. The minimum clearance of a line is the most important governing factor. As an example, the B.P.A. of the U.S.A. have selected the maximum e.s. field gradient to be 9 kV/m at 1200 kV for their 1150 kV line and in order to do so used a minimum clearance at midspan of 23.2 m whereas they could have selected 17.2 m based on clearance required for switching-surge insulation recommended by the National Electrical Safety Council.

(*b*) *Animals*

Experiments carried out in cages under e.h.v. lines have shown that pigeons and hens are affected by high e.s. field at about 30 kV/m. They are unable to pick up grain because of chattering of their beaks which will affect their growth. Other animals get a charge on their bodies and when they proceed to a water trough to drink water, a spark usually jumps from their nose to the grounded pipe or trough.

(*c*) *Plant Life*

Plants such as wheat, rice, sugarcane, etc., suffer the following types of damage. At a field strength of 20 kV/m (r.m.s.), the sharp edges of the stalk give corona discharges so that damage occurs to the upper portion of the grain-bearing parts. However, the entire plant does not suffer damage. At 30 kV/m, the by-products of corona, namely ozone and N_2O become intense. The resistance heating due to increased current prevents full growth of the plant and grain. Thus, 20 kV/m can be considered as the limit and again the safe value for a human being governs line design.

(*d*) *Vehicles*

Vehicles parked under a line or driving through acquire electrostatic charge if their tyres are made of insulating material. If parking lots are located under a line, the minimum recommended safe clearance is 17 m for 345 kV and 20 m for 400 kV lines. Trucks and lorries will require an extra 3 m clearance. The danger lies in a human being attempting to open the door and getting a shock thereby.

(*e*) *Others*

Fences, buried cables, and pipe lines are important pieces of equipment to require careful layout. Metallic fences parallel to a line must be grounded preferably every 75 m. Pipelines longer than 3 km and larger than 15 cm in diameter are recommended to be buried at least 30 m laterally from the line centre to avoid dangerous eddy currents that could cause corrosion. Sail boats, rain gutters and insulated walls of nearby houses are also subjects of potential danger. The danger of ozone emanation and harm done to sensitive tissues of a human being at high electric fields can also be included in the category of damage to human beings living near e.h.v. lines.

7.5 METERS AND MEASUREMENT OF ELECTROSTATIC FIELDS

The principle on which a meter for measuring the e.s. field of an e.h.v. line is based is very simple. It consists of two conducting plates insulated from each other which will experience a potential difference when placed in the field. This can be measured on a voltmeter or an ammeter through a current flow. There exist 3 configurations for the electrodes in meters used in practice: (1) Dipole, (2) Spherical Dipole, and (3) Parallel Plates. The dimensions and other details are given in the following tabular form. Also see Fig. 7.11.

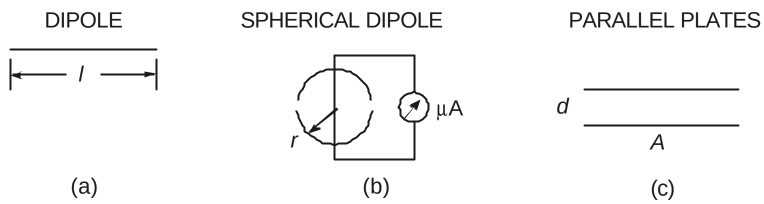

Fig. 7.11 Measurement of E.S. field. (a) Dipole. (b) Spherical dipole. (c) Parallel plates.

Table 7.1 Meters for E.S. Field Measurement

(1)	*Electrode Shape*	*Dipole*	*Spherical Dipole*	*Parallel Plates*
(2)	*Major Dimensions*	Effective length, l	Radius, r	Distance, d, Surface area, A
(3)	*Open-circuit Voltage* (as voltage source)	*E.l.*	–	*E.d*
(4)	*Short-circuit Current* (as current source)	–	$3\pi r^2 w e_0 E$ ($C = 3\pi e_0 r^2$)	$w e_0 A E$ ($C = e_0 A/d$)

The formula for the spherical dipole, which consists of two hemispheres insulated from each other, is very accurate and has been recommended as a standard. The two insulated hemispheres are connected by a micro-ammeter whose scale is calibrated in terms of kV/m of the electric field. On the other hand, the parallel plate meter is very easy to fabricate. A small digital voltmeter can be used by attaching a copper-clad printed-circuit board with its insulated side placed on top of the casing. The input to the meter is taken from the top copper-clad side and the casing.

The procedure for measurement consists of attaching the meter to a long (2 m) insulated rod and placing it in the field at the desired height. The insertion of the meter and rod as well as the human-body should not distort the field.

The meters must be first calibrated in a high voltage laboratory. One procedure is to suspend two horizontal plane parallel electrodes with constant separation. A suggested type is 6 m × 6 m wire mesh electrodes separated by 1 m. These will be accurate to within 5%. The meter is placed in the centre of this parallel-plate arrangement and a known voltage is gradually applied until about 100 kV/m is reached. The following application rules may be followed:

1. The instrument should be capable of measuring at least the vertical component of electric field. Up to a height of 3 or 4 m above ground, the horizontal component is very small and the total 50 Hz field is nearly the same as its vertical component.

2. If the instrument is not held in hand, it should be mounted at about 2 m above ground.
3. It should be battery powered in case a power supply for the electronic circuitry is necessary.
4. The r.m.s. value is preferably measured by a full-wave rectifier circuit and suitably calibrated.
5. Analogue indication may be preferable to digital representation as it disturbs the field.
6. The instrument may have full-scale readings of 3, 10, 30, and 100 kV/m or other suitable ranges for legible reading.
7. It should be designed for outdoor use and portable. A pole at least 2 m long must go with the instrument if hand-held.

7.6 ELECTROSTATIC INDUCTION ON UNENERGIZED CIRCUIT OF A D/C LINE

We shall end this chapter with some discussion of electrostatic and electromagnetic induction from energized lines into other circuits. This is a very specialized topic useful for line crew, telephone line interference etc. and cannot be discussed at very great length. EHV lines must be provided with wide enough right-of-way so that other low-voltage lines are located far enough, or when they cross the crossing must be at right angles.

Consider Fig. 7.12 in which a double-circuit line configuration is shown with 3 conductors energized by a three-phase system of voltages $V_1 = V_m \sin wt, V_2 = V_m \sin(wt - 120°)$ and $V_3 = V_m \sin(wt + 120°)$. The other circuit consisting of conductors 4, 5 and 6 is not energized. We will calculate the voltage on these conductors due to electrostatic induction which a line-man may experience. Now,

$$V_4 = \frac{q_1}{2\pi e_0}\ln(I_{14}/A_{14}) + \frac{q_2}{2\pi e_0}\ln(I_{24}/A_{24}) + \frac{q_3}{2\pi e_0}\ln(I_{34}/A_{34}) \quad ...(7.37)$$

$$= \frac{q_1}{2\pi e_0}P_{14} + \frac{q_2}{2\pi e_0}P_{24} + \frac{q_3}{2\pi e_0}P_{34}$$

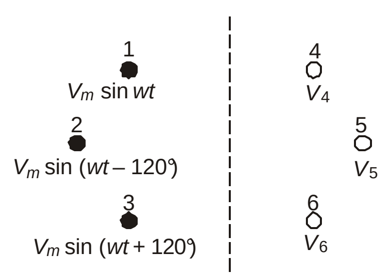

Fig. 7.12 D/C line: One line energized and the other unenergized to illustrate induction.

The charge coefficients q_1, q_2, q_3 are obtained from the applied voltages.

$$\begin{bmatrix} V_1 \\ V_2 \\ V_3 \end{bmatrix} = \begin{bmatrix} P_{11}, & P_{12}, & P_{13} \\ P_{21}, & P_{22}, & P_{23} \\ P_{31}, & P_{32}, & P_{33} \end{bmatrix} \begin{bmatrix} q_1 \\ q_2 \\ q_3 \end{bmatrix} (1/2\pi e_0) = [P][q](1/2\pi e_0) \quad ...(7.38)$$

so that $$[q/2\pi e_0] = [M][V] \quad ...(7.39)$$

$$\begin{aligned} V_4 &= V_m.P_{14}[M_{11}\sin wt + M_{12}\sin(wt-120°) + M_{13}\sin(wt+120°)] \\ &\quad + V_m P_{24}[M_{21}\sin wt + M_{22}\sin(wt-120°) + M_{23}\sin(wt+120°)] \\ &\quad + V_m P_{34}[M_{31}\sin wt + M_{32}\sin(wt-120°) + M_{33}\sin(wt+120°)] \\ &= V_m[(P_{14}M_{11} + P_{24}M_{21} + P_{34}M_{31})\sin wt \\ &\quad + (P_{14}M_{12} + P_{24}M_{22} + P_{34}M_{32})\sin(wt-120°) \\ &\quad + (P_{14}M_{13} + P_{24}M_{23} + P_{34}M_{33})\sin(wt+120°)] \\ &= V_m[\lambda_1 \sin wt + \lambda_2 \sin(wt-120°) + \lambda_3 \sin(wt+120°)] \end{aligned} \quad ...(7.40)$$

In phasor form,

$$V_4 = V[\lambda_1\angle 0° + \lambda_2\angle -120° + \lambda_3\angle 120°], \text{r.m.s.} \quad ...(7.41)$$

$$V_4 = V(\lambda_1^2 + \lambda_2^2 + \lambda_3^2 - \lambda_1\lambda_2 - \lambda_2\lambda_3 - \lambda_3\lambda_1)^{1/2} \quad ...(7.42)$$

Similarly, $$V_5 = V(\lambda_4^2 + \lambda_5^2 + \lambda_6^2 - \lambda_4\lambda_5 - \lambda_5\lambda_6 - \lambda_6\lambda_4)^{1/2} \quad ...(7.43)$$

and $$V_6 = V(\lambda_7^2 + \lambda_8^2 + \lambda_9^2 - \lambda_7\lambda_8 - \lambda_8\lambda_9 - \lambda_9\lambda_7)^{1/2} \quad ...(7.44)$$

where

$$\left.\begin{aligned} \lambda_1 &= P_{14}M_{11} + P_{24}M_{21} + P_{34}M_{31} \\ \lambda_2 &= P_{14}M_{12} + P_{24}M_{22} + P_{34}M_{32} \\ \lambda_3 &= P_{14}M_{13} + P_{24}M_{23} + P_{34}M_{33} \\ \lambda_4 &= P_{15}M_{11} + P_{25}M_{21} + P_{35}M_{31} \\ \lambda_5 &= P_{15}M_{12} + P_{25}M_{22} + P_{35}M_{32} \\ \lambda_6 &= P_{15}M_{13} + P_{25}M_{23} + P_{35}M_{33} \\ \lambda_7 &= P_{16}M_{11} + P_{26}M_{21} + P_{36}M_{31} \\ \lambda_8 &= P_{16}M_{12} + P_{26}M_{22} + P_{36}M_{32} \\ \text{and} \quad \lambda_9 &= P_{16}M_{13} + P_{26}M_{23} + P_{36}M_{33} \end{aligned}\right\} \quad ...(7.45)$$

Example 7.3. A 230-kV D/C line has the dimensions shown in Figure 7.13. The phase conductor is a single Drake 1.108 inch (0.028 m) diameter. Calulate the voltages induced in conductors of circuit 2 when circuit 1 is energized assuming (a) no transposition, and (b) full transposition.

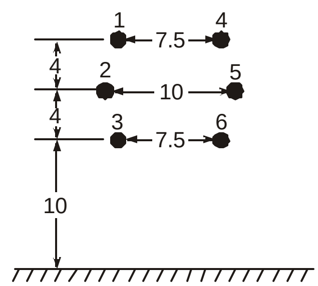

Fig. 7.13 D/C 230-kV line dimensions.

Solution. The Maxwell's Potential coefficients for the energized circuit are as follows:
P_{11} = ln (36/0.014) = 7.852, P_{22} = ln (28/0.014) = 7.6,
P_{33} = ln (20/0.014) = 7.264
P_{12} = ln (32.02/4.19) = 2.0335, P_{13} = ln (28/8) =1.253,
P_{23} = ln (24.03/4.19) = 1.747.

$$\therefore \qquad [P]_u = \begin{bmatrix} 7.852, & 2.0335, & 1.253, \\ 2.0335, & 7.6, & 1.747 \\ 1.253, & 1.747, & 7.264 \end{bmatrix};$$

$$[M]_{\text{ut}} = [P]_{ut}^{-1} = \begin{bmatrix} 0.1385, & -.0334, & -.0159 \\ -.0334, & .1474, & -.0297 \\ -.0159, & -.0297, & .14755 \end{bmatrix}$$

P_{14} = ln (36.77/7.5) =1.59, P_{24} = ln (33.175/9.62) = 1.238,
P_{34} = ln (29/10.97) = 0.972
$P_{15} = P_{24}$ = 1.238, P_{25} = ln (29.73/10) = 1.09,
P_{35} = ln (25.55/9.62) = 0.9765
$P_{16} = P_{34}$ = 0.972, $P_{26} = P_{35}$ = 0.9765,
P_{36} = ln(21.36/7.5) = 1.0466.

These values give, from equations (7.42) to (7.45), with $V = 230/\sqrt{3}$,

λ_1 = 0.1634, λ_2 = 0.1005, λ_3 = 0.0813, $\therefore$ V_4 = 9.76 kV.
λ_4 = 0.1196, λ_5 = 0.09035, λ_6 = 0.092, $\therefore$ V_5 = 3.9 kV.
λ_7 = 0.0854, λ_8 = 0.0804, λ_9 = 0.11, $\therefore$ V_6 = 3.65 kV.

For the completely transposed line, the induced voltage is the average of these three voltages which amounts to $\frac{1}{3}(9.76 + 3.9 + 3.65) = 5.77$ kV.

7.7 INDUCED VOLTAGE IN INSULATED GROUND WIRES

Normally, in all high voltage and e.h.v. lines which use overhead ground wires for lightning protection, it is usual to tie them firmly to the tower top so that they are grounded directly and are at ground potential which is considered as zero. Consequently, only the phase conductors experience a voltage with respect to ground. However, in recent years, the shield wires strung above the phase conductors are being insulated from the tower structure in order to utilize them for the following purposes:

(*a*) To serve as conducting wires for carrier communication and protection. This is also being taken over by fibre-optic links.

(*b*) To tap power at power frequency at a voltage lower than the power-frequency transmission voltage in order to feed rural loads along the line route.

In order also to serve the primary purpose of shielding against lightning, the insulators on which the "ground" wires are mounted should be provided with a spark gap which flashes over at the high lightning voltage. We will now discuss this problem of induced voltage on insulated ground wires due to the power-frequency voltage carried by the phase conductors, assuming that the voltages of the shield wires are floating. The shield wires are made from ACSR instead of galvanized steel in order to reduce both the series resistance and inductance.

At first, the bundle charge on the three phase conductors (for a S/C line) are calculated at power frequency in the usual manner from equation (7.4) or (7.38). Then, by using equations (7.37) to (7.42) and designating the insulated shield wires as 4,5,..., the voltage induced in them can be calculated. For example, in a 400-kV line with two insulated shield wires, calculation yields an induced voltage of about 8.6% of the line-to-ground voltage of the phase condutors which amounts to roughly 21 kV, r.m.s., at 420 kV exccitation of the three phases, or about 20 kV for 400 kV. This is shown in the following example.

Example 7.4. A 400-kV horizontal configuration S/C line of the UPSEB type has the details given in Example 4.16 in Chapter 4. The salient dimensions are as follows:

Phase conductors:	Average height	— 9.81 metres;
	Phase spacings	— 11.3 metres;
	Conductor	— 2 × 3.18 cm diameter at bundle spacing of 45.72 cm.
Ground wires:	Height above ground	— 20.875 metres. Neglect sag.
	Horizontal spacing	— 16 metres. Two numbers.

Calculate the voltage induced in the insulated ground wires as a percentage of power-frequency voltage of the phase conductors using the line-to-ground value.

Solution. The equivalent bundle radius is $r_{eq} = (r.B)^{1/2} = 0.0815\,\text{m}$. The Maxwell's Potential Coefficients are as follows:

Self — $P_{11} = P_{22} = P_{33} = \ln(2 \times 9.81/0.0815) = 5.44$;

Mutual—Outer to inner: $P_{12} = P_{23} = 0.695$;

Outer to outer: $P_{13} = 0.285$.

By inverting matrix [P] and evaluating the charge coefficients, there result for the phase conductors, with V = phase-to-ground voltage,

$$q_1/2\pi e_0 = 187 \times 10^{-3} V\angle 0° - 23 \times 10^{-3} V\angle -120° - 6.9 \times 10^{-3} V\angle 120°$$

$$q_2/2\pi e_0 = -23 \times 10^{-3} V\angle 0° + 189.7 \times 10^{-3} V\angle -120° - 23 \times 10^{-3} V\angle 120°$$

$$q_3/2\pi e_0 = -6.9 \times 10^{-3} V\angle 0° - 23 \times 10^{-3} V\angle -120° + 187 \times 10^{-3} V\angle 120°$$

Since the ground wires insulated from the tower are located symmetrically with respect to the phase conductors, the voltages induced in both will be equal. Designating any one of them as No. 4, the mutal potential coefficients between this wire and the three phase conductors are calculated as follows:

Image distances:

$I_{14} = [(20.875 + 9.81)^2 + 3.3^2]^{1/2}$

$= 30.864$ metres;

$I_{24} = [30.685^2 + 8^2]^{1/2} = 31.71\text{m};$

$I_{34} = [30.685^2 + 19.3^2]^{1/2} = 36.25\text{m};$

Aerial distances:

$A_{14} = [3.3^2 + 11.065^2]^{1/2} = 11.5466.$

$A_{24} = [8^2 + 11.065^2]^{1/2} = 13.654;$

$A_{34} = [19.3^2 + 11.065^2]^{1/2} = 22.247\text{m}.$

$\therefore \quad P_{14} = \ln(30.864/11.5466) = 0.9832; P_{24} = 0.8426 : P_{34} = 0.4822.$

Then, $\quad V_4 = (q_1/2\pi e_0).P_{14} + (q_2/2\pi e_0).P_{24} + (q_3/2\pi e_0).P_{34}$

$= [0.1638\angle 0° + 0.126\angle -120° + 0.065\angle 120°]V$

$\therefore \quad V_4/V = (0.1638^2 + 0.126^2 + 0.065^2 - 0.1638 \times 0.126$

$- 0.126 \times 0.065 - 0.065 \times 0.1638)^{1/2}$

$= (0.046931 - 0.039476)^{1/2} = 0.08634 = 8.634\%.$

At $\quad V = 420$ kV, line-to-line $= 420/\sqrt{3}$ kV, line-to-ground,

$V_4 = 0.08634 \times 242.49 = 20.94$ kV to ground ≈ 21 kV, r.m.s.

At 400 kV, $\quad V_4 = 20$ kV to ground

The insulator supporting the overhead shield wires must be rated for this voltage class.

7.8 MAGNETIC FIELD EFFECTS

An overhead line generates an electrostatic field in its vicinity because of the voltage at which it is energized and the charge in its conductors trapped in its capacitance network. In addition, the line generates a magnetic field in its vicinity due to the load current flowing in the conductors. The intensity of the magnetic field is proportional to the currents so that it varies with the load condition. However, in e.h.v. lines, the load factor seldom if ever is lower than 75% so that the load current stays above 75% rated value most of the time. In calculating the magnetic field, we will assume that the current flowing is the rated full-load current. The following Table gives the values of rated current for e.h.v. lines based upon the details of Table 2 in Chapter II.

Nominal kV	*Reactance*	*Length*	*Load, MW 3ph*	*Cond. Current, Amps.*
400	0.327	400 km	612	883
	ohm/km	600	408	588
	at 50 Hz	800	306	441
500	0.3	400	1040	1200
		600	695	800
		800	520	600
750	0.272	600	1720	1327
		800	1290	995
		1000	1032	796

These values are based on the following assumptions:

(*a*) Equal voltage magnitudes at both ends;

(*b*) Power angle of 30° based on stability considerations;

(*c*) $P_{3ph} = E_s E_r \sin\delta/(L.x); E_s = E_r = E$;

(*d*) $I = E\sin\delta/\sqrt{3}Lx = P_{3ph}/\sqrt{3}E$.

7.9 MAGNETIC FIELD OF 3-PHASE LINES

7.9.1 Single Circuit Horizontal Configuration

Most e.h.v. transmission lines consist of one 3-phase circuit on a tower with horizontal configuration of the 3 phases. In Chapter 3, we have discussed the method of calculation of the inductance matrix of a multi-conductor line from the Maxwell Potential Coefficient matrix. Based on Maxwell's method of images, we will now calculate the magnetic field generated at any point in space in the vicinity of the 3-phase line. In most applications, the field intensity at ground level is the most important quantity. But the equations derived will be very general.

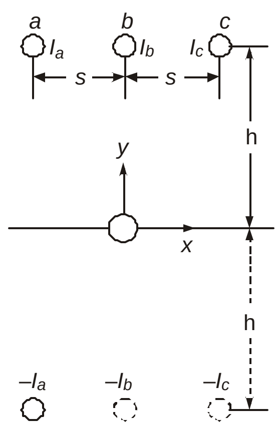

Fig. 7.14

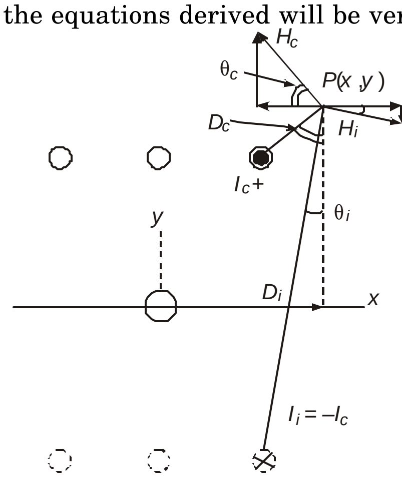

Fig. 7.15

Figure 7.14 shows the 3 overhead conductors and the ground surface replaced by image conductors below the ground surface. This assumes that the ground surface is a flux line. The origin of a coordinate system is placed on the ground underneath the centre-phase. The conductors are at height h above ground and the phase separation is s.

At the point P (x, y), the components of magnetic field are as follows:

(*a*) Due to the conductor current, from Fig. 7.15:

$$H_c = I/2\pi D_c, \qquad \text{...(7.46)}$$

where

$$D_c = \sqrt{(x-s)^2 + (y-h)^2} \qquad \text{...(7.47)}$$

Assume the direction of I_c to be out of the paper. Then the direction of H-field is counter-clockwise at P as shown. Its horizontal and vertical components are :

(*i*) Hor. comp. : $$H_c\cos\theta_c = -\frac{I_c}{2\pi}\frac{1}{D_c}\frac{y-h}{D_c} = -\frac{I}{2\pi}\frac{y-h}{(x-s)^2+(y-h)^2} \qquad \text{...(7.48)}$$

(*ii*) Vert. comp.: $H_c \sin\theta_c = \dfrac{I_c}{2\pi}\dfrac{1}{D_c}\dfrac{x-s}{D_c} = \dfrac{I}{2\pi}\dfrac{x-s}{(x-s)^2+(y-h)^2}$ ...(7.49)

(*b*) Due to the image current:

$$H_i = \frac{I_c}{2\pi}\frac{1}{D_i}, \text{ where } D_i = \sqrt{(x-s)^2+(y+h)^2} \quad ...(7.50)$$

This is directed in the clockwise sense as shown in Figure 7.15, since the current in the image conductor is assumed to flow into the paper, opposite to the direction of current in the actual overhead conductor. The horizontal and vertical components of this magnetic field will be:

(*iii*) Hor. comp.: $H_i \cos\theta_i = \dfrac{I_c}{2\pi}\dfrac{1}{D_i}\dfrac{y+h}{D_i} = \dfrac{I_c}{2\pi}\dfrac{y+h}{(x-s)^2+(y+h)^2}$ ...(7.51)

(*iv*) Vert. comp.: $H_i \sin\theta_i = -\dfrac{I_c}{2\pi}\dfrac{1}{D_i}\dfrac{x-s}{D_i} = -\dfrac{I_c}{2\pi}\dfrac{x-s}{(x-s)^2+(y+h)^2}$ ...(7.52)

From the figure we observe that the horizontal and vertical components of H_c are directed in the opposite sense to those due to H_i. Therefore, the total horizontal and vertical components of the H-field at point $P(x, y)$ due to the conductor current I_c and image current

$I_i = -I_c$ will be readily seen to be:

$$H_h = H_c \cos\theta_c + H_i \cos\theta_i = \frac{I_c}{2\pi}\left[\frac{y+h}{(x-s)^2+(y+h)^2} - \frac{y-h}{(x-s)^2+(y+h)^2}\right] \text{Amp/metre.} \quad ...(7.53)$$

$$H_v = H_c \sin\theta_c + H_i \sin\theta_i = \frac{I_c}{2\pi}\left[\frac{x-s}{(x-s)^2+(y-h)^2} - \frac{x-s}{(x-s)^2+(y+h)^2}\right] \text{Amp/metre.} \quad ...(7.54)$$

The corresponding flux densities are:

$$B_h = \mu_0 H_h, \text{and } B_v = \mu_0 H_v, \textit{Tesla}, \quad ...(7.55)$$

where $\mu_0 = 4\pi\times10^{-7}$ Henry/metre.

Following the above procedure, we can extend the equations to calculate the magnetic field at $P(x, y)$ due to the combined effect of all 3 conductor-currents. Let the three currents be:

$$I_a = I\angle 0°, I_b = I\angle -120°, \text{and } I_c = I\angle +120° \text{ Amps.}$$

Then:

$$H_{ht} = \frac{I_a}{2\pi}\left[\frac{y+h}{(x+s)^2+(y+h)^2} - \frac{y-h}{(x+s)^2+(y-h)^2}\right] + \frac{I_b}{2\pi}\left[\frac{y+h}{x^2+(y+h)^2} - \frac{y-h}{x^2+(y-h)^2}\right] + \frac{I_c}{2\pi}\left[\frac{y+h}{(x-s)^2+(y+h)^2} - \frac{y-h}{(x-s)^2+(y-h)^2}\right], \text{Amp/metre.} \quad ...(7.56)$$

$$H_{vt} = \frac{I_a}{2\pi}\left[\frac{x+s}{(x+s)^2+(y-h)^2} - \frac{x+s}{(x+s)^2+(y+h)^2}\right]$$

$$+\frac{I_b}{2\pi}\left[\frac{x}{x^2+(y-h)^2}-\frac{x}{x^2+(y+h)^2}\right]$$

$$+\frac{I_c}{2\pi}\left[\frac{x-s}{(x-s)^2+(y-h)^2}-\frac{x-s}{(x-s)^2+(y+h)^2}\right], \text{Amp/metre.} \qquad ...(7.57)$$

In particular, on the ground surface where animals and human beings live, the magnetic-field components at a distance x from the line centre will be, with y = 0:

$$H_{ht} = \frac{I_a}{2\pi}\frac{2h}{(x+s)^2+h^2}+\frac{I_b}{2\pi}\frac{2h}{x^2+h^2}+\frac{I_c}{2\pi}\frac{2h}{(x-s)^2+h^2} \qquad ...(7.58)$$

$$H_{vt} = \frac{I_a}{2\pi}\left[\frac{x+s}{(x+s)^2+h^2}-\frac{x+s}{(x+s)^2+h^2}\right]+\frac{I_b}{2\pi}\times 0+\frac{I_c}{2\pi}\times 0 = 0. \qquad ...(7.59)$$

Since we have assumed the ground surface to be a flux line, the vertical component of H due to any phase-current is zero, and the magnetic field at the ground surface is entirely in the horizontal direction.

Magnitudes of H_{ht} and H_{vt}. In equations (7.56) and (7.57), the three phase-currents I_a, I_b and I_c are phasors with generally equal magnitudes I and having a phase difference of 120° with respect to each other. They can be written as:

$$I_a = I\angle 0° = I(1+j0); I_b = I\angle -120° = I(-0.5-j0.866); \text{ and}$$

$$I_c = I\angle +120° = I(-0.5+j0.866).$$

It is convenient to abbreviate the six geometric factors from equations (7.56) and (7.57), thus:

Horizontal components:

$$K_a = \frac{y+h}{(x+s)^2+(y+h)^2}-\frac{y-h}{(x+s)^2+(y-h)^2} \qquad ...(7.60)$$

$$K_b = \frac{y+h}{x^2+(y+h)^2}-\frac{y-h}{x^2+(y-h)^2} \qquad ...(7.61)$$

$$K_c = \frac{y+h}{(x-s)^2+(y+h)^2}-\frac{y-h}{(x-s)^2+(y-h)^2} \qquad ...(7.62)$$

Vertical components:

$$J_a = \frac{x+s}{(x+s)^2+(y-h)^2}-\frac{x+s}{(x+s)^2+(y+h)^2} \qquad ...(7.63)$$

$$J_b = \frac{x}{x^2+(y-h)^2}-\frac{x}{x^2+(y+h)^2} \qquad ...(7.64)$$

$$J_c = \frac{x-s}{(x-s)^2+(y-h)^2}-\frac{x-s}{(x-s)^2+(y+h)^2} \qquad ...(7.65)$$

Then, equations (7.56) and (7.57) may be written in phasor forms as follows:

$$H_{ht} = \frac{I}{2\pi}\left[K_a + K_b(-0.5 - j0.866) + K_c(-0.5 + j0.866)\right]$$

$$= \frac{I}{2\pi}\left[\{K_a - 0.5(K_b + K_c)\} + j0.866(K_c - K_b)\right] \quad ...(7.66)$$

The magnitude $|H_{ht}|$ will then be obtained as:

$$|H_{ht}| = \frac{I}{2\pi}\left[\{K_a - 0.5(K_b + K_c)\}^2 + 0.75(K_c - K_b)^2\right]^{1/2}$$

$$= \frac{I}{2\pi}(K_a^2 + K_b^2 + K_c^2 - K_aK_b - K_bK_c - K_cK_a)^{1/2}, \text{Amp/metre} \quad ...(7.67)$$

Similarly, the magnitude $|H_{vt}|$ will be:

$$|H_{vt}| = \frac{I}{2\pi}(J_a^2 + J_b^2 + J_c^2 - J_aJ_b - J_bJ_c - J_cJ_a)^{1/2}, \text{ Amp/metre} \quad ...(7.68)$$

The corresponding values of flux density will be:

$$|B_{ht}| = \mu_0|H_{ht}| \text{ and } |B_{vt}| = \mu_0|H_{vt}|, \text{Tesla.} \quad ...(7.69)$$

Example 7.5 The details of a horizontal 750-kV line are as follows:
Voltage: 750 kV, line-to-line; **Load:** 1900 MW, 3-phase.
Current: 1.4626 kilo Amps in each phase.
Line height: 18 metres; **Phase spacing:** 15 m.
Calculate and plot the *B*-field intensity at ground level from the
Line centre ($x/h = 0$) to a distance of $x/h = 10$.

Solution. Figure 7.16 shows the result. Note that the scale is expanded for x/h = 6 to 10 because of the low values of flux density. The figure is symmetrical about the line centre and only one half is shown. The maximum value of flux density of 215 milli Gauss (0.215 Gauss = 21.5 μ Tesla) occurs at x/h = 1.1.

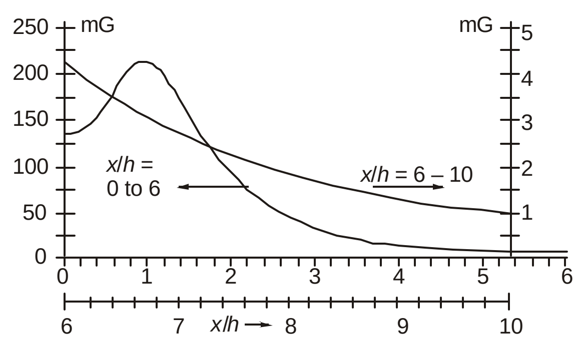

Fig. 7.16

7.9.2 Double-Circuit Vertical Configuration of 3-Phase Line

Figure 7.17 shows a double-circuit (D/C) 3-phase transmission line with a height to the middle phase of h. In this figure, the 6 conductors are shown as distributed uniformly on a circle of radius R. This may not always be the case in practice, but it is not difficult to use the actual dispositon of conductors in any given case for evaluating the magnetic field. The phase configurations can be of two types: (*i*) *abc* - *cba*, and (*ii*) *abc* - *abc*. Of the two the former is more comonly encountered. It is left as an exercise at the end of the chapter for the reader to evaluate the magnetic field for the latter case of *abc* - *abc*. Each has its own advantages and disadvantages, especially on what is known as "low-reactance" configuration. The lower the line reactance, the larger will be the power carried by the line. But we will not enter into a discussion of this topic here.

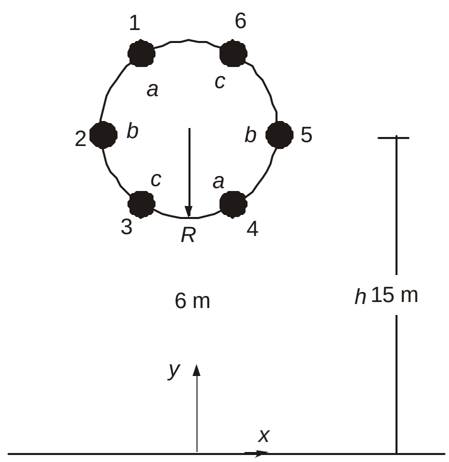

Fig. 7.17

Using Figure 7.17 for the geometry of the phase-conductors and phase-configuration *abc* - *cba*, we now write down the magnetic-field components at a point $P\ (x, y)$ in a manner similar to the single-circuit horizontal line of Figs. 7.14 and 7.15.

With the origin placed on ground surface underneath the line centre and the positions of the phase-conductors shown as 1 to 6, the coordinates of the 6 conductors will be as follows:

$$\begin{aligned}
&\text{Conductor 1: } x_1 = -\frac{1}{2}R, && y_1 = h + \frac{\sqrt{3}}{2}R, && \text{Current} = I_a;\\
&\text{Conductor 2: } x_2 = -R, && y_2 = h, && \text{Current} = I_b;\\
&\text{Conductor 3: } x_3 = -\frac{1}{2}R, && y_3 = h - \frac{\sqrt{3}}{2}R, && \text{Current} = I_c;\\
&\text{Conductor 4: } x_4 = \frac{1}{2}R, && y_4 = h - \frac{\sqrt{3}}{2}R, && \text{Current} = I_a;\\
&\text{Conductor 5: } x_5 = R, && y_5 = h, && \text{Current} = I_b;\\
&\text{Conductor 6: } x_6 = \frac{1}{2}R, && y_6 = h + \frac{\sqrt{3}}{2}R, && \text{Current} = I_c;
\end{aligned} \qquad \text{...(7.70)}$$

Referring to Fig. 7.18 and following earlier analysis, we can write down the values of horizontal and vertical components of H-field due to the current I_n in conductor n and its image current $-I_n$. The values of n range from 1 to 6 for the indicated positions of the phase conductors. Conductor n has the coordinates $C(x_n, y_n)$.

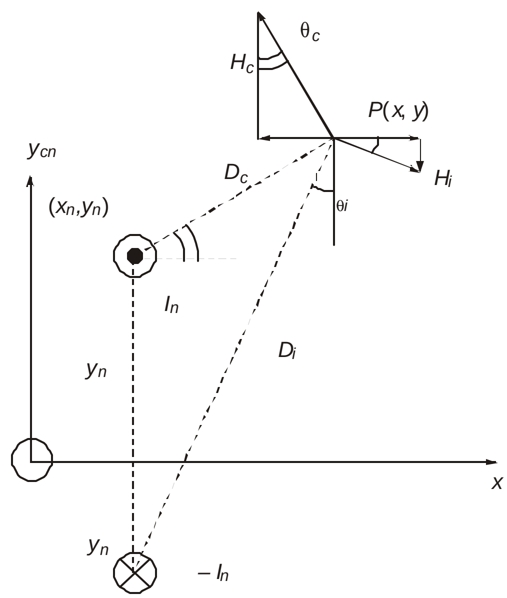

Fig. 7.18

Magnetic Fields: See Fig. 7.18.

Due to the conductor current, $$H_c = \frac{I_n}{2\pi}\frac{1}{D_c} \quad ...(7.71)$$

where $$D_c^2 = (x - x_n)^2 + (y - y_n)^2. \quad ...(7.72)$$

Its horizontal component is $$-H_c \sin\theta_c = -\frac{I_n}{2\pi}\frac{y - y_n}{D_c^2} \quad ...(7.73)$$

The vertical component is $$+H_c \cos\theta_c = \frac{I_n}{2\pi}\frac{x - x_n}{D_c^2} \quad ...(7.74)$$

Due to the image current, $$H_i = \frac{I_n}{2\pi}\frac{1}{D_i} \quad ...(7.75)$$

where $$D_i^2 = (x - x_n)^2 + (y + y_n)^2. \quad ...(7.76)$$

Its horizontal component is $$+H_i \cos\theta_i = \frac{I_n}{2\pi}\frac{y + y_n}{D_i^2} \quad ...(7.77)$$

The vertical component is $$-H_i \sin\theta_i = -\frac{I_n}{2\pi}\frac{x - x_n}{D_i^2} \quad ...(7.78)$$

The total horizontal component will be: $$H_h = \frac{I_n}{2\pi}\left[\frac{y + y_n}{D_i^2} - \frac{y - y_n}{D_c^2}\right] \quad ...(7.79)$$

and total vertical component is $$H_v = \frac{I_n}{2\pi}\left[\frac{x-x_n}{D_c^2} - \frac{x-x_n}{D_i^2}\right] \quad ...(7.80)$$

Combining the effect of all 6 conductors, we can write down:

$$H_{\text{ht}} = \frac{I_a}{2\pi}\left[\frac{y+y_1}{(y+y_1)^2+(x-x_1)^2} - \frac{y-y_1}{(x-x_1)^2+(y-y_1)^2}\right.$$

$$\left.+\frac{y+y_4}{(y+y_4)^2+(x-x_4)^2} - \frac{y-y_4}{(x-x_4)^2+(y-y_4)^2}\right]$$

$$+\frac{I_b}{2\pi}\left[\frac{y+y_2}{(x-x_2)^2+(y+y_2)^2} - \frac{y-y_2}{(x-x_2)^2+(y-y_2)^2}\right.$$

$$\left.+\frac{y+y_5}{(x-x_5)^2+(y+y_5)^2} - \frac{y-y_5}{(x-x_5)^2+(y-y_5)^2}\right]$$

$$+\frac{I_c}{2\pi}\left[\frac{y+y_3}{(x-x_3)^2+(y+y_3)^2} - \frac{y-y_3}{(x-x_3)^2+(y-y_3)^2}\right.$$

$$\left.+\frac{y+y_6}{(x-x_6)^2+(y+y_6)^2} - \frac{y-y_6}{(x-x_6)^2+(y-y_6)^2}\right] \quad ...(7.81)$$

$$= \frac{I_a}{2\pi}(K_1+K_4) + \frac{I_b}{2\pi}(K_2+K_5) + \frac{I_c}{2\pi}(K_3+K_6) \quad ...(7.82)$$

$$= \frac{I_a}{2\pi}K_a + \frac{I_b}{2\pi}K_b + \frac{I_c}{2\pi}K_c. \quad ...(7.83)$$

$$\therefore \quad |H_{ht}| = \frac{I}{2\pi}(K_a^2 + K_b^2 + K_c^2 - K_aK_b - K_bK_c - K_cK_a)^{1/2} \quad ...(7.84)$$

Similarly, the total vertical component of the H-field will be:

$$H_{vt} = \frac{I_a}{2\pi}\left[\frac{x-x_1}{(x-x_1)^2+(y-y_1)^2} - \frac{x-x_1}{(x-x_1)^2+(y+y_1)^2}\right.$$

$$\left.+\frac{x-x_4}{(x-x_4)^2+(y-y_4)^2} - \frac{x-x_4}{(x-x_4)^2+(y+y_4)^2}\right]$$

$$+\frac{I_b}{2\pi}\left[\frac{x-x_2}{(x-x_2)^2+(y-y_2)^2} - \frac{x-x_2}{(x-x_2)^2+(y+y_2)^2}\right.$$

$$\left.+\frac{x-x_5}{(x-x_5)^2+(y-y_5)^2} - \frac{x-x_5}{(x-x_5)^2+(y+y_5)^2}\right]$$

$$+\frac{I_c}{2\pi}\left[\frac{x-x_3}{(x-x_3)^2+(y-y_3)^2}-\frac{x-x_3}{(x-x_3)^2+(y+y_3)^2}\right.$$

$$\left.+\frac{x-x_6}{(x-x_6)^2+(y-y_6)^2}-\frac{x-x_6}{(x-x_6)^2+(y+y_6)^2}\right] \quad ...(7.85)$$

$$=\frac{I_a}{2\pi}(J_1+J_4)+\frac{I_b}{2\pi}(J_2+J_5)+\frac{I_c}{2\pi}(J_3+J_6) \quad ...(7.86)$$

$$=\frac{I_a}{2\pi}J_a+\frac{I_b}{2\pi}J_b+\frac{I_c}{2\pi}J_c \quad ...(7.87)$$

$$\therefore \quad |H_{vt}|=\frac{I}{2\pi}(J_a^2+J_b^2+J_c^2-J_aJ_b-J_bJ_c-J_cJ_a)^{1/2} \quad ...(7.88)$$

Ground-level Field: $Y = 0$. $D_c = D_i$.

For this case, equations (7.81) and (7.85) are as follows:

$$K_a=\frac{2y_1}{(x-x_1)^2+y_1^2}+\frac{2y_4}{(x-x_4)^2+y_4^2} \quad ...(7.89)$$

$$K_b=\frac{2y_2}{(x-x_2)^2+y_2^2}+\frac{2y_5}{(x-x_5)^2+y_5^2} \quad ...(7.90)$$

$$K_c=\frac{2y_3}{(x-x_3)^2+y_3^2}+\frac{2y_6}{(x-x_6)^2+y_6^2} \quad ...(7.91)$$

$$J_a=J_b=J_c=0. \quad \therefore \quad H_{vt}=0 \text{ as before.}$$

We notice that K_a, K_b, K_c as well as J_a, J_b, J_c in equations (7.82), (7.83), (7.86) and (7.87) have been written as the sum of two terms:

$$K_a=K_1+K_4, K_b=K_2+K_5, K_c=K_3+K_6; \quad ...(7.92)$$

$$J_a=J_1+J_4, J_b=J_2+J_5, J_c=J_3+J_6. \quad ...(7.93)$$

One advantage in writing like this is that later on when we evaluate the magnetic field of a 6-phase line, there will be 6 conductors. Their currents will be diplaced by 60° and it will prove easy to evaluate the resulting field. The values of x_1 to x_6 and y_1 to y_6 are given in equation (7.70).

Example 7.6. Figure 7.17 shows the details of a D/C 3-phase line. The line height to the middle phases is 15 metres while the 6 conductors are distributed uniformly on a circle of radius 6 m. The total 3-phase load is 240 MW at 230 kV, line-to-line, giving a current of 300 Amps in each conductor.

Calculate and plot the magnitude of flux density near the line along the ground surface only, as the distance from line centre is varied from $x = 0$ to $x = 5\,h = 75$ metres.

Solution. At ground level, $|H_{vt}| = |B_{vt}| = 0$. Only the horizontal component survives. The values of x_1 to x_6 and y_1 to y_6 are given in equations (7.70), where $h = 15$ m and $R = 6$ m.

Figure 7.19 Shows the results of computation of the ground-level flux density. It has a maximum (r.m.s.) value of B = 40 mG at x/h = 0.4 and decreases or attenuates rapidly to nearly zero at x/h = 4, or, x = 60 m from line centre.

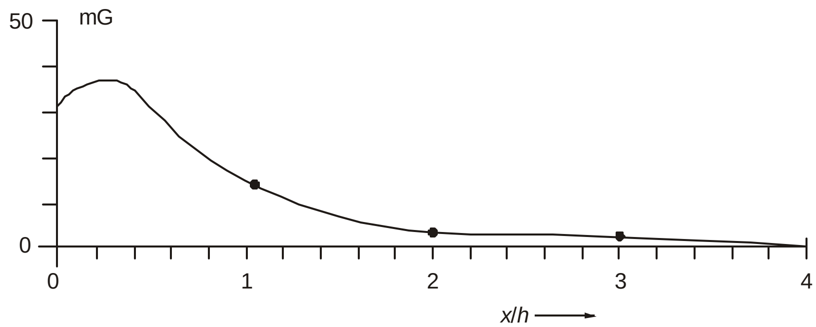

Fig. 7.19

7.10 MAGNETIC FIELD OF A 6-PHASE LINE

In Fig. 7.17, let it be assumed that the currents in conductors 1 to 6 are as follows:

$$\begin{aligned} I_1 &= I\angle 0°, I_2 = I\angle -60° = I(0.5 - j0.866), \\ I_3 &= I\angle -120° = I(-0.5 - j0.866), I_4 = I\angle -180° = -I_1 = -I, \\ I_5 &= I\angle -240° = I(-0.5 + j0.866) = -I_2, \\ I_6 &= I\angle -300° = I\angle 60° = I(0.5 + j0.866) = -I_3. \end{aligned} \quad ...(7.94)$$

Then, it is easy to observe that

$$H_{ht} = \frac{I_1}{2\pi}K_1 + \frac{I_2}{2\pi}K_2 + \frac{I_3}{2\pi}K_3 + \frac{I_4}{2\pi}K_4 + \frac{I_5}{2\pi}K_5 + \frac{I_6}{2\pi}K_6 \quad ...(7.95)$$

$$= \frac{I}{2\pi}[K_1 + K_2(0.5 - j0.866) + K_3(-0.5 - j0.866) - K_4$$
$$+ K_5(-0.5 + j0.866) + K_6(0.5 + j0.866)] \quad ...(7.96)$$

$$= \frac{I}{2\pi}[\{K_1 - K_4 + 0.5(K_2 - K_3 - K_5 + K_6)\} + j0.866(-K_2 - K_3 + K_5 + K_6)] \quad ...(7.97)$$

The magnitude of the horizontal component is

$$|H_{ht}| = \frac{I}{2\pi}\Big[\{K_1 - K_4 + 0.5(K_2 - K_3 - K_5 + K_6)\}^2$$
$$+ 0.75(K_2 + K_3 - K_5 - K_6)^2\Big]^{1/2}, \quad \text{Amp/metre.} \quad ...(7.98)$$

The values of K_1 to K_6 can be obtained from equation (7.81).

Similarly, the magnitude of the vertical component of magnetic field is:

$$|H_{vt}| = \frac{I}{2\pi}\Big[\{J_1 - J_4 + 0.5(J_2 - J_3 - J_5 + J_6)\}^2$$
$$+ 0.75(J_2 + J_3 - J_5 - J_6)^2\Big]^{1/2}, \quad \text{Amp/metre} \quad ...(7.99)$$

where the values of J_1 to J_6 are obtained from equation (7.85).

The corresponding flux densities are:

$$|B_{ht}| = \mu_0 |H_{ht}|, \text{and} |B_{vt}| = \mu_0 |H_{vt}|, \qquad \text{Tesla.} \qquad ...(7.100)$$

Example 7.7. Assume that a 138-kV 6-phase line with conductor-conductor voltage (and conductor-tower) voltage being equal to 138 kV. The conductors occupy the same positions as for the 3-phase D/C line considered in Example 7.6 earlier. The load is also nearly equal and the conductor-current is 300 Amperes.

Calculate and plot the horizontal component of $|B_{ht}|$ at ground level only.

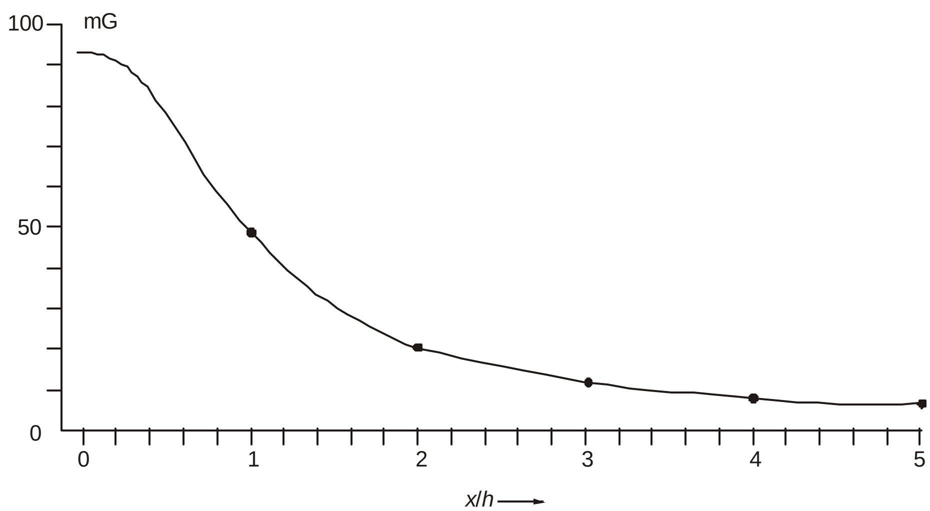

Fig. 7.20

Solution. Figure 7.20 shows the result of calculating $|B_{ht}|$ from equation (7.98) and (7.100) at ground level, $y = 0$.

We observe that the maximum value of $|B_{ht}|$ at ground level is 92 mG which is higher than for an equivalent 3-phase D/C line shown in Fig. 7.19.

7.11 EFFECT OF POWER-FREQUENCY MAGNETIC FIELDS ON HUMAN HEALTH

Magnetic fields are basically energy reservoirs with an energy density of e = $B^2/2\mu_0$, Joules/m^3, where B is in Tesla and $\mu_0 = 4\pi \times 10^{-7}$ Henry/metre. This energy is known to influence tissues in the human body in everyday activities. Some of the effects are known to be beneficial such as being used medically for healing broken bones, but most are harmful and pose health hazards among which have been counted cancer of many types. These cancers are: leukemia or blood cancer, lymphoma which weakens the immune system of the body to cancerous conditions, nervous disorders leading to brain damage such as altzheimer disease, breast cancer in both female and male species, and several other dangerous conditions too numerous to enumerate here. The magnetic radiation at low frequency emanating from Video Display Terminals such as are used by secretaries in banks, offices and so on is suspected to cause not only skin rash, eye problems, tissue cancer but more importantly are known to give rise to spontaneous abortions in pregnant women operators thereby forcing an end to pregnancy. The study of health hazards associated with power-frequency (50 and 60 Hz) magnetic fields has gained world-wide importance in medical, biological, physics and engineering fields and is the subject of intensive study, including the magnetic-field radiation from e.h.v. lines and distribution lines. We will only describe and discuss a few basic facts and mechanisms that give rise to health hazards associated with magnetic fields.

It is also believed but not proved with certainty that the power-frequency magnetic field induces a voltage in the tissue which in turn yields a current flow due to the electrical conductivity of the tissue (about 0.1 to 0.2 Siemen/metre). Some workers discount this theory because the cell walls are made from proteins which act as insulation barriers to the current flow. Moreover, the energy fed by this mechanism is considered too low, below even the thermal or Johnson noise of the ions in the cell at the body temperature (37°C or 310°K). Therefore, other mechanisms are sought for to explain the influence of magnetic fields on cancer-producing conditions.

Some international organizations such as the World Health Organization (WHO), International Radiation Protection Association (IRPA) as also other national organizations of different countries have given guidelines for limiting the magnetic field in homes or in occupations such as line workers. In homes where children and adults live and the electrical wiring carries power-frequency current, the resulting magnetic field experienced continuously has been suspected to cause cancerous conditions in the occupants. This observation was published in medical, biological and electrical literature for the first time in North America in 1979 by two scientists in Denver City, Colorado State, U.S.A. Their names are Nancy Wertheimer and Edward Leeper, the former a psychiatrist with the Denver Department of Public Health and the latter a physicist. Prior to that date in 1966, two Russian scientists had published their report on their findings that electricians working with electrical distribution lines — both males and females — experienced breast cancer. They suspected the magnetic field of the current-carrying lines to be the primary cause and advised the government to limit the exposure of workers to the magnetic field. The resulting Russian guidelines are as follows.

Exposure Hours	1	2	3	4	5	6	7	8
B-Field, Gauss	754	616	503	402	314	251	201	176

(The reader should convert the Gauss values given above to Ampere/metre).

Since then many international and national organizations have suggested the same limits. This is known as an "occupational hazard".

For the general public the exposure is about 1 to 2 hourse per day in public places where nearby distribution lines can give rise to exposure to magnetic fields. Also, in many countries, schools and shopping centres are located near high-voltage transmission lines and have been suspected as causing cancerous conditions in the school-children and shop-workers. There are many such instances of magnetic fields at power frequency being associated, along with other causes, with cancer-producing circumstances.

According to the WHO and IRPA Guidelines, any cancerous or other internal health defects inside the body can only be diagonozed by observing conditions on the surface of the body or by other diagnostic examinations. Based on experience gained all over the world, they have related the measured current density on the surface of the body or organ with the following health hazards:

Surface Current *Density,* mA/m^2	*Health Effects*
<1	Absence of any established effects.
1 –10	Minor biological effects reported.
10 –100	Well-established effects: (*a*) Visual defects (called Magneto-Phosphene effect); (*b*) Possible nervous-system defects.
100 – 1000	Changes in central nervous-system excitability (onset of brain damage) established; Stimulations thresholds; Possible health hazards.
> 1000	Extra systoles; Ventricular fibrillation (heart condition); Definite health hazards.

(*Note:* $(10 \text{mA/m}^2 = 1 \mu\text{A/cm}^2)$).

The surface current density measured on a cylindrical organ of radius r and electrical conductivity σ is related to the flux density at a frequency *f* as follows:

$$J_{\text{rms}} = \pi f \sigma r B_{\text{rms}}, \text{Amp/m}^2 \quad ...(7.101)$$

where J_{rms} = rms value of current density,

B_{rms} = rms value of flux density in Tesla,

f = frequency, Hz,

σ = electrical conductivity of the tissue, Siemens/metre,

and r = radius of the cylinder, metre.

This is derived as follows:

The flux density is $B(t) = \sqrt{2} B_{rms} \sin \omega t, \text{where } \omega = 2\pi f$. It induces a voltage in the cylinder of radius r equal to $v = \pi r^2 \text{dB}/dt = 2\sqrt{2}\pi^2 f r^2 B_{\text{rms}}$, volts. On the surface, the resulting voltage gradient is $e = v/2\pi r = \sqrt{2}\pi f r B_{\text{rms}}$. This gives an rms value of surface current density equal to $J_{\text{rms}} = \sigma e_{\text{rms}} = \pi f \sigma r B_{\text{rms}}, \text{Amp/m}^2$.

Example 7.8. For a current density of 1 mA/m^2 = 10^{-4} A/m^2, with f = 50 Hz and σ = 0.2 S/m, calculate the values of B_{rms} required to establish this current density on cylinders with r = 10 inches (Torso), 5 inches (heart and head), 2.5 inches (arm), 1.0 inch, 0.5 inch and 0.25 inch (fingers).

Solution. From equation $(7.101), B_{\text{rms}} = (J_{\text{rms}}/\pi f \sigma).\frac{1}{r}$, Tesla. (1 Tesla = 10,000 Gauss = 10^4 Gauss).

***r*, inches**	10	5	2.5	1.0	0.5	0.25
B_{rms}, Gauss	1.25	2.5	5	12.5	25	50

The WHO and IRPA Guidelines recommend that for electrical workers a current density of 5 mA/m^2 should not be exceeded on the surface of the torso with a radius of 10 inches = 25 cm. For the general public, the limit of current density on the torso is 1 mA/m^2. At 1mA/m^2, there is no onset of any visible health defect, while at 5 mA/m^2 there is just a chance of some defect but the workers are in general protected by a suitable uniform. Thus, the flux-density limits are about 5 Gauss for electrical workers and 1 Gauss for the general public.

There are considerations governing the limiting value of flux desnsity other than surface current density as proposed by the WHO and IRPA Guidelines. But these are highly specialized topics and will not be discussed here.

Review Questions and Problems

1. What is the effect of high electrostatic fields on human beings under a line? Why does a normal human being not experience a shock when walking underneath a line? Why do birds survive even though they come into contact with e.h.v. lines ?
2. Describe the difference between primary shock current and secondary shock current. What is the meaning of 'let-go' current?
3. A 400-kV horizontal line has 2 conductors of 3.18 cm diameter in a bundle with B = 0.4572 metre spacing. The line height and phase spacing are H = 15 m and S = 12 m. A D/C 230-kV line runs parallel to it with its centre 25 metres from the centre of the 400 kV line. The heights of the conductors are 18, 14, and 10 metres with equal horizontal spacings of 10 metres between conductors. Calculate the voltages induced in the 3 conductors closest to the 400-kV line if the voltage is 420 kV, line-to-line. Assume both lines to be fully transposed.
4. A 1150 kV Δ line has conductors at heights 26 m and 44 m with 24 m spacing between the lowest conductors. Each phase is equipped with 8 × 46 mm diameter conductor on a circle of 1.2 metre diameter. At 1200 kV, calculate the e.s. field at ground level at distances from the line centre d =0, 13, 26, 39, and 52 metres.
5. A double-circuit 400–kV line has conductors displaced 8 m from line centre. The heights of conductors are 13, 23, 33 m above ground. A neighbouring D/C 220-kV line has one circuit at 10 m horizontal separation from the nearest circuit of the 400-kV line. Its conductors are 10, 14, 18 m above ground. The conductors of the 400–kV line are 2 × 3.18 cm dia with 45.72 cm spacing. Calculate: (*a*) The voltage induced in the 3 conductors of one 400–kV circuit when the other circuit is energized at 420–kV. [28.4, 9.85, 7.23 kV]. (*b*) The voltage induced in the conductors of the nearest 220–kV circuit when only one of the (closest) 400–kV circuits is energized at 420–kV, [12,77, 13.72, 14.25 kV]. (*c*) Repeat (*b*) when both 400–kV circuits are energized at 420–kV. Assume phase voltages (*a*, *b*, *c*; *c*, *b*, *a*) for the two circuits for the top, middle, and bottom conductors. (The Maxwell's Potential coefficient Matrix for 400–kV line is now 6 ×6). [21.5, 15.2, 14.74 kV].

   (*d*) Compare cases (*a*), (*b*), and (*c*), and give your comments on the voltages experienced by a lineman.

6. Repeat worked example 7.5 for the 750-kV horizontal line when 50% series compensation is used and plot the lateral profile of the magnetic field on Fig. 7.16.
7. Repeat worked example 7.6 when the phase configuration is abc – abc. Compare the intensity of resulting magnetic field and superimpose on it the result of Example 7.6, Fig. 7.19. Which configuration results in more favourable circumstances as far as lower magnetic field near the line?
8. A 3–phase 230 kV D/C line has the dimensions shown, with all dimensions in metres. The phase configuration is abc – cba with currents as follows: $I_1 = I_6 = 300\angle 0°$ Amps; $I_2 = I_5 = 300\angle -120°$; $I_3 = I_4 = 300\angle +120°$. The origin of coordinate system is at ground level under the line centre as shown. Evaluate the following:

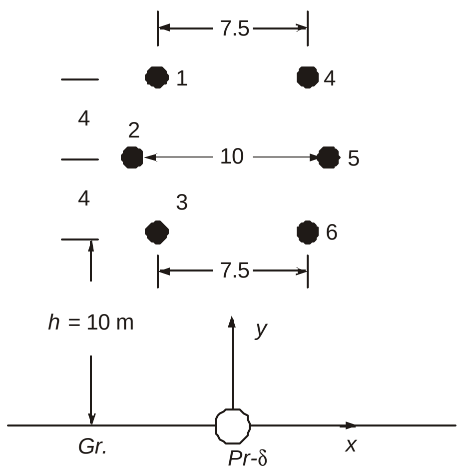

Fig. 7.21

(*a*) Write down the coordinates of the 6 conductors : (x_1, y_1) to (x_6, y_6).

(*b*) Calculate and plot the intensity of the *B*-field along ground for $x = 0$ to $x = 5\ h$, where $h = 10$ metres.

(*c*) Give the value of x at which the maximum *B*-field occurs.

9. A 6-phase transmission line has the same dimensions as the 3-phase 230 kV D/C line of problem 8. Its conductors carry the same current of 300 Amps. Assume the currents to be: $I_1 = 300\angle 0°$ Amps; $I_2 = 300\angle -60°$; $I_3 = 300\angle -120°$;

   $I_4 = 300\angle -180°$; $I_5 = 300\angle -240°$; and $I_6 = 300\angle -300°$.

   Calculate the intensity of the *B*-field along ground only for $x/h = 0$ to 5. Take the origin of the coordinate system on ground under the line centre. Plot the values on the same figure as in Problem 8 of the 230–kV D/C line.
10. Convert the *B*-values given in the table in Section 7.11 to *H*-values.

11. (*a*) Using a limiting energy value of S = 5 x 10^{-3} Joule/kg per year of continuous exposure to a magnetic field, calculate the r.m.s. value of the B-field at 50 Hz that should not be exceeded. Take tissue density of $\delta = 2\text{gm}/cc = 2000\,\text{kg}/m^3$.

(*b*) Derive the formula $B_{\text{rms}} = 0.2823/\sqrt{S.\delta/f,\mu}$ Tesla, where δ = tissue density in kg/m^3, and f = frequency.

[Hint : Let $B(t) = \sqrt{2}B_{\text{rms}} \sin \omega t$; Energy density $e = B^2/2\mu_o$, Joule/m^3; If tissue volume = V and weight = W, then the energy/kg = $(B^2/2\mu_o)(V/W)$; Average energy per cycle $= B_{\text{rms}}^2/(2\mu_o\delta)$. Then calculate energy in 1 year which should be equated to S Joule/kg.]

8

Theory of Travelling Waves and Standing Waves

8.1 TRAVELLING WAVES AND STANDING WAVES AT POWER FREQUENCY

On an electrical transmission line, the voltages, currents, power and energy flow from the source to a load located at a distance L, propagating as electro-magnetic waves with a finite velocity. Hence, it takes a short time for the load to receive the power. This gives rise to the concept of a wave travelling on the line which has distributed line parameters r, l, g, c per unit length. The current flow is governed mainly by the load impedance, the line-charging current at power frequency and the voltage. If the load impedance is not matched with the line impedance, which will be explained later on, some of the energy transmitted by the source is not absorbed by the load and is reflected back to the source which is a wasteful procedure. However, since the load can vary from no load (infinite impedance) to rated value, the load impedance is not equal to the line impedance always; therefore, there always exist transmitted waves from the source and reflected waves from the load end. At every point on the intervening line, these two waves are present and the resulting voltage or current is equal to the sum of the transmitted and reflected quantities. The polarity of voltage is the same for both but the directions of current are opposite so that the ratio of voltage to current will be positive for the transmitted wave and negative for the reflected wave. These can be explained mathematically and have great significance for determining the characteristics of load flow along a distributed-parameter line.

The same phenomenon can be visualized through standing waves. For example, consider an open-ended line on which the voltage must exist with maximum amplitude at the open end while it must equal the source voltage at the sending end which may have a different amplitude and phase. For 50 Hz, at light velocity of 300×10^3 km/sec, the wavelength is 6000 km, so that a line of length L corresponds to an angle of ($L \times 360°/6000$). With a load current present, an additional voltage caused by the voltage drop in the characteristic impedance is also present which will stand on the line. These concepts will be explained in detail by first considering a loss-less line ($r = g = 0$) and then for a general case of a line with losses present.

8.1.1 Differential Equations and Their Solutions

Consider a section of line Δx in length situated at a distance x from the load end. The line length is L and has distributed series inductance l and shunt capacitance c per unit length, which are calculated as discussed in Chapter 3. The inductance is ($l.\Delta x$) and capacitance ($c.\Delta x$) of the differential length Δx. The voltages on the two sides of l are $(V_x + \Delta V_x)$ and V_x, while the currents on the two sides of c are $(I_x + \Delta I_x)$ and I_x. From Figure 8.1 the following equations can be written down:

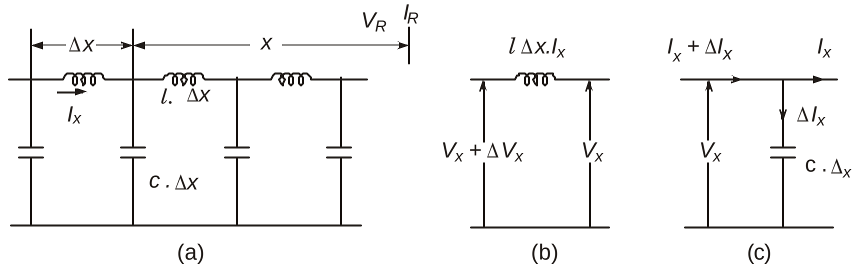

Fig. 8.1 Transmission line with distributed inductance and capacitance.

$$(V_x + \Delta V_x) - V_x = \Delta V_x = (jwl\,.\Delta x) I_x \quad ...(8.1)$$

and

$$(I_x + \Delta I_x) - I_x = \Delta I_x = (jwc\,.\Delta x) V_x \quad ...(8.2)$$

By making Δx infinitesimal, the changes in voltage and current along the line are expressed as differential equations thus:

$$dV_x/dx = z.\ I_x \text{ and } dI_x/dx = y.\ V_x \quad ...(8.3)$$

where $z = jwl$ and $y = jwc$, the series impedance and shunt capacitive admittance at power frequency. Since all quantities are varying sinusoidally in time at frequency $f = w/2\pi$, the time-dependence is not written, but is implicit.

By differentiating (8.3) with respect to x and substituting the expressions for dV_x/dx and dI_x/dx, we obtain independent differential equations for V_x and I_x as follows:

$$d^2V_x/dx^2 = z.\ y.\ V_x = p^2 V_x \quad ...(8.4)$$

and

$$d^2 I_x/dx^2 = z.y.I_x = p^2 I_x \quad ...(8.5)$$

where

$$p = \sqrt{z.y} = jw\sqrt{lc} = jw/v = j2\pi/\lambda \quad ...(8.6)$$

which is the propagation constant, v = velocity of propagation, and λ = wavelength. Equation (8.4) and (8.5) are wave equations with solutions

$$V_x = A e^{px} + B e^{-px} \quad ...(8.7)$$

and

$$I_x = (1/z)\,dV_x/dx = \left(\frac{p}{z}\right).(A e^{px} - B e^{-px})$$

$$= \sqrt{\frac{y}{z}}(A e^{px} - B e^{-px}) \quad ...(8.8)$$

The two constants A and B are not functions of x but could be possible functions of t since all voltages and currents are varying sinusoidally in time. Two boundary conditions are now necessary to determine A and B. We will assume that at $x = 0$, the voltage and current are V_R and I_R. Then, $A + B = V_R$ and $A - B = Z_0 I_R$, where $Z_0 = \sqrt{z/y} = \sqrt{l/c}$ = the characteristic impedance of the line.

Then, $$V_x = \frac{1}{2}(V_R + Z_0 I_R)e^{j2\pi x/\lambda} + \frac{1}{2}(V_R - Z_0 I_R)e^{-j2\pi x/\lambda} \quad ...(8.9)$$

and $$I_x = \frac{1}{2}(V_R/Z_0 + I_R)e^{j2\pi x/\lambda} - \frac{1}{2}(V_R/Z_0 - I_R)e^{-j2\pi x/\lambda} \quad ...(8.10)$$

We can also write them as

$$V_x = V_R.\cos(2\pi x/\lambda) + jZ_0 I_R \sin(2\pi x/\lambda) \quad ...(8.11)$$

and $$I_x = I_R.\cos(2\pi x/\lambda) + j(V_R/Z_0).\sin(2\pi x/\lambda) \quad ...(8.12)$$

Now, both V_R and I_R are phasors at power frequency and can be written as $V_R = V_R.e^{(jwt+\phi)}$, and $I_R = I_R.\exp[(jwt + \phi - \phi_L)]$ where ϕ_L = internal angle of the load impedance $Z_L\angle\phi_L$.

We can interpret the above equations (8.11) and (8.12) in terms of standing waves as follows:

(1) The voltage V_x at any point x on the line from the load end consists of two parts: $V_R \cos(2\pi x/\lambda)$ and $jZ_0 I_R \sin(2\pi x/\lambda)$. The term $V_R \cos(2\pi x/\lambda)$ has the value V_R at $x = 0$ (the load end), and stands on the line as a cosine wave of decreasing amplitude as x increases towards the sending or source end. At $x = L$, it has the value $V_R.\cos(2\pi L/\lambda)$. This is also equal to the no-load voltage when $I_R = 0$. Figure 8.2(a) shows these voltages. The second term in equation (8.11) is a voltage contributed by the load current which is zero at $x = 0$ and $Z_0 I_R \sin(2\pi L/\lambda)$ at the source end $x = L$, and adds vectorially at right angles to I_R as shown in Figure 8.2 (c).

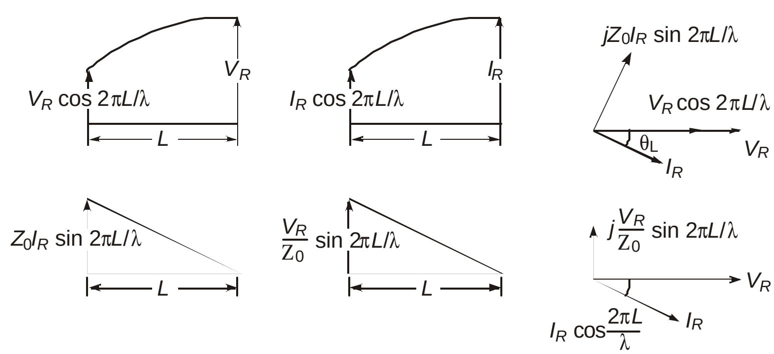

Fig. 8.2. Standing waves of (a) voltage, and (b) current at power frequency.

(2) The current in equation (8.12) also consists of two parts. $I_R \cos(2\pi x/\lambda)$ and $j(V_R/Z_0)\sin(2\pi x/\lambda)$. At no load, $I_R = 0$ and the current supplied by the source is $j(V_R/Z_0)\sin(2\pi L/\lambda)$ which is a pure charging current leading V_R by 90°. These are shown in Fig. 8.2(b) and the vector diagram of 8.2(c).

A second interpretation of equations (8.9) and (8.10) which are equivalent to (8.11) and (8.12) is through the travelling wave concept. The first term in (8.9) is $\frac{1}{2}(V_R + Z_0 I_R)e^{jw(t+x/v)}$ after introducing the time variation. At $x = 0$, the voltage is $(V_R + Z_0 I_R)/2$ which increases as x does, i.e., as we move towards the source. The phase of the wave is $e^{jw(t+x/v)}$. For a constant value of $(t + x/v)$, the velocity is $dx/dt = -v$. This is a wave that travels from the source to the load and therefore is called the forward travelling wave. The second term is $\frac{1}{2}(V_R - Z_0 I_R)e^{jw(t-x/v)}$ with the phase velocity $dx/dt = +v$, which is a forward wave from the load to the source or a backward wave from the source to the load.

The current also consists of forward and backward travelling components. However, for the backward waves, the ratio of voltage component and current component is $(-Z_0)$ is seen by the equations (8.9) and (8.10) in which the backward current has a negative sign before it.

8.2 DIFFERENTIAL EQUATIONS AND SOLUTIONS FOR GENERAL CASE

In Section 8.1, the behaviour of electrical quantities at power frequencies on a distributed-parameter line was described through travelling-wave and standing-wave concepts. The time variation of all voltages and currents was sinusoidal at a fixed frequency. In the remaining portions of this chapter, the properties and behaviour of transmission lines under any type of excitation will be discussed. These can be applied specifically for lightning impulses and switching surges. Also, different types of lines will be analyzed which are all categorized by the four fundamental distributed parameters, namely, series resistance, series inductance, shunt capacitance and shunt conductance. Depending upon the nature of the transmitting medium (line and ground) and the nature of the engineering results required, some of these four parameters can be used in different combinations with due regard to their importance for the problem at hand. For example, for an overhead line, omission of shunt conductance g is permissible when corona losses are neglected. We shall develop the general differential equations for voltage and current by first considering all four quantities (r, l, g, c) through the method of Laplace Transforms, studying the solution and interpreting them for different cases when one or the other parameter out of the four loses its significance. As with all differential equations and their solutions, boundary conditions in space and initial or final conditions in time play a vital role.

8.2.1 General Method of Laplace Transforms

According to the method of Laplace Transform, the general series impedance operator per unit length of line is $z(s) = r + ls$, and the shunt admittance operator per unit length is $y(s) = g + cs$, where s = the Laplace-Transform operator.

Consider a line of length L energized by a source whose time function is $e(t)$ and Laplace Transform $E(s)$, as shown in Fig. 8.3. Let the line be terminated in a general impedance $Z_t(s)$.

We will neglect any lumped series impedance of the source for the present but include it later on. Also, $x = 0$ at the terminal end as in Section 8.1.2. Let the Laplace Transforms of voltage and current at any point x be $V(x, s)$ and $I(x, s)$.

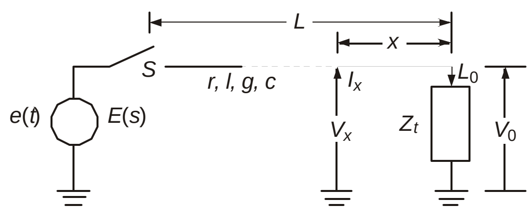

Fig. 8.3 Distributed-parameter transmission line with source $E(s)$ and terminating impedance $Z_t(s)$.

Then, the following two basic differential equations will hold as for the steady-state excitation discussed earlier:

$$\partial V(x,s)/\partial x = z(s).I(x,s) \text{ and } \partial I(x,s)/\partial x. = y(s).V(x,s) \quad ...(8.13)$$

For simplicity in writing, we may omit s in all terms but only remember that we are discussing the properties of the Laplace-Transforms of all quantities. The solutions for voltage and current in equation (8.13) will be

$$V(x) = A.e^{px} + B.e^{-px} \quad ...(8.14)$$

and $$I(x) = (p/z).(Ae^{px} - Be^{-px}) \quad ...(8.15)$$

where again, p = the propagation constant = $\sqrt{z.y}$ ...(8.16)

Also, $(p/z) = \sqrt{y/z} = Y_0$ and $(z/p) = \sqrt{z/y} = Z_0$, the characteristic or surge impedance.

For this problem, the boundary conditions are:

(1) At $x = L$, $V(L)$ = source voltage = $E(s)$; and

(2) At $x = 0$, $V(0) = Z_t.\ I(0)$. Using them in (8.14) and (8.15) yields

$$A = (Z_t + Z_0)E(s)/[(Z_t + Z_0)e^{pL} + (Z_t - Z_0)e^{-pL}] \quad ...(8.17)$$

and $$B = (Z_t - Z_0)A/(Z_t + Z_0) \quad ...(8.18)$$

$$\therefore \quad V(x) = \frac{\cosh px + (Z_0/Z_t)\sinh px}{\cosh pL + (Z_0/Z_t)\sinh pL}E(s) \quad ...(8.19)$$

and $$I(x) = \frac{1}{z}\frac{\partial V}{\partial x} = \sqrt{\frac{y}{z}}.\frac{\sinh px + (Z_0/Z_t)\cosh px}{\cosh pL + (Z_0/Z_t)\sinh pL}E(s) \quad ...(8.20)$$

These are the general equations for voltage V and current I at any point x on the line in operational forms which can be applied to particular cases as discussed below.

Line Terminations

For three important cases of termination of an open-circuit, a short circuit and $Z_t = Z_0$, the special expressions of equations (8.19) and (8.20) can be written.

Case 1. *Open Circuit.* $Z_t = \infty$

$$\left.\begin{aligned} V_{oc}(x,s) &= \cosh px.E(s)/\cosh pL \\ I_{oc}(x,s) &= \sqrt{y/z}.\sinh px.E(s)/\cosh pL \end{aligned}\right\} \quad ...(8.21)$$

Case 2. *Short-Circuit*. $Z_t = 0$

$$\left.\begin{aligned} V_{sc}(x,s) &= \sinh px.E(s)/\sinh pL \\ I_{sc}(x,s) &= \sqrt{y/z}\cosh px.E(s)/\sinh pL \end{aligned}\right\} \quad ...(8.22)$$

Case 3. *Matched Line*. $Z_t = Z_0$

$$\left.\begin{aligned} V_m(x,s) &= (\cosh px + \sinh px).E(s)/(\cosh pL + \sinh pL) \\ I_m(x,s) &= \sqrt{y/z}(\cosh px + \sinh px).E(s)/(\cosh pL + \sinh pL) \end{aligned}\right\} \quad ...(8.23)$$

The ratio of voltage to current at every point on the line is

$$Z_0 = \sqrt{z/y}\ .$$

$$[\sqrt{y/z} = Y_0 = \sqrt{(g+cs)/(r+ls)} = 1/Z_0.]$$

Source of Excitation

The time-domain solution of all these operational expressions are obtained through their Inverse Laplace Transforms. This is possible only if the nature of source of excitation and its Laplace Transform are known. Three types of excitation are important:

(1) *Step Function*. $e(t) = V$; $E(s) = V/s$, where V = magnitude of step

(2) *Double-Exponential Function*. Standard waveshapes of lightning impulse and switching impulse used for testing line and equipment have a shape which is the difference between two exponentials. Thus $e(t) = E_0\ (e^{-\alpha t} - e^{-\beta t})$ where E_0, α and β depend on the timings of important quantities of the wave and the peak or crest value. The Laplace Transform is

$$E(s) = E_0(\beta - \alpha)/(s+\alpha)(s+\beta) \quad ...(8.24)$$

(3) *Sinusoidal Excitation*. When a source at power frequency suddenly energises a transmission line through a circuit breaker, considering only a single-phase at present, at any point on the voltage wave, the time function is $e(t) = V_m \sin\ (wt + \phi)$, where $w = 2\pi f$, f = the power frequency, and ϕ = angle from a zero of the wave at which the circuit breaker closes on the positively-growing portion of the sine wave. Its Laplace Transform is

$$E(s) = V_m(w.\cos\phi + s.\sin\phi)/(s^2 + w^2) \quad ...(8.25)$$

Propagation Factor. For the general case, the propagation factor is

$$p = \sqrt{z.y} = \sqrt{(r+ls)(g+cs)} \quad ...(8.16)$$

In the sections to follow, we will consider particular cases for the value of p, by omitting one or the other of the four quantities, or considering all four of them.

Voltage at Open-End. Before taking up a detailed discussion of the theory and properties of the voltage and current, we might remark here that for the voltage at the open end, equation (8.21) gives

$$\begin{aligned} V(0, s) &= E(s)/\cosh pL = 2.E(s)/(e^{pL} + e^{-pL}) \\ &= 2E(s)(e^{-pL} - e^{-3pL} + e^{-5pL} - \ldots) \end{aligned} \quad ...(8.26)$$

Under a proper choice of p this turns out to be a train of travelling waves reflecting from the open end and the source, as will be discussed later. Equation (8.26) also gives standing waves consisting of an infinite number of terms of fundamental frequency and all its harmonics.

8.2.2 The Open-Circuited Line: Open-End Voltage

This is a simple case to start with to illustrate the procedure for obtaining travelling waves and standing waves. At the same time, it is a very important case from the standpoint of designing insulation required for the line and equipment since it gives the worst or highest magnitude of over-voltage under switching-surge conditions when a long line is energized by a sinusoidal source at its peak value. It also applies to energizing a line suddenly by lightning. The step response is first considered since by the Method of Convolution, it is sometimes convenient to obtain the response to other types of excitation by using the Digital Computer (see any book on Operational Calculus).

Travelling-Wave Concept: Step Response

Case 1. First omit all losses so that $r = g = 0$. Then,

$$p = s\sqrt{lc} = s/v \qquad ...(8.27)$$

where v = the velocity of e.m. wave propagation.

$$\therefore \quad V_0(s) = 2V/s(e^{sL/v} + e^{-sL/v}) = 2V(e^{-sL/v} - e^{-3sL/v} + \ldots)/s \qquad ...(8.28)$$

Now, by the time-shifting theorem, the inverse transform of

$$2V.e^{-ksL/v}/s = 2V.\ U(t - kL/v) \qquad ...(8.29)$$

where $U(t - kL.v) = 0$ for $t < kL/v$

$= 1$ for $t > kL/v$.

We observe that the time function of open-end voltage obtained from equations (8.28) and (8.29) will be

$$V_0(t) = 2V[U(t-L/v) - U(t-3L/v) + U(t-5L/v)\ldots] \qquad ...(8.30)$$

This represents an infinite train of travelling waves. Let $L/v = T$, the time of travel of the wave from the source to the open end. Then, the following sequence of voltages is obtained at the open end.

t	T	$2T$	$3T$	$4T$	$5T$	$6T$	$7T$	$8T$	$9T$...
V_0	$2V$	$2V$	0	0	$2V$	$2V$	0	0	$2V$...

A plot of the open-end voltage is shown in Fig. 8.4(*a*) from which it is observed that

(1) the voltage reaches a maximum value of twice the magnitude of the input step,

(2) it alternates between $2V$ and 0, and

(3) the periodic time is $4T$, giving a frequency of $f_0 = 1/4T$.

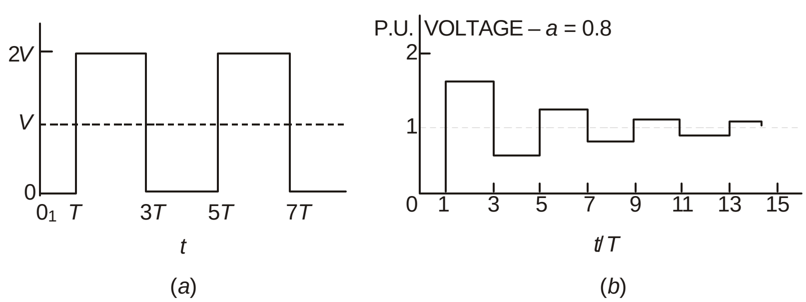

Fig. 8.4 Step response of transmission line. (*a*) Losses neglected. (*b*) Losses and attenuation included

Since all losses have been omitted, attenuation is absent and the amplitude between successive maxima does not decrease. The open-end voltage can never stabilize itself to a value equal to the excitation voltage.

Case 2. *Omit g*

For this case, $p = \sqrt{(r+ls)cs}$ or $p^2 = lcs^2 + rcs.$

Then, $p^2 = (\sqrt{lc})^2 (s + r/2l)^2 - r^2c/4l$ ...(8.31)

The last term ($r^2c/4l$) is usually negligible compared to the first. For example, consider $r = 1$ ohm/km, $l = 1.1$ mH/km and $c = 10$ nF/km. Then, $r^2c/4l = 2.25 \times 10^{-6}$. Therefore, we take $p = s/v + r/2lv = s/v + \alpha$, where $\alpha = r/2lv$ = attenuation constant in Nepers per unit length.

Now, equation (8.26) becomes, with $E(s) = V/s$ for step,

$$V_0(s) = 2V/(e^{pL} + e^{-pL})s = 2V(e^{-pL} - e^{-3pL} + e^{-5pL} - \ldots)/s$$

$$= (2V/s)(e^{-\alpha L}.e^{-sL/v} - e^{-3\alpha L}.e^{-3sL/v} + e^{-5\alpha L}.e^{-5sL/v} - \ldots) \qquad \text{...(8.32)}$$

The time response contains the attenuation factor exp $(-k\alpha L)$ and the time shift factor exp $(-ksL/v)$ = exp $(-kTs)$. The inverse transform of any general term is $2V$.exp $(-k\alpha L).U(t - kL/v)$. Let a = exp $(-\alpha L)$, the attenuation over one line length which the wave suffers. Then the open end voltage of (8.32) becomes, in the time domain,

$$V_0(t) = 2V[a.U(t-T) - a^3.U(t-3T) + a^5.U(t-5T)\ldots] \qquad \text{...(8.33)}$$

With the arrival of each successive wave at intervals of $2T = 2L/v$, the maximum value also decreases while the minimum value increases, as sketched in Fig. 8.4 (*b*) for $a = 0.96$ and 0.8. The voltage finally settles down to the value V, the step, in practice after a finite time. But theoretically, it takes infinite time, and because we have neglected the term ($r^2c/4l$), the final value is a little less than V as shown below. The values of attenuation factor chosen above (0.96 and 0.8) are typical for a line when only the conductor resistance is responsible for energy loss of the wave and when a value of 1 ohm/km for ground-return resistance is also taken into account. (For $a = 0.96$, see next page).

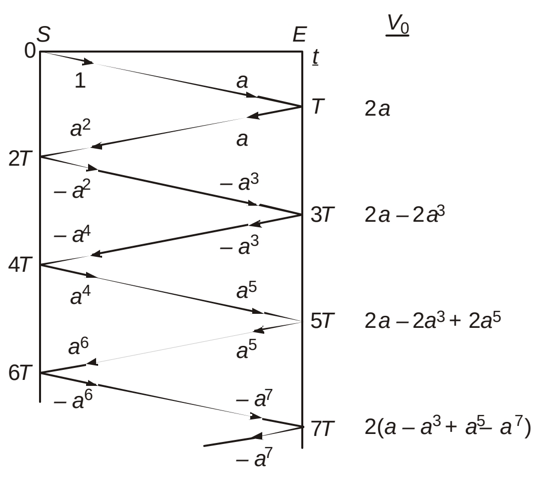

Fig. 8.5 The Bewley Lattice Diagram.

The following tabular form gives a convenient way of keeping track of the open-end voltage and Fig. 8.5 shows a graphical sketch which is due to Bewley. It is known as the Bewley Lattice Diagram. Note the systematic method employed in finding the voltage after any number of reflections.

Time t/T	$V_0(t)$	*a = 0.96*	*a = 08*
1	$V_1 = 2V.a$	1.92 V	1.6 V
2	$V_2 = 2V.a$		
3	$V_3 = 2V(a - a^3) = V_1 - a^2V_1$	0.15 V	0.576 V
4	$V_4 = V_3$		
5	$V_5 = 2V(a - a^3 + a^5) = V_1 - a^2V_3$	1.78 V	1.23 V
6	$V_6 = V_5$		
7	$V_7 = 2V(a - a^3 + a^5 - a^7) = V_1 - a^2V_5$	0.28 V	0.81 V
8	$V_8 = V_7$		
9	$V_9 = 2V(a - a^3 + a^5 - a^7 + a^9) = V_1 - a^2V_7$	1.66 V	1.08 V
10	$V_{10} = V_9$		
⋮			
N	$V_N = V_1 - a^2V_{N-2}$		
$N + 1$	$V_{N+1} = V_N$		

According to this procedure, the final value is

$$V_\infty = 2Va(1 - a^2 + a^4 - a^6 + \ldots) = 2Va/(1 + a^2) \quad \ldots(8.34)$$

Example 8.1. For a = 0.96 and 0.8, find the final value of open-end voltage and the % error caused by omitting the term ($r^2c/4l$) in equation (8.31)

Solution. (*a*) a = 0.96, V_∞ = 0.9992 V, error = 0.08%.

(*b*) a = 0.8, V_∞ = 0.9756 V, error = 2.44%.

8.2.3 The Bewley Lattice Diagram

Before we consider another form for p, let us discuss the Lattice Diagram for keeping account of the infinite number of reflections on a line when suddenly energized by a source. A horizontal line is drawn to represent the line and two vertical lines at the ends on which equal intervals of time T are marked as shown. The diagram begins at the top left corner at the source and proceeds along the line OT. The attenuation a is also shown for one travel. At the open end, the wave reflects completely as a. To the right is marked $2a$ which is the voltage at the open end after one travel time. Arrows show the progress of the wave. At T, the wave reflects and reaches the source at time $2T$ with an amplitude a^2, and since the source voltage has to remain constant at + 1, the wave arriving at the source is reflected negatively and shown as $-a^2$. When this reaches the open end at time $3T$, it has the value ($-a^3$). Again, at the end, this wave doubles and a reflection ($-a^3$) travels back to the source. The total voltage at the open end is now $(a + a - a^3 - a^3) = 2(a - a^3)$ which is the sum of all voltages marked on the inclined lines up to time $3T$. Proceeding in this manner, we observe that in order to keep the source voltage at + 1, continued reflections have to take place with negative signs at the source and positive signs at the open end.

8.2.4 $r/l = g/c = \beta$

If the above condition is satisfied, then

$$p = \sqrt{(r+ls)(g+cs)} = \sqrt{lc}\,[(s+r/l)(s+g/c)]^{1/2} = (s+\beta)/v$$

$$= s/v + r/lv. \qquad ...(8.35)$$

The step response is the same as before in Section 8.2.2 and Fig. 8.4(b), but the attenuation factor is now $b = \exp(-\beta L/v) = \exp(-2\alpha L/v) = a^2$. The voltage attenuates more rapidly than when $g = 0$.

Example 8.2. For $a = 0.96$ and 0.8, find the resulting attenuation factor when $r/l = g/c$, assuming line length L to be equal in both cases. Also calculate the maximum values of the surge in the two cases in p.u.

Solution. (1) $a = e^{-\alpha L} = 0.96 \quad \therefore \quad b = a^2 = 0.9216$

Maximum value of surge is the first peak = 1.8432 p.u.

(2) $a = e^{-\alpha L} = 0.8. \quad \therefore \quad b = a^2 = 0.64.$

$\therefore$ First peak = 1.28 p.u.

The relation $r/l = g/c$ is also known as the distortionless condition in which any waveshape of voltage applied at one end will travel without distortion of waveshape but will be attenuated. The relation is very useful in telephone and telegraph work where artificial loading coils are used to increase the value of inductance in cable transmission for which g and c are high while l is low.

The case of including all four parameters (r, l, g, c) in the propagation constant p leads to complicated expressions for the Inverse Laplace Transform involving Bessel Functions but, as will be shown in the next section, will yield easier solutions when the standing wave concept is resorted to.

8.3 STANDING WAVES AND NATURAL FREQUENCIES

In this method, the inverse Laplace Transform is evaluated by the Method of Residues and instead of an infinite number of reflections caused by both ends, we obtain the solution as the sum of an infinite number of frequencies which consist of a fundamental frequency and its harmonics. The infinite series of terms can be truncated after any suitable number of harmonics to yield engineering results. We will first show that the method yields the same result as the travelling-wave concept for a simple case, and then proceed with the Standing-wave Method for more complicated cases for $p = \sqrt{(r+ls)(g+cs)}$.

8.3.1 Case 1–Losses Neglected $r = g = 0$

The Laplace Transform of the open-end voltage, equation (8.26), can be written as (with $r = g = 0$), for a step input,

$$V_0 = V/s.\ \cosh pL = V/s.\ \cosh (s\sqrt{lc}L) \qquad ...(8.36)$$

The locations of the poles of the expression where the denominator becomes zero are first determined. Then the residues at these poles are evaluated as described below, and the time response of the open-end voltage is the sum of residues at all the poles.

Location of Poles. The denominator is zero whenever $s = 0$ and $\cosh s\sqrt{lc}L = 0$. Now, $\cosh j\theta = \cos\theta$ which is zero whenever $\theta = \pm(2n + 1)\pi/2, n = 0, 1, 2, \ldots$ Thus, there are an infinite number of poles where $\cosh(s\sqrt{lc}L)$ becomes zero. They are located at

$$\sqrt{lc}Ls = \pm j(2n+1)\pi/2.$$

$$\therefore \quad s = \pm j(2n+1)\pi/2\sqrt{lc}L = \pm jw_n \text{ and } pL = \pm j(2n+1)\pi/2 \quad \ldots(8.37)$$

where
$$w_n = (2n+1)\pi/2\sqrt{lc}L = (2n+1)\pi v/2L = (2n+1)\pi/2T \quad \ldots(8.38)$$

upon using the property that $v = 1/\sqrt{lc}$ and $T = L/v$. We also observe that (lL) and (cL) are the total inductance and capacitance of the line of length L, and $\pi/2T = 2\pi/4T = 2\pi f_0$, with f_0 = fundamental frequency. This was the same as was obtained in the travelling-wave concept.

Residues

In order to calculate the residue at a simple pole, we remove the pole from the denominator, multiply by e^{st} and evaluate the value of the resulting expression at the value of s given at the pole.

(1) At $s = 0$:

$$\text{Residue} = \left.\frac{V.e^{st}}{\cosh(\sqrt{lc}Ls)}\right|_{s=0} = V, \text{ the input step.}$$

(2) At the infinite number of poles, the procedure is to take the derivative of $(\cosh pL)$ with respect to s and evaluate the value of the resulting expression at each value of s at which $\cosh pL = 0$. Thus, the residues at the poles of $(\cosh pL)$ are found by the operation

$$V_{(n+)} = \left.\frac{V}{s}\frac{e^{st}}{\frac{d}{ds}(\cosh pL)}\right|_{\substack{s = jw_n \\ pL = j(2n+1)\pi/2}} \quad \ldots(8.39)$$

Now, $\frac{d}{ds}\cosh \sqrt{lc}Ls = \sqrt{lc}L.\sinh(\sqrt{lc}.Ls) = \sqrt{lc}.L\sinh pL$. But at $pL = j(2n+1)\pi/2$, $\sinh pL = j\sin(2n+1)\pi/2 = j(-1)^n$.

$$\therefore \quad V(n+) = \frac{V}{jw_n}.\frac{\exp(jw_n t)}{j(-1)^n.\sqrt{lc}.L} = -(-1)^n.V.2\exp(jw_n t)/(2n+1)\pi \quad \ldots(8.40)$$

upon using equation (8.38).

Similarly, at $s = -jw_n$, the residue will be the complex conjugate of equation (8.40). Now using $e^{j\theta} + e^{-j\theta} = 2\cos\theta$, the sum of all residues and therefore the time response is

$$V_0(t) = V\left[1 - \sum_{n=0}^{\infty}(-1)^n.\frac{4}{(2n+1)\pi}.\cos\frac{(2n+1)\pi}{2L\sqrt{lc}}.t\right] \quad \ldots(8.41)$$

The first or fundamental frequency for $n = 0$ is $f_0 = 1/4L\sqrt{lc} = 1/4T$ and its amplitude is $(4/\pi)$. Let $\theta = \pi t/2L\sqrt{lc}$. Then equation (8.41) can be written as

$$V_0(t) = V\left[1 - \frac{4}{\pi}\left(\cos\theta - \frac{1}{3}\cos 3\theta + \frac{1}{5}\cos 5\theta - \ldots\right)\right] \quad \ldots(8.42)$$

Now, the Fourier series of a rectangular wave of amplitude V is

$$\frac{4V}{\pi}\left(\cos\theta - \frac{1}{3}\cos 3\theta + \frac{1}{5}\cos 5\theta - \ldots\right).$$

Therefore, the open-end voltage response for a step input when line losses are neglected is the sum of the step input and a rectangular wave of amplitude V and fundamental frequency $f_0 = 1/4T$. This is the same as equation (8.30) and Fig. 8.4(*a*). Therefore, the travelling-wave concept and standing-wave method yield the same result.

8.3.2 General Case (*r*, *l*, *g*, *c*)

Instead of deriving the open-end voltage response for every combination of (r, l, g, c), we will develop equations when all four parameters are considered in the propagation constant, and then apply the resulting equation for particular cases. Now,

$$p = \sqrt{(r + ls)(g + cs)}$$

The poles of (cosh pL) are located as before when $pL = \pm j(2n + 1)\pi/2$, $n = 0, 1, 2, \ldots, \infty$. The values of s at these poles will be obtained by solving the quadratic equation

$$(r + ls)(g + cs)L^2 = -(2n + 1)^2\pi^2/4 \quad \ldots(8.43)$$

This gives

$$s = -\frac{1}{2}\left(\frac{r}{l} + \frac{g}{c}\right) \pm j\sqrt{\frac{rg}{lc} + (2n+1)^2\frac{\pi^2}{4L^2lc} - \frac{1}{4}\left(\frac{r}{l} + \frac{g}{c}\right)^2} \quad \ldots(8.44)$$

or

$$s = -a \pm jw_n$$

where

$$a = \frac{1}{2}(r/l + g/c) \quad \ldots(8.45)$$

and

$$w_n^2 = rg/lc - \frac{1}{4}(r/l + g/c)^2 + (2n+1)^2\pi^2/4L^2lc \quad \ldots(8.46)$$

Now

$$\frac{d}{ds}\cosh pL = L.\ \sinh(pL).\ (dp/ds)$$

where sinh $pL = j(-1)^n$ at the pole, and

$$\frac{dp}{ds} = \frac{1}{2}\left.\frac{2lcs + (rc + gl)}{\sqrt{(r + ls)(g + cs)}}\right|_{s=-a+jw_n} = \frac{1}{2}\frac{2lc(-a + jw_n) + (rc + gl).}{j(2n+1)\pi/2L} \quad \ldots(8.47)$$

$$\therefore \left.\frac{d}{ds}\cosh pL\right|_{s=-a+jw_n} = j(-1)^n.\ 2L^2lc\ w_n/(2n + 1)\pi \quad \ldots(8.48)$$

Thus, the residues at the poles $s = 0$, $s = -a + jw_n$, $s = -a - jw_n$ are found to be

(1) At $s = 0. V_0 = \left.\dfrac{Ve^{st}}{\cosh L\sqrt{(r+ls)(g+cs)}}\right|_{s=0} = V/\cosh L\sqrt{rg}$ ...(8.49)

(2) At $s = -a + jw_n$.

$$V(n+) = \left.\frac{V.e^{st}}{s(d.\cosh pL/ds)}\right|_{s=-a+jw_n} = \frac{-(-1)^n.e^{-at}(2n+1)\pi}{2L^2lcw_n}\frac{e^{jw_nt}}{w_n+ja}V \quad ...(8.50)$$

(3) At $s = -a - jw_n$.

$$V(n-) = \frac{-(-1)^n e^{-at}(2n+1)\pi}{2L^2lc\,w_n}.\frac{e^{-jw_nt}}{w_n-ja}.V \quad ...(8.51)$$

The sum of all residues and therefore the open-end voltage for step input will be, with $\tan\phi = a/w_n$,

$$V_0(t) = V\left[\frac{1}{\cosh L\sqrt{rg}} - \sum_{n=0}^{\infty}\frac{(-1)^n(2n+1)\pi.e^{-at}}{L^2.lc.w_n.\sqrt{a^2+w_n^2}}.\cos(w_nt-\phi)\right] \quad ...(8.52)$$

Particular cases

(1) When $r = g = 0$, the lossless condition, $a = 0$, $\phi = 0$, $\cosh L\sqrt{rg} = 1$, and $L^2/cw_n^2 = (2n+1)^2\pi^2/4$. The resulting open-end voltage reduces to equation (8.41).

(2) When $g = 0$, $a = r/2l$, $w_n = [(2n+1)^2\pi^2/4L^2lc - (r/2l)^2]^{1/2}$.

$\cosh L\sqrt{rg} = 1.$ $\quad\therefore\quad$ $\sqrt{a^2+w_n^2} = (2n+1)\pi/2L\sqrt{lc}$

(3) When $r/l = g/c$, the distortionless condition, $r/l = g/c = b$.

$a = \frac{1}{2}(r/l+g/c) = r/l, rg/lc - \frac{1}{4}(r/l+g/c)^2 = 0, w_n = (2n+1)\pi/2L\sqrt{lc}$.

The natural frequency becomes equal to that when losses are omitted, equations (8.38). All harmonics have same attenuation.

At the velocity of light, for different lengths of line L, the following values of fundamental frequencies and travel time are found from the expressions $T = L/300$ ms, with L in km and $f_0 = 1/4T$.

L, km	100	200	300	400	500	750	1000
T, ms	0.333	0.667	1.0	1.333	1.667	2.5	3.333
f_0, *Hz*	750	375	250	187.5	150	100	75

These frequencies are important for calculating ground-return resistance and inductance according to Carson's Formulae.

8.4 OPEN-ENDED LINE: DOUBLE-EXPONENTIAL RESPONSE

The response of an open-ended line when energized by a step input was described in Section 8.3 where the Laplace Transform of the step was $E(s) = V/s$. In considering lightning and switching surges, the excitation function is double exponential with the equation, as shown in Fig. 8.6(*a*),

$$e(t) = E_0(e^{-\alpha t} - e^{-\beta t}) \qquad ...(8.53)$$

Its Laplace Transform is

$$E(s) = E_0[1/(s+\alpha) - 1/(s+\beta)] = E_0(\beta-\alpha)/(s+\alpha)(s+\beta) \qquad ...(8.54)$$

Now, the operational expression of the open-end voltage is

$$V_0(s) = E(s)/\cosh pL = E_0(\beta-\alpha)/(s+\alpha)(s+\beta)\cosh pL \qquad ...(8.55)$$

where $p = \sqrt{(r+ls)(g+cs)}$, as before,

The poles of (8.55) are located at $s = -\alpha, -\beta,$ and $-a \pm jw_n$, where by equations (8.45) and (8.46),

$$a = \frac{1}{2}(r/l + g/c) \text{ and } w_n = \sqrt{(2n+1)^2\pi^2/4L^2lc + rg/lc - a^2}.$$

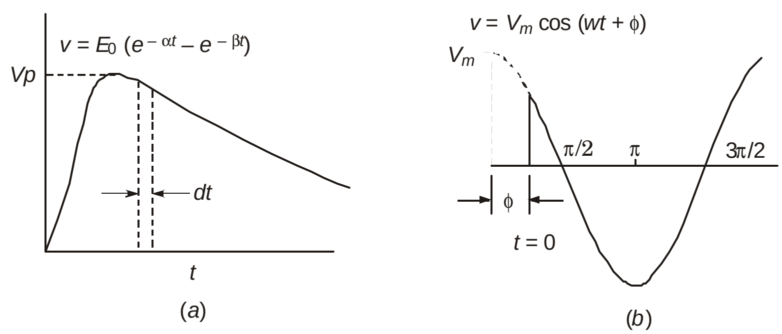

Fig. 8.6 (*a*) Double-exponential wave: $e(t) = E_0(e^{-\alpha t} - e^{-\beta t})$
(*b*) Sine wave of excitation switched at any point on the wave.

Residues

(1) At $s = -\alpha . V(-\alpha) = \dfrac{E_0(\beta-\alpha)e^{-\alpha t}}{(\beta-\alpha).\cosh L\sqrt{(r-l\alpha)(g-c\alpha)}}$ ...(8.56)

(2) At $s = -\beta . V(-\beta) = \dfrac{E_0(\beta-\alpha)e^{-\beta t}}{(\alpha-\beta)\cosh L\sqrt{(r-l\beta)(g-c\beta)}}$ ...(8.57)

(3) At $s = -a + jw_n$.

$$\frac{d}{ds}\cosh pL \,\Big|_{s=-a+jw_n} = j(-1)^n.2L^2lcw_n/(2n+1)\pi \qquad ...(8.58)$$

$$\therefore \quad V(n+) = \frac{E_0(\beta-\alpha).e^{(-a+jw_n)t}.(2n+1)\pi}{(\alpha-a+jw_n)(\beta-a+jw_n)j2L^2.lcw_n} \qquad ...(8.59)$$

(4) At $s = -a - jw_n$. $V(n-)$ = complex conjugate of $V(n+)$.

The sum of all residues will become

$$V_0(t) = \frac{E_0 e^{-\alpha t}}{\cosh L\sqrt{(r-l\alpha)(g-c\alpha)}} - \frac{E_0 e^{-\beta t}}{\cosh L\sqrt{(r-l\beta)(g-c\beta)}}$$

$$- E_0 \sum_{n=0}^{\infty} \frac{(-1)^n (\beta-\alpha)(2n+1)\pi e^{-at}}{L^2 lc\, w_n} \frac{1}{\sqrt{A_n^2 + B_n^2}} \cos(w_n t + \phi_n) \quad ...(8.60)$$

where $A_n = (\alpha - a)(\beta - a) - w_n^2,\ B_n = (\alpha + \beta - 2a) w_n$ ...(8.61)

and $\tan \phi_n = A_n / B_n$.

Equation (8.60) can be written out explicitly for various combinations of *r, l, g, c* such as discussed before. These are:

(1) Lossless line : $r = g = 0$.

(2) Neglect g. $g = 0$.

(3) Distortionless line. $r/l = g/c$.

(4) All four parameters considered. Equation (8.60).

8.5 OPEN-ENDED LINE: RESPONSE TO SINUSOIDAL EXCITATION

When a sine-wave of excitation source is suddenly switched on to an open-ended line, at an angle ϕ after a positive peak, its time function is $e(t) = V_m \cos(wt + \phi)$, where $w = 2\pi f$ and f = power frequency. Its Laplace-Transform is

$$E(s) = V_m (s.\cos\phi - w.\sin\phi)/(s^2 + w^2) \quad ...(8.62)$$

The resulting open-end voltage becomes

$$V_0(s) = V_m (s.\cos\phi - w.\sin\phi)/(s^2 + w^2).\cosh pL \quad ...(8.63)$$

The poles are now located at $s = \pm jw, -a \pm jw_n$, with a and w_n obtained from equations (8.45) and (8.46). The residue at each pole is evaluated as before and the resulting open-end voltage is as follows:

Let $J = (rg - w^2 lc)L^2, K = w(rc + lg)L^2$

$$a = \frac{1}{2}(r/l + g/c), w_n = [(2n+1)^2 \pi^2 / L^2 lc + rg/lc - a^2]^{1/2}$$

$$p_1 = 0.5(\sqrt{J^2 + K^2} + J)^{0.5}, q_1 = 0.5(\sqrt{J^2 + K^2} - J)^{0.5}$$

$$F = \cosh p_1 . \cos q_1, G = \sinh p_1 . \sin q_1, \tan\theta = G/F,$$

$$p_2 = a^2 + w^2 - w_n^2.$$

Then, $$V_0(t) = \frac{V_m.\cos(wt+\phi-\psi)}{[F^2+G^2]^{1/2}} + V_m \sum_{n=0}^{\infty} \frac{(-1)^n (2n+1)\pi e^{-at}}{L^2 lcw_n (p_2^2 + 4a^2 w_n^2)}$$
$$\times[\cos\phi\{w_n(p_2 - 2a^2)\cos w_n t - a(p_2 + 2w_n^2)\sin w_n t\}$$
$$+ w\sin\phi.(p_2.\cos w_n t - 2aw_n.\sin w_n t)] \quad ...(8.64)$$

It consists of a steady-state response term, and the transient response with an infinite number of frequency components which decay with the time constant $\tau = 1/a$.

8.6 LINE ENERGIZATION WITH TRAPPED-CHARGE VOLTAGE

Hitherto, we have been considering a line with no initial voltage trapped in it at the time of performing the switching or excitation operation with a voltage source such as the step, double-exponential or sinusoidal. When some equipment is connected between line and ground, such as a shunt-compensating reactor or a power transformer or an inductive potential transformer or during rain, the trapped charge is drained to ground in about half-cycle (10 ms on 50 Hz base). Therefore, when a switching operation is performed, the line is "dead". But there are many situations where the line is re-energized after a de-energization operation with a voltage trapped in it. This voltage in a 3-phase line has a value equal to the peak value of voltage with sinusoidal excitation or very near the peak. The resulting open-end voltage is higher than when trapped charge is neglected. The response or behaviour of the open-end voltage when there is an initial voltage V_t will now be discussed.

The basic differential equations for the line, Fig. 8.7, are

$$\partial V_x/\partial x = (r + l.\partial/\partial t)I_x, \quad \text{and} \quad \partial I_x/\partial x = (g + c.\partial/\partial t)V_x \quad ...(8.65)$$

As before, let $z = r + ls$ and $y = g + cs$. Then taking the Laplace

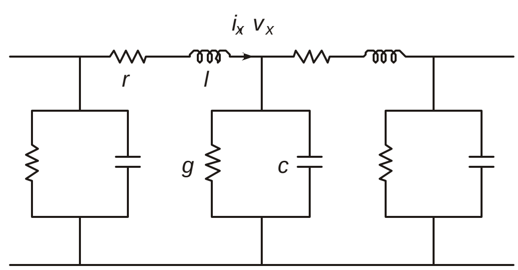

Fig. 8.7 Distributed-parameter line with all four parameters (r, l, g, c).

Transforms with the conditions that at t = 0, i = 0 and $v = V_t$, the trapped voltage, there results for the Laplace-Transform of voltage at any point x,

$$\partial^2 V_x(s)/\partial x^2 - p^2 V_x(s) + zcV_t = 0 \quad ...(8.66)$$

The complimentary function is obtained with V_t = 0 which is $V_{xc} = Ae^{px} + Be^{-px}$. The particular integral will be (cV_t/y), and the complete solution is

$$V_x(s) = Ae^{px} + Be^{-px} + cV_t/y \quad ...(8.67)$$

This can be verified by substituting in equation (8.66).

The boundary conditions are (1) at $x = L$, $V_L = E(s)$ and (2) at $x = 0$, $V_0 = Z_t I_0$. Then, A and B have the values, with $Z_0 = \sqrt{z/y} = z/p$, the characteristic impedance,

$$A = (Z_t + Z_0)E(s)/D + (V_t c/y)(Z_0 \exp(-pL) - Z_t - Z_0)/D \quad ...(8.68)$$

and $$B = (Z_t - Z_0)E(s)/D - (V_t c/y)(Z_0 \exp(-pL) + Z_t - Z_0)/D \quad ...(8.69)$$

with $$D = (Z_t + Z_0)\exp(pL) + (Z_t - Z_0)\exp(-pL) \quad ...(8.70)$$

When $V_t = 0$, these equations reduce to equations (8.17) and (8.18). The current, even with trapped charge, is

$$I_x = (1/z).\partial V_x / \partial x = Y_0.(A \exp(px) - B \exp(-px)) \quad ...(8.71)$$

which is the same as equation (8.15).

Combining equations (8.68), (8.69) and (8.67), since A and B also contain the trapped-voltage term,

$$V_x = E(s).\frac{\cosh px + (Z_0/Z_t)\sinh px}{\cosh pL + (Z_0/Z_t)\sinh pL} - \frac{V_t c}{y}$$

$$\frac{\cosh px + (1 - \exp(-pL))(Z_0/Z_t)\sinh px}{\cosh pL + (Z_0/Z_t)\sinh pL} \quad ...(8.72)$$

For an open-ended line, $Z_0/Z_t = 0$, and the voltage at any point x on the line from the open end is

$$V_{x0} = E(s).\cosh px/\cosh pL - (V_t\, c/y) \cosh px/\cosh pL \quad ...(8.73)$$

In particular, at the open end,

$$V_0 = E(s)/\cosh pL - V_t/(s + g/c)\cosh pL \quad ...(8.74)$$

When $V_t = 0$ this reduces to equation (8.26) which we have been dealing with in previous sections. The inverse transforms of the first term $E(s)/\cosh pL$ in equation (8.74) have already been obtained for step, double-exponential and sinusoidal excitations, which are equations (8.52), (8.60) and (8.64). To these will be added the response due to the trapped charge, the second term in (8.74).

The poles are now at $s = -g/c$, and $s = -a \pm jw_n$, with a and w_n given by equations (8.45) and (8.46).

(1) At the simple pole $s = -g/c$, the residue is

$$V_1 = V_t.e^{st}/\cosh L\sqrt{(r + ls)(g + cs)}\,|_{s=-g/c} = V_t.\exp[-(g/c)t] \quad ...(8.75)$$

(2) The residue at $s = -a + jw_n$ is

$$V(n+) = \frac{-(-1)^n V_t \exp(-at).(2n+1)\pi}{2L^2 lc\, w_n} . \frac{\exp(jw_n t)}{w_n + j(a - g/c)} \quad ...(8.76)$$

(3) At the pole $s = -a - jw_n$, the residue is equal to the complex conjugate of $V(n+)$, thus $V(n-) = [V(n+)]^*$.

The sum of all residues and the resulting contribution to the open-end voltage due to the trapped voltage finally becomes

$$V_t.\exp[-(g/c)t] - V_t \sum_{n=0}^{\infty} (-1)^n . \frac{\exp(-at).(2n+1)\pi}{L^2.lc.w_n\{w_n^2 + (a-g/c)^2\}^{1/2}} \cos(w_n t - \psi) \qquad ...(8.77)$$

where $\tan \Psi = (a - g/c)/w_n$ ...(8.78)

Both terms decay with their own time constants. Note that when $g = 0$, the trapped-charge voltage is always present in the open-end voltage in spite of a line resistance r being present.

8.7 CORONA LOSS AND EFFECTIVE SHUNT CONDUCTANCE

When surges propagate on transmission lines they suffer attenuation or decrease in amplitude due to energy lost in the conductor resistance, ground resistance, and corona. This is particularly beneficial in the case of lightning and switching surges. In the previous discussions, a shunt conductance g has been included which represents the corona loss element. We will now derive an approximate expression for this quantity assuming the voltage to be of the double-exponential form. It was shown in Chapter 5 that for unidirectional surges the corona loss in Joules per unit length is given by the expression

$$W_e = \frac{1}{2} KC(V_m^2 - V_0^2) \qquad ...(8.79)$$

where C = capacitance of conductor per unit length, K = the increase in capacitance when corona is present, V_m = peak value of voltage attained and V_0 = corona-inception voltage, peak value.

This was obtained from the q-V relation approximated to a trapezoidal form, Fig. 5.3.

Let the waveshape of the double-exponential be

$$e(t) = E_0(e^{-\alpha t} - e^{-\beta t}) \qquad ...(8.80)$$

where E_0, α and β depend on the timings of front and 50% value on tail, and the crest voltage. Typical values of α, β, E_0 are given below:

	α	β	E_0/V_m
Lightning Impulse 1.2/50 μs	14.5×10^3	2.45×10^6	1.035
Switching Surge 250/2500 μs	320	12×10^3	1.13

Denoting by g_e "effective conductance" per unit length the differential energy loss is $(g_e e^2.dt)$ per unit length, and the total energy loss in the full wave is *

$$W_e = \int_0^{\infty} g_e.e^2.dt = g_e.E_0^2 \int_0^{\infty} (e^{-\alpha t} - e^{-\beta t})^2 dt = \frac{\beta - \alpha}{2\alpha\beta} g_e.E_0^2 \qquad ...(8.81)$$

* In practice the limits of integration are not 0 and ∞ but the times when the voltage equals corona-inception and extinction values. These depend on the peak of surge. This can be worked out on a case-by-case basis.

Equating this to $\frac{1}{2}KC(V_m^2 - V_0^2)$, the effective conductance per unit length is

$$g_e = \{\alpha\beta/(\beta - \alpha)\}KC.(V_m^2 - V_0^2)/E_0^2 \quad ...(8.82)$$

In practice, the crest value of voltage V_m for both lightning and switching surges is 2.5 to 3 times the crest value of corona-inception voltage V_0, and E_0 is approximately equal to V_m. Therefore the factor $(V_m^2 - V_0^2)/E_0^2$ is nearly unity. An approximation for g_e will then be

$$g_e \approx \alpha\beta KC/(\beta - \alpha) \text{ and } g_e/C = \alpha\beta K/(\beta - \alpha) \quad ...(8.83)$$

The value of K is about 0.7.

Example 8.3. A 400 kV line has C = 10 nF/km. For lightning and switching surge type of voltage, calculate the effective conductance per unit length assuming $(V_m^2 - V_0^2)/E_0^2 = 1$.

Solution.

(*a*) *For lightning* : $g_e = \alpha\beta KC/(\beta - \alpha)$

$= 14.5 \times 2.45 \times 0.7 \times 10^{-5}/2.436 = 102\ \mu$ mho/km

(*b*) *For switching* : $g_e = (320 \times 12 \times 0.7/11.68)\ 10^{-8} = 2.3\ \mu$ mho/km

Example 8.4. A 300 km line is to be represented by a model consisting of 12 π sections for the above 400-kV line. Find the values of resistances to be connected in shunt for each section.

Solution. Let line length be L and number of π sections be N. Then each π-section is equivalent to a length of line of (L/N) km. The total conductance is $G_e = g_e L/N$ mhos and the corresponding resistance is $R_e = N/g_e L$.

(*a*) *For lightning-impulse* : $R_e = 12/(102 \times 10^{-6} \times 300) = 392$ ohms

(*b*) *For switching-surge*: $R_e = 12/(2.3 \times 10^{-6} \times 300) = 17.4$ kilohms

Note that because of the lower resistance to be connected in shunt for the lightning case, the voltage loses energy faster than for the switching surge and the wave attenuation is higher. In general, lightning surges attenuate to 50% value of the incident surge in only 10 km whereas it may only be 80% for switching surges after a travel of even as far as 400 km.

8.8 THE METHOD OF FOURIER TRANSFORMS

The method of Fourier Transforms when applied to propagation characteristics of lightning and switching surges is comparatively of recent origin and because of the availability of powerful Digital Computers offers a very useful tool for evaluating transient performance of systems, especially when distributed parameter lines occur in combination with lumped system elements. These are in the form of series source impedance, resistors in circuit breakers, shunt reactors for line compensation, transformers, bus bars, bushing capacitances, and entire sub-stations at the receiving end.

In previous sections, a solution for voltage at the open end of a line was derived in closed form by both the travelling-wave and standing-wave methods using the time-shifting theorem and residues by using the Laplace Transform. The Fourier Transform parallels the Laplace Transform with (1) the substitution of $s = a + jw$ in all quantities in their operational form, (2) separating real and j-parts in the resulting expression for a voltage or current under investigation, and (3) finally calculating the Inverse Fourier Transform (IFT) by performing an indicated numerical integration, preferably using the Digital Computer. We will illustrate the method for obtaining the open-end voltage considered before and then extend it to include other types of line termination and series and shunt impedances. Specific cases useful for design of insulation of lines will be taken up in chapter 10 on Switching Surges.

The open-end voltage was found to be, equation (8.26),

$$V_0(s) = E(s)/\cosh pL \text{ where } p = f(r, l, g, c)$$

For a step input, $E(s) = V/s$, and in general $p = \sqrt{(r+ls)(g+cs)}$. Substitute $s = a + jw$. Then,

$$V_0(a+jw) = V/(a+jw).\cosh L\sqrt{\{r+l(a+jw)\}\{g+c(a+jw)\}} \quad ...(8.84)$$

We can separate the real and j-parts easily. Let $\cosh pL$ be written as the complex number $(M + jN)$. Then,

$$V_0 = V/(a+jw)(M+jN) = V/\{(aM-wN)+j(aN+wM)\}$$

$$= V.\frac{(aM-wN)-j(aN+wM)}{(aM-wN)^2+(aN+wM)^2} = P + jQ \quad ...(8.85)$$

The real and j-parts of the required open-end voltage are

$$P = V(aM-wN)/D, \text{and} Q = -V(aN+wM)/D \quad ...(8.86)$$

where $D = (aM-wN)^2 + (aN+wM)^2$, the denominator ...(8.87)

The inverse transform is then given by the integral

$$V_0(t) = F^{-1}[V_0(a+jw)] = \frac{2}{\pi}\int_0^\infty P.e^{at}.\cos wt.\sigma_f.dw, \quad ...(8.88)$$

where σ_f is called the "sigma factor" which helps in convergence of the integral. In a practical situation, because of the upper limits being 0 and ∞, division by zero occurs. In order to obviate this, a lower limit for $w = W_i$ is assumed (could be a value of 10) and the integration is terminated at a final value $w = W_F$. The sigma factor is then written as

$$\sigma_f = \sin(\pi w/W_F)/(\pi w/W_F) \quad ...(8.89)$$

and the desired integral becomes

$$V_0(t) = \frac{2e^{at}}{\pi}\int_{W_i}^{W_F} P.\cos wt.\frac{\sin(\pi w/W_F)}{(\pi w/W_F)}.dw \quad ...(8.90)$$

The j-part could also be used and is then written as

$$V_0(t) = -\frac{2}{\pi}e^{at}\int_{W_i}^{W_F} Q.\sin wt.\frac{\sin(\pi w/W_F)}{(\pi w/W_F)}.dw \quad ...(8.91)$$

The numerical integration can be carried out by utilizing any of the several methods available in books on Numerical Methods, such as (*a*) the trapezoidal rule, (*b*) Simpson's Rule, (*c*) Gauss's method, and finally by the application of (*d*) the Fast-Fourier Transform. These are considered beyond the scope of this book.

There are several factors which are now discussed on the choice of values for several quantities such as a, W_i and W_F, which are very critical from the point of view of application of this method. First, the values of M and N are found as follows:

Let

$$pL = L\sqrt{\{r + l(a + jw)\}\{g + c(a + jw)\}} = m + jn \qquad \text{...(8.92)}$$

Then, $(m + jn)^2 = J + jK$ where ...(8.93)

and

$$\left.\begin{aligned} J &= L^2\{(r + la)(g + ca) - lc\,w^2\} \\ K &= L^2\{(r + la)cw + (g + ca)lw\} \end{aligned}\right\} \qquad \text{...(8.94)}$$

$\therefore$ $m^2 - n^2 = J$ and $2\,mn = K$ with $K > 0$ ...(8.95)

$\therefore$ Solving for m and n in terms of J and K, there are

$$m = \left[\frac{1}{2}(\sqrt{J^2 + K^2} + J)\right]^{1/2} \; and \; n = \left[\frac{1}{2}(\sqrt{J^2 + K^2} - J\right]^{1/2} \qquad \text{...(8.96)}$$

Then, cosh $(m + jn)$ = cosh m. cos $n + j$ sinh m sin n = $M + jN$ or

$$M = \cosh m.\cos n \text{ and } N = \sinh m.\sin n \qquad \text{...(8.97)}$$

The use of the Fourier-Transform Method for very fast-rising input voltages such as the step function is very important and any choice of values for a, W_i and W_F used for this type of excitation will hold for other types. From experience, the following rules are formulated which should be tried out for each case and the final values chosen:

(1) The choice of the converging factor "a" which is the real part of the Fourier-Transform operator $s = (a + jw)$ is very crucial. If T_f = final value of time up to which the response is to be evaluated, then a rule is to choose $(a\,T_f)$ = 1 to 4. For example, for a switching-surge study carried out to one cycle on 50 Hz base, that is 20 ms, the value of a = 50 to 200. If the calculation is to proceed up to 40 ms, two cycles, then choose a = 50 to 200 for the first 20 ms, and 25 to 100 for the next 20 ms.

(2) The choice of final value of $w = W_F$ at which the integration of (8.90) or (8.91) is to be truncated is governed by the rise time of the phenomenon. The shortest rise time occurs for a step function (theoretically zero) and W_F may be as large as 10^6, but for other wave-shapes it may be 10^5.

(3) The choice of interval (Δw) depends on the accuracy required. The number of ordinates chosen for integration is $N_0 = (W_F - W_i)/\Delta w$. This can be 500 to 1000 so that the choice of W_F will determine the frequency step to be used.

Chapter 10 will describe some calculations using this method.

8.9 REFLECTION AND REFRACTION OF TRAVELLING WAVES

The methods described earlier can be very usefully applied to simple but important system configurations and the Fourier Transform method can handle entire systems given sufficient computer time. In may situations, several components are connected in series and a wave travelling on one of these propagates in a different component with a different value. This is caused by the discontinuity at the junction which gives rise to reflected and refracted (or transmitted) waves. They are described by reflection and refraction factors which are derived as follows:

The voltage and current at any point on a line was found to be, equations (8.19) and (8.20), and Fig. 8.3,

$$V = \frac{\cosh px + (Z_0/Z_t)\sinh px}{\cosh pL + (Z_0/Z_t)\sinh pl} E(s) \quad ...(8.19)$$

$$I = \frac{1}{Z_0} \frac{\sinh px + (Z_0/Z_t)\cosh px}{\cosh pL + (Z_0/Z_t)\sinh pL} E(s) \quad ...(8.20)$$

These resulted from the general solutions, equations (8.14) and (8.15),

$$V(x) = Ae^{px} + Be^{-px} \text{ and } I(x) = \frac{1}{Z_0}(Ae^{px} - Be^{-px})$$

The voltage and current consist of two parts:

$$V(x) = V_1 + V_2, \text{ and } I(x) = I_1 + I_2 = \frac{1}{Z_0}V_1 - \frac{1}{Z_0}V_2 \quad ...(8.98)$$

We counted $x = 0$ from the terminal, Fig. 8.3, (at the impedance Z_t) while $x = L$ at the source end. The term e^{px} increases as we move from Z_t to the source which is an unnatural condition. But the concept of a wave decreasing in magnitude as one moves from the source end into the line is a natural behaviour of any phenomenon in nature. Consequently, this is a forward travelling wave from the source. When losses are neglected, $p = \sqrt{lc} = 1/v$ where v = velocity of e.m. propagation. The current also consists of two parts: (1) $I_1 = Ae^{px}/Z_0 = V_1/Z_0$ which is the forward-travelling component. The ratio of voltage to current is + Z_0, the characteristic impedance of line. (2) $I_2 = -Be^{-px}/Z_0 = -V_2/Z_0$, which is the backward-travelling component from the terminal end to the source. The ratio of voltage to current is ($-$ Z_0).

Let us re-write the expression in (8.19) as

$$V = \frac{e^{px}(1 + Z_0/Z_t) + e^{-px}(1 - Z_0/Z_t)}{e^{pL}(1 + Z_0/Z_t) + e^{-pL}(1 - Z_0/Z_t)} E(s) \quad ...(8.99)$$

At $x = 0$, the surge is incident on Z_t where the incident voltage has the magnitude $(1 + Z_0/Z_t)\, E(s)/D$, where D = the denominator of equation (8.99).

The total voltage across Z_t is

$$V = V_i + V_r$$

where V_i = the incident voltage and V_r = reflected voltage. The voltage V is also called the refracted voltage or transmitted voltage. At the junction of line and Z_t, from equation (8.99), we have the relation

$$K_r = \frac{\text{Reflected Voltage}}{\text{Incident Voltage}} = \frac{1 - Z_0/Z_t}{1 + Z_0/Z_t} = \frac{Z_t - Z_0}{Z_t + Z_0} = \begin{pmatrix}\text{Reflection}\\ \text{Coefficient}\end{pmatrix} \quad ...(8.100)$$

The refraction or transmission coefficient is defined as

$$K_t = \frac{\text{Total Voltage at junction}}{\text{Incident Voltage at junction}}$$

$$= \frac{(1 + Z_0/Z_t) + (1 - Z_0/Z_t)}{1 + Z_0/Z_t} = 2Z_t/(Z_t + Z_0) \quad ...(8.101)$$

We also note that

$$K_t = 1 + K_r \quad ...(8.102)$$

Similarly, for the current. The total current can be written at $x = 0$, or at the junction of line and Z_t, as

$$I = \frac{1}{Z_0} \frac{(1 + Z_0/Z_t) + (Z_0/Z_t - 1)}{(1 + Z_0/Z_t)e^{pL} + (1 - Z_0/Z_t)e^{-pL}} E(s) = I_i + I_r \quad ...(8.103)$$

The ratio of reflected component of current to the incident current at the junction, or the reflection coefficient, is

$$J_r = I_r/I_i = (Z_0/Z_t - 1)/(Z_0/Z_t + 1)$$

$$= -(Z_t - Z_0)/(Z_t + Z_0) = -K_r \quad ...(8.104)$$

while the transmission coefficient is

$$J_t = I/I_i = (2Z_0/Z_t)/(1 + Z_0/Z_t) = 2Z_0/(Z_t + Z_0) = (Z_0/Z_t)K_t \quad ...(8.105)$$

The reflection coefficients for voltage and current, K_r and J_r, are of opposite sign since they are backward travelling components. The refraction coefficients for voltage and current are of the same sign.

These coefficients are usually derived in a simpler manner (without proving the relations between incident, reflected and refracted waves) as follows:

Consider the equations

where
$$\left.\begin{aligned} V_t &= V_i + V_r \text{ and } I_t = I_i + I_r \\ V_t &= Z_t I_t, V_i = Z_0 I_i, \text{ and } V_r = -Z_0 I_r \end{aligned}\right\} \quad ...(8.106)$$

Then, $Z_t I_t = Z_0 I_i - Z_0 I_r$ giving $I_i - I_r = Z_t I_t / Z_0$ ...(8.107)

Since $I_i + I_r = I_t$, we obtain

$$2I_i = (1 + Z_t/Z_0)I_t \text{ giving } I_t = 2Z_0 I_i / Z_t + Z_0) = J_t I_i \quad ...(8.108)$$

and
$$2I_r = (1 - Z_t/Z_0)I_t \text{ giving } I_r = I_i(Z_0 - Z_t)/(Z_0 + Z_t) = J_r I_t \quad ...(8.109)$$

Similarly, $V_t/Z_t = (V_i - V_r)/Z_0$ or $V_i - V_r = (Z_0/Z_t)V_t$ and $V_i + V_r = V_t$.

These yield $V_t = [2Z_t/(Z_t + Z_0)]V_i = K_t V_i$ ...(8.110) and $V_r = V_t - V_i = (K_t - 1)V_i = V_i(Z_t - Z_0)/(Z_t + Z_0) = K_r V_i$ ...(8.111)

These coefficients can be used very effectively in order to find junction voltages in simple cases which are experienced in practice. Let us consider certain special cases.

	Case	Z_t	K_t	K_r	J_t	J_r
(1)	Open circuit	∞	+ 2	+ 1	0	– 1
(2)	Short circuit	0	0	– 1	+ 2	+ 1
(3)	Matched	Z_0	+ 1	0	+ 1	0
(4)	Two outgoing lines	$Z_0/2$	+ 2/3	– 1/3	+ 4/3	+ 1/3
(5)	*n* outgoing lines	Z_0/n	2/(n + 1)	$\frac{-(n-1)}{(n+1)}$	$\frac{2n}{(n+1)}$	$\frac{(n-1)}{(n+1)}$

Example 8.5. An overhead line with Z_0 = 400 ohms continues into a cable with Z_c = 100 ohms. A surge with a crest value of 1000 kV is coming towards the junction from the overhead line. Calculate the voltage in the cable.

Solution. $K_t = 2Z_c/(Z_c + Z_0) = 200/500 = 0.4$.

Therefore, cable voltage = 400 kV, crest.

Example 8.6. In the above example, the end of the cable is connected to a transformer whose impedance is practically infinite to a surge, when the bushing capacitance is omitted. Calculate the transformer voltage.

Solution. When the 400 kV voltage reaches the junction of cable and transformer, it reflects positively with K_r = + 1 and K_t = + 2.

Therefore

Transformer voltage = 800 kV.

Example 8.7. A 750-kV transmission line has a surge impedance of 275 ohms and the transformer to be connected to it has a surge impedance of 1100 ohms for its h.v. winding. The length of winding is 5 km and its far end is connected to a zero resistance ground. A surge of 2400 kV is coming in the line which is to be limited to 1725 kV at the transformer bushing by using a short cable. (*a*) Calculate the surge impedance and voltage rating of the cable to be interposed between line and transformer. (*b*) Calculate the voltage at the h.v. terminal of the winding as soon as the first reflection arrives from the grounded end. See Fig. 8.8.

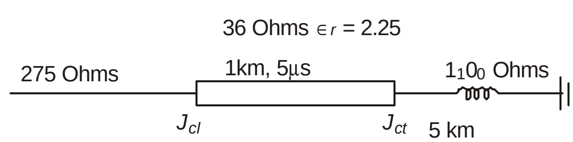

Fig. 8.8 Circuit diagram for Example 8.7.

Solution. If V_i = incident voltage from line, V_c = voltage at junction of line and cable, and V_t voltage of transformer h.v. winding at the junction of cable and transformer, then:

$$V_c = V_i.2Z_c/(Z_c + Z_1) = 2Z_c \times 2400/(Z_c + 275).$$

Similarly,

$$V_t = V_c.2Z_t/(Z_t + Z_c) = 2200\,V_c/(1100 + Z_c)$$

Thus we obtain with all surge impedances in kilohms.

$$1725 = 4.4Z_c \times 2400/[(Z_c + 0.275)(1.1 + Z_c)]$$

giving $$Z_c^2 - 4.74674\,Z_c + 0.3025 = 0.$$

This yields the more reasonable value of Z_c = 64.6 ohms. (The other value is 4682 ohms). With this cable, the voltages at the two ends of the cable are V_c = 913 kV at the junction of line and 1725 kV at the junction of transformer. Therefore, the impulse voltage level of cable will be chosen as 1725 kV, the same as the transformer.

(*b*) The reflection at zero-resistance ground of the transformer winding is total and negative. Therefore, the transformer terminal voltage should drop suddenly from 1725 kV to zero, but because of the cable the junction voltage falls by $(2Z_c/(Z_c + Z_t)) \times (-1725) = -191.4$ kV. Therefore, the junction voltage is (1725 – 191.4) = 1533.6 kV.

8.10 TRANSIENT RESPONSE OF SYSTEMS WITH SERIES AND SHUNT LUMPED PARAMETERS AND DISTRIBUTED LINES

Up to Section 8.8 we considered the equations and solutions of a transmission line only when energized by the different types of sources. In practice, lumped elements are connected to lines. In this section we will consider the development of equations suitable for solution based on transform methods or finite difference methods using the Digital Computer. The actual procedure for solution is left to Chapter 10 where some examples will be given.

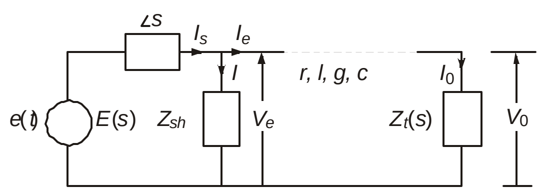

Fig. 8.9 Transmission system with source, series impedance, shunt impedance, distributed-parameter line, and terminating impedance.

Figure 8.9 shows a general single-line diagram of a source $E(s)$ energizing the line with distributed-parameters (r, l, g, c per unit length). There is an impedance Z_s in between the source and line which normally is composed of the transient reactance x' of the synchronous machine and any resistance that can be included in the circuit breaker during the switching operation. A shunt impedance Z_{sh} is also in the circuit which can represent the shunt-compensating reactor. The line is terminated with an impedance Z_t which consists of a transformer, shunt reactor, or an entire substation. For the present, only single-phase representation is used which we can extend to a complete 3-phase system as will be done in Chapter 10.

Let $z = r + ls$ and $y = g + cs$ as before ...(8.112)

Then, at any point x from the termination Z_t, the equations are

$$\partial V/\partial x = zI \text{ and } \partial I/\partial x = yV \quad ...(8.113)$$

$$\left.\begin{aligned} &\text{with solutions} \quad V = Ae^{px} + Be^{-px} \\ &\text{and} \quad I = (p/z)(Ae^{px} - Be^{-px}) \end{aligned}\right\} \quad ...(8.114)$$

The boundary conditions are : (1) at $x = L$, $V = V_e$, the voltage at the line entrance, and (2) at $x = 0$, $V(0) = I(0).Z_t$. Using

$$Z_0 = \sqrt{z/y} = z/p,$$

we obtained the solutions, equations (8.19) and (8.20) for the voltage and current at any point on the line as follows;

$$V(x) = \frac{\cosh px + (Z_0/Z_t)\sinh px}{\cosh pL + (Z_0/Z_t)\sinh pL}.V_e \quad ...(8.115)$$

and $$I(x) = \frac{1}{Z_0}.\frac{\sinh px + (Z_0/Z_t)\cosh px}{\cosh pL + (Z_0/Z_t)\sinh pL}.V_e \quad ...(8.116)$$

At the end of the line, $x = 0$, the voltage and current are

$$V(0) = V_e/[\cosh pL + (Z_0/Z_t)\sinh pL] \quad ...(8.117)$$

and $$I(0) = V(0)/Z_t \quad ...(8.118)$$

At the entrance to the line, $x = L$, they are

$$V(L) = V_e \text{ and } I(L) = \frac{1}{Z_0}.\frac{\sinh pL + (Z_0/Z_t)\cosh pL}{\cosh pL + (Z_0/Z_t)\sinh pL}.V_e \quad ...(8.119)$$

Therefore, if the voltage V_e is found in terms of the known excitation voltage of source (step, double exponential, or sinusoidal) then all quantities in equations (8.115) to (8.119) are determined in operational form. By using the Fourier Transform method, the time variation can be realized.

Referring to Fig. 8.9, the following equations can be written down:

$$I_{sh} = V_e/Z_{sh}, I_s = I_{sh} + I(L), V_e = E(s) - Z_s I_s \quad ...(8.120)$$

$$\therefore \quad V_e = E(s) - Z_s(I_{sh} + I(L))$$

$$= E(s) - \frac{Z_s}{Z_{sh}}V_e - \frac{Z_s}{Z_0}\frac{\sinh pL + (Z_0/Z_t)\cosh pL}{\cosh pL + (Z_0/Z_t)\sinh pL}V_e \quad ...(8.121)$$

Solving for V_e, the voltage at the line entrance, we obtain

$$V_e = E(s)\frac{(1 + Z_s/Z_{sh} + Z_s/Z_t)\cosh pL + (Z_0/Z_t + Z_sZ_0/Z_{sh}Z_t + Z_s/Z_0)\sinh pL}{\cosh pL + (Z_0/Z_t)\sinh pL}$$

...(8.122)

When $Z_s = 0$ and $Z_{sh} = \infty$, the entrance voltage equals the source voltage $E(s)$.

12

Power-Frequency Voltage Control and Overvoltages

12.1 PROBLEMS AT POWER FREQUENCY

Power-frequency voltage is impressed on a system continuously as compared to transients caused by faults, lightning, and switching operations. Certain abnormal conditions arise when overvoltages of a sustained nature can exist in systems which have to be guarded against. Insulation levels will be governed by these, and it is very important to know all the factors which contribute to such overvoltages. E.H.V. lines are longer than and their surge impedance lower than lines at 345 kV and lower voltages. Also, e.h.v. lines are used more for point-to-point transmission so that when load is dropped, a large portion of the system is unloaded and voltage rise could be more severe than when there is a vast interconnected network. Due also to the high capacitance of e.h.v. lines possibility of self-excitation of generators is quite serious. Shunt reactors are employed to compensate the high charging current, which not only prevent overvoltages during load dropping but also improve conditions for load flow, and the risk of self-excitation can also be counteracted. In order to improve conditions, variable static VAR systems can also be employed as well as switched capacitors which introduce harmonics into the system. Finally, the use of series capacitors to increase line loading in long lines might bring about the danger of subsynchronous resonance in which electrical conditions in generators can produce torques which correspond to the torsional frequencies of the shaft and result in mechanical damage.

The system at power frequency consists of lumped-parameter network elements connected to distributed-parameter transmission lines, and the calculations are best handled through generalized constants in matrix form.

12.2 GENERALIZED CONSTANTS

We have already derived equations for voltage and current at any point on a distributed-parameter line in Chapter 10 in terms of the voltage at the entrance to the line for any general line termination impedance, Z_t. They are, for a line of length L,

$$E(x) = E_e \frac{\cosh px + (Z_0/Z_t)\sinh px}{\cosh pL + (Z_0/Z_t)\sinh pL} \qquad \text{...(12.1)}$$

$$I(x) = \frac{E_e}{Z_0}.\frac{\sinh px + (Z_0/Z_t)\cosh px}{\cosh pL + (Z_0/Z_t)\sinh pL} \quad ...(12.2)$$

In the steady state, the propagation constant and surge impedance are

$$p = \sqrt{(r + jwl)(g + jwc)} \text{ and } Z_0 = \sqrt{(r + jwl)/(g + jwc)} \quad ...(12.3)$$

Also, at the load end, $x = 0$, $E_0 = Z_t I_0$ so that

$$E_0 = E_e/[\cosh pL + (Z_0/Z_t)\sinh pL] \quad ...(12.4)$$

This can be written for the entrance voltage as

$$E_e = (\cosh pL)E_0 + (Z_0.\sinh pL).(E_0/Z_t)$$
$$= E_0.\cosh pL + I_0.Z_0 \sinh pL \quad ...(12.5)$$

Similarly, from equation (12.2), at $x = 0$ and at $x = L$,

$$I_0 = (E_e/Z_t)/[\cosh pL + (Z_0/Z_t)\sinh pL) \quad ...(12.6)$$

and
$$I_e = \frac{E_e}{Z_0}[\sinh pL + (Z_0/Z_t)\cosh pL]/[\cosh pL + (Z_0/Z_t)\sinh pL] \quad ...(12.7)$$

$$= \left(\frac{1}{Z_0}\sinh pL\right)E_e/[\cosh pL + (Z_0/Z_t)\sinh pL]$$
$$+ (\cosh pL).(E_e/Z_t)/[\cosh pL + (Z_0/Z_t)\sinh pL]$$

$$= \left(\frac{1}{Z_0}\sinh pL\right)E_0 + (\cosh pL)I_0 \quad ...(12.8)$$

Equations (12.5) and (12.8) give expressions for the voltage and current at the entrance to the line in terms of the voltage and current at the output or load end.

These can be re-written as

$$\left.\begin{aligned} E_e &= A.E_0 + B.I_0 \\ \text{and} \quad I_e &= C.E_0 + D.I_0 \end{aligned}\right\} \quad ...(12.9)$$

For steady-state conditions, we will designate the line entrance as the source end and the load end as the receiving end. The subscripts "*s*" and "*r*" will be used to indicate these. Thus,

$$E_s = AE_r + BI_r \text{ and } I_s = CE_r + DI_r \quad ...(12.10)$$

We observe that

$$A = D = \cosh pL = \cosh \sqrt{ZY} \quad ...(12.11)$$

$$B = Z_0.\sinh pL = \sqrt{\frac{Z}{Y}}.\sinh\sqrt{ZY} \quad ...(12.12)$$

$$C = \frac{1}{Z_0}.\sinh pL = \sqrt{Y/Z}.\sinh\sqrt{ZY} \quad ...(12.13)$$

$$\left.\begin{aligned} \text{where} \quad Z &= (r + jwl)L = \text{total series impedance of line} \\ \text{and} \quad Y &= (g + jwc)L = \text{total shunt admittance of line} \end{aligned}\right\} \quad ...(12.14)$$

In dealing with steady-state voltages and currents on an overhead line, we can take $g = 0$. For underground cables, this is not valid.

From (12.11) to (12.13) we note that

$$AD - BC = \cosh^2 pL - \sinh^2 pL = 1 \qquad ...(12.15)$$

The propagation constant p can be written in various forms.

$$p = \sqrt{(r + j\omega l) j\omega c} = \alpha + j\beta, \qquad ...(12.16)$$

where $\alpha^2 = \dfrac{\omega^2 lc}{2}\left[\sqrt{1 + 4r^2/\omega^2 l^2} - 1\right]$

and $\beta^2 = \dfrac{\omega^2 lc}{2}\left[\sqrt{1 + 4r^2/\omega^2 l^2} + 1\right] \qquad ...(12.17)$

For the case where the resistance is low enough such that

$$2r \ll \omega l, \sqrt{1 + (2r/\omega l)^2} = 1 + 2r^2/\omega^2 l^2,$$

we have $\alpha^2 = r^2 c/l$ and $\beta^2 = \omega^2 lc(1 + r^2/\omega^2 l^2) \qquad ...(12.18)$

The real part α of p is the attenuation constant and is approximately

$$\alpha = r\sqrt{c/l} = r/Z_{00} \qquad ...(12.19)$$

where Z_{00} = surge impedance of line when $r = 0$.

Also, if we define v_0 = velocity of propagation of e.m. wave on a resistance-less line, $v_0 = 1/\sqrt{lc}$ and we have

$$Z_{00} = v_0 l = 1/v_0 c \text{ and } \alpha = r/v_0 l = v_0 rc \qquad ...(12.20)$$

The j-part β of p is the phase-shift constant and it is approximately

$$\beta = \frac{\omega}{v_0}\sqrt{1 + r^2/\omega^2 l^2} \approx \frac{\omega}{v_0}\left(1 + \frac{1}{2} r^2/\omega^2 l^2\right) \qquad ...(12.21)$$

The wavelength is related to the frequency by $f\lambda = v_0$.

$$\therefore \quad \beta = \frac{2\pi}{\lambda}(1 + r^2/2\omega^2 l^2) \qquad ...(12.22)$$

For a line without losses.

$$\alpha = 0 \text{ and } \beta = 2\pi/\lambda \qquad ...(12.23)$$

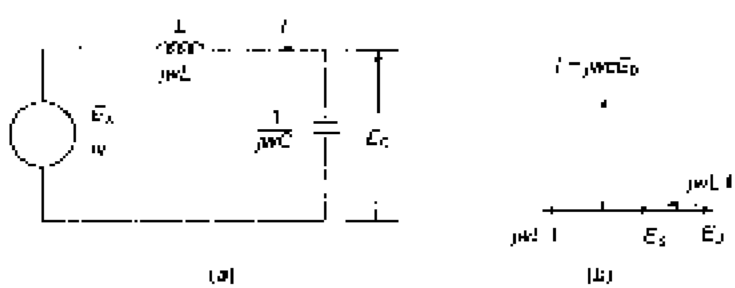

Fig. 12.1 Ferranti effect in lumped L-C circuit excited by sine wave of voltage, and phasor diagram

The wavelength λ at 50 Hz is 6000 km based on light velocity of 300,000 km/sec. Therefore, for a line of 100 km, $2\pi L/\lambda = 6°$. This usually indicates that on an uncompensated line at no load, and when line resistance is negligible, the phase difference between the source voltage and receiving end voltage is 6° for every 100 km of line length at 50 Hz.

12.3 NO-LOAD VOLTAGE CONDITIONS AND CHARGING CURRENT

When there is no-load at the receiving end, $I_r = 0$, the control of voltage at line ends poses certain problems due to overvoltage conditions. Unlike dc lines, ac lines have the shunt charging current flowing through the series inductance of line causing a rise in the output voltage at the receiving end. This is the well-known "Ferranti Effect." Consider a simple series L-C circuit with lumped inductance and capacitance, as shown in Figure 12.1 (*a*) and the phasor diagram of voltages and currents in 12.1 (*b*). By proper voltage division, the source voltage will be

$$E_s = (1/jwc + jwL)E_r/(1/jwc) = (1 - w^2LC)E_r \quad ...(12.24)$$

This shows that E_s is less than E_r and in phase with it. The voltage drop in the inductive reactance due to the charging current of the capacitor, $I = jwC\,E_r$, is substracting from the load voltage to give the source voltage.

In a distributed-parameter line, neglecting series resistance for understanding the phenomenon, equation (12.5) gives at no load,

$$E_s = (\cosh jwL/v_0)E_r = E_r.\cos(wL/v_0) = E_r.\cos(2\pi L/\lambda) \quad ...(12.25)$$

Since cos $wL/v_0 \le 1$, the source voltage is lower than the receiving-end voltage. Normally, the source voltage is held constant at the station bus so that the receiving-end bus voltage rises with line length.

Example 12.1. Calculate the expected p.u. value of load-end voltage for various line lengths from 100 km to 1000 km at no load. Neglect line resistance and assume source-end voltage to be held constant at 1 p.u.

Solution. The following table shows all values.

L, km	100	200	300	400	500	600	700	800	900	1000
$(2\pi L/\lambda)°$	6°	12°	18°	24°	30°	36°	42°	48°	54°	60°
$\cos(2\pi L/\lambda)$	0.9945	0.978	0.951	0.9135	0.866	0.809	0.743	0.669	0.588	0.5
E_r/E_s	1.0055	1.022	1.05	1.095	1.155	1.236	1.346	1.494	1.7	2

If we continue this table, we soon find that the ratio E_r/E_s on a resistanceless line increases to infinity for a line whose length is equal to one quarter wavelength or 1500 km, and then will decrease.

Since the standard specifications state the maximum operating voltages for given nominal system voltages, some measures must be taken to control the voltage rise at no load at the receiving end. This requires shunt inductive reactive vars to be provided. If the equipment is connected only at one end, usually the load end, then a synchronous condenser can be used operating in the under-excited condition. However, shunt-compensating reactors either of the fixed type or variable type are used at both ends, and in recent years, static var systems of the switchable type using high-speed thyristor switches are coming into practice.

Example 12.2. Determine the limiting lengths for uncompensated lines if the voltages at the two ends must be held at the following sets of values. Neglect resistance and assume no-load condition.

(*a*) E_s = 400 kV, E_r = 420 kV,

(*b*) E_s = 380 kV, E_r = 420 kV,

(*c*) E_s = 750 kV, E_r = 765 kV,

(*d*) E_s = 735 kV, E_r = 750 kV,

(*e*) E_s = 720 kV, E_r = 750 kV,

Note that in all cases, $E_s < E_r$.

Solution. Since $E_s = E_r \cos(2\pi L/\lambda)$, the line length is

$$L = (\lambda/2\pi)[\cos^{-1}(E_s/E_r)] = \frac{100}{6}\cos^{-1}(E_s/E_r), \text{km.}$$

For the given data, the line lengths will be

(*a*) 296 km, (*b*) 420 km, (*c*) 189 km, (*d*) 191 km, (*e*) 271 km.

Note that the larger the difference between E_s and E_r, the longer will be the line length allowed without shunt reactor compensation.

Charging Current and MVAR

The current supplied by the source into the line at no load (I_r = 0) is, from equation (12.10)

$$I_s = CE_r = \frac{1}{Z_0}\sinh pL.E_r\,. \quad \text{...(12.26)}$$

When resistance is neglected,

$$Z_{00} = \sqrt{l/c} \text{ and } p = jw/v_0 = j2\pi/\lambda\,.$$

$$\therefore \quad I_s = j\sqrt{\frac{c}{l}}\sin(wL/v_0).E_r = jE_r.\sqrt{\frac{c}{l}}.\sin(2\pi L/\lambda) \quad \text{...(12.27)}$$

It leads the receiving-end voltage by 90°. An effective capacitance for the distributed line connected across the receiving-end voltage E_r and drawing the same current has the value

$$c_0 = \frac{1}{wZ_{00}}\sin(2\pi L/\lambda), \text{ Farad.} \quad \text{...(12.28)}$$

The corresponding charging reactive power supplied by the source per phase will be

$$Q_0 = E_s.I_0 = E_s.E_r\sqrt{\frac{c}{l}}.\sin(2\pi L/\lambda)\,. \quad \text{...(12.29)}$$

If E_s and E_r are line-to-line voltages in kV, r.m.s., then Q_0 will be the 3-phase charging MVAR. Also,

$$Q_0 = E_s^2.\sqrt{\frac{c}{l}}.\tan(2\pi L/\lambda), \text{since } E_r = E_s/\cos(2\pi L/\lambda) \quad \text{...(12.30)}$$

Note that for a resistanceless line, when $L = \lambda/2$, there is no charging current, and furthermore, $E_r = -E_s$.

Example 12.3. For a 400 kV line, l = 1 mH/km and c = 11.1 nF/km, and E_s = 400 kV from the source, line-line, r.m.s. Calculate the charging MVAR for line lengths varying from 100 km to 1000 km. Neglect resistance.

Solution. $Z_{00} = \sqrt{l/c}$ = 300 ohms.

L, km	100	200	300	400	500	600	700	800	900	1000
$\tan\left(\frac{6L}{100}\right)^\circ$	.105	.213	.325	.445	.577	.727	.9	1.11	1.38	1.732
$Q_0, MVAR$	56	113.4	173.3	237.5	308	387.5	480	592	734	924
Q_0/L	.56	.567	.578	.594	.616	.646	.686	.74	.816	.924

For normally-encountered distances from 300 km to 600 km, the charging MVAR per 100 km is 58 to 65 with an average of 60 MVAR for each 100 km length.

Example 12.4. Repeat example 12.3 for a 750 kV line with surge impedance of Z_{00} = 250 ohms. Take line lengths from 400 km to 1000 km.

Solution. $E_s^2/Z_{00} = 2250 MW. Q_0 = 2250 \tan(6L/100)^\circ$.

L, km	400	500	600	700	800	900	1000
Q_0, *MVAR*	1001	1298	1635	2025	2500	3096	3897

For lines between 400 and 1000 km, the charging MVAR is 250 to 390 per 100 km (With an average value of 300 MVAR/100 km).

Example 12.5. For the 400-kV and 750-kV lines, calculate the surge-impedance loading, SIL.

Solution. The surge-impedance load is equal to the MVA delivered to a load equal to Z_{00}. This is

$$\text{SIL} = E_s^2/Z_{00}.$$

For 400 kV line, SIL = $400^2/300$ = 533.3 MVA.

For 750 kV line, SIL = $750^2/250$ = 2250 MVA.

Example 12.6. For a 400 kV 400 km line, 50% of the line-charging MVAR is to be compensated by connecting shunt reactors. Calculate the approximate MVAR required in these.

Solution. From example 12.3, the charging MVAR supplied by the source is 237.5 MVAR. For 50% compensation, the shunt reactors have to provide approximately 120 MVAR. In practice, 60 MVAR reactors will be connected at each end of line.

More accurate shunt reactor compensation will be calculated in later sections, including line resistance.

12.4 THE POWER CIRCLE DIAGRAM AND ITS USE

Equation (12.10) can also be written for E_r and I_r in terms of E_s and I_s as follows, with $AD - BC$ = 1, and $A = D$:

$$\begin{bmatrix} E_r \\ I_r \end{bmatrix} = \begin{bmatrix} A, & B \\ C, & D \end{bmatrix}^{-1} \begin{bmatrix} E_s \\ I_s \end{bmatrix} = \begin{bmatrix} A, & -B \\ -C, & D \end{bmatrix} \begin{bmatrix} E_s \\ I_s \end{bmatrix} \quad ...(12.31)$$

Also, $I_r = (E_s - AE_r)/B$ ...(12.32)

All these quantities are complex numbers. The receiving-end power is

$$W_r = P_r + jQr = E_r I_r^* = E_r (E_s^* - A^* E_r^*)/B^* \quad ...(12.33)$$

If we consider E_r as reference giving $E_r = E_r\angle 0°$, then the sending-end voltage $E_s = |E_s| \angle\delta$, where the angle δ is called the power angle. Also let $A = |A| \angle\theta_a$ and $B = |B| \angle\theta_b$. Then

$$W_r = P_r + jQ_r = \frac{E_r \angle\theta_b}{|B|}(|E_s| \angle -\delta - E_r.|A| \angle -\theta_a)$$

$$= \frac{E_r |E_s|}{|B|}\angle(\theta_b - \delta) - \frac{E_r^2 |A|}{|B|}\angle(\theta_b - \theta_a) \quad ...(12.34)$$

Separating the real and j-parts, there result

$$P_r = \frac{E_r |E_s|}{|B|}\cos(\theta_b - \delta) - \frac{E_r^2 |A|}{|B|}\cos(\theta_b - \theta_a) \quad ...(12.35)$$

and $$Q_r = \frac{E_r |E_s|}{|B|}\sin(\theta_b - \delta) - \frac{E_r^2 |A|}{|B|}\sin(\theta_b - \theta_a) \quad ...(12.36)$$

These can be re-written as

$$\left.\begin{aligned} P_r + \frac{E_r^2 |A|}{|B|}\cos(\theta_b - \theta_a) &= \frac{E_r |E_s|}{|B|}\cos(\theta_b - \delta) \\ Q_r + \frac{E_r^2 |A|}{|B|}\sin(\theta_b - \theta_a) &= \frac{E_r |E_s|}{|B|}\sin(\theta_b - \delta) \end{aligned}\right\} \quad ...(12.37)$$

Then, eliminating δ by squaring and adding the two equations, we obtain the locus of P_r against Q_r to be a circle with given values of A and B, and for assumed values of E_r and $|E_s|$ as follows:

$$\left\{P_r + \frac{E_r^2 |A|}{|B|}\cos(\theta_b - \theta_a)\right\}^2 + \left\{Q_r + \frac{E_r^2 |A|}{|B|}\sin(\theta_b - \theta_a)\right\}^2$$

$$= \left(\frac{E_r |E_s|}{|B|}\right)^2 \quad ...(12.38)$$

The coordinates of the centre of the receiving-end power-circle diagram are

$$\left.\begin{aligned} x_c &= -\frac{E_r^2 |A|}{|B|}\cos(\theta_b - \theta_a), \text{MW, and} \\ y_c &= -\frac{E_r^2 |A|}{|B|}\sin(\theta_b - \theta_a), \text{MVAR.} \end{aligned}\right\} \quad ...(12.39)$$

The radius of the circle is

$$R = E_r.|E_s|/|B|, \text{MVA}. \quad ...(12.40)$$

Figure 12.2 shows the receiving-end circle diagram. If the receiving-end voltage is held constant, as is usually dictated by the load, the centre of the circle is fixed, but the radius will depend on the value of the sending-end voltage, E_s. Therefore, for a chosen variation in $|E_s|$, a system of circles with centre at C and proper radius given by equation (12.40) can be drawn. The power-circle diagram and the geometrical relations resulting from it are extremely useful to a design engineer and an operating engineer to determine the status of power flow, reactive power flow, compensation requirements for voltage control and many properties concerning the system. These will be illustrated through typical examples.

Referring to Figure 12.2, the angle $\angle OCP_m = (\theta_b - \theta_a)$ and from equations (12.35) and (12.36), when $P_r = 0$, that is when the circle intersects the vertical axis at O'.

$$R \cos(\theta_b - \delta_0) = |x_c|, \text{ giving } \angle O'CP_m = (\theta_b - \delta_0) \qquad ...(12.41)$$

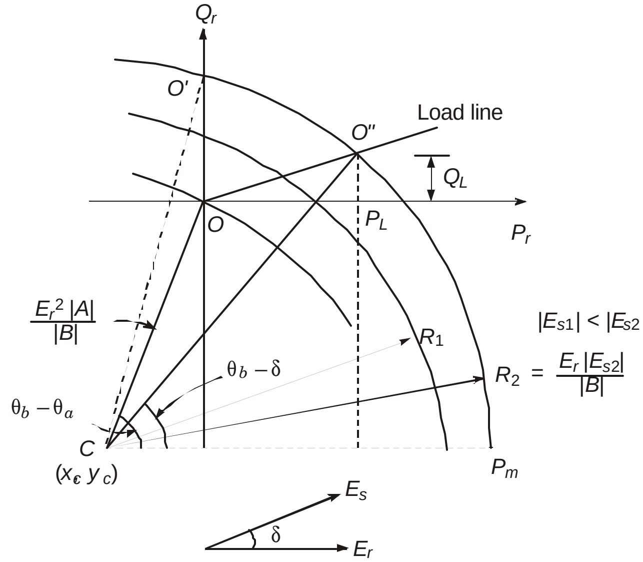

Fig. 12.2 Receiving-end circle diagram for calculating reactive compensation for voltage control at buses.

It is therefore a simple matter to find the angle δ_0 at no-load. For any other load, the load line is drawn with given MW and MVAR along the horizontal and vertical axes shown as P_L and Q_L. Let the circle intersect the load line at O''. Then, $\angle O''CP_m = \theta_b - \delta$, from equation (12.35). Because of geometrical construction using instruments, there will be slight inherent error involved in the results but will serve engineering purposes. However, with the aid of Digital Computers, great accuracy can be achieved from the properties relating to the circle diagram.

Maximum Power

For a given set of E_r, E_s, A and B, the maximum power that can be transmitted, P_m, is

$$P_{\max} = R - |x_c| = \frac{E_r |E_s|}{|B|} - \frac{E_r^2 |A|}{|B|} \cos(\theta_b - \theta_a) \qquad ...(12.42)$$

and the corresponding power angle is

$$\delta_{\max} = \theta_b - \angle O'CP_m \qquad ...(12.43)$$

For the case when resistance is neglected,

$$A = \cosh pL = \cos wL/v_0, \text{ giving } \theta_a = 0, \text{ and}$$

$$B = \sqrt{l/c}.\sinh jwL/v_0 = j\sqrt{l/c}.\sin wL/v_0, \text{giving } \theta_b = 90°.$$

$$\therefore \quad P_{max} = E_r\,|E_s|/|B| = E_r\,|E_s|/(Z_{00}\text{'}\sin wL/v_0) \quad ...(12.44)$$

From (12.35) and (12.36), with $\theta_a = 0$ and $\theta_b = 90°$,

$P_r = E_r\,|E_s|.\sin\delta/|B|$, which is maximum when $\delta = 90°$ and so $P_{max} = E_r|E_s|/|B|$. We observe from equation (12.44) that $|B| = Z_{00}.\sin wL/v_0$. Normally, resistances should not be neglected since the line losses for a given system status are one of the governing quantities in system design and compensation calculations.

Example 12.7. The following details are given for a 750-kV 3-phase line: Resistance r = 0.014 ohm/km, inductance l = 0.866 mH/km, reactance x = 0.272 ohm/km at 50 Hz, c = 12.82 nF/km giving a susceptance of $y = 4.0275 \times 10^{-6}$ mho/km, velocity $v_0 = 3 \times 10^8$ m/s = 3×10^5 km/sec, line length = 500 km. Calculate items (*a*) and (*b*) below, and work parts (*c*) and (*d*). Give proper units for all quantities.

(*a*) $Z = L(r + jwl), Y = jwcL, Z_{00} = \sqrt{l/c}$.

(*b*) The generalized constants A, B, C, and D, in both polar and rectangular forms.

(*c*) For E_r = 750 kV and $|E_s|$ = 0.98 E_r, determine the coordinates of the centre of the receiving-end power-circle diagram and the radius.

(*d*) Find the power angle δ for transmitting a load of 2000 MW at 750 kV at the receiving-end at unity power factor.

Solution.

(*a*)

$$Z = 500(0.014 + j0.272) = 7 + j136 = 136.2\angle 87°, \text{ ohms.}$$

$$Y = j500 \times 4.0275 \times 10^{-6} = j\,2.014 \times 10^{-3} = 2.014 \times 10^{-3}\angle 90°, \text{ mho.}$$

$$Z_{00} = \sqrt{0.866/12.82} \times 10^3 = 260 \text{ ohms.}$$

(*b*)

$$\sqrt{ZY} = (136.2 \times 2.014 \times 10^{-3})^{1/2}\angle 88.5° = 0.5237\angle 88.5°$$

$$= 0.0137 + j0.5235. \qquad (0.5235 \text{ radian} = 30°)$$

$$\sqrt{Z/Y} = (136.2/2.014 \times 10^{-3})^{1/2}\angle -1.5°$$

$$= 260\angle -1.5° = 259.9 - j6.8 \text{ ohms.}$$

$$\therefore \quad A = D = \cosh\sqrt{ZY} = \cosh 0.0137.\cos 0.5235 + j\sinh 0.0137.\sin 0.5235$$

$$= 0.86625 + j0.00685 = 0.8663\angle 0.45°$$

[At no load, without compensation, for E_r = 750 kV, $E_s = AV_r$ = 650 kV, line-line].

$$C = \sqrt{Y/Z}\sinh\sqrt{ZY} = \sinh(0.0137 + j\,0.5235)/260\angle -1.5°$$

$$= (\sinh 0.0137.\cos 0.5235 + j\cosh 0.0137.\sin 0.5235)/260\angle -1.5°$$

$$= 0.50024\angle 88.64°/260\angle -1.5° = 1.924 \times 10^{-3}\angle 90.14°.$$

$$= (-0.0047 + j1.923994)\,10^{-3} \text{ mho.}$$

$$B = Z_0 \sinh\sqrt{ZY} = 0.50024\angle 88.64° \times 260\angle -1.5°$$

$$= 130\angle 87.14° = 6.486 + j129.84 \text{ ohms.}$$

(*c*) *Centre* : $x_c = -E_r^2\,|A|\cos(\theta_b - \theta_a)/|B|$

$= -750^2.0.8663 \cos(87.14° - 0.45°)/130$

$= -216.6$ MW

$y_c = -3748.5.\ \sin 86.69° = -3742.25$ MVAR

Radius : $R = E_r|E_s|/|B| = 0.98 \times 750^2/130 = 4240$ MVA.

(*d*) From the geometry of the circle diagram, Figure 12.2, or, from equation (12.35),

$2000 + 216.6 = 4240 \cos(87.14° - \delta)$, giving

$\delta = 87.14° - 58.48° = 28.66°$.

[The surge impedance for a lossless line is Z_{00} = 260 ohms. The SIL is $750^2/260$ = 2163 MW. At this load with 6°/100 km, the power angle would be 30° for 500 km length of line].

Example 12.8. In the previous example, calculate the reactive compensation to be provided across the load at the receiving end for (*a*) no-load condition, and (*b*) at full rated load of 2000 MW at 0.95 power factor lag. State the nature of reactive compensation used in the two cases.

Solution.

(*a*) The no-load point is O' on the circle diagram, Figure 12.2. By geometry, $(Q_0 + 3742.25)^2 + 216.6^2 = 4240^2$, which gives Q_0 = 492.25 MVAR showing that the compensation is inductive. The point O' falls above the origin O. See Figure 12.3.

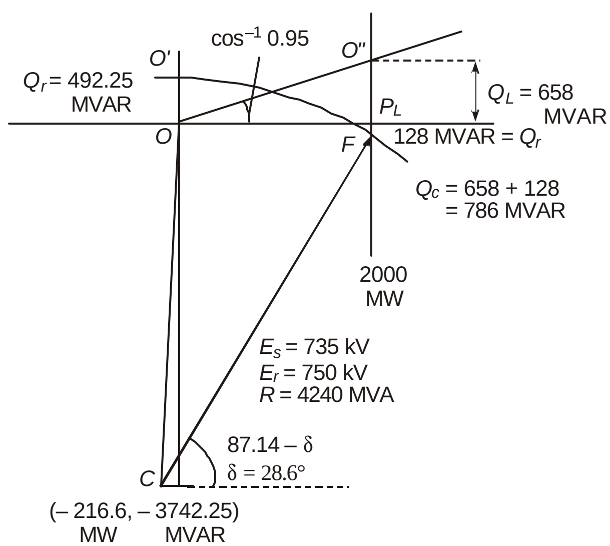

Fig. 12.3 Circle diagram for Example 12.8.

(*b*) For locating the full-load point at 0.95 lag, a line *OL* is drawn from the origin at $\cos^{-1} 0.95 = 18.2°$ in the 1st quadrant since the reactive power of load is positive, i.e., inductive, equal to Q_L = 2000 tan 18.2° = 658 MVAR. From the circle diagram,

$$(|y_c| - P_L F)^2 + (P_L + |x_c|)^2 = R^2$$

or, $$(3742.25 - P_L F)^2 + (2000 + 216.6)^2 = 4240^2$$

giving $P_L F$ = 128 MVAR, capacitive, since the point F was taken below the horizontal or power axis. This is the total reactive power required at the receiving end across the load for the given voltage and load conditions. To this must be added 658 MVAR of the load itself in order to obtain the rating of the compensating equipment, which not only has to override the 658 MVAR inductive of the load but also provide 128 MVAR capacitive. Therefore, the rating of the compensating equipment will be 658 + 128 = 786 MVAR, capacitive. From equation (12.35), the power angle is δ = 28.66°, which can also be obtained from equation (12.36) by using Q_r= – 128 MVAR.

From the above example, it may be observed that at no load inductive compensation is necessary amounting to 492.25 MVAR and at full load the compensation required is capacitive amounting to 786 MVAR. The ratio of inductive to capacitive MVAR's is 492.25/786 = 0.626.

Example 12.9. If in the previous example, the sending-end voltage is raised to 750 kV, the same as E_r, calculate the compensation to be provided (*a*) at no load, (*b*) at full load, and (*c*) the power angle δ in the two cases.

Solution. Since E_r, A, and B are the same, the coordinates of the centre of the receiving-end circle diagram stay the same at (– 216.6 MW, – 3742.25 MVAR). But the new radius is R = $750^2/130$ = 4327 MVA.

(*a*) At no load: $(Q_0 + 3742.25)^2 + 216.6^2 = 4327^2$ giving

Q_0 = 580 MVAR, inductive.

(*b*) At full load: $(3742.25 - P_L F)^2 + 2216.6^2 = 4327^2$ giving

$P_L F$ = 26 MVAR, capacitive. Therefore, adding 658 MVAR of the load, the compensating equipment must provide a reactive power of 684 MVAR, capacitive. Since the load can vary from no-load to full-load, this will be in the nature of switched capacitors. The ratio of inductive MVAR to capacitive MVAR = 580/684 = 0.848. Notice that power can flow in an ac system from a point at any voltage to another of equal voltage or even at higher voltage, provided the proper type and sufficient amount of reactive compensation is utilized. This is impossible in a dc system.

(*c*) The power angles are $\delta_0 = 0°$ and $\delta_l = 28.5°$.

12.5 VOLTAGE CONTROL USING SYNCHRONOUS CONDENSERS

From the generalized constants (A, B, C, D) of a given input port and output port, the power-circle diagram or the corresponding geometrical relations can be utilized for deciding the proper compensating MVAR's to be provided at the receiving end when a set of magnitudes for E_r and E_s at the two ends of the line are specified. When the load has a lagging power factor or even a unity power factor, generally the control of voltage is achieved by providing leading power factor or capacitive compensation at the receiving end. This can take the form of switched capacitors, usually connected to the low-voltage tertiary of the substation transformer at the load end. At no-load, usually inductive reactive compensation is required if the sending-end voltage is to be raised to stay within the standard specifications. This is provided by either the switched type (regulated) or constant type (unregulated).

The synchronous condenser provides both types of MVAR's, lagging or leading, that is inductive or capacitive. The synchronous motor runs without a shaft load and is enclosed in an explosion-proof casing which is filled with hydrogen at above atmospheric pressure in order to minimize rotational losses, and to ensure that any leakage of gas will be from the inside to external air, thus preventing an explosive mixture to be formed. The reactive powers generated by the motor are controlled by varying the dc field excitation of the rotor, under-excitation providing inductive MVAR's and over-excitation yielding capacitive MVAR's. Because of limitations imposed on excitation, the synchronous phase modifier can provide only 60 to 70% of its rated capacity at lagging power factor (under-excited condition) and full rated leading reactive power (over-excited condition).

The design of the rating of the synchronous phase modifier (or condenser for short) and the voltage conditions are illustrated below. The general equation satisfied by the real and reactive powers at the load end at any point on the circle is

$$(P_r + |x_c|)^2 + (Q_r + |y_c|)^2 = R^2 \quad \text{...(12.45)}$$

At no load, the point O' in Figure 12.2, obviously $P_r = 0$. The reactive power is

$$Q_0 = \sqrt{R^2 - x_c^2} - |y_c| \quad \text{...(12.46)}$$

At full load, point O'' in Figure 12.2 or 12.3,

$$(P_L + |x_c|)^2 + (|y_c| - Q_r)^2 = R^2 \quad \text{...(12.47)}$$

∴ The total reactive power required at the receiving end is

$$Q_r = |y_c| - \sqrt{R^2 - (P_L + |x_c|)^2} \quad \text{..(12.48)}$$

The capacitive MVAR required in the synchronous condenser is then

$$Q_c = Q_L + Q_r = Q_L + |y_c| - \sqrt{R^2 - (P_L + |x_c|)^2} \quad \text{...(12.49)}$$

If we use the relation $Q_0 = mQ_c, (m < 1)$, then the equation to be satisfied by the radius of the circle, which is the only quantity involving the sending-end voltage E_s will be, when values for E_r, A, B, P_L, Q_L are specified,

$$m\sqrt{R^2 - (P_L + |x_c|)^2} + \sqrt{R^2 - x_c^2} = (1+m)|y_c| + mQ_L \quad \text{...(12.50)}$$

When all quantities except R are specified, equation (12.50) will yield the value of $R = E_r |E_s|/|B|$, from which the sending-end voltage is determined. This is shown by the following example.

Example 12.10. For Example 12.9, taking E_r = 750 kV and m = 0.7 for the synchronous condenser, determine (*a*) the sending-end voltage, and (*b*) the proper rating of the synchronous condenser.

Solution. The data given are

$E_r = 750$, $A = 0.8663\angle 0.45°$, $B = 130\angle 87.14°$, $x_c = -216.6$,

$y_c = -3742.25$, P_L = 2000 MW, Q_L = 658 MVAR inductive, and $m = 0.7$.

(*a*) Solving equation (12.50) for R there results

$R = 4272 = 750 \times E_s/130$.

∴ The sending-end voltage has the magnitude

$E_s = 4272 \times 130/750 = 740$ kV, line-line.

(*b*) The synchronous-condenser rating is $Q_c = Q_L + Q_r$, from equation (12.49).

$$Q_r = 3742.25 - \sqrt{4272^2 - (2000 + 216.6)^2}\text{, from equation (12.48)}$$

$$= 90 \text{ MVAR, capacitive at full load.}$$

$\therefore \quad Q_c = 90 + 658 = 748$ MVAR, over-excited.

As a check, the under-excited reactive power required at no load is given by equation (12.46) as

$$Q_0 = \sqrt{4272^2 - 216.6^2} - 3742.25 = 519 \text{ MVAR, inductive.}$$

The ratio of under-excited to over-excited MVAR's is

$$Q_0/Q_c = 519/748 = 0.694 \approx 0.7.$$

The rating of the synchronous condenser would be about 750 MVAR when delivering capacitive reactive power at over-excited condition of operation.

In order to use the circle diagram, a series of circles should be drawn with several chosen values of magnitude of E_s and picking values of compensation required at no load and full load. The value yielding a ratio of $m = Q_0/Q_c = 0.7$ will be the magnitude of the sending-end voltage, E_s.

12.6 CASCADE CONNECTION OF COMPONENTS–SHUNT AND SERIES COMPENSATION

In the previous sections, the (A, B, C, D) constants of only the line were considered. It becomes evident that through the example of the 750 kV line parameters, it is impossible to control the voltages within limits specified by IS and IEC by providing compensation at one end only by synchronous condensers, or by switched capacitors if the voltages are to vary over wider limits than discussed. In practice, shunt-compensating reactors are provided for no-load conditions which are controlled by the line-charging current entirely, and by switched capacitors for full-load conditions when the load has a lagging power factor.

Generalized Equations

For no-load conditions, $Z_t = \infty$, and the equations for sending-end and receiving-end voltages are, Figure 12.4,

$$E_r = E_s/[\cosh pL + (Z_0/Z_{sh})\sinh pL] \qquad \text{...(12.51)}$$

For simplicity, let $r = 0$. Then,

$$p = jw/v_0 = j2\pi/\lambda, Z_0 = Z_{00} = \sqrt{l/c}, Z_{sh} = jX_{sh},$$

so that $$E_s/E_r = \cos 2\pi L/\lambda + (Z_{00}/X_{sh})\sin 2\pi L/\lambda. \qquad \text{...(12.52)}$$

When the ratio E_s/E_r is given for a system, the value of X_{sh} is easily determined. In particular, when $E_s = E_r$,

$$Z_{sh} = Z_{00}/(\text{cosec } 2\pi L/\lambda - \cot 2\pi L/\lambda). \qquad \text{...(12.53)}$$

Example 12.11. For the 750-kV line of previous examples, $L = 500$ km, $\lambda = 6000$ km at 50 *Hz* and $Z_{00} = 260$ ohms. Assuming $E_s = E_r = 750$ kV, calculate the reactance and 3-phase MVAR required at load end in the shunt-compensating reactor. Neglect line resistance.

Solution. $2\pi L/\lambda = 30°$ at 6° per 100 km of length of line.

$\therefore \quad X_{sh} = 260/(\text{cosec } 30° - \cot 30°) = 3.73 \times 260 = 970$ ohms.

This is necessary at load end connected between line and ground so that there will be 3 such reactors for the 3-phases.

Current through each reactor $I_{sh} = 750/970\sqrt{3} = 0.4464$ kA.

$\therefore$ MVAR of each reactor per phase = 750 × 0.4464/ $\sqrt{3}$ = 193.3.

Total 3-phase MVAR at load end = 580 MVAR.

Chain Rule

For the reactor only, the generalized constants are given by, see Figure 12.4,

$$\begin{bmatrix} E_s \\ I_s \end{bmatrix} = \begin{bmatrix} 1, & 0 \\ -jB_{sh}, & 1 \end{bmatrix} \begin{bmatrix} E_r' \\ I_r' \end{bmatrix} \quad ...(12.54)$$

where $B_{sh} = 1/X_{sh}$ = admittance of each reactor per phase.

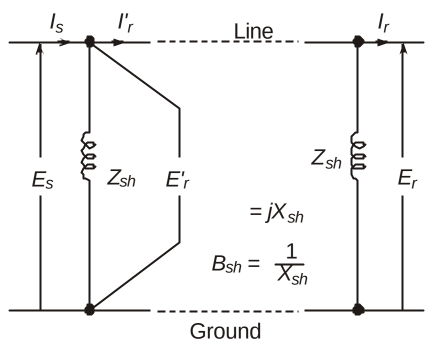

Fig. 12.4 Transmission line with shunt-reactor compensation for voltage control at no load.

If (E_s, I_s) refer to the input voltage and current from the source and (E_r, I_r) the output quantities at the load end, then the generalized constants (A_T, B_T, C_T, D_T) for the entire system is obtained by chain multiplication of the three matrices for the cascade-connected components. This is

$$\begin{bmatrix} A_T, & B_T \\ C_T, & D_T \end{bmatrix} = \begin{bmatrix} 1, & 0 \\ -jB_{sh}, & 1 \end{bmatrix} \begin{bmatrix} A, & B \\ C, & D \end{bmatrix}_{Line} \begin{bmatrix} 1, & 0 \\ -jB_{sh}, & 1 \end{bmatrix}$$

$$= \begin{bmatrix} A, & B \\ C, & D \end{bmatrix}_{Line} - jB_{sh} \begin{bmatrix} B, & 0 \\ 2A - jB_{sh}B, & B \end{bmatrix} \quad ...(12.55)$$

where A, B, C, D refer only to the line, equations (12.11) to (12.13). These are, in general, complex quantities whereas B_{sh} is a real number.

When once the total generalized constants (A_T, B_T, C_T, D_T) are calculated, the receiving-end power-circle diagram can be drawn and all requirements for compensation can be determined. The main requirement for the shunt reactors is control of voltage at no-load. For this case,

$$E_s = A_T E_r = (A - jB_{sh}B)E_r$$

$$\therefore \quad B_{sh} = (A - E_s/E_r)/jB = j(E_s/E_r - A)/B \quad ...(12.56)$$

For Example 12.11, for $E_s = E_r = 750$ kV,

$$B_{sh} = j(1 - 0.866)/j130 = 1.0308 \times 10^{-3} \text{ mho}$$

giving X_{sh} = 970 ohms.

12.6.1 Shunt Reactor Compensation of Very Long Line with Intermediate Switching Station

For very long lines, longer than 400 km at 400 kV, or at higher voltages, an intermediate station is sometimes preferable in lieu of series-capacitor compensation which will be discussed in the next section. Figure 12.5 shows the arrangement where each line section has the generalized constants $(A, B, C, D)_{Line}$, and each of the four shunt reactors has an admittance of $(-jB_{sh})$ and reactance (jX_{sh}). Then, by using the chain rule of multiplication, the total generalized constants (A_T, B_T, C_T, D_T) relating (E_s, I_s) with (E_r, I_r) will be as follows, upon using equation (12.55).

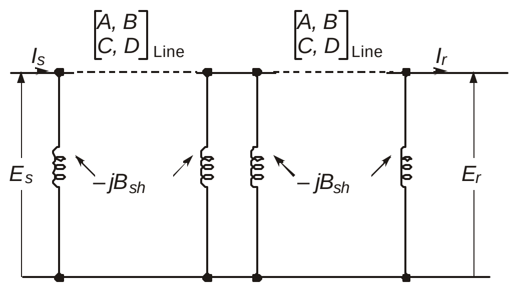

Fig. 12.5 Extra-long line with shunt reactors at ends and at an intermediate station.

$$\begin{bmatrix} A_T, & B_T \\ C_T, & D_T \end{bmatrix} = \begin{bmatrix} A - jB_{sh}B, & B \\ C - j2B_{sh}A - B_{sh}^2 B, & D - jB_{sh}B \end{bmatrix}^2$$

$$= \begin{bmatrix} A^2 + BC, & 2AB \\ 2AC, & A^2 + BC \end{bmatrix} - B_{sh}^2 B \begin{bmatrix} 2B, & 0 \\ 6A, & 2B \end{bmatrix}$$

$$- jB_{sh} \begin{bmatrix} 4AB & B^2 \\ 2BC + 4A^2 + 2B_{sh}^2 B^2, & 4AB \end{bmatrix} \quad ...(12.57)$$

For $B_{sh} = 0$, this reduces to

$$\begin{bmatrix} A_T, & B_T \\ C_T, & D_T \end{bmatrix}_{B_{sh}=0} = \begin{bmatrix} A^2 + BC, & 2AB \\ 2AC, & A^2 + BC \end{bmatrix} = \begin{bmatrix} A, & B \\ C, & D \end{bmatrix}^2 \quad ...(12.58)$$

The voltage and current at the intermediate station are

$$\begin{bmatrix} E_r' \\ I_r' \end{bmatrix} = \begin{bmatrix} A - jB_{sh}B, & B \\ C - j2AB_{sh} - B_{sh}^2 B, & D - jB_{sh}B \end{bmatrix} \begin{bmatrix} E_r \\ I_r \end{bmatrix} \quad ...(12.59)$$

Example 12.12. In example 12.11, shunt compensating reactors of 580 MVAR are provided at each end. Calculate the % compensation of charging MVAR provided by these shunt reactors. Neglect line resistance.

Solution. The generalized constants for the line are

$$A = 0.866,\ B = j130, \text{ and } C = j\frac{1}{Z_{00}}\sin 2\pi L/\lambda = j\frac{1}{260}\sin 30^\circ$$

$$= j1.923 \times 10^{-3} \text{ mho.}$$

∴ Charging MVAR of line without shunt reactors is

$$Q_0 = CE_s^2 = j1.923 \times 10^{-3} \times 750^2 = 1082 \text{ MVAR.}$$

With shunt reactors, with $B_{sh} = 1.0308 \times 10^{-3}$ mho, from equation (12.55),

$$C_T = C - j2A\,B_{sh} - B_{sh}^2 B = j(1.923 - 1.7854 - 0.138)10^{-3} \approx 0.$$

∴ % compensation is total or 100%.

Example 12.13. For the examples 12.11 and 12.12, instead of 580 MVAR, allow 60% shunt reactor compensation to maintain E_s = 750 kV. Calculate the MVAR of the shunt reactors at each end, and the voltage at the receiving end at no-load.

Solution. % compensation = 100 $(C - C_T)/C$, giving

$$C_T = (1 - 0.6)\ C = 0.4\ C = j0.4 \times 1.923 \times 10^{-3} \text{ mho}$$
$$= j0.7692 \times 10^{-3} \text{ mho.}$$

But $$C_T = C - j2A\ B_{sh} - B_{sh}^2 B,$$

or $j0.7692 \times 10^{-3} = j1.923 \times 10^{-3} - j2 \times 0.866 \times B_{sh} - j130\ B_{sh}^2$.

Solving the quadratic equation for B_{sh} results

$$B_{sh} = 0.6358 \times 10^{-3} \text{ mho.}$$

∴ 3-phase MVAR of each shunt-reactor bank at 750 kV will be

$$Q_{sh} = B_{sh}E_s^2 = 0.6358 \times 10^{-3} \times 750^2 = 358 \text{ MVAR.}$$

[Note that this may be approximately 60% of 580 MVAR which was required for 100% compensation.]

With these reactors connected, the receiving-end voltage will not be 750 kV. It is calculated as follows:

$$A_T = A - jB_{sh}\,B = 0.866 + 0.6358 \times 10^{-3} \times 130 = 0.9486.$$

∴ $$E_r = E_s/A_T = 790.6 \text{ kV.}$$

The compensation is a bit low since the bus voltage at the receiving end is higher than 765 kV, which is specified by *IS* and *IEC*. *If* E_r is to be held at 765 kV, then E_s must be lowered. Since A_T = 0.9486, E_s = 0.9486 × 765 = 726 kV. Then, the shunt-reactor rating will be

$$Q_{shs} = 726^2 \times 0.6358 \times 10^{-3} = 335 \text{ MVAR at the sending end,}$$

and $Q_{shr} = 765^2 \times 0.6358 \times 10^{-3} = 372$ MVAR at the receiving end.

A compromise of 350 MVAR would be selected and the voltages at the two ends adjusted.

Example 12.14. A 400-kV line is 800 km long. Its inductance and capacitance per km are l = 1 mH/km and c = 11.1 nF/km (Z_{00} = 300 ohms). The voltages at the two ends are to be held at 400 kV at no load. Neglect resistance. Calculate

(*a*) MVAR of shunt-reactors to be provided at the two ends and at an intermediate station midway with all four reactors having equal reactance.

(*b*) The *A, B, C, D* constants for the entire line with the shunt reactors connected.

(*c*) The voltage at the intermediate station. (Use 6°/100 km).

Solution. Refer to Figure 12.5 and equations (12.57) and (12.59). For one 400-km section:

(*a*) $A = D = \cos 24° = 0.9135$, $B = j300 \sin 24° = j122$ ohm and

$C = (\sin 24°)/300 = j1.356 \times 10^{-3}$ mho.

The total A_T from end to end for 800 km is

$$A_T = A^2 + BC - 2B_{sh}^2 B^2 - j4ABB_{sh}$$

$$= 0.669 + 445.8B_{sh} + 29{,}768B_{sh}^2 .$$

But since $E_s = E_r$, the value of $A_T = 1$.

By using this value of A_T and solving for B_{sh} yields $B_{sh} = 0.709 \times 10^{-3}$ mho. The MVAR of each of the reactors at the two ends will be

$$Q_e = 400^2 \times 0.709 \times 10^{-3} = 113.4 \text{ MVAR, 3-phase unit.}$$

(*b*) The *A, B, C, D* constants for the entire line are found as follows:

From equation (12.55), for each 400-km section,

$$A - jB_{sh}B = 0.9135 + 0.709 \times 10^{-3} \times 122 = 1$$

$$C - jB_{sh}(2A - jB_{sh}B) = j1.356 \times 10^{-3} - j0.709 \times 10^{-3} \times (1.827 + 0.709 \times .122)$$

$$= 0.$$

$$\therefore \quad \begin{bmatrix} A_T, & B_T \\ C_{T,} & D_T \end{bmatrix} = \begin{bmatrix} 1, & j122 \\ 0, & 1 \end{bmatrix}^2 = \begin{bmatrix} 1, & j244 \\ 0, & 1 \end{bmatrix}$$

(*c*) At the intermediate station, $E_r' = 1.E_s = 400\text{kV}$.

12.6.2 Series-Capacitor Compensation at Line Centre

In order to increase the power-handling capacity of a line, the magnitude of B must be reduced, as shown in equations (12.35) and (12.44). In normal practice, $\theta_b \approx 90^\circ$ and $\theta_a \approx 0$ for very low series line resistance. Therefore, $P = E_r E_s . \sin\delta / B$. We also observe that the value of B is very nearly equal to the series inductive reactance of the line so that by employing capacitors connected in series with the line, the power-handling capacity of a line can be increased for chosen values of E_s, E_r and δ. All these three quantities are limited from considerations of highest equipment voltages and stability limits. Usually, the series capacitor is located at the line centre when one capacitor only is used, or at the one-third points if two installations are used. On a very long line with intermediate station, the series capacitor can be located here. In this section we will only consider the generalized constants when a series capacitor is located at the line centre without intermediate shunt-reactor compensation. Thus, the system considered consists of equal shunt reactor admittances B_{sh} at the two ends and a capacitor with reactance x_c at the line centre, as shown in Figure 12.7.

For each half of the line section of length $L/2$,

$$A' = D' = \cosh\sqrt{ZY/4}, B' = Z_0 \sinh\sqrt{ZY/4},$$

$$C' = \frac{1}{Z_0}\sinh\sqrt{ZY/4} \qquad \text{...(12.60)}$$

where Z and Y refer to the total line of length L. The surge impedance is not altered even though the line length is halved.

For the series capacitor, Figure 12.6(*b*), the voltages and currents on the two sides are related by

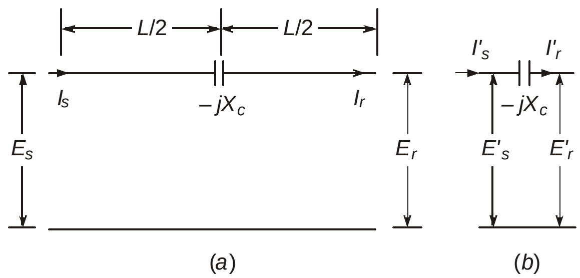

Fig. 12.6 Transmission line with series-capacitor compensation in middle of line.

$$\begin{bmatrix} E_s' \\ I_s' \end{bmatrix} = \begin{bmatrix} 1, & -jx_c \\ 0, & 1 \end{bmatrix} \begin{bmatrix} E_r' \\ I_r' \end{bmatrix} \quad \text{...(12.61)}$$

Thus, for the two half-sections of line with the capacitor separating them, the total generalized constants will be, by the chain rule of multiplication, (Figure 12.6*a*),

$$\begin{bmatrix} A_T, & B_T \\ C_T, & D_T \end{bmatrix} = \begin{bmatrix} \cosh\sqrt{ZY/4}, Z_0 \sinh\sqrt{ZY/4} \\ \dfrac{1}{Z_0}\sinh\sqrt{ZY/4}, \cosh\sqrt{ZY/4} \end{bmatrix} \begin{bmatrix} 1, & -jx_c \\ 0, & 1 \end{bmatrix} \times$$

$$\begin{bmatrix} \cosh\sqrt{ZY/4}, Z_0 \sinh\sqrt{ZY/4} \\ \dfrac{1}{Z_0}\sinh\sqrt{ZY/4}, \cosh\sqrt{ZY/4} \end{bmatrix} = \begin{bmatrix} \cosh\sqrt{ZY}, Z_0 \sinh\sqrt{ZY} \\ \dfrac{1}{Z_0}\sinh\sqrt{ZY}, \cosh\sqrt{ZY} \end{bmatrix}$$

$$-j\frac{x_c}{2Z_0}\begin{bmatrix} \sinh\sqrt{ZY}, Z_0(\cosh\sqrt{ZY}+1) \\ \dfrac{1}{Z_0}(\cosh\sqrt{ZY}-1), \sinh\sqrt{ZY} \end{bmatrix} \quad \text{...(12.62)}$$

$$= \begin{bmatrix} A, & B \\ C, & D \end{bmatrix}_{\text{Line}} - j\frac{x_c}{2Z_0}\begin{bmatrix} \sinh pL, Z_0(\cosh pL+1) \\ \dfrac{1}{Z_0}(\cosh pL-1), \sinh pL \end{bmatrix} \quad \text{...(12.63)}$$

With no series capacitor, $x_c = 0$, equation (12.63) reduces to the generalized constants of the line.

Shunt Reactors at Both Ends and Series Capacitor in Middle of Line

If shunt-compensating reactors of admittance B_{sh} are located at both ends of line, the total generalized constants with series capacitor located in the line centre can be obtained in the usual way by using the chain rule, from Figure 12.7. It is left to the reader to verify the result.

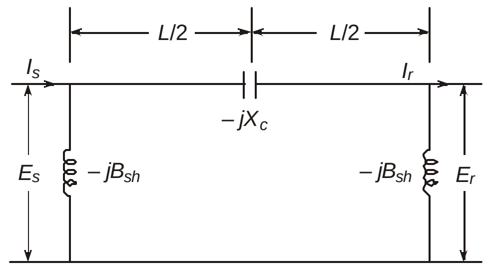

Fig. 12.7 Transmission line with series capacitor in middle and shunt reactors at ends.

$$\begin{bmatrix} A_T, & B_T \\ C_T, & D_T \end{bmatrix} = \begin{bmatrix} A, & B \\ C, & D \end{bmatrix}_{\text{Line}} - jB_{sh}\begin{bmatrix} B,0 \\ 2A - jB_{sh}B, B \end{bmatrix}$$

$$- j\frac{x_c}{Z_0}\begin{bmatrix} \sinh pL, \; Z_0(\cosh pL + 1) \\ \frac{1}{Z_0}(\cosh pL - 1), \sinh pL \end{bmatrix}$$

$$- \frac{x_c B_{sh}}{2}\begin{bmatrix} \cosh pL + 1, & 0 \\ \frac{2}{Z_0}\sinh pL - jB_{sh}(\cosh pL + 1), & \cosh pL + 1 \end{bmatrix} \quad ...(12.64)$$

We must point out that all quantities except x_c and B_{sh} are complex numbers with a magnitude and phase angle.

If shunt reactors are not used, $B_{sh} = 0$, then equation (12.64) reduces to (12.63). If no series capacitor is used, equation (12.55) results.

The value of capacitance is chosen such that its reactance amounts to a chosen percentage of the series inductive reactance of the line. For example, if 50% series capacitance is to be provided for a 800 km 400 kV line having a series inductive reactance of j 244 ohms, the capacitive reactance is $-j$ 122 ohms. The required capacitance will be $C = 1/wx_c = 26$ μF at 50 Hz. The power-handling capacity of a line with 50% series compensation will increase to double that without series capacitor.

While the power-handling capacity can be increased, series capacitor compensation results in certain harmful properties in the system, chief among them are:

(*a*) Increased short-circuit current. Note that for a short-circuit beyond the capacitor location, the reactance is very low. At the load-side terminal of the capacitor, a short-circuit will result in infinite current for 50% compensation.

(*b*) Sub-harmonic or sub-synchronous resonance conditions during load changes and short-circuits. This has resulted in unexpected failures to long shafts used in steam-turbine-driven alternators and exciters when one or more of the resulting sub-harmonic currents due to series compensation can produce shaft torques that correspond to one of the several resonance frequencies of the shaft, called torsional modes of oscillation or critical speeds. This aspect will be discussed in some detail and counter measures used against possible failure will be described in the next section.

12.7 SUB-SYNCHRONOUS RESONANCE IN SERIES-CAPACITOR COMPENSATED LINES

12.7.1 Natural Frequency and Short-Circuit Current

With series compensation used, the power-handling capacity of a single circuit is approximately

$$P = E_r E_s . \sin\delta / X_s \quad ...(12.65)$$

where $$X_s = X_L - X_c = X_L(1-m) \quad ...(12.66)$$

with $m = X_c/X_L$ = degree of compensation, and the reactances are at power frequency f_0. The approximation occurs because we have considered the series inductive reactance X_L to be lumped. At any other frequency f,

$$X_L(f) = 2\pi f L_L = \text{total inductive series reactance of line}$$

and $$X_c(f) = 1/2\pi f C = \text{series capacitive reactance of capacitor.}$$

∴ The resonance frequency occurs when $X_L(f_e) = X_c(f_e)$ giving

$$2\pi f_e L_L = 1/2\pi f_e C \quad ...(12.67)$$

We can introduce the power frequency f_0 by re-writing equation (12.67)

as $$(2\pi f_0 L_L)(f_e/f_0) = 1/[2\pi f_0 C.(f_e/f_0)] \text{ at resonance.}$$

Consequently,

$$(f_e/f_0)^2 = 1/(2\pi f_0 L_L).(2\pi f_0 C) = X_c/X_L = m\,. \quad ...(12.68)$$

Thus, the electrical resonance frequency is $f_e = f_0\sqrt{m}$ ...(12.69)

The reduction of series reactance also reflects as decrease in effective length to $L_e = (1-m)L$.

For f_0 = 50 Hz and 60 Hz, and for various degrees of series compensation, the following table gives the resonant frequencies and effective length which are also plotted in Figure 12.8.

$m = X_c/X_L$	0.1	0.2	0.3	0.4	0.5	0.6	0.7	0.8	0.9	1.0
% compensation	10	20	30	40	50	60	70	80	90	100
f_e/f_0	0.3162	0.447	0.548	0.632	0.707	0.775	0.837	0.894	0.949	1
f_e *for* 50*Hz*	15.8	22.4	27.4	31.6	35.36	38.7	41.8	44.7	47.4	50
f_e *for* 60*Hz*	18.97	26.8	32.9	37.95	42.4	46.5	50.2	53.7	56.9	60
$L_e/L = 1 - m$	0.9	0.8	0.7	0.6	0.5	0.4	0.3	0.2	0.1	0

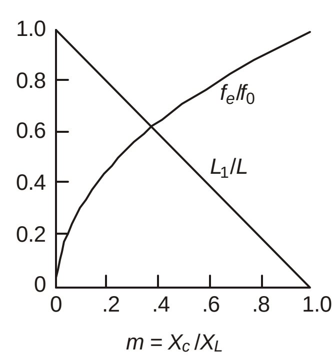

Fig. 12.8 Variation of resonance frequency f_e and effective length L_e of line with degree of series compensation (X_C/X_L).

For a single line with series compensation between 40% and 70%, the line can resonate at frequencies between 63.25% and 83.7% of the power frequencies. Any disturbance in the line giving rise to currents at these frequencies will increase the voltage across the series capacitor and therefore the line drop to extremely high values which are limited only by the line resistance. The voltage across the capacitor during normal operation is $V_c = X_c I$, where I = current flowing in line.

Example 12.15. A 50-Hz 750 kV line with l = 0.866 mH/km is 500 km long. It is provided with 50% series compensation connected in the middle of line. The power delivered at 750 kV is 2000 MW 3-phase per circuit at unity power factor. Neglect shunt capacitance and line resistance and assume the line inductance to be lumped. Calculate

(*a*) the reactance and capacitance of series capacitor,

(*b*) the voltage drop across it at full load,

(*c*) the current flowing through it and the voltage across it during a sustained short-circuit occurring

  (*i*) on the source-side terminal of the capacitor,

  (*ii*) on the load-side terminal of the capacitor, and

  (*iii*) across the load.

(*d*) the same as in (*c*) without the series capacitor.

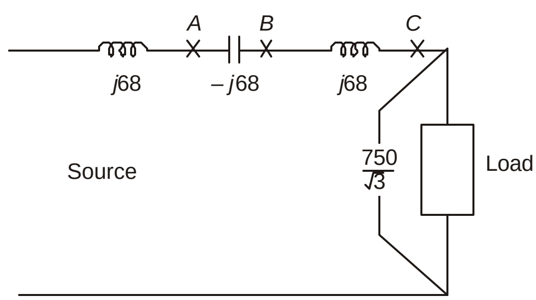

Fig. 12.9. Illustrating dangers of increased short-circuit currents with series-capacitor compensation for faults at various important locations.

Assume that no other generating area is supplying the load. See Figure 12.9.

Solution. Total series reactance of 250 km of line at 50 Hz is

$314 \times 0.866 \times 10^{-3} \times 250 = 68$ ohms.

(*a*) For 50% compensation, X_c = 68 ohms and C = 46.8 μF.

(*b*) At full load, $I = 2000/750\ \sqrt{3}$ = 1.54 kA = 1540 Amps.

∴ Voltage across capacitor V_c = 68 × 1.54 = 104.7 kV.

(*c*) (*i*) For a short-circuit to ground occurring at point A, the capacitor will discharge through the fault and its voltage will become zero. There will be an oscillatory stage consisting of a circuit with the capacitor, line reactance of j68 ohms and the load impedance.

(*ii*) For a short-circuit at point *B*, we observe that the steady-state component of current is infinity and dangerously high voltage will exist across the capacitor. Under such a condition, arrangements must be made to bypass the capacitor by a gap that will flashover at a preset overvoltage value. This is normally set at 2.2 p.u. where 1 p.u. voltage = voltage across capacitor during normal operation which was calculated as 104.7 kV. These protective schemes will be described later on.

(*iii*) When a short-circuit occurs at point *C*, the sustained r.m.s. value of current is

$$I_{sc} = 750/68\sqrt{3} = 6.368 \text{ kA} = 4.135 \times \text{full-load current.}$$

The voltage across the capacitor will be $V_c = 750/\sqrt{3} = 433\,\text{kV}$. This is the lowest value of voltage across the capacitor for a short-circuit occurring at any place on the line between points *B* and *C*.

(*d*) Without the series capacitor, the currents during short circuit at points *A* or *B* and *C* will be 6.368 kA and 3.184 kA respectively. Consequently, using a series capacitor has increased the short-circuit level of the system.

Protective Schemes for Series Capacitor

Some of the methods used in practice for protecting series capacitors from damage due to overvoltages and overcurrents are described below and shown in Figure 12.10. In some schemes, the capacitor banks are protected by a sparkover gap that will either short-circuit the capacitor or otherwise use a voltage-limiting surge arrester of the gap-SiC type or gapless ZnO type. When the short-circuit in the system is cleared, the capacitor is re-inserted in order to preserve the stability of the system. The re-insertion transient can be very high and cause gap flashover. This is prevented by either parallel resistor or SiC and ZnO arresters. The sparkover voltage of the gap *G* is between 2.2 and 3.5 p.u. of normal capacitor voltage at full rated current.

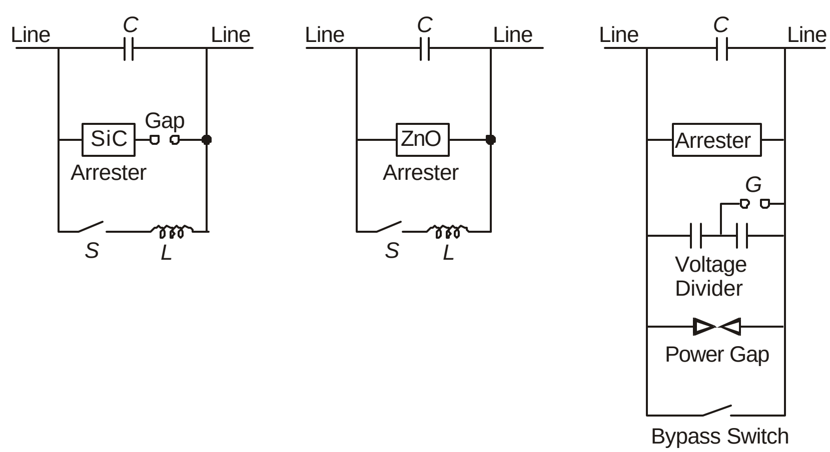

Fig. 12.10 Protective schemes for series capacitors during abnormal conditions.

12.7.2 Sub-Synchronous Resonance Problem and Counter Measures

As pointed out before, electrical resonance frequencies lower than synchronous frequency f_0 exist when series-capacitor compensation is used. The frequency f_0 corresponds to the steady-state speed of the rotor in large power stations. With steam-turbine-driven generating units (designated T.G. units), the shaft or shaft portions connecting the HP, IP, LP stages of the turbine and the generator-exciter are very long, with their own characteristic torsional mechanical resonant frequencies. When the electrical system operates in such a manner that the rotating fields in the generator due to sub-synchronous currents produce torques of the same frequency as one of the mechanical torsional frequencies of the shaft and of the correct phase, torques up to 10 times the break away or ultimate strength of the shaft can be reached resulting in shaft damage. This phenomenon of electromechanical interaction between electrical resonant circuits of the transmission system and the torsional natural frequencies of the T-G rotor is known as "Sub-Synchronous Resonance", and designated SSR.

The phenomenon of SSR has been studied very extensively since 1970 when a major transmission network in the U.S. experienced shaft failure to its T-G unit with series compensation in the 500 kV lines. This has now gone into technical literature as a classic problem and known as Project Navajo. The phenomenon, however, had been known to exist for a few years according to many experts who predicted such a phenomenon in series-compensated lines connected to T-G units. As a result of extensive study of Project Navajo, countermeasures to combat the SSR problem have been designed and are operating successfully. The SSR failure must therefore be considered as one of the governing factors in design of series-compensated lines when they are used for evacuating power from large thermal power stations. The combined cost of series-capacitor installation and the countermeasures is lower than the cost of additional transmission lines required when no series-compensation is used. We shall briefly describe the SSR problem and the countermeasures, since torque interactions in the generator belong to the realm of synchronous-machine theory which is outside the scope of this book.

Figure 12.11 (*a*) shows the torque and speed conditions in the generator which cause failure of the shaft, while conditions when countermeasures are taken to suppress the breaking torque are shown in Figure 12.11(*b*). Three distinct problems have been identified in SSR problem which are called

1. Induction Generator Effect,
2. Torsional Interaction, and
3. Transient Torque Problem.

The first two are known as steady-state problems while the last one occurs when system conditions change due to short-circuits and switching operations.

12.7.2.1 *Induction Generator Effect*

The electrical resonance frequencies, f_e, produce sinusoidal perturbations in the generator which are superimposed on the synchronously-rotating field at f_0. The resulting torque variation produced on the rotor is also sinusoidal and occurs at the same speed as the perturbing field. When the frequency of perturbation is $f_m = f_0 - f_e$, the torque perturbation is in phase with the speed perturbation. This phenomenon is called "negative damping" and is the main cause of SSR oscillations. During the SSR condition, a large current flows in the stator circuit giving rise to large torques.

Thus, at sub-synchronous frequencies causing resonance, the reactance of the system viewed from the generator terminals is zero and the resistance may be negative. This condition gives rise to self excitation of the oscillatory currents at this natural frequency and dangerous conditions will build up progressively. The shaft mechanical life is usually represented in graphical form as shown in Figure 12.11(*c*). If the magnitude of torque is below the level shown as ∞ , no damage to the shaft occurs and its life can be counted as infinity. However, if the torque oscillation exceeds the level marked 0, the fatigue life of the shaft becomes zero which indicates that the shaft will fail. This is also known as the "Once-in-a-Lifetime Torque Limit."

Normally, the long shaft of a T-G set consists of sections with varying dimensions, resulting in different values of stiffness and damping giving rise to several modes of torsional resonance frequencies. An example of the Navajo Project electrical and mechanical torsional frequencies are given in the table below.

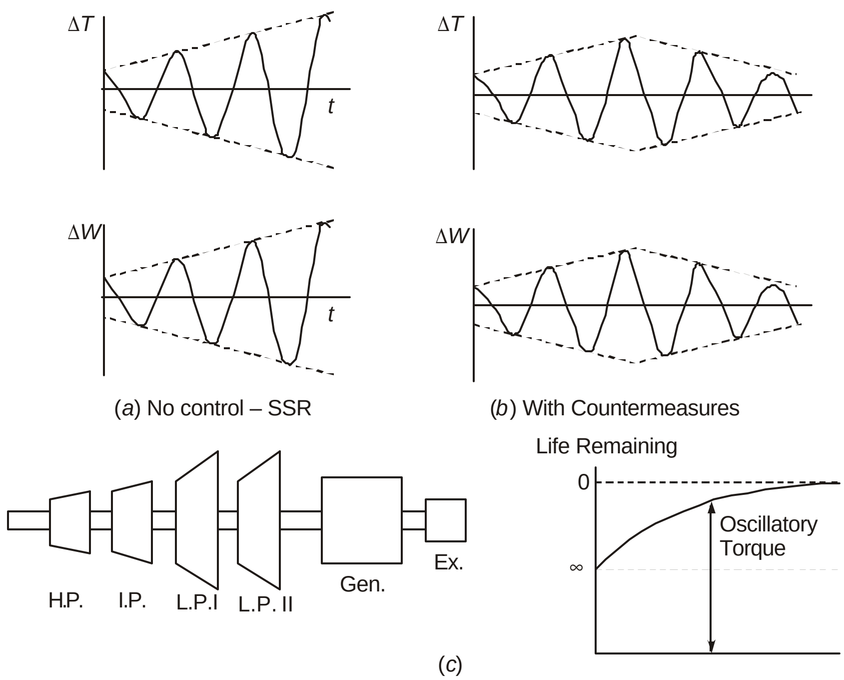

Fig. 12.11 Sub-synchronous Resonance condition.
(*a*) Variation of torque and angular velocity without counter measures.
(*b*) Same, with countermeasures.
(*c*) Life-strength of shafts of T-G units.

Electrical System

Natural Frequencies, f_e	44.5	43.5	30.7	28.3	25.5	10.5	10
Torsional Frequencies	44.2	39.8	34	26.7			6.8
Mode Number	1	2	3	4			5

Remedy for Countering Induction Generator Effect

The principles on which counter measures to combat the self-excitation problem and the resulting induction-generator effect are based on the following ideas:

1. *Addition of pole-face or amortisseur windings to reduce the rotor resistance* of generator at the sub-synchronous frequencies, which help to produce a net damping (positive resistance) at the slip frequencies. They are used in salient-pole generators to prevent hunting but are not normally used in cylindrical-rotor turbo-generators. But the SSR problem has shown the need for incorporating them in round-rotor generators also.
2. *Addition of series reactance in stator circuit.* This will help to detune the resonant network as viewed from the generator terminals. The leakage inductance of transformer can also be increased. However, the drawback of increased series reactance is the reduction of stability margin, and it is also not easy to design the large reactors required for the high load currents they have to carry.
3. *System switching and unit tripping*. During potentially dangerous SSR conditions, system switching can take the form of shorting the series capacitors as described in the previous section, or isolating the generator from the system by switching it to an uncompensated line if this is available in order that power flow is not interrupted. But this requires that the system must be designed for such a scheme, and withstanding the transients resulting from switching operations.
4. *Armature-current relay protection*. This relay senses the sub-synchronous-frequency armature currents in the range of 25% to 75% of power frequency at a level of 5% of rated current, when these frequencies are known to cause *SSR* danger. The relay will trip the generator under sustained sub-synchronous oscillations. There must be a further discrimination for current level or torque changes that take place under low magnitude sustained conditions and high level changes under fault conditions. These may vary from 1% of rated current under sustained conditions to 300% under faults.

12.7.2.2 *Torsional Interaction*

Dangerous conditions for a shaft exist when an electrical resonance frequency or minimum reactance occurs very near one of the natural torsional modes of the T-G shaft. These frequencies are the eigenvalues of the spring-mass-damping model of the electro-mechanical system equations. The analysis of this problem is considered beyond the scope of this book, since the mechanical damping inherent in the turbine increases when loaded and therefore the problem is non-linear. Torsional interaction takes place at an electrical resonance frequency which is near the complement of a torsional resonant frequency, that is, complement frequency = synchronous frequency f_0 – torsional resonance frequency f_m. When this condition exists, even a small voltage generated by the oscillating rotor can give rise to large SS current in the stator resulting in large undamped torques which keep growing.

Solution to Problem

1. *Dynamic Stabilizer*. This is a shunt reactor controlled by thyristors whose value is modulated by the oscillatory currents in the stator, or the rotor velocity deviations. The reactor introduces enough current in the armature at the critical sub-synchronous frequency so as to cancel the current resulting from the transmission system with its series capacitor.

2. *Reduction in Series-Capacitor Compensation or Complete Removal*. The flashing of gaps across the series-compensation capacitor prevents the dangerous condition.
3. *Filters*. Filters in series with the generator increase the effective circuit resistance. These are known as Line Filters. They have to carry the full load current.

However, static blocking filter connected at the neutral end of the h.v. winding of the generator-transformer offers a better solution. The scheme is shown in Figure 12.12. The *N* separate filters in series are each tuned in parallel resonance to block current at the offending frequency giving rise to the torsional modes. The resistances of the filters are in the range 200 to 600 ohms and have high *Q*.

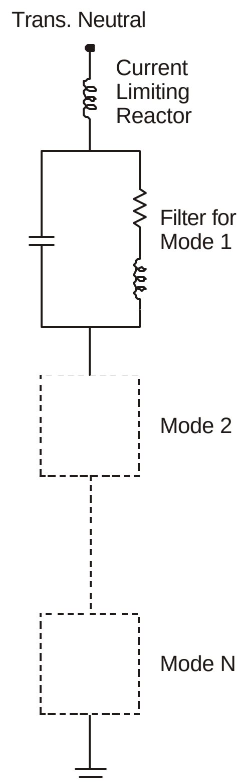

Fig. 12.12 Filters used at transformer neutral for blocking sub-synchronous currents.

This can also be augmented by a device known as Excitation Damping Control which acts on the Automatic Voltage Regulator by injecting a sinusoidal signal of proper phase which is obtained from a rotor-motion sensor.

4. *Other Remedies*. Except for pole-face amortisseur windings, all countermeasures used for eliminating the induction generator effect also help to reduce the torsional-interaction problem. In addition, a torsional-motion relay is used to detect excessive mechanical stresses in the shaft. This picks up signals from toothed wheels and proximity magnetic pick-ups at each end of the shaft. Filters are used to convert these signals proportional to the modal oscillations. It acts as a back-up protection as

it is too slow in action. Its main function is to trip the generator in the event of excessive sustained torques.

12.7.2.3 *Transient Torque Problem*

Dangerous transient torques are obtained during faults in the system or when making switching operations to change system configuration. Two types of fault conditions must be considered for their relative severity, as shown in Figure 12.13.

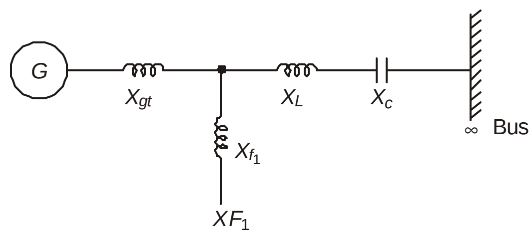

(*a*)

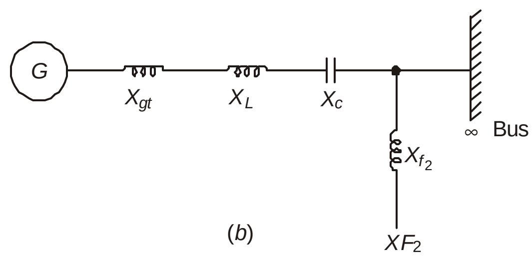

(*b*)

Fig. 12.13 Sub-synchronous conditions during faults on a system giving rise to transient torques of large amplitude.

In Figure 12.13(*a*) a fault occurs on the generator side of the transmission line. In this case the series capacitor will be charged to high voltage by the infinite bus. Before the fault occurs the natural frequency f_e is determined by X_{gt}, X_L and X_c of the generator-transformer, line, and the capacitor. This could be a complement to a rotor torsional mode frequency f_n, that is $f_e + f_n = f_0$ or $f_n = f_0 - f_e$, where f_0 = average synchronous frequency (50 or 60 Hz). When the fault is cleared, the capacitor will discharge partly through the generator at frequency f_e to produce an amplified torque.

On the other hand, referring to Figure 12.13 (*b*), if a fault occurs at F_2 on the infinite-bus side, sub-synchronous current will flow into the fault and until the fault is cleared, torque amplification occurs. This case is worse than the previous case of fault at F_1. Nearly 10 times the once-in-a-lifetime torque level (0 life-time in Figure 12.11 (*c*)) may be reached. In general, transient torques are large-amplitude problems and very sudden.

Remedy for Transient Torque Problem

Transient torques can be controlled by some of the schemes described before. These are: (*a*) Static Blocking Filter; (*b*) Series Line Filter; (*c*) Tripping the Generator or Unit Tripping

Scheme; (*d*) Increased Series Reactance; and (*e*) Flashing the Series Capacitor which will also decrease the short-circuit current magnitude.

12.7.2.4 *Summary of SSR Problem and Countermeasures*

In series-capacitor compensated systems, electrical resonant frequencies below the synchronous frequency exist which lie in the range of torsional frequencies of the T-G shaft. These cause electro-mechanical sub-synchronous frequency oscillation leading to shaft failure in one of the several modes of excitation. Three types of SSR problems exist: (1) Induction Generator Effect caused by self-excitation and negative damping; (2) Torsional Interaction when the electrical resonant frequency is the complement of one of the torsional frequencies; (3) Transient Torque problems occurring during system faults and switching operations.

The remedies or countermeasures utilized in removing the shaft-failure problem may consist of the following five categories:

(1) *Filtering and Damping*: These utilize

(*a*) Static Blocking Filter, (*b*) Line Filter, (*c*) Bypass Damping Filter, (*d*) Dynamic Filter, (*e*) Dynamic Stabilizer, (*f*) Excitation System Damper.

(2) *Relaying and Detecting*: These are

(*a*) Torsional Motion Relay, (*b*) Armature Current Relay, (*c*) Torsional Monitor.

(3) *System Switching and Unit Tripping.*

(4) *Modification to Generator and System:* These include

(*a*) T-G modifications for new units altering stiffness, inertia and damping of rotors, (*b*) Generator Series Reactance, (*c*) Pole-Face Amortisseur Winding.

(5) *Removal or Short-Circuiting the Series Capacitor*

This is already provided in the system during normal course for limiting short-circuit currents in the system.

12.8 STATIC REACTIVE COMPENSATING SYSTEMS (STATIC VAR)

In the previous section, one type of reactor compensation for countering SSR was mentioned as a Dynamic Filter which uses thyristors to modulate the current through a parallel-connected reactor in response to rotor speed variation. The advent of high-speed high-current switching made possible by thyristors (silicon-controlled-rectifiers) has brought a new concept in providing reactive compensation for optimum system performance. Improvements obtained by the use of these static var compensators (SVC) or generators (SVG) or simply static var systems (SVS) are numerous, some of which are listed below:

1. When used at intermediate buses on long lines, the steady-state power-handling capacity is improved.
2. Transient stability is improved.
3. Due to increased damping provided, dynamic system stability is improved.
4. Steady-state and temporary voltages can be controlled.
5. Load power factor can be improved thereby increasing efficiency of transmission and lowering of line losses.
6. Damping is provided for SSR oscillations.

7. Overall improvement is obtained in power-transfer capability and in increased economy.
8. The fast dynamic response of SVC's have offered a replacement to synchronous condensers having fast excitation response.

In principle, when the voltage at a bus reduces from a reference value, capacitive Vars have to be provided, whereas inductive Vars are necessary to lower the bus voltage. Figure 12.14 shows schematically the control characteristics required and the connection scheme. The automatic voltage regulator AVR provides the gate pulses to the proper thyristors to switch either capacitors or inductors. The range of voltage variation is not more than 5% between no load and full load.

Many schemes are in operation and some of them are shown in Figure 12.15 and described below.

12.8.1 SVC Schemes

1. *The TCR-FC System* (Figure 12.15 (*a*)).

This is the Thyristor Controlled Reactor-Fixed Capacitor system and provides leading vars from the capacitors to lagging vars from the thyristor-switched reactors. Because of the switching operation, harmonics are generated. Since there are 6 thyristors for the 3-phases, 6-pulse harmonics are generated in addition to the 3rd. These must be eliminated if they are not to affect normal system operation.

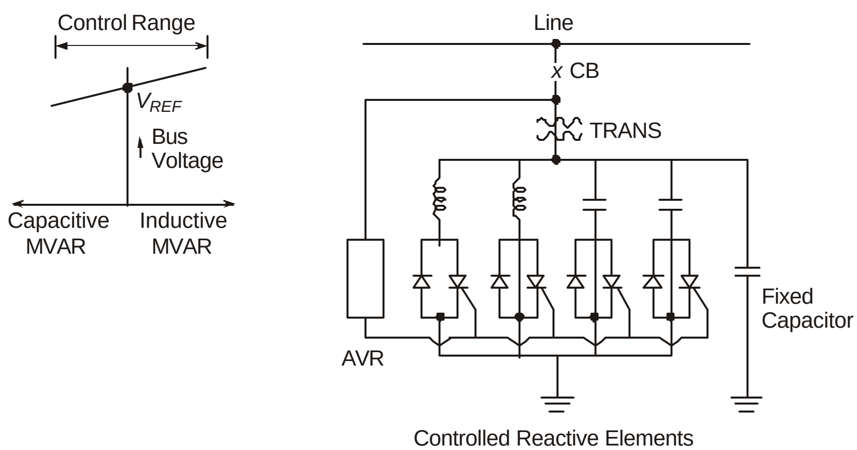

Fig. 12.14 General circuit of Static Var Systems with controlled reactive elements and control range exercised.

This can be improved by using a large number of small reactors to reduce harmonics which normally depend on the reactor size. However, it requires correspondingly larger number of thyristor switches. This is known as segmented TCR-FC.

By using two transformers, one in Y/Δ and the other in Y/Y, and dividing the fixed capacitors and controlled reactors into two groups, 12 thyristors can be used in a 12-pulse configuration. The lowest harmonic will be the 12th (600 Hz or 720 Hz in 50 or 60 Hz system). It introduces complications in transformer design, and requires more thyristors. The gate-firing angle control is made more difficult because of the 30° phase shift between the secondary voltages of the Y/Δ and Y/Y transformers.

(2) *The TCT Scheme* (Thyristor Controlled Transformer)

A transformer of special design with almost 100% leakage impedance is controlled on the secondary side by thyristor switches. By connecting the 3 phases in Δ, 3rd harmonics are eliminated. This system has better over-load capacity and can withstand severe transient overvoltages. But it is more expensive than TCR scheme. See Figure 12.15(*b*).

(3) *TSC-TCR Scheme* (Figure 12.15)(*c*))

This is Thyristor Switched Capacitors and Thyristor-Controlled Reactors, It has TCR's and capacitance changed in discrete steps. The capacitors serve as filters for harmonics when only the reactor is switched.

(4) *MSC-TCR Compensator Scheme*

This is the Mechanically Switched Capacitor-Thyristor Controlled Reactors scheme. It utilizes conventional mechanical or SF_6 switches instead of thyristors to switch the capacitors. It proves more economical where there are a large number of capacitors to be switched than using TSC (thyristor-switched capacitors). The speed of switching is however longer and this may impair transient stability of the system.

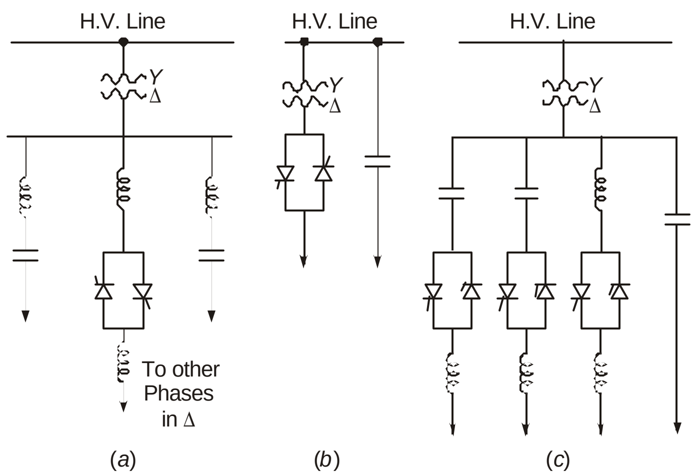

Fig. 12.15 Different types of Static Var Compensators.
(*a*) TCR-FC System, (*b*) TCT scheme, (*c*) TSC-TCR scheme

(5) *SR Scheme* (Saturated Reactor)

In some schemes for compensation, saturated reactors are used. Fixed capacitors are provided as usual. A slope-correction capacitor is usually connected in series with the saturated reactor to alter the B-H characteristics and hence the reactance.

General Remarks

In all SVC schemes, harmonics generated by the switching operation are very important from the point of view of telephone and other types of interference, for example, signals. Filters are therefore an integral part of these Var compensating schemes. Fast-action of these SVC schemes with proper protection can offer great advantages in controlling voltages under load rejection. Most modern schemes utilize fibre optics for gate firing.

The current-voltage relationships as a function of firing angle are shown in Figure 12.16(*a*) and (*b*) for switched reactors and capacitors respectively.

A complete 3-phase bank of switched reactor or capacitor connected in Δ is schematically shown in Figure 12.16, which eliminates triplen harmonics.

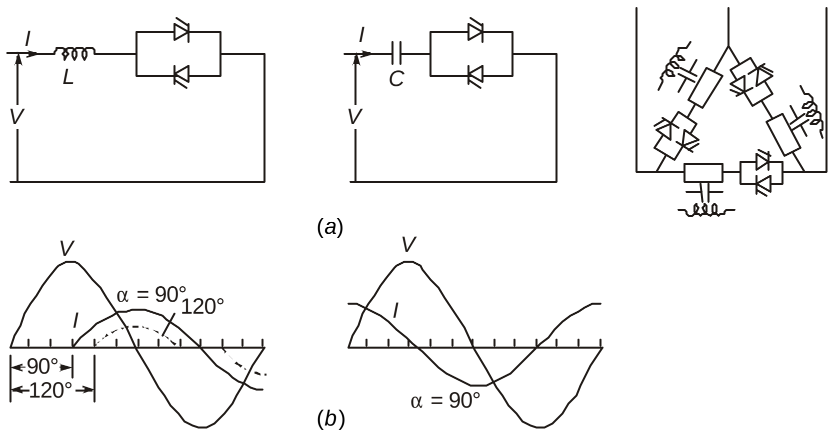

Fig. 12.16. Voltage-current relationships in switched reactor and capacitor with variation in firing angle α.

12.8.2 Harmonics Injected into Network by TCR

Figure 12.17 shows filter capacitors and the TCR's connected to the low-voltage winding of a step-down transformer. This may be a 2-winding or in most cases a 3-winding transformer having primary, secondary and low-voltage tertiary. We will analyse the problem of harmonic generation, filter design and the resulting harmonic injection into the system through the transformer windings. When the TCR's are connected in Δ, the 3rd harmonic and its multiples are eliminated. The low-voltage winding feeding the TCR's may be connected either in Δ or *Y* as shown in Figure 12.18. The harmonics present are therefore of orders 5, 7, 11, 13, etc., that is ($2n \pm 1$) times the fundamental where $n = 3k$, $k = 1, 2, 3, \ldots$ This gives rise to both positive-sequence and negative-sequence currents.

The amplitude of a harmonic depends entirely on the firing angle of the thyristors, denoted by α. Since the current is purely inductive, it will lag behind the transformer voltage by 90° in so far as the fundamental is concerned. For full conduction, $\alpha = 90°$ from a voltage zero. Figure 12.19 shows the relation between voltage and current for $\alpha = 90°$ and for $\alpha > 90°$. When $\alpha = 90°$, no harmonics are generated, obviously. For a general value of α, the fundamental component of current is

$$I_1 = \frac{2}{\pi} I \int_{\alpha}^{\pi-\alpha} \sin\theta . \sin\theta d\theta = \frac{2}{\pi} I \left[\pi - \alpha - \frac{1}{2} \sin 2(\pi - \alpha)\right] \quad \ldots(12.70)$$

When $\alpha = \pi/2, I_1 = I$ in equation (12.70) so that the value I can be considered as the amplitude of the fundamental when the reactors are conducting fully over the entire cycle.

When α changes, the amplitude of fundamental also changes, which is as shown in the following table and calculated from equation (12.70):

α =	90°	105°	120°	135°	150°	165°	180°
I_1/I =	1	0.674	0.391	0.182	0.058	0.0075	0

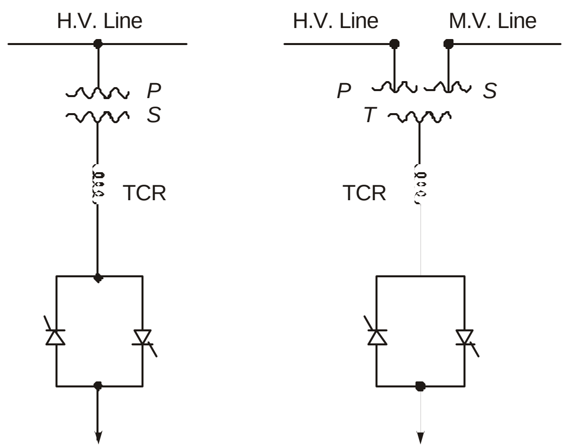

Fig. 12.17 Harmonic injection by TCR into a high-voltage system through 2-winding and 3-winding transformers.

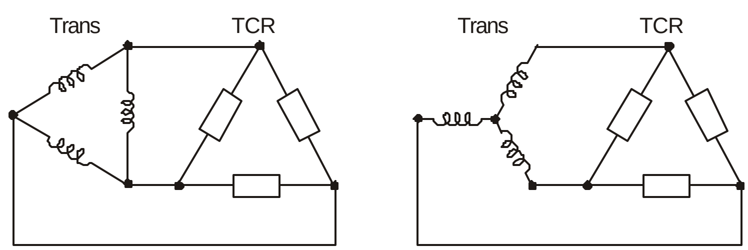

Fig. 12.18 Connection of TCR to Δ and Y-connected transformer windings.

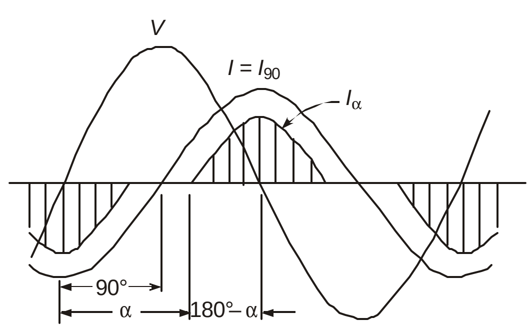

Fig. 12.19 Voltage waveform and current waveforms for $\alpha = 90°$ (full conduction of TCR) and $\alpha > 90°$, for calculation of harmonics. (I_{90} = current under full conduction of thyristor and no harmonics).

***n*-th harmonic**

The n-th harmonic of current generated by the switching operation is given by

$$I_n = \frac{2}{n\pi} I \int_{\alpha}^{\pi-\alpha} \sin\theta . \sin n\theta . d\theta$$

$$= \frac{2I}{n\pi}\left[\frac{1}{n+1}\sin(n+1)\alpha - \frac{1}{n-1}\sin(n-1)\alpha\right]$$

or $$= \frac{2I}{n\pi}\left[\frac{1}{n-1}\sin(n-1)(\pi-\alpha) - \frac{1}{n+1}\sin(n+1)(\pi-\alpha)\right] \quad ...(12.71)$$

Because the reactor has n times the reactance for the n-th harmonic as compared to its value for the fundamental, the factor n is introduced in the denominator. Now, as α is changed the amplitude of the n-th harmonic generated also changes so that there is a particular value α_{mn} for α at which the amplitude of the n-th harmonic attains maximum value. This is obtained by letting $dI_n/d\alpha = 0$ and solving for α thus:

$$dI_n/d\alpha = (2I/n\pi)[\cos(n+1)(\pi-\alpha) - \cos(n-1)(\pi-\alpha)] = 0 \quad ...(12.72)$$

$$\therefore \quad \cos(n+1)(\pi-\alpha) = \cos(n-1)(\pi-\alpha), \quad ...(12.73)$$

and furthermore, since n is an odd integer, there is

$$\cos(n+1)\alpha_{mn} = \cos(n-1)\alpha_{mn}$$

or, $$\sin n\,\alpha_{mn} \times \sin\alpha_{mn} = 0. \quad ...(12.74)$$

Consequently,

either $$\sin n\,\alpha_{mn} = 0 \text{ giving } \alpha_{mn} = j\pi/n, \alpha_{mn} > 90° \quad ...(12.75)$$

or, $$\sin\alpha_{mn} = 0 \text{ giving } \alpha_{mn} = j\pi, \quad ...(12.76)$$

where j = an integer = 0, 1, 2,... Also, since $j\pi/n > \pi/2$ from equation (12.75) we obtain $j > n/2$, where n = harmonic order.

For various harmonic orders, the following table gives the values of firing angles α_{mn} in order to achieve maximum amplitude of that harmonic current.

n	5	7	11	13	17	19
j	3	4	6	7	9	10
α_{mn}	$3\pi/5$	$4\pi/7$	$6\pi/11$	$7\pi/13$	$9\pi/17$	$10\pi/19$
$(j\pi/n)$	108°	102.9°	98.2°	96.9°	95.3°	94.7°

For $\alpha = \pi/2 = 90°$, then n-th harmonic current $I_n = 0 (n \neq 1)$ so that no harmonics are generated for full conduction of the thyristors. However, since the firing angle changes continuously the condition $\alpha = 90°$ does not exist all the time and so harmonics are continuously generated and injected into the connected system. However, the reactive power generated by the TCR is due only to the fundamental component of current and the voltage. This is, by using equation (12.70),

$$Q_\alpha = 3\frac{1}{\sqrt{2}} I_1 V_{ph} = \frac{3\sqrt{2}}{\pi}\left[\pi - \alpha - \frac{1}{2}\sin 2(\pi-\alpha)\right] I\,V_{ph}$$

$$= 1.35\left[\pi - \alpha - \frac{1}{2}\sin 2(\pi - \alpha)\right] I\,V_{ph}$$

$$= 0.78\left[\pi - \alpha - \frac{1}{2}\sin 2(\pi - \alpha)\right] I\,V_{l-l} \qquad ...(12.77)$$

When the values of $\alpha_{mn} = j\pi/n$ are substituted in equation (12.71) for I_n, the amplitude of the n-th harmonic is

$$I_n, \alpha_{mn} = \frac{2I}{n\pi}\left[\frac{1}{n+1}\sin(n+1)\alpha_{mn} - \frac{1}{n-1}\sin(n-1)\alpha_{mn}\right] \qquad ...(12.78)$$

The following table gives values of $(I_n, \alpha_{mn}/I)$ for various harmonics according to equation (12.78):

n	5	7	11	13	17	19
α_{mn}	$3\pi/5$	$4\pi/7$	$6\pi/11$	$7\pi/13$	$9\pi/17$	$10\pi/19$
$(I_n, \alpha_{mn}/I)$	0.0505	0.0259	0.0105	0.0075	0.0044	0.00

Thus, if no filters are used the 5-th harmonic injected into the network reaches 5.05% of the fundamental (or a little over 5% of current I obtain for $\alpha = 90°$ or full conduction). Usually such high values of harmonics are not permitted. A maximum limit set by power utilities is more like $(5/n)$ where n is the harmonic order. Therefore, under such a restriction taken as example , the 5th harmonic should be kept below 1%, the 7th harmonic below (5/7)% = 0.715% of the maximum amplitude of the fundamental occurring at full conduction, $\alpha = 90°$. Note that without a filter the 7th harmonic injected into the system is 0.0259 = 2.59% instead of 0.715%. We will now consider the problem of suppressing some harmonics injected into the system by using suitable filters.

12.8.3 Design of Filters for Suppressing Harmonics Injected into the System

Figure 12.20 shows a schematic diagram of a possible series L-C filter used for offering low impedance to any desired harmonic current of order n. The equivalent circuit referred to the high-voltage side is as shown in Figure 12.20(b). The harmonic current generated by the TCR is shown as a current source I_n. The transformer and line reactances are x_t and x_l, respectively, at the fundamental frequency of the system. Therefore, at the harmonic frequency $(n\omega_0)$ where $\omega_0 = 2\pi f_0$, the angular frequency at the fundamental frequency f_0, the filter impedance is

$$x_F = x_{FL} + x_{FC} = n\omega_0 L - 1/n\omega_0 C \qquad ...(12.78)$$

∴ The current injected into the line is, neglecting resistances,

$$I_1 = jx_F I_n/[j(x_F + x_t + x_l)] = \frac{n\omega_0 L - 1/n\omega_0 C}{n(\omega_0 L + x_t + x_l) - 1/n\omega_0 C} I_n \qquad ...(12.79)$$

Here, all quantities are referred to the same voltage level.

Let $\eta = \dfrac{I_l}{I_n} \times 100 = \%I_l$ in terms of the generated I_n. Then the required value of capacitor can be found out for a set limiting value η for the harmonic. In the previous section this limit was taken to be $(5/n)\%$. If a = turns ratio of the transformer, then

$$\frac{\eta}{100} = \frac{(n\omega_0 L_F - 1/n\omega_0 C_F)a^2}{n(\omega_0 L_F a^2 + x_t + x_l) - a^2/n\omega_0 C_F} \quad \text{...(12.80)}$$

where L_F, C_F = actual values of filter inductance and capacitance connected to the low-voltage winding of the step-down transformer, and x_t, x_l are actual values of transformer and line reactances referred to the high-voltage side at the fundamental frequency f_0 or angular frequency ω_0. Examples will make clear the design and operation of the filter for a given simple system.

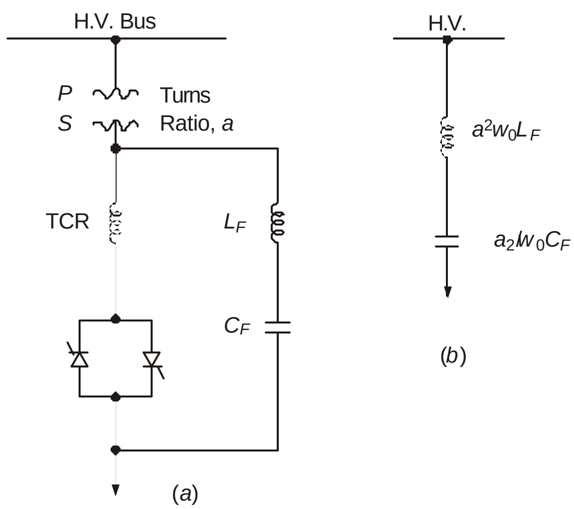

Fig. 12.20 Arrangement of TCR and filter for suppression of harmonics.
(*a*) Actual connection to transformer secondary.
(*b*) Inductive and capacitive reactances referred to primary by turns ratio *a*.

Example 12.16. A 100 MVA 230 kV 50 Hz transformer has x_t = 12% and is connected to a line 200 km long which has an inductance of 1 mH/km. The filter, connected to the l.v. 33 kV side of the transformer, is required to suppress the 5-th harmonic generated by the TCR to 1% of I_n. Calculate the value of filter capacitor if the filter inductance used is 2 mH.

Solution. The given data are:

$x_t = 0.12 \times 230^2/100 = 63.48$ ohms

$x_l = 314 \times 0.2 = 62.8$ ohms

$a = 230/33 = 6.97$

$\omega_0 L_F = 314 \times 2 \times 10^{-3} = 0.628$ ohm at 50 Hz.

$\eta = 1\% = 0.01.$

n = 5-th harmonic = 5.

$\therefore$ From equation (12.80)

$$0.01 = \frac{(5 \times 0.628 - 1/1570 C_F)6.97^2}{5(0.628 \times 6.97^2 + 63.48 + 62.8) - 6.97^2/1570 C_F}$$

Let $K = 1/1570\ C_F$, the reactance of filter capacitor for the 5-th harmonic frequency of 250 Hz. Then,

$$0.01 = (3.14 - K)\ 48.58/(783.944 - 48.58K),$$

giving $K = 3.0103$ and $C_F = 10^6/(1570 \times 3.0103)$, μF = 211.6 μF.

Example 12.17. Using the values of filter inductance and capacitance of the previous example which have limited the 5-th harmonic injected into the line to 1% of the generated 5-th harmonic:

(*a*) Calculate the 7-th harmonic injected into the line;

(*b*) If the 7-th harmonic generated by the TCR = 2.586% of fundamental, as calculated for the value of $\alpha_{mn} = 4\pi/7 = 102.9°$ in the previous section, calculate the % of 7-th harmonic injected into the line on base of fundamental current I obtained when the firing angle $\alpha = 90°$.

Solution. Note that the capacitive reactance is now 5/7-th of that at the 5-th harmonic frequency.

$$I_l/I_7 = \frac{(7 \times 0.628 - 5 \times 3.0103/7)6.97^2}{7(0.628 \times 6.97^2 + 63.48 + 62.8) - 6.97^2 \times 3.0103 \times 5/7}$$

$$= 0.11.$$

Therefore, of the 7-th harmonic generated by the TCR 11% enters the line through the transformer and the filter absorbs the remaining 89%. Note that while the filter was designed to limit the 5-th harmonic injected into the line to 1% of the amplitude of 5-th harmonic generated, it has allowed 11% of the 7-th harmonic generated into the line.

(*b*) Since the 7-th harmonic generated is 2.59% of the fundamental, the resulting 7-th harmonic current injected into the line is 2.59 × 0.11 = 0.2845% of the fundamental amplitude.

Note that if the limiting value of any harmonic injected into the line is set at say $(5/n)$% of the fundamental, then the allowable 7-th harmonic content injected into the line would be (5/7)% = 0.715%. Therefore, in this example, the filter has kept the 7-th harmonic to 0.2845%, which is below the specified limit. Thus the filter is quite effective for both the 5-th and the 7th harmonics.

Example 12.18. A 3-winding 400 kV/220 kV/33 kV transformer with grounded wye/grounded wye/delta connection has ratings of 250 MVA, 200 MVA, and 50 MVA for the primary, secondary and tertiary, respectively. The equivalent Y circuit representation of the leakage reactances of the three windings referred to the 400-kV winding and 250 MVA are $Z_p = j0.0375$ p.u., $Z_s = j0.0625$ p.u., and $Z_t = j0.0625$ p.u.

The line connected to the 400 kV side is 400 km long and the 220-kV winding is connected to a line of 200 km in length. Both lines have a series inductance of 1 mH/km. Line resistances are negligible.

The filter connected to the tertiary 33 kV winding has filter inductance of 2 mH and capacitance of 200 μF. These are in series and the combination is connected in parallel with the TCR's.

(*a*) Draw the equivalent circuit of the transformer windings and line inductive reactances including the filter referred to the 400-kV side on base of 400-kV and 250-MVA for the fundamental frequency.

(*b*) Draw the equivalent circuit for the 5-th harmonic of current generated by the switched TCR.

(*c*) Calculate the % of 5-th harmonic currents injected into the 400-kV and 220-kV lines through the transformer windings.

Solution. The base impedance on 400-kV and 250-MVA is $Z_{B400} = 400^2/250 = 640$ ohms. Referred to the 220-kV side, $Z_{B220} = 220^2/250 = 193.6$ ohms, and for the 33-kV side, $Z_{B33} = 33^2/250$ = 4.356. Reactances at fundamental frequency (50 Hz):

Lines: $400\text{ kV} - x_{l400} = j314 \times 1 \times 10^{-3} \times 400/640 = j0.196$ p.u.

$220\text{ kV} - x_{l220} = j314 \times 1 \times 0^{-3} \times 200/193.6 = j0.243$ p.u.

Filter: $x_{LF} = j314 \times 2 \times 10^{-3}/4.356 = j0.144$ p.u.

$x_{CF} = -j10^6/314 \times 200 \times 4.356 = -j3.655$ p.u.

(*a*) The equivalent circuit for the fundamental frequency is shown in Figures 12.21(*a*) and (*b*).

(*b*) Equivalent circuit for 5-th harmonic:

For the 5-th harmonic current, all inductive reactances calculated above are multiplied by 5, while the filter capacitive reactance is divided by 5. The resulting equivalent circuit is shown in Figures 12.21(*c*) and (*d*).

(*c*) The generated harmonic current is shown as the current source. This divides into two parts, one part flowing through the tertiary winding connected to the other two transformer windings and the two lines, while the remaining part is absorbed by the filter. The current injected into the tertiary is consequently from the equivalent circuit of Figure 12.21(*d*),

$$I_1 = \frac{-j(0.731 - 0.72)}{-j0.011 + j0.3125 + \dfrac{j1.1675 \times j1.5275}{j1.1675 + j1.5275}} \times I_5$$

$$= (-0.011/0.9632)\, I_5 = -0.0114\, I_5.$$

This can be further divided into the 400-kV and 220-kV lines as follows:

$$I_{400} = \frac{1.5275}{1.5275 + 1.1675} |I_1| = 0.567\,|I_1| = 0.00646\,|I_5|$$

$$= 0.646\% \text{ of } I_5.$$

$$I_{220} = (0.0114 - 0.00646)\, I_5 = 0.00494\, I_5 = 0.494\% \text{ of } I_5.$$

Note further that the maximum amplitude of the 5-th harmonic is 5.05% of fundamental generated by the TCR so that the filter has been quite effective in keeping the 5-th harmonic injected into the two lines much less than (5/*n*)%, if this is the limit set by the power utility.

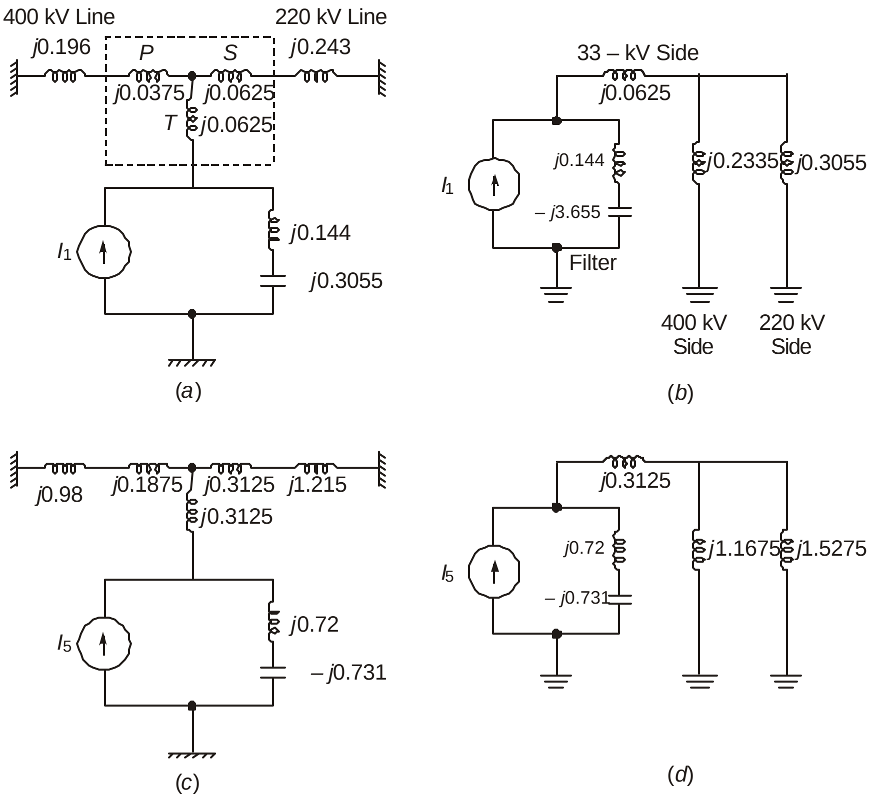

Fig. 12.21 Equivalent circuits for Example 12.18.
(*a*), (*b*): Fundamental frequency.
(c), (*d*): 5th harmonic frequency.

12.9 HIGH PHASE ORDER TRANSMISSION

For e.h.v. transmission requirements, either ac 3-phase or bipolar dc is used. Since such high voltage lines run mostly in the countryside, space for right-of-way does not pose as severe a problem as near metropolitan areas. However, wherever insulation clearances have to be optimized and lines have to be compacted, the use of higher than 3-phases on the same tower can be adopted. This is a recent development and studies are being carried out on a very extensive basis. One transmission line using 6 phases has already been commissioned in the U.S.A. and more are envisaged. We shall give here a brief discussion of a six-phase system only in so far as the transmission line is concerned and operating in the steady state. Transients and faults are not considered.

In a 3-phase system, the three voltages with respect to ground can be written as the phasors.

$$V_a = V\angle 0°, V_b = V\angle -120° \text{ and } V_c = V\angle 120° \quad ...(12.81)$$